Targeting Lopinavir to the Mesenteric Lymphatic System by Lipophilic Ester Prodrug Approach for Improved Treatment of HIV/AIDS

Chaolong Qin

School of Pharmacy

University of Nottingham

Nottingham

United Kingdom

Thesis submitted to The University of Nottingham for the degree of Doctor in Philosophy

TABLE OF CONTENTS

ACKNOWLEDGEMENTS

I would like to express my utmost gratitude to my supervisor Dr. Pavel Gershkovich who has shown his trust, patience, motivation, enthusiasm, rigour, and immense knowledge in supervision throughout my Ph.D. The completion of my project and thesis would not be possible without his support and nurturing. I'd also like to extend my gratitude to my supervisors Professor Peter M. Fischer and Dr. Michael J. Stocks for their support towards the medicinal chemistry aspect of the project, Professor Dr. Yuntao Wu at George Mason University (US) for partaking in our collaborative research and Dr. Christophe Fromont for his supervision during organic synthesis experiments.

A special thanks to my wife, Dr. Sijia He for her constant emotional and academic support, who assumes a greater responsibility towards the family during my Ph.D study. I am also very grateful to my lovely daughter, Victoria A. Qin, who brings so much joy laughter and happiness into my life and has inspired me to become a better father as well as my parents and mother-in-law for their financial and emotional support.

I also had great pleasure working with my previous/current colleagues and friends at the University of Nottingham. I gratefully acknowledge the effort of other members in Gershkovich group - Miss. Wanshan Feng and Mr. YenJu Chu for their invaluable contribution to my Ph.D study. I'd like to especially thank an ex-colleague, Dr. Jong Bong Lee, who provided me lot of support during the early stages of my Ph.D. He was always generous in sharing his enormous knowledge and always showed great patience to answer my questions. I would like to recognize the assistance that I received from Dr. Atheer Zgair, Dr. Joseph Ali, Dr. Carlos Sanders-Velez, Mr. Teerapong Monmaturapoj, Miss. Adelaide Jewell, Miss. Alice

Brookes, Miss. Abigail Wong and Mr. Liuhang Ji in our group. I also very grateful to Dr. Lei Yang, Dr. Zhi Yuan Kok, Dr. Divneet Kaur, Dr. Bashir Rumah and Miss. Ruiling Liu for their contributions towards my Ph.D. project. I am also grateful to the undergraduate, MSc and Ph.D. students who took part in my project which include Mr. Mattia Berton, Miss. Sara Bettonte, Miss. Concepción Medrano-Padial, Mr. Allen Alonso Rodríguez Ugalde, Miss. Daria Vetrugno, Miss. Shi Ying Ee, Mr. Charles Sheriston and Miss. Yeong Yeu Teo.

Chaolong Qin

LIST OF PUBLICATIONS

1. List of publications originating from this thesis:

Qin, C., Feng, W., Chu, Y., Lee, J., Berton, M., Bettonte, S., Teo, Y., Stocks, M., Fischer, P. and Gershkovich, P. (2020). Development and validation of a cost-effective and sensitive bioanalytical HPLC-UV method for determination of lopinavir in rat and human plasma. *Biomedical Chromatography*, 34 (11), e4934.

Qin, C., Chu, Y., Feng, W., Fromont, C., He, S., Ali, J., Lee, J., Zgair, A., Berton, M., Bettonte, S., Liu, R., Yang, L., Monmaturapoj, T., Medrano-Padial, C., Ugalde, A., Vetrugno, D., Ee, S.Y., Sheriston, C., Wu, Y., Stocks, M., Fischer, P. and Gershkovich, P. (2020). Targeted delivery of lopinavir to HIV reservoirs in the mesenteric lymphatic system by lipophilic ester prodrug approach. *Journal of Controlled release.* Online ahead of print.

2. Additional publications:

Lee, J., Radhi, M., Cipolla, E., Gandhi, R., Sarmad, S., Zgair, A., Kim, T., Feng, W., **Qin, C.**, Adrower, C., Ortori, C., Barrett, D., Kagan, L., Fischer, P., de Moor, C. and Gershkovich, P. (2019). A novel nucleoside rescue metabolic pathway may be responsible for therapeutic effect of orally administered cordycepin. *Scientific Reports*, 9(1).

He, S., Fu, Y., Guo, J., Spear, M., Yang, J., Trinité, B., **Qin, C.**, Fu, S., Jiang, Y., Zhang, Z., Xu, J., Ding, H., Levy, D., Chen, W., Petricoin, E., Liotta, L., Shang, H. and Wu, Y. (2019). Cofilin hyperactivation in HIV infection and targeting the cofilin pathway using an anti-α4β7 integrin antibody. *Science Advances*, 5(1), p.eaat7911.

Lee, J., Zgair, A., Malec, J., Kim, T., Kim, M., Ali, J., **<u>Qin, C.</u>**, Feng, W., Chiang, M., Gao, X., Voronin, G., Garces, A., Lau, C., Chan, T., Hume, A., McIntosh, T., Soukarieh, F., Al-Hayali, M., Cipolla, E., Collins, H., Heery, D., Shin, B., Yoo, S., Kagan, L., Stocks, M., Bradshaw, T., Fischer, P. and Gershkovich, P. (2018). Lipophilic activated ester prodrug approach for drug delivery to the intestinal lymphatic system. *Journal of Controlled Release*, 286, pp.10-19.

Lee, J., Adrower, C., **<u>Qin, C.</u>**, Fischer, P., de Moor, C. and Gershkovich, P. (2017). Development of Cordycepin Formulations for Preclinical and Clinical Studies. *AAPS PharmSciTech*, 18(8), pp.3219-3226.

LIST OF ABBREVIATIONS

ART	Antiretroviral treatment
AUC	Area under curves
AIDS	Acquired immunodeficiency syndrome
AZT	Zidovudine
BLT	Bone marrow/liver/thymus
COVID-19	Coronavirus disease
C_0	Concentration extrapolated to time zero
C_{max}	Maximum plasma drug concentration
C_{min}	Minimum plasma drug concentration
C_{trough}	The lowest plasma drug concentration before the next dose
CL	Clearance
CMs	Chylomicrons
CBD	Cannabidiol
CEs	Carboxylesterases
CYP3A4	Cytochrome P450 3A4
CCR5	CC-chemokine receptor 5
CXCR4	CXC-chemokine receptor
DMSO	Dimethyl sulfoxide
DDT	4,4-Dichlorodiphenyltrichloroethane
DDIs	Drug-drug interactions
DC	Dendritic cell
DCM	Dichloromethane
DMF	N,N-Dimethylformamide
DMEM	Dulbecco-modified Eagle’s medium
DNA	Deoxyribonucleic acid
DMAP	4-dimethylaminopyridine
EDTA	Ethylenediaminetetraacetic acid
EDCI	1-Ethyl-3-[N,N-dimethylaminopropyl]-carbodiimide
ELISA	Enzyme-linked immunosorbent assay
Env	Envelope protein
FDA	Food and Drug Administration (US)

FFA	Free fatty acid
F_{oral}	Oral bioavailability
FaSSIF	Fasted state simulated intestinal fluid
FBS	Fetal bovine serum
GI	Gastrointestinal
GALT	Gut-associated lymphoid tissue
GFP	Green fluorescent protein
Gag	Golyprotein
HPLC	High-performance liquid chromatography
HIV	Human immunodeficiency virus
HQC	High concentration quality control samples
HMGB1	High mobility group box 1
HEK293	Human embryonic kidney 293 cells
HR-MS	High resolution mass spectrometry
HSP90	Heat Shock Protein 90
HAND	HIV associated neurocognitive disease
IV	Intravenous administration
IS	Internal standard
IC_{50}	50% inhibition concentration
IC_{90}	90% inhibition concentration
IL-1	Interleukin-1
ILF	Isolated lymphoid follicles
INSTIs	Integrase inhibitors
KBr	Potassium bromide
KS	Kaposi sarcoma
LPV	Lopinavir
LPV/r	Lopinavir/ritonavir
LLOQ	Lower limit of quantification
LC-MS/MS	Liquid Chromatography-tandem mass spectrometry
LQC	Low concentration quality control samples
LPS	Lipopolysaccharide
Log P	Partition co-efficient
Log $D_{7.4}$	Distribution coefficient at pH = 7.4
LRA	Latency-reversing agent

LP	Lamina propria
LCT	Long-chain triglyceride
LPL	Lipoprotein lipase
MSM	Men who have sex with men
M-tropic	Macrophage-tropic
LN	Lymph node
NaF	Sodium fluoride
NaTc	Sodium taurocholate
NCA	Non-compartmental analysis
MQC	Medium concentration quality control samples
MLN	Mesenteric lymph nodes
NMR	Nuclear magnetic resonance
NK	Natural killer
NRTIs	Nucleoside reverse transcriptase inhibitors
NNRTIs	Non–nucleoside reverse transcriptase inhibitors
NMP	*N*-Methyl-2-pyrrolidone
PIs	Protease inhibitors
PI	Propidium iodide
PA-IC_{90}	Protein binding-adjusted IC_{90}
PO	Oral administration
PBS	Phosphate buffered saline
PCP	*Pneumocystis* pneumonia
Pol	Reverse transcriptase
QC	Quality control samples
RPMI	Roswell Park Memorial Institute Medium
RES	Reticuloendothelial system
RBC	Red blood cell
RTV	Ritonavir
RE	Relative error
RSD	Relative standard deviation
Rev	Revelation
RNA	Ribonucleic acid
SARS-CoV-2	Severe acute respiratory syndrome coronavirus 2
SD	Standard deviation

SIV	Simian immunodeficiency virus
SLNs	Solid lipid nanoparticles
S-SNEDDS	Solid self-nanoemulsifying drug delivery system
TDM	Therapeutic drug monitoring
TLR4	Toll-like receptor 4
TG	Triglyceride
THC	Δ9-tetrahydrocannabinol
THF	Tetrahydrofuran
TLC	Thin-layer chromatography
TCL-tropic	T-cell line-tropic
TPV	Tipranavir
$t_{1/2}$	Half-life
t_{max}	Time to reach plasma peak concentration
t_{max-1}	One hour before t_{max}
UV	Ultra-violet
V_{ss}	Volume of distribution at steady state

ABSTRACT

Human immunodeficiency virus (HIV) is a lifelong disease that can destroy human immune system, thereby leading to life-threatening acquired immune deficiency syndrome (AIDS). Combined antiretroviral therapy (cART) can efficiently suppress HIV replication, but the cessation of cART usually results in viral rebound, mostly due to the presence of viral reservoirs. The mesenteric lymphatic system, including mesenteric lymph nodes (MLNs), is an important viral reservoir. In this work, lopinavir (LPV), a protease inhibitor, was selected as a drug candidate for mesenteric lymphatic targeting. In this work we focused on two main aims as follows: (1) development and validation of a sensitive HPLC-UV bioanalytical method for determination of LPV for pharmacokinetics and biodistribution studies in rats; (2) discovery of a novel lipophilic ester prodrug approach, combined with oral lipid-based drug delivery, to efficiently deliver lopinavir (LPV) to the mesenteric lymph and MLNs.

A simple and sensitive HPLC-UV bioanalytical method for determination of LPV in rat plasma was developed and validated. The plasma sample preparation procedure includes a combination of protein precipitation using cold acetonitrile and liquid-liquid extraction with *n*-hexane–ethyl acetate (7:3, *v*/*v*). A good chromatographic separation was achieved with a Phenomenex Gemini (C18, 150 mm × 2.0 mm, 5 μm) column at 40°C with gradient elution, at 211 nm. Calibration curves were linear in the range 10–10,000 ng/mL, with a lower limit of quantification (LLOQ) of 10 ng/mL using 100 μL of plasma. The accuracy and precision in all validation experiments were within the criteria range set by the guidelines of the Food and Drug Administration (FDA). This method was successfully applied to a preliminary pharmacokinetic study in rats following intravenous bolus administration of LPV. Moreover, the method was subsequently fully validated for human plasma allowing its use in therapeutic

drug monitoring. In conclusion, this novel and simple bioanalytical method for determination of LPV is useful for pharmacokinetic and drug delivery studies in rats, as well as therapeutic drug monitoring in human patients.

The combined antiretroviral therapy (cART) can efficiently suppress HIV replication, but the cessation of cART usually results in viral rebound, mostly due to the presence of viral reservoirs. The mesenteric lymphatic system, including mesenteric lymph nodes (MLNs), is an important viral reservoir into which antiretroviral drugs poorly penetrate. In this work, we proposed a novel lipophilic ester prodrug approach, combined with oral lipid-based formulation, to efficiently deliver lopinavir (LPV) to the mesenteric lymph and MLNs. A series of prodrugs was designed using an *in-silico* model for prediction of affinity to chylomicrons (CMs), and then synthesised. The potential for mesenteric lymphatic targeting and bioconversion to LPV in physiologically relevant media was assessed *in vitro* and *ex vivo*. Subsequently, LPV and selected prodrug candidates were evaluated for their *in vivo* pharmacokinetics and biodistribution in rats. Oral co-administration of lipids alone could not facilitate the delivery of unmodified LPV to the mesenteric lymphatic system and resulted in undetectable levels of LPV in these tissues. However, a combination of the lipophilic prodrug approach with lipid-based formulation resulted in efficient targeting of LPV to HIV reservoirs in mesenteric lymph and MLNs. The maximum levels of LPV in mesenteric lymph were 1.6- and 16.9-fold higher than protein binding-adjusted IC_{90} (PA-IC_{90}) of LPV for HIV-1 (140 ng/mL) following oral administration of simple alkyl ester prodrug and activated ester prodrug, respectively. Moreover, the concentrations of LPV in MLNs were 1.1- and 7.2-fold higher than PA-IC_{90} following administration of simple alkyl ester prodrug and activated ester prodrug, respectively. Furthermore, the bioavailability of LPV was also substantially increased following oral administration of activated ester prodrug compared to unmodified LPV. This approach, especially if can be translated to other antiretroviral drugs, has potential for reducing the size of HIV reservoirs within the mesenteric lymphatic system.

Therefore, oral co-administration of lipophilic ester prodrugs and dietary lipids can improve the concentration of prodrugs and the release of the parent drug LPV in the mesenteric lymphatic system. The concentrations of LPV recovered in the mesenteric lymph and lymph nodes were significantly high and exceeded the therapeutic levels of LPV following administration of prodrug **7**. In addition, the increase in systemic exposure to LPV following administration of prodrug **7** is of potentially high clinical importance as it could avoid drug-drug interaction issues caused by co-administration of ritonavir. Therefore, prodrug **7** could be potentially selected for future development for the treatment of HIV.

Following the investigation of lipophilic ester prodrug approach, five self-immolative codrugs were also designed using *in-silico* model for prediction of affinity to chylomicrons (CMs), and then synthesised. The lead compound codrug **4** showed high affinity to artificial CMs (around 60%), good stability in FaSSIF (degradation half-life: 30.5 min). The half-life of codrug **4** was nearly 5-fold shorter and 24-fold longer compared to prodrugs **1** (shortest alkyl ester) and **7** (activated ester), respectively, in rat plasma. Therefore, codrug **4** was selected for the subsequent *in vivo* studies. Unfortunately, the levels of codrug or released LPV could not be detected in plasma at any sampled time points during pharmacokinetic study. Although the reason for these *in vivo* results is unclear, it is likely that first-pass intestinal or hepatic metabolic loss is the main cause of lack of measurable levels of codrug **4** or LPV in plasma. Further investigation will be needed to assess the feasibility of self-immolative codrug approach.

In conclusion, in this PhD project, we have focused on the optimisation of drug delivery for maximising exposure of mesenteric lymphatic system, an important difficult-to-penetrate HIV reservoir, to the antiretroviral drug LPV. A sensitive bioanalytical method for the determination of LPV in rat plasma was a crucial part of this whole project as the measurement of drug concentrations in samples were achieved by means of HPLC-UV. Following the assessment of a series of stability, CM association, and *in vivo* studies, it was shown that the activated ester prodrug exhibited significantly efficient delivery of the active drug to the mesenteric lymph and lymph nodes. The results of the prodrug approach indicated that the delivery of high levels of antiretroviral drugs to viral reservoirs can be beneficial to improve the treatment of HIV/AIDS.

LIST OF FIGURES

LIST OF TABLES

1. INTRODUCTION

1.1. HIV and AIDS

1.1.1. Historical preview

In the early 1980s, several reports announced a new infectious disease among men who have sex with men (MSM) which caused a high mortality rate in the US [1–5]. It was diagnosed as the deficiency of human cellular immune function, leading to Kaposi sarcoma (KS), *Pneumocystis* pneumonia (PCP) or other opportunistic infections, and is now known as acquired immune deficiency syndrome (AIDS) [2]. The human immunodeficiency virus subtype 1 (HIV-1) was first isolated from T cells of infected patients by Luc Montagnier's group in 1983 [6]. Later on, other two groups of scientists isolated and characterised HIV-1, which suggested the relationship between HIV-1 and AIDS [7,8].

1.1.2. HIV infection and immune response

1.1.2.1. HIV life cycle in host cells

There are two subtypes of HIV: HIV-1 and HIV-2. HIV-1 is a highly virulent subtype that is found worldwide. In this PhD work, we mainly focused on the improvement of antiretroviral treatment for HIV-1 infection. It is well documented that there are several critical stages of the HIV life cycle, which represent specific targets for each class of antiretroviral drugs (**Figure 1-1**) [9]. Initially, the introduction of HIV infection to target cells is mediated by interaction with surface receptor CD4 and the co-receptors CC-chemokine receptor 5 (CCR5), CXC-chemokine receptor (CXCR4) or CCR5/CXCR4 [10]. The tropism of HIV is determined by the interaction of HIV envelope (Env) glycoprotein gp120 with the specific co-receptor on the surface of target cells [11]. HIV-1 isolates that target CCR5 co-receptor are known as macrophage-tropic (M-tropic) or R5 viruses [12–14], whereas HIV-1 isolates that target CXCR4 co-receptor are known as T-cell line-tropic (TCL-tropic) or X4 viruses [15,16]. Once an HIV-1 virion fuses into the cytoplasm of target cell, the single-stranded viral RNA is transcripted into cDNA by reverse transcriptase [17]. The proviral DNA is then integrated into cellular DNA, permanently becoming a part of the genome of the infected cell [18]. After transcription of integrated viral DNA, mRNA is exported to cytoplasm for translation. At the end, all essential viral components are assembled near the cytoplasm membrane and immature virions are released and become infectious after maturation [19].

Mature infectious HIV-1 target host cells that express CD4 receptors on the surface, including T lymphocytes, monocytes, macrophages and dendritic cells (DCs). HIV-1 infection of target cells can happen *via* both cell-free virions and cell-to-cell transmission [20,21]. It is well known that viral cell-to-cell transmission is more efficient than cell-free viral infection [22–24]. In general, HIV infection of CD4+ cells results in one of the following outcomes: (1) turning into productively infected cells that release free infectious virions; (2) turning into latent HIV-infected cells; (3) undergoing programmed cell death [25].

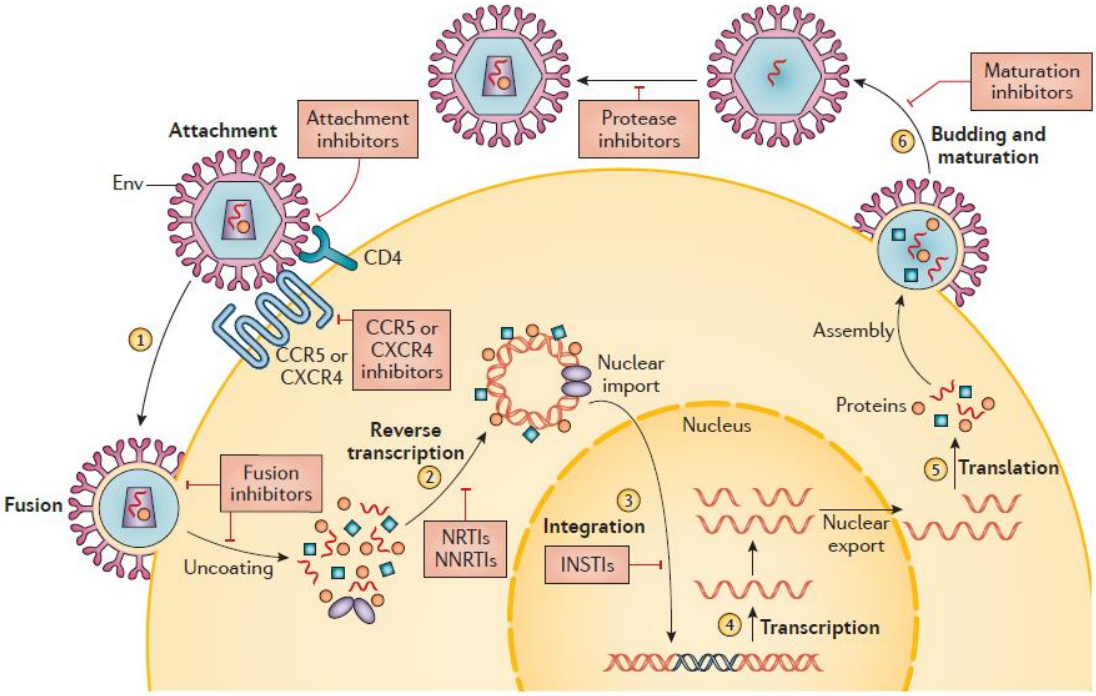

Figure 1 - 1. HIV life cycle and potential target for antiretroviral drugs. HIV attaches to host cells through interaction with CD4 receptor and either CC-chemokine receptor 5 (CCR5) or CXC-chemokine receptor 4 (CXCR4) through envelope glycoprotein (Env) (step 1). Once fusion of cell membrane occurs, the viral particles are released into the cytosol, and viral RNA is subsequently reverse transcripted into cDNA (step 2). The viral cDNA is transported into nucleus, then integrated with host genome (step 3). In step 4, proviral DNA is transcripted into mRNA by host enzyme transcriptase. After transcription, these mRNA are transported back to the cytosol for translation into viral RNA and proteins (step 5). Following assembly, the virus is budding out of the host cells and then is processed to maturation by HIV protease (step 6). Adapted from [9].

1.1.2.2. Immune response

In early HIV-1 infection stage, increased levels of proinflammatory cytokines (such as interleukin-1 (IL-1)) and extrinsic factors (such as lipopolysaccharide (LPS), which migrates from the gastrointestinal tract to systemic circulation) can be detected in patients' blood [26]. Following the stimulation, natural killer (NK) cells and natural killer T (NKT) cells are activated during acute HIV-1 infection. Natural killer and nature killer T cells control the replication of HIV-1 by promoting DCs-mediated CD8+ T cell immune responses [27,28].

Subsequently, HIV-1-specific CD8+ T cells start to reduce the rate of HIV-1 replication following post infection, thereby decreasing the levels of plasma viral load to the viral set point [29]. The viral set point is the viral load of a person infected with HIV, which stabilizes following a period of acute HIV infection. Meanwhile, the number of CD4+ T cells drops dramatically, especially in gut-associated lymphoid tissue (GALT) which contains a high proportion of effector and memory CD4+ T cells in the body [30,31]. It has been reported that nearly 80% of CD4+ T cells are depleted in GALT during the early acute phase of SIV-infected macaques or HIV-1-infected patients [30,32–34]. The SIV infection of macaques is an extremely valuable animal model for the study of HIV infection and human AIDS. Experimental inoculation of SIV to macaques will lead to a similar pathogenesis to humans who are infected with HIV. More importantly, the characterisation of immunologic and virologic parameters can be easily monitored and quantified throughout the study [35].

1.2. HIV reservoirs

1.2.1. Establishment of HIV reservoirs

HIV reservoirs are known as cellular and anatomical compartments where HIV can escape and hide from both, efficient ART (a combination therapy can reduce the viral load in the blood to undetectable levels) and immune response. It has been demonstrated that viral reservoirs are established in the very early stages of HIV-1 infection. Chun *et al*. [36] found that the initial antiretroviral treatment in HIV-1-infected individuals as early as 10 days following the onset of symptoms of primary infection cannot prevent the establishment of latent infected CD4+ T cells in viral reservoirs. Following this important finding, Chun *et al.* [37] demonstrated that efficient administration of ART in seven patients at early acute HIV-1 infection stage was able to significantly reduce the size of latent viral reservoirs, thereby achieving better clinical outcomes. These results are in agreement with other published studies on SIV-infected macaques, in which the establishment of SIV reservoirs happened within 3 days post-infection (p.i.) [38–41]. Early efficient ART in SIV-infected macaques (at day 3 p.i.) substantially reduced the size of latent HIV reservoirs within lymphoid tissues compared with treatments at later time points, but still failed to completely eliminate viral reservoirs [41].

1.2.2. HIV reservoirs under efficient ART

HIV-induced AIDS was one of the main causes of morbidity and mortality worldwide in the early 1990s before the appearance of antiretroviral drugs. In current clinical practice, ART is capable of suppressing the plasma viral load below the limit of detection (<50 copies/mL) in patients [42]. However, a rapid viral rebound (within several weeks) was observed in the vast majority of HIV-infected patients who discontinued suppressive ART [43–45] (**Figure 1-2**). Rothenberger *et al*. [46] demonstrated solid clinical evidence for the existence of HIV reservoirs within lymphoid tissues, which led to a large number of cases of viral rebound in peripheral blood following treatment interruption. The reasons for persistence of viral reservoirs are described as follows: (1) latent cellular reservoirs where proviral DNA integrates with host genome; (2) ongoing replication reservoirs in which presently known antiretroviral drugs have poor penetration; (3) immune dysfunctions fail to control viral replication and neutralise viruses [47]. The HIV-1 latent reservoirs can be formed within days of initial infection, and they have an extremely long half-life (44 months) even in patients undergoing suppressive ART [48–50]. These latent HIV-infected CD4+ T cells do not express viral RNA and proteins, thereby remaining invisible to effective ART and immune system. Following immune activation, the latent HIV-infected CD4+ T cells transcribe proviral DNA into viral RNA, thereby assembling virions that will become infectious upon maturation (**Figure 1-1**)

[51]. A number of studies have reported that ongoing HIV replication is attributed to the low levels of antiretroviral drugs in these difficult-to-penetrate tissues within viral reservoirs, especially in GALT [52–55]. In addition, an irreversible depletion of mucosal CD4+ T cells was observed in the gastrointestinal tract during acute infection stage, and only limited number of CD4+ T cells were repopulated following effective ART [56], which led to immune dysfunction. Therefore, development of an efficient therapeutic strategy to eliminate viral reservoirs and reconstitute immune function is an urgent unmet need for the development of an HIV cure.

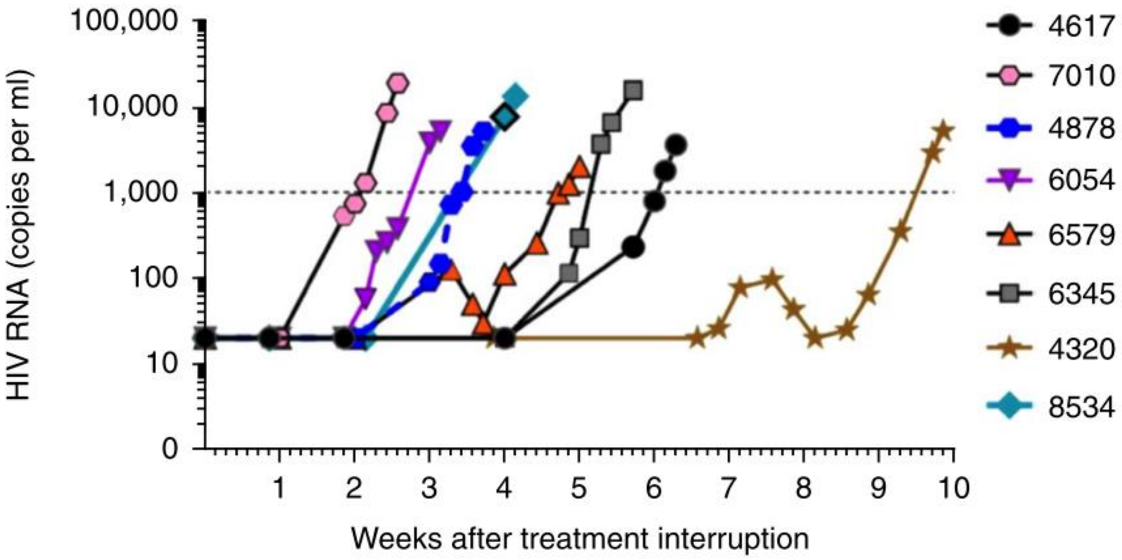

Figure 1 - 2. Plasma viral load rebound following treatment interruption in 8 Fiebig I acutely treated participants. Median (range) time to viral load rebound > 20 copies per ml was 26 (13–48) days. The numbers on the right side of the figure represent patient ID numbers. Adapted from [43].

1.3. Current antiretroviral therapy (ART)

1.3.1. Historical preview

Since the appearance of HIV/AIDS, discovery, development and optimization of an effective antiretroviral therapy has been the major goal. In 1987, zidovudine (AZT) was the first approved anti-HIV drug by the Food and Drug Administration (FDA), which showed significant reduction of plasma viral load following administration in HIV-infected patients [57]. After the successful application of AZT in HIV-infected patients, other classes of antiretroviral drugs with activity at different stages of the HIV life cycle were developed (**Figure 1-1**). In the late of 20th century, a novel combination antiretroviral therapy (cART), also known as the ‘AIDS cocktail’ therapy, was introduced to reduce plasma viral load to undetectable levels in patients [58,59]. Nowadays, with early initiation of cART, people living with HIV can have a near-normal life expectancy. Currently, there are more than 30 different approved antiretroviral compounds for HIV treatment in clinical settings [60].

1.3.2. Antiretroviral agents for the treatment of HIV-1

There are five distinct classes of antiretroviral drugs categorised based on their mechanism of action on the HIV life cycle in host target cells (**Figure 1-1**). Antiretroviral agents include viral entry inhibitors (such as attachment inhibitors, CCR5/CXCR4 antagonists and fusion inhibitors), nucleoside reverse transcriptase inhibitors (NRTIs), non–nucleoside reverse transcriptase inhibitors (NNRTIs), integrase inhibitors (INSTIs) and protease inhibitors (PIs) [61]. To achieve a good outcome of the treatment, three or four different classes of antiretroviral agents are used as a combination therapy.

1.3.3. HIV protease inhibitors

HIV protease belongs to the family of aspartic proteinases, which hydrolyses the HIV Gag and Gag-Pol polyprotein precursors and leads to viral maturations [62]. In this work, we focused on protease inhibitors (PIs). PIs were designed as substrates or peptidomimetic ‘transition-state’ analogues, which inhibit HIV protease from cleaving viral polyproteins during the viral maturation [63,64].

Lopinavir (LPV), an orally administered PI, was initially approved by the FDA for co-administration with low-dose ritonavir under the brand name Kaletra (LPV/r) [65]. It has been reported that the oral bioavailability of LPV in humans is less than 1%, and around 25% in rats [66]. Poor oral bioavailability of LPV is related to extensive intestinal and hepatic first-pass metabolism by cytochrome P450 3A4 (CYP3A4) [67]. As a result, ritonavir, which is a potent inhibitor of CYP3A4, was utilized to increase the systemic exposure to LPV [66,68]. LPV/r has been consistently recommended as a PI for use in second-line ART regimens since 2006 [69]. Moreover, LPV/r is still recommended as the preferred PI therapy for second-line ART regimen, alternative first-line ART regimen in children, and in special situations in neonates according to the latest WHO guidelines [70]. Most importantly, over 70% patients in developing countries undergoing second-line therapy are receiving LPV/r [71]. Therefore, LPV/r is one of the most widely used PIs.

1.3.4. Potential strategies under current investigation for elimination of HIV reservoirs

1.3.4.1. 'Shock and kill' strategy

In 2012, Archin *et al*. reported a proof-of-concept study, which demonstrated that vorinostat (VOR) can stimulate latent HIV-infected CD4+ T cells, and proposed a novel strategy for eradication of latent viral reservoirs [72]. In 2013, this strategy was termed as 'shock and kill' [73], which includes a two-step process: first, latency-reversing agents (LRAs) are applied to stimulate latent HIV-infected CD4+ T cells (the shock part); second, the infectious virions are produced by activated cells and killed by effective ART or immune system (the kill part). In the past few years, numerous LRAs were developed [74–77] and the proposed 'shock and kill' strategy was studied in both HIV-infected individuals [72,78,79] and SIV-infected macaques [75,80]. However, some important drawbacks of 'shock and kill' strategy have been reported. This includes: (1) the degree of the activation of resting CD4+ T cells exhibits large variation among individuals, suggesting LRAs may not strong enough for latent viral reservoirs stimulation in all patients [81]; (2) chronic HIV-infected patients with severely destroyed immune system may fail to efficiently respond to LRA-stimulated CD4+ T cells compared with acute HIV infection [82,83]; (3) LRA-stimulated CD4+ T cells are likely to produce viral RNA and proteins in tissues to which antiretroviral drugs poorly penetrate, such as brain, thereby leading to HIV associated neurocognitive disease (HAND) [84]. Due to these limitations, 'shock and kill' strategy remains controversial to proceed with large-scale clinical studies.

1.3.4.2. ‘Block and lock’ strategy

“Block and lock” strategy includes a two-step process as follows: (1) prevent latent HIV-infected CD4+ T cells from activation (the block part); (2) prevent all proviral DNA from transcription even after the interruption of ART (the lock part). ‘Block and lock’ strategy is a novel strategy without clinical data; most of the studies are under the development with cell lines and/or primary cell models [82,85–88]. In addition, a limited number of preclinical studies have been carried out in recent years. One study showed that Tat inhibitor dCA delayed viral rebound for up to 19 days following treatment interruption in bone marrow/liver/thymus (BLT) humanized mice latency models [89]. Another study demonstrated that (Heat Shock Protein 90) HSP90 inhibitors could delay viral rebound up to 11 weeks following treatment interruption [90]. However, there is no evidence to confirm ‘block and lock’ strategy can maintain the latent viral reservoirs silent for an extended period of time [91]. Further studies of ‘block and lock’ strategy are needed.

1.3.4.3. ‘Kick and go’ strategy

The development of antibody-based therapies is becoming another promising strategy for the cure of HIV. In recent years, it became known that integrin α4β7, highly expressed on CD4+ T cells [92,93], is associated with both HIV and SIV infection risk [94]. Therefore, integrin α4β7 has become an interesting antigenic target for the treatment of HIV/AIDS. It has been demonstrated that anti-α4β7 antibody can modulate the cofilin pathway and repair T cell migratory defect, and restore T cell migration and repopulation in gut [95]. This ‘kick and go’ strategy can potentially contribute to immune reconstitution, thereby controlling viral replication within HIV reservoirs, especially GALT. Another interesting finding shows that integrin α4β7 is able to efficiently incorporate into HIV, which facilitates viral infection of α4β7-expressing cells [96]. Both important findings provide further mechanisms detailing the protective effects of anti-α4β7 antibody (ACT-1) in SIV-infected macaques from a virology and immunology perspective [97,98]. However, phase I and phase II clinical studies showed that anti-α4β7 antibody (Vedolizumab) cannot effectively suppress viral rebound following the discontinuation of ART in patients [99,100]. A further investigation showed that administration of higher dose of Vedolizumab (300 mg) did result in lower viral rebound, compared to a lower dose (150 mg) [100]. Therefore, continuing investigation of anti-α4β7 antibody is necessary to interpret its potential role in future clinical studies.

All these novel strategies above for the elimination of viral reservoirs are still under investigation, which means they are not at a stage to replace current antiretroviral therapy in clinical settings. However, it is necessary to continue investigation of therapeutic strategies for reducing the size of viral reservoirs, thereby improving the treatment outcomes of HIV-infected patients.

1.4. Lymphatic system

1.4.1. Lymphatic transport system

The lymphatic system is not a closed system. It comprises of lymphatic capillaries, collecting vessels, lymph nodes, trunks and ducts, which drains the lymph from capillaries back to the systemic circulation [101]. The lymph from the upper right quadrant drains into the right thoracic duct, and lymph from the rest part of the body (including intestinal lymphatics) drains into the left thoracic duct (**Figure 1-3**). In this study, we took advantage of the physiological intestinal lymphatic transport of lipids and lipophilic molecules to deliver drugs to the gut-associated lymphoid tissue (GALT) *via* the oral route.

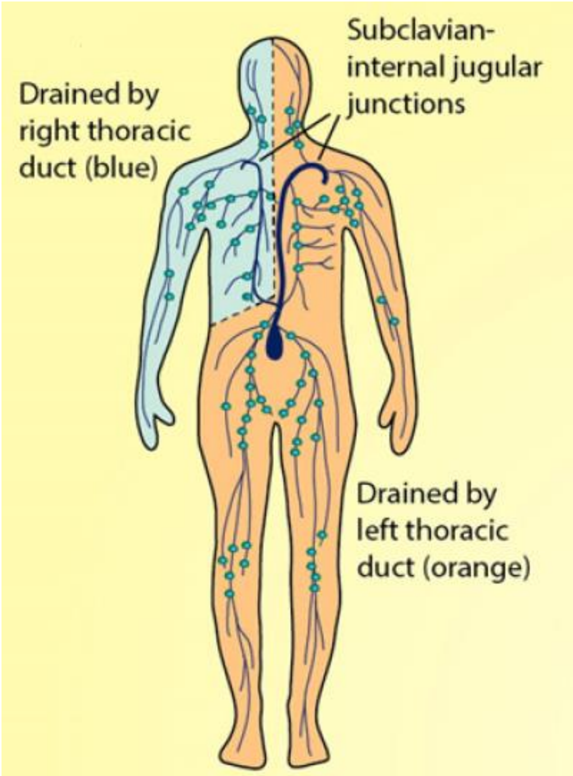

Figure 1 - 3. Schematic diagram of the lymph transport and lymphatic system. Adapted from [102].

1.4.2. Gut-associated lymphoid tissue (GALT)

The GALT is the largest secondary lymphoid tissue in the body [103], and includes the lamina propria (LP), intestinal epithelium, Peyer's patches, isolated lymphoid follicles (ILF) and mesenteric lymph nodes (MLNs) [103,104]. The MLNs are the largest gatherings of lymph nodes in the body [104], which drains lymphocytes, immunoglobulins and other proteins from the jejunum, ileum, cecum, and ascending colon [105]. Subsequently, these components flow from MLNs *via* the thoracic duct to the systemic circulation [104].

1.4.3. Gut-associated lymphoid tissue (GALT) involvement in HIV infection

A disruption of mucosal homeostasis due to HIV infection (discussed in Section 1.2.2.), may contribute to the severe migration of bacteria and their products across the intestinal barrier to the systemic circulation [106]. Briefly, the antigens can be taken up by dendritic cells within the wall of small intestine by Peyer's patches, then carried to the MLNs where dendritic cells present antigens to T lymphocytes [107]. Subsequently, the memory and naïve T lymphocytes are activated by the antigens in gut lymphoid tissues (mainly MLNs), as well as in peripheral blood [108]. Therefore, the MLNs are a crossover point between the intestinal antigen presentation and systemic immune response. As discussed in Section 1.1.2.2., GALT (mainly MLNs) contains the largest numbers of CD4+ T cells, which subsequently develop into the largest HIV cellular reservoirs in HIV-infected individuals.

Many studies have demonstrated that GALT possesses the largest proportion of viral RNA/DNA in HIV-1-infected patients during suppressive ART [34,109–111], and rebounding virions in systemic circulation emerge from this important reservoir [46,112–114]. Estes *et al*. [54] comprehensively analysed some key organs in SIV-infected monkeys, and found that around 98% of SIV RNA+ cells were in GALT under otherwise efficient ART. To note, Siddiqui *et al*. [53] and Horiike *et al*. [55] reported that MLNs contain substantially higher numbers of HIV-infected cells, compared to peripheral LNs, in SIV-infected macaques after half year or one year of fully suppressive cART. Furthermore, Rabezanahary *et al*. [115] recently found the evidence of early viral seeding in MLNs (but not peripheral LNs) despite early administration of cART treatment in SIV-infected macaques, as well as maintaining higher replicative rate in MLNs than peripheral LNs during the whole infection stage (**Figure**

1-4). Taken together, these studies indicate that efficient delivery of antiretroviral drugs to the GALT (MLNs) is potentially much more important than to peripheral LNs throughout the acute and chronic HIV infection stages.

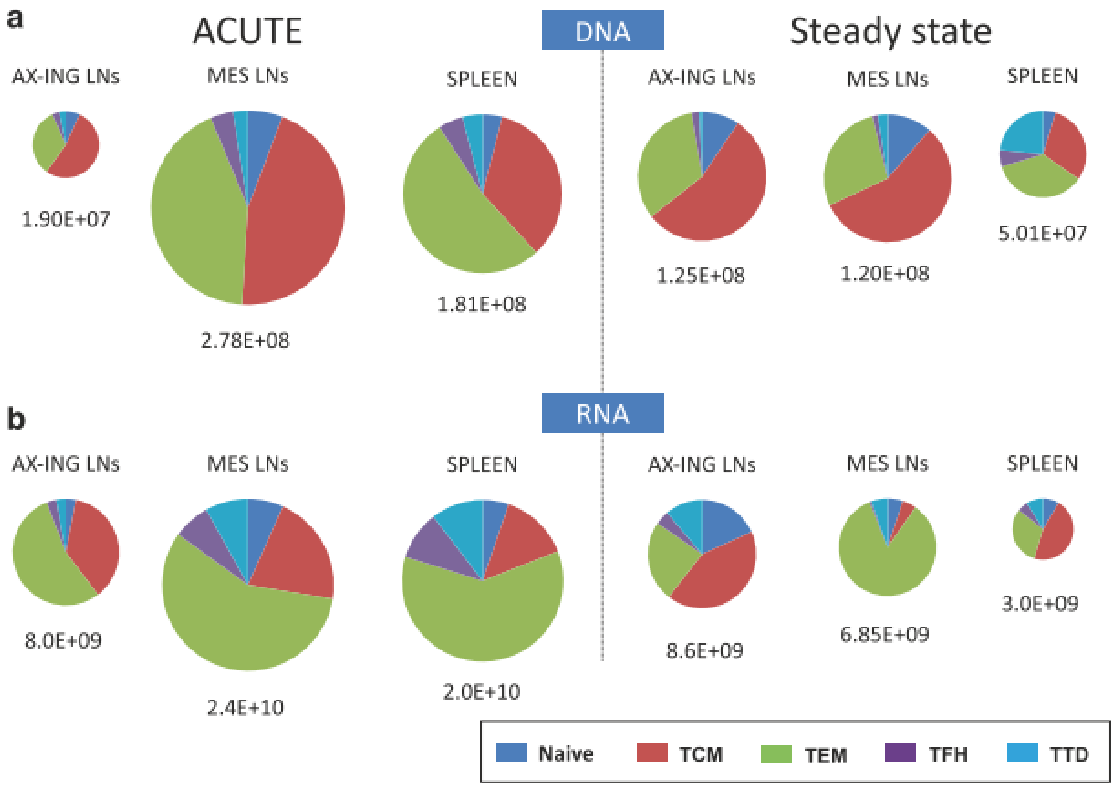

Figure 1 - 4. The size is proportional to the relative amount of SIV DNA or RNA in total CD4+ T cells per organ (the absolute value is indicated below each graph and the size of the Ax-Ing LNs pie graph at the acute phase is used as reference). Ax-Ing LNs, axillary-Inguinal lymph nodes; Mex LNs, mesenteric lymph nodes, Naïve, naïve T cells; TCM, central memory T cells; TEM, effector memory T cells; TFH, follicular helper T cells; TTD, terminally differentiated T cells. Adapted from [115].

1.4.4. Intestinal lymphatic transport as drug delivery approach

1.4.4.1. Conventional drug delivery routes

In general, most orally administered drugs will transport into the small intestinal wall and be absorbed to hepatic portal vein *via* mesenteric vessels, then to the liver before reaching the systemic blood circulation. The bioavailability of orally administered drugs could be affected by intestinal and hepatic first-pass metabolism. In general, the liver is a major site of first-pass metabolism following oral administration [116]. However, there are several routes for drug delivery which can bypass hepatic first-pass metabolism, such as intestinal lymphatic delivery [117–120], transdermal delivery, inhalation, sublingual and rectal administration [116], thereby increasing the drug exposure in systemic circulation.

1.4.4.2. The physiological process of dietary lipid absorption

In the mid-18th century, a famous Scottish anatomist William Hunter founded a doctrine of 'absorbent system', which demonstrated absorption into the lymphatic system rather than blood veins [121,122]. Furthermore, he and his younger brother John Hunter worked together to trace the path of lymphatic vessels by injection of mercury. By the late 20th century, processes involving intestinal digestion and absorption of dietary lipids were well documented [123–125]. Dietary lipids absorption consists of 4 main steps, including: digestion in the GI lumen, uptake into the enterocyte, intracellular processing and transport into mesenteric lymphatic system [126,127]. Lipids are initially digested by pancreatic lipase/co-lipase complexes in the lumen of the small intestine. Hydrolysis products (fatty acids and 2-monoaclyglycerol) are incorporated into bile salt micelles, and then transported into the cells across the brush-border membrane of the intestinal enterocyte [128]. Triglycerides are re-synthesised in smooth endoplasmic reticulum. At the same time, primordial chylomicrons (CMs) are assembled in rough endoplasmic reticulum [129,130]. Primordial CMs and a fusion (core expansion) of TG droplets are transported into Golgi apparatus, packed into vesicles and then released to the basolateral side [131]. CMs consist of LCTs (85-92%) as a central lipid core, and a layer of phospholipids (6-12%), cholesterol (1-3%), and apolipoproteins (1-2%)

[132]. Once the newly formed CMs arrive from thoracic duct the systemic blood circulation, the LCTs are hydrolysed by the activity of lipoprotein lipase (LPL) on the luminal surface of capillaries of certain tissues [133]. The released fatty acids can be rapidly taken up by skeletal muscle, heart and adipose tissue, and CM remnants are delivered to the liver for further metabolism [133,134].

1.4.4.3. Intestinal lymphatic transport of lipophilic drugs

The intestinal lymphatic pathway is physiological mechanism of absorption of dietary lipids, fat-soluble vitamins, and macromolecules molecules into the systemic circulation [104,117,118]. In addition, the intestinal lymphatic system represents an important compartment related to the pathophysiology of lymphomas, metastatic tumours, as well as HIV infection. Therefore, efficient promotion of drug exposure and activity in intestinal lymphatic system may potentially improve the treatment of lymphomas, tumour metastases [135] and reduce the size of HIV reservoirs [136].

It has been reported that lipophilic drugs with a distribution coefficient at pH 7.4 (log $D_{7.4}$) value more than 5, as well as a triglyceride (TG) solubility in excess of 50 mg/mL have potential to be absorbed into intestinal lymphatics following oral administration with LCT or other lipids [135,137]. In 2005, Gershkovich *et al.* [138] reported a linear relationship between the intestinal lymphatic transport *in vivo* and the degree of association of drugs with CMs *ex vivo* (**Figure 1-5**). As a result, the enterocyte-derived CMs were essential carriers to deliver lipophilic compounds to intestinal lymphatic system, instead of hepatic portal vein transport (**Figure 1-6**) [117,118,139]. In the further investigation, an *in-silico* modelling tool was developed to predict the affinity of drugs to CMs using a combination of eight different molecular physicochemical parameters of tested compound [137]. The *in-silico* modelling can efficiently predict drug potential for intestinal lymphatic targeting; therefore it has been used to predict the CMs association (%) with designed molecules in this work.

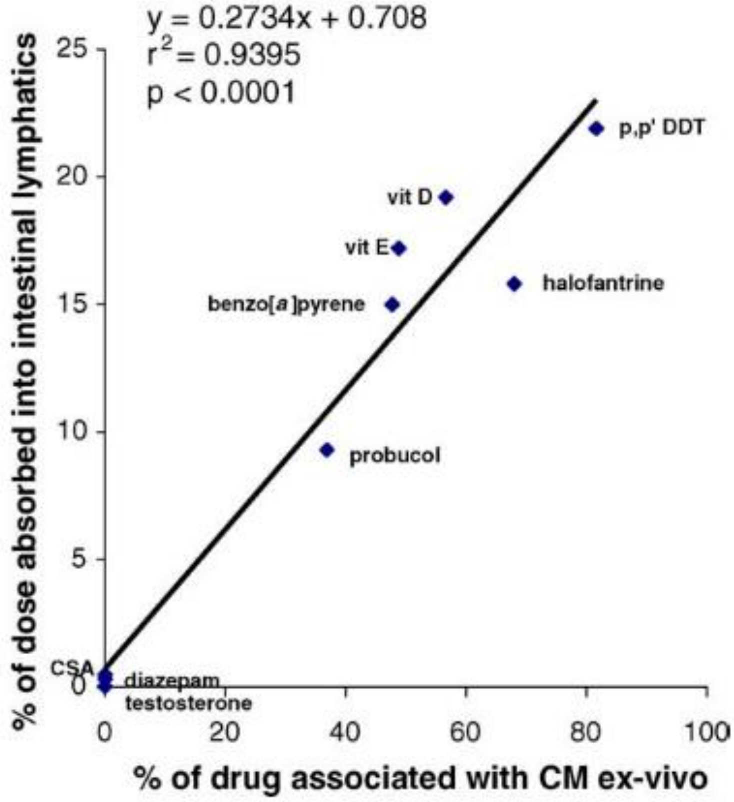

Figure 1 - 5. Lymphatic absorption of tested drugs (% of dose) *in vivo* vs. the degree of drug-chylomicrons association *ex vivo* (% of amount). Adapted from [138].

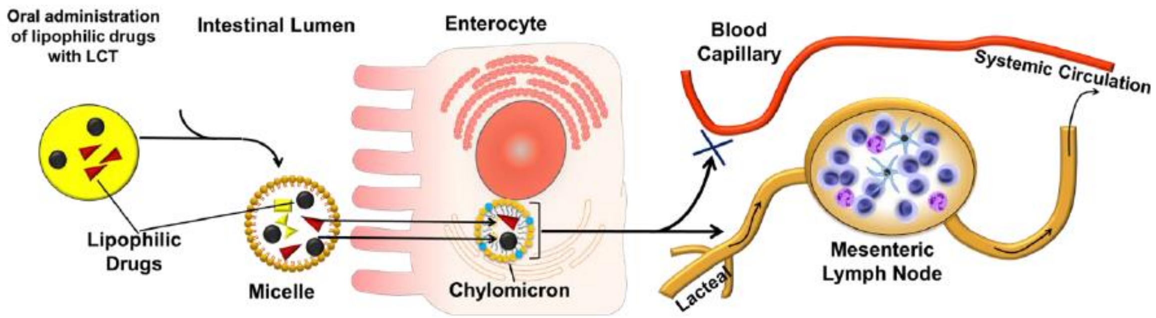

Figure 1 - 6. Targeted delivery of lipophilic compounds to the mesenteric lymphatic system using the physiological pathway of dietary lipids absorption. Adapted from [139].

1.5. Current approaches for delivery of antiretroviral drugs to the reticuloendothelial system (RES) and lymphatic system.

1.5.1. Erythrocyte-based drug approach for delivery of antiretroviral drugs to HIV reservoirs within reticuloendothelial system (RES)

In 1970s, scientists started to use red blood cells (RBCs) as natural biological carriers for drug delivery to the reticuloendothelial system (RES), such as lymphoid organs, bone marrow and liver [140]. In 1990s, this strategy was applied for antiretroviral drugs delivery to the lymphatic system [140,141]. One of the main advantages of using the erythrocyte as a carrier is due to its high potential for drug-erythrocyte delivery to the RES [142,143] – are primarily responsible for clearing and recycling iron from erythrocytes [144]. Magnani *et al.* [145] successfully encapsulated ddTCP (nucleoside analogue) into erythrocytes and selectively delivered the drug to viral cellular reservoirs such as macrophage cells, resulting in a reduction of typical syndromes over 3 months treatment in the murine model of AIDS. Further investigation of this strategy revealed similar results following administration of two encapsulated nucleoside analogues (AZT + Didanosine (DDI)) with erythrocytes in mice [146]. In addition, the combination of AZT + DDI with erythrocytes in brain significantly reduced the levels of viral DNA, compared to administration of AZT + DDI alone. Similarly, a few other studies demonstrated that encapsulation of antiretroviral drugs within erythrocytes can efficiently inhibit viral replication in HIV-infected macrophages *in vitro* [147,148]. However, large variations for erythrocytes in drug loading, strict storage conditions for drug-loaded erythrocytes and possible contamination make this approach unsuitable for applications in the large scale treatment of HIV/AIDS [149].

1.5.2. Conventional approaches for delivery of antiretroviral drugs to HIV reservoirs within lymphatic system

1.5.2.1. Liposomes

Around the 1980s, liposome technology was developed and applied for drug delivery, some of which are commercially available for clinical treatments or are undergoing clinical trials in recent years [150]. A conventional liposome is a spherical vesicle composed of an aqueous core and one or more phospholipid bilayers, which closely resemble the structure of cell membranes [151]. The function of liposomes is to incorporate either lipophilic or hydrophilic drugs into the opposing phase of this vesicle, allowing targeted delivery of drugs into tissues [151]. Recently, many studies have reported selective delivery of antiretroviral drugs to HIV reservoirs in lymphatic system using liposome drug delivery approaches [152–154]. Bestman-Smith *et al.* [152] reported that the levels of antibodies in MLNs following a single subcutaneous injection of antibody-incorporated sterically stabilized immunoliposomes were 1.6-fold higher, compared to conventional liposomes in mice. In the study carried out by Kaur *et al*. [153], a mannose-coated liposomes of zidovudine led to increase in the percentage of administered dose present in LNs (cervical, mediastinal, and above colon) by nearly 15-fold compared to free zidovudine at 2 h after subcutaneous injection in rats. In another study, indinavir was investigated for evaluation of drug delivery to the peripheral LNs following subcutaneous injection of free indinavir or indinavir-incorporated in sterically stabilized immunoliposomes in mice [154]. This study showed that indinavir-incorporated in sterically stabilized immunoliposomes could selectively and efficiently deliver 126-fold higher levels of indinavir to LNs, compared to administration of free indinavir. This drug-incorporated liposome approach highlights an efficient therapeutic strategy for delivery of antiretroviral drugs to viral reservoirs for the treatment of HIV/AIDS. The main drawback of this approach is that following subcutaneous administration only limited number of peripheral lymph nodes draining the lymph from the injection site can be targeted [155].

1.5.2.2. Solid Lipid Nanoparticles and other nanoformulations

Solid lipid nanoparticles (SLNs) are known as nanostructured lipid carriers, which consist of surfactant-stabilized lipids in a solid state at both room and normal body temperature. SLNs possess higher drug entrapment, better stability and controllable drug release compared to the liposome delivery system [156,157]. There are three models for drug incorporation, including: homogenous matrix model, drug-enriched shell model and drug-enriched core model [158]. The nanoformulations are commonly administered by routes of subcutaneous or intramuscular injection [159–165], and are likely to be taken up into the local lymphatic system, then delivered to lymphatic tissues due to their similar size (50-1000 nm [166]) to CMs. Studies in another group, lopinavir (LPV), ritonavir (RTV), tenofovir (TFV) and lamivudine (3TC) were efficiently delivered to the superficial lymph nodes following a single subcutaneous administration of antiretrovirals-SLNs in nonhuman primates [160–162]. One of the most promising results showed that the levels of LPV, RTV, TFV and 3TC in lymph node mononuclear cells (LNMCs) were 4.1-, 23.1-, 5.0- and 1.9-fold higher than peripheral blood mononuclear cells (PBMCs), respectively, at day 8 following subcutaneous administration of the 4-in-1 drug combination nanoparticle approach [162]. It is also reported that rilpivirine, dolutegravir and cabotegravir were effectively delivered to the superficial lymph nodes following a single intramuscular injection of antiretrovirals-containing nanoformulations to mice [163–165]. For example, the levels of cabotegravir in LNs following intramuscular administration of the latest nanoformulation in mice were significantly higher, compared to the first-generation nanoformulation, and drug concentration maintained above therapeutic levels for up to 364 days [165]. Moreover, several studies showed that the nanoparticle-based drug delivery approach could achieve long-acting efficacy of antiretroviral drugs in systemic circulation [159–165]. As a result, this approach would not only improve the tissue biodistribution profiles of antiretroviral drugs but would also enhance patient adherence to ART regimens. However, the main disadvantage of this approach is that only superficial lymphatic tissues could achieve sufficient levels of drug, probably due to the fact that drug-loaded nanoparticles are being preferably taken up from anatomical injection areas.

In addition to the promising results above, studies from other groups investigating antiretroviral drug distribution to HIV reservoirs by the SLNs approach indicated similar outcomes [167–170]. Their results showed that the levels of stavudine in LNs following oral [168] and intravenous [169] administration of stavudine-SLNs formulation in rats were significantly higher, compared to free stavudine. In addition, Dandagi *et al*. [168] showed that the levels of stavudine in LNs and brain following oral administration of stavudine-SLNs formulation were 4- and 11-fold higher, respectively, compared to free stavudine. Makwana *et al*. [170] developed a novel SLNs approach using hot homogenisation technique followed by ultrasonication method which achieved high levels of efavirenz in the mesenteric lymph fluid at 4 and 6 h sampling time points following oral administration of the novel efavirenz-SLNs formulation in rats. Therefore, nanoformulation approaches showed high potential for delivery of antiretroviral drugs to the lymphatic tissues for reducing or even eliminating HIV anatomical reservoirs.

1.6. Current prodrug approaches for delivery of active drugs to the mesenteric lymphatic system

In recent years, TG-mimetic and long-chain fatty acid ester prodrug approaches were studied for delivery of prodrugs and active drugs to systemic circulation *via* intestinal lymphatic transport [171–176]. However, these studies mainly focused on the % of dose in lymphatic versus portal relative contribution to systemic bioavailability, as well as systemic bioavailability when administered orally in animals. For example, it is reported that the absolute bioavailability of released docetaxel following oral administration of TG-mimetic docetaxel prodrug in rats was over 4-fold higher than unmodified docetaxel [172]. In other work, when TG-mimetic and long-chain fatty acid ester prodrug approaches were applied to mycophenolic acid (MPA) in dogs, the % of dose of both MPA and its prodrugs were measured in lymph [174]. The % of 2-MPA-TG dose in lymph was as high as 36.4 % following oral administration, while the % of released MPA dose was the same as the % obtained after administration of free MPA. In addition to TG-mimetic and long-chain fatty acid ester prodrug approaches, activated ester prodrug approaches were applied to efficiently deliver parent drugs to the lymphatic system [177,178]. As an example, a study carried out by Lee *et al*. found that the maximum levels of active drug bexarotene in MLNs were 17-fold higher following oral administration of activated ester prodrug in rats, compared to unmodified bexarotene [177]. In another example, the levels of tenofovir diphosphate (TFV-DP) (pharmacologic-active moiety of TFV) in inguinal lymph nodes were 6.4-fold higher following oral administration of TFV novel prodrug in HIV-infected patients, compared to commercially available prodrug TDF [178]. These previous studies combined suggest that the levels of antiretroviral drugs in HIV reservoirs (mesenteric lymph and MLNs) can be potentially improved by lipophilic ester prodrug approaches.

1.7. Current codrug approaches to improve the activity of antiretroviral drugs

The codrug approach is more complex than prodrug approach. In general, two different drugs are conjugated *via* labile covalent bond (enzymatic cleavable linker) as a carrier to deliver to the HIV-infected cells, thereby exerting their pharmacological effects simultaneously [179–181]. There are three different categories of antiretroviral codrugs: (1) codrugs targeting the same HIV enzyme [182,183]; (2) codrugs targeting different HIV enzymes [184,185]; and (3) codrugs containing one antiretroviral drug to target one HIV enzyme and one non-antiretroviral drug with potent anti-inflammatory pharmacological effects [186] or additive/synergistic effects [187]. One study carried out by Matsumoto *et al*. [184] showed that the anti-HIV-1 activity of one hybrid molecule (AZT and KNI-727 [PI]) (EC_{50} = 0.1 nM) in Molt-4 cells was 62- and 920-fold higher compared to that of either AZT (EC_{50} = 6.2 nM) or KNI-727 (EC_{50} = 92 nM), respectively. In another example, the anti-HIV-1 activity of one hybrid molecule (AZT conjugated with κ-carrageenan) (EC_{50} = 6.8 nM) in MT-4 cells was 116- and 4-fold higher than κ-carrageenan (EC_{50} = 788 nM) and AZT (EC_{50} = 25 nM), respectively [187]. Taken together, the overall aim of the codrug approach above is to achieve higher antiretroviral activity, compared to individual parent drugs.

1.8. Project hypotheses and aims

Despite antiretroviral therapy (ART) is capable of suppressing viral load to undetectable levels in the blood, viral RNA/DNA remains detectable in anatomical and cellular reservoirs into which antiretroviral drugs poorly permeate. Mesenteric lymph nodes (MLNs) harbour the vast majority of viral RNA/DNA in presence of ART. Therefore, the main hypothesis of this PhD project is that improving the intestinal lymphatic transport of lipophilic prodrug by oral co-administration with dietary lipids could deliver antiretroviral drug (LPV) to MLNs above therapeutic levels.

The rationale behind lipophilic prodrug approach is based on the physiological process of lipid digestion and absorption, which directly associates with intestinal lymphatic transport of lipophilic drugs. LPV without chemical modifications has negligible association with chylomicrons. This indicates that LPV could not be delivered to the mesenteric lymphatic system following oral administration without chemical modifications. Therefore, the key aspect of this work is to design and synthesize lipophilic ester prodrugs which possess the necessary physicochemical properties for improvement of association with CMs. Another critical aspect is to ensure the rapid release of active drug from prodrug as soon as it reaches the effect-site in the lymphatic system.

Specific objectives of this work include:

Chapter 3:

- Development of a simple and sensitive HPLC-UV method for determination of lopinavir in rat plasma
- Validation of the developed method in rat plasma in different storage conditions
- Application of the method to pre-clinical pharmacokinetic study in rats
- Application and validation of the method in human plasma in different storage conditions

Chapter 4

- Design of LPV prodrugs by means of *in-silico* modelling for prediction of drug association with CMs
- Chemical synthesis and characterisation of designed prodrugs
- Assessment of mesenteric lymphatic targeting potential of the prodrugs using *in vitro* and *ex vivo* CMs association experiments
- Evaluation of the bioconversion of the prodrugs to the active drug (LPV) in physiologically relevant media *in vitro*
- *In vivo* assessment of the pharmacokinetics of LPV and selected prodrugs
- *In vivo* assessment of the biodistribution of LPV and selected prodrugs to the mesenteric lymph and mesenteric lymph nodes
- *In vitro* antiretroviral efficacy evaluation of LPV and selected prodrugs

Chapter 5

- Design of LPV codrugs by means of *in-silico* modelling for prediction of drug association with CMs
- Chemical synthesis and characterisation of designed codrugs
- Assessment of mesenteric lymphatic targeting potential of the codrugs using *in vitro* artificial CMs association experiments
- Evaluation of the bioconversion of the codrugs to the active drug (LPV) in physiologically relevant media *in vitro*
- *In vivo* assessment of the pharmacokinetics of selected codrug

2. MATERIALS AND METHODS

2.1. Materials

Lopinavir (LPV, CAS: 192725-17-0), Corning 96-well Transwell®, Costar Spin-X Centrifuge Tubes, butyric acid, hexanoic acid, octanoic acid, decanoic acid, dodecanoic acid and 2-(2-acetamidoacetamido) acetic acid were purchased from Fisher Scientific (Leicestershire, UK); 2-butoxyacetic acid was from Enamine (Riga, Latvia). Thin-layer chromatography (TLC) Silica gel 60 Å F254 plates were purchased from Merck (Darmstadt, Germany). Cannabidiol (CBD, CAS: 13956-29-1) was purchased from THC Pharm (Frankfurt, Germany). 4,4-Dichlorodiphenyltrichloroethane (DDT, CAS: 50-29-3) was purchased from Sigma Aldrich (Dorset, UK). Ritonavir (CAS: 155213-67-5), Intralipid®, esterase from porcine liver, NaF, sodium taurocholate (NaTc), lecithin, EDTA, KBr, NaCl, NaOH (pellets), NaH_2PO_4, propylene glycol, sesame oil, serum triglyceride determination kit, 1-ethyl-3-[N,N-dimethylaminopropyl]-carbodiimide (EDCI), *O*-acetylsalicyloyl chloride, salicylic acid, butyryl chloride, hexanoyl chloride, octanoyl chloride, decanoyl chloride, DMSO-d_6, 4-dimethylaminopyridine (DMAP), magnesium sulfate, anhydrous dichloromethane (DCM), anhydrous *N*-Methyl-2-pyrrolidone (NMP), anhydrous N,N-Dimethylformamide (DMF), G418 (antibiotics) and puromycin were from Sigma-Aldrich (Gillingham, UK or St. Louis, MO, USA). Rat plasma was purchased from Sera Laboratories (West Sussex, UK) and human plasma from TCS Biosciences (Buckingham, UK). Lipofectamine 2000, Roswell Park Memorial Institute (RPMI) 1640, Dulbecco-modified Eagle's medium (DMEM), penicillin-streptomycin and fetal bovine serum (FBS) were purchased from Invitrogen (Carlsbad, CA, USA). The HIV Rev-dependent GFP indicator Rev-A3R5-GFP cells were provided by Virongy (Virginia, USA). HEK293T cells were kindly provided by Dr. Yuntao Wu. The infectious HIV-1 molecular clone pNL4-3 was obtained from the NIH AIDS Reagent Program. HPLC-grade water was obtained from PURELAB® Ultra system (ELGA LabWater, UK). All other research reagents used were of HPLC analytical grade or higher.

2.2. Bioanalytical methods for determination of lopinavir and its prodrugs/codrugs in plasma and tissues

2.2.1. Plasma sample preparation

This methodology was used to generate experimental results described in Chapters 3-5

All samples went through the same process of combination of protein precipitation and liquid-liquid extraction for HPLC-UV analysis. Ten microliters of IS was added to 100 µL of rat plasma in a 16 mm × 150 mm glass tube. Then 300 µL of cold acetonitrile (-20°C) was added, followed by vortex-mixing for 1 min. HPLC-grade water (300 µL) was then added and vortex-mixed again for 1 min [188]. A volume of 3 mL of extraction solvent, consisting of a mixture n-hexane–ethyl estate (7:3, *v*/*v*), was added and the samples were vortex-mixed for 3 min. Following centrifugation (1160 *g*, 10°C, 10 min), the upper organic layers were transferred to fresh tubes using Pasteur pipette and evaporated under nitrogen at 40°C (Techne DRI- Block type DB-3D, Cambridge, UK). Dry residues were reconstituted in 100 µL of mobile phase (50% acetonitrile in water), vortex-mixed for 10 min and then transferred to HPLC vials.

2.2.2. Validation of the stability of prodrugs in rat plasma

This methodology was used to generate experimental results described in Chapter 4

The stability assessment was performed by spiking prodrug solution in acetonitrile into rat plasma supplemented with 10 mg/mL of NaF. For the validation of prodrug **1**, samples were kept on ice for 5 min, followed by centrifugation (3000 *g*, 0°C, for 3 min) to mimic the procedure of blood collection and plasma separation. Following centrifugation, the ‘separated plasma’ samples were placed on ice for 1 h to mimic the time frame of temporary storage of samples during pharmacokinetic studies, and then kept frozen at -80°C (for 24 h) until analysis. For the validation of prodrug **7**, plasma samples were kept on ice for 5 min and immediately centrifuged (3000 *g*, 0°C, for 3 min). Following centrifugation, proteins were immediately precipitated by 300 µL cooled (-20°C) acetonitrile and samples were processed for HPLC analysis. Sample preparation procedure and chromatography conditions are described in Sections 2.2.1 and 2.2.5. All experiments were performed in triplicates (data are shown as mean ± SD). Tested prodrugs were stable at these conditions (97.6 ± 6.6% remaining of prodrug **1**; 92.3 ± 8.0% remaining of prodrug **7**).

2.2.3. Tissue sample preparation

This methodology was used to generate experimental results described in Chapters 4 and 5

Tissues were harvested at the end of pharmacokinetic studies and biodistribution studies at t_{max} observed in plasma during pharmacokinetic studies and 1 h before t_{max} time points. Tissues were thawed on the ice bath, then weighed. HPLC-grade water was added to tissues (1:3, *w/v*) collected from *in vivo* studies following administration of LPV. NaF solubilised in HPLC-grade water (10 mg/mL) was added to tissues (1:3, *w/v*) harvested from *in vivo* studies following administration of LPV prodrugs. Prepared samples were then homogenised (POLYTRON® PT 10-35 GT, Kinematica AG, Luzern, Switzerland) on ice bath prior to sample preparation for analysis. Sample preparation was identical to Section 2.2.1.

2.2.4. Validation of the stability of prodrugs in homogenised MLNs

This methodology was used to generate experimental results described in Chapter 4

Prodrug **7** solution was spiked into homogenised blank MLNs with water (1:3, *w/v*) and placed on ice for 10 min (mimicking the time frame of lymph nodes isolation procedure), then stored in dry ice for 1 h and transferred to -80°C (for 24 h) until analysis. The prepared homogenates were thawed at ambient temperature and treated with NaF to achieve a final NaF concentration of 10 mg/mL, following by homogenisation on ice bath within 30 second to mimic the time frame of homogenisation procedure. Sample preparation procedure and chromatography conditions were described in Sections 2.2.3 and 2.2.5. All experiments were performed in triplicates (data are shown as mean ± SD). Prodrug **7** was stable in homogenised MLNs (93.9 ± 9.8% remaining).

2.2.5. Chromatography conditions

This methodology was used to generate experimental results described in Chapters 3-5

The HPLC-UV system consisted of a Waters Alliance 2695 separations module equipped with a Waters 996 photodiode array detector. Separation was accomplished at 40°C using an analytical C18 Gemini column (150 mm × 2.0 mm I.D.) with a particle size of 5 µm, coupled with a guard column (2 mm × 4mm) with a particle size of 3 µm (Phenomenex, Macclesfield, UK). All compounds were monitored at λ = 211 nm. The temperature of autosampler was maintained at 4°C and the column was kept at 40°C. Complete HPLC running conditions for all tested compounds including column, guard column and mobile phase are described in **Table 2-1** and **Table 2-2**. Empower™ 2 software was used for data acquisition and analysis.

Table 2- 1. Analytical method conditions for compounds studied in Chapter 4

Compounds	Moblie phase (%) Acetonitrile	water	column [a]	Flow rate (mL/min)	UV length (nm)	Internal standard	Reconstitution solvent [b]
Prodrug **1**	55	45	C18	0.5	211	CBD [g]	55%
Prodrug **2**	65	35	C18	0.5	211	CBD	65%
Prodrug **3**	70	30	C18	0.5	211	CBD	70%
Prodrug **4**	80	20	C18	0.5	211	CBD	80%
Prodrug **5**	85	15	C18	0.5	211	CBD	85%
Prodrug **1**, **6** and **7**	Gradient 1[c]		C18	0.3	211	CBD	50%
Prodrug **2**	Gradient 2[d]		C18	0.3	211	CBD	50%
Prodrug **3**	Gradient 3[e]		C18	0.5	211	CBD	50%
Prodrug **4** and **5**	Gradient 4[f]		C18	0.5	211	CBD	50%

[a] C18: Gemini C18 2.0 × 150 mm, 110Å, 5 µm particle size, coupled with a guard column (2 mm x 4mm) with a particle size of 3 µm

[b] Reconstitution solvent expressed as % of acetonitrile in HPLC-grade water.

[c] Gradient 1: Acetonitrile 50% at 0-9.5 min, increase to 65% at 9.5-11.5 min, 65% at 11.5-20 min, decrease to 50% at 20-21 min, 50% at 21-25 min.

[d] Gradient 2: Acetonitrile 50% at 0-9.5 min, increase to 70% at 9.5-11.5 min, 70% at 11.5-20 min, decrease to 50% at 20-21 min, 50% at 21-25 min.

[e] Gradient 3: Acetonitrile 50% at 0-6.5 min, increase to 80% at 6.5-10 min, 80% at 10-15 min, decrease to 50% at 15-16 min, 50% at 16-24 min.

[f] Gradient 4: Acetonitrile 50% at 0-6.5 min, increase to 85% at 6.5-10 min, 85% at 10-15 min, decrease to 50% at 15-16 min, 50% at 16-24 min.

[g] CBD: Cannabidiol

Table 2- 2. Analytical method conditions for compounds studied in Chapter 5

Compounds	**Moblie phase (%)**		**column** [a]	**Flow rate (mL/min)**	**UV length (nm)**	**Internal standard**	**Reconstitution solvent** [b]
	Acetonitrile	**water**					
Codrug **1**	Gradient 1[c]		C18	0.3	211	CBD[e]	50%
Codrug **2**	Gradient 2[d]		C18	0.3	211	DDT[f]	50%
Codrug **3-5**	Gradient 2		C18	0.3	211	CBD	50%

[a] C18: Gemini C18 2.0 × 150 mm, 110Å, 5 µm particle size, coupled with a guard column (2 mm x 4mm) with a particle size of 3 µm

[b] Reconstitution solvent expressed as % of acetonitrile in HPLC-grade water.

[c] Gradient 1: Acetonitrile 50% at 0-9.5 min, increase to 70% at 9.5-11.5 min, 70% at 11.5-20 min, decrease to 50% at 20-21 min, 50% at 21-25 min.

[d] Gradient 2: Acetonitrile 50% at 0-9.5 min, increase to 70% at 9.5-11.5 min, 70% at 11.5-20 min, increase to 85% at 20-22 min, 85% at 22-26 min, then decrease to 50% at 26-27 min, 50% at 27-32 min.

[e] CBD: cannibidiol

[f] DDT: 4,4-dichlorodiphenyltrichloroethane

2.3. Chemical synthesis

2.3.1. Lopinavir prodrug synthesis

This methodology was used to generate experimental results described in Chapter 4

The synthesis of ester prodrugs was based on previously reported chemical approach with slight modifications [189]. Corresponding carboxylic acid to generate prodrugs **1-7** (1.59 mmol), 1-ethyl-3-(3-dimethylaminopropyl) carbodiimide (EDCI) (1.59 mmol) and 4-dimethylaminopyridine (DMAP) (0.032 mmol) were dissolved in anhydrous dichloromethane (DCM) (10 mL) and stirred at room temperature under N_2 for 15 min before adding LPV (0.159

mmol). The reaction mixture was then allowed to stir overnight and monitored by TLC and LC-MS. The mixture was added to saturated $NH_4CH_3CO_2$ (30 mL), then extracted with ethyl acetate (20 mL × 3). The combined organic layers were washed with saturated $NaHCO_3$ (30 mL) and brine (30 mL), then dried over anhydrous $MgSO_4$, filtered, and the solvent evaporated *in vacuo*. The crude product was purified by column chromatography on silica using a gradient DCM/tetrahydrofuran (THF) 5:1. The purified fractions were pooled and fully evaporated to dryness. Final compound (20 mg) was dissolved in DMSO-d_6 for NMR determination.

2.3.2. Codrug (lopinavir + salicylic acid) synthesis

This methodology was used to generate experimental results described in Chapter 5

Salicylic acid (0.72 mmol) was dissolved in anhydrous NMP (5 mL) with a drop of anhydrous DMF at 0°C under N_2. Triethylamine (1 mmol) was added, and the mixture was stirred for 1 min at 0°C. Then desired acid chloride (0.72 mmol) was added into the mixture drop by drop at 0°C, temperature was gradually increased to room temperature. After 2 h, reaction completion was monitored by LC-MS. Product was purified by column chromatography on silica using a gradient DCM/ethyl acetate 20:1. The product was weighed (0.1 mmol) then was dissolved in anhydrous DCM (with 2 drops of anhydrous DMF) at 0°C under N_2. Thionyl chloride (0.25 mmol) was added drop by drop and stirred at room temperature. Reaction completion was monitored by LC-MS. After 1.5 h, the reaction mixture was evaporated to dryness, then dissolved in anhydrous NMP. LPV (0.16 mmol) and trimethylamine (3.6 mmol) were dissolved in anhydrous NMP in a new flask, and stirred at 0°C for 1 min. *O*-acetylsalicyloyl chloride (0.8 mmol) was added to the reaction mixture drop by drop. Temperature was changed gradually from 0°C to room temperature with stirring overnight at 50°C. Reaction completion was monitored by LC-MS. The reaction was monitored by thin layer chromatography (TLC) using a mobile phase of 20% ethyl acetate in DCM and LC-MS. The mixture was added to saturated $NH_4CH_3CO_2$ (30 mL), then extracted with ethyl acetate (20 mL × 3). The combined organic layers were washed with saturated $NaHCO_3$ (30 mL) and brine (30 mL), then dried over anhydrous $MgSO_4$, filtered, and the solvent evaporated *in vacuo*. The crude product was purified by column chromatography on silica using a gradient DCM/ethyl acetate 5:1. The purified eluents were pooled and fully evaporated to dryness. Final compound (20 mg) was dissolved in DMSO-d_6 for NMR determination.

2.3.3. Characterisation of synthesised molecules

This methodology was used to generate experimental results described in Chapters 4 and 5

^{1}H NMR and ^{13}C NMR spectra (Bruker 400 Ultrashield Spectrometer) were recorded at 400 and 100 MHz, respectively, at ambient temperature. Chemical shifts (δ) were reported in parts per million (ppm) relative to DMSO-d_6 (^{1}H, δ = 2.50 ppm; ^{13}C, δ = 39.52 ppm [190]). ^{1}H NMR data was reported as follows: chemical shift, integration, multiplicity (s = singlet, d = doublet, t = triplet, q = quartet, m = multiplet) and coupling constants (J) were recorded in Hz. The spectra were analysed using MestReNova 12.0.1 software. High-resolution mass spectrometry was performed using a Bruker MicroTOF II with electrospray ionisation (ESI). The liquid chromatograph-tandem mass spectrometry (LC-MS) system consisted of a Shimadzu UFLCXR module equipped with an Applied Biosystems API2000. An analytical C18 Gemini-NX column (50 mm × 2 mm I.D.) with a particle size of 3μm (Phenomenex, Macclesfield, UK) was used at 40°C to accomplish a chromatographic separation. All compounds were monitored at 220 nm (channel 2) and 254 nm (channel 1). Short gradient method: pre-equilibration for 1 min at 5% solvent B, then increase to 98% B in 2 min, 98% B for 2 min, decrease to 5% B in 0.5 min, then 5% B for 1 min. Long gradient method: pre-equilibration for 1 min at 5% B, then

5% B for 0.5 min and increase to 98% B in 8 min, 98% B for 2 min, decrease to 5% B in 0.5 min, then 5% for 1 min. Both methods underwent at flow rate of 0.5 mL/min. Solvent A: 0.1% formic acid in water; solvent B: 0.1% formic acid in acetonitrile. Thin-layer chromatography (TLC) was performed using Silica gel 60 Å F254 plates (Merck, Darmstadt, Germany). Compounds were purified *via* column chromatography using ISOLUTE SPE columns (Flash Silica II 5g/25mL) (Biotage, Hengoed, UK). Reagents and solvents for prodrugs characterisation were purchased from Sigma-Aldrich (Gillingham, UK) and Fisher Scientific (Leicestershire, UK), and were used without further purification.

2.4. *In vitro* and *ex vivo* CMs association assay

2.4.1. Preparation of artificial emulsion (Intralipid®)

Intralipid® 20% (Sigma, Gillingham, UK) was diluted with phosphate buffered saline (PBS, PH 7.4) to yield a triglyceride (TG) concentration of 1 mg/mL [137,177]. The TG concentration was measured by serum TG determination kit according to the manufacture's protocol (Sigma, Gillingham, UK) using a BIO-TEK FL600™ plate reader (BIO-TEK INSTRUMENTS, INC. Vermont, USA). The fresh prepared artificial emulsion was then used to assess the uptake efficiency of tested compounds, which is described in Section 2.4.3.

2.4.2. Isolation of human plasma-derived chylomicrons

The protocol for preparation of human plasma-derived CMs was approved by the Faculty of Medicine and Health Sciences Research Ethics Committee, Queens Medical Centre, Nottingham University Hospitals (BT12102015 CBS SoP). Three healthy male participants between 30-40 years old were enrolled after providing informed consent. Study participants received a high-fat breakfast (equivalent to a full English breakfast [177]). Three to four hours following the meal, 30 mL of blood was collected into heparinised Vacutainer® Blood Collection tubes, and plasma was separated by centrifugation (800 *g*, 10 min, 15°C).

The separation of CMs from human plasma was performed as previously described [138,177]. A density of 1.1 g/mL was achieved by gently mixing 4 mL of plasma with KBr (0.57 g). Standard solutions with densities of 1.006, 1.019 and 1.063 g/mL were prepared by dissolving appropriate amount of KBr in PBS. Density gradient layers were built by layering standard solutions of different densities on the top of plasma in a 12-mL polyallomer ultracentrifuge tube. Samples were ultracentrifuged (SORVALL® Ultracentrifuge; TH-641 Rotor, 268,350 *g*, 35 min, 15°C) and the upper layer (approximately 1 mL) containing CMs fraction, was collected by glass Pasteur pipettes. TG concentrations were measured using the serum TG determination kit and were adjusted to 1 mg/mL TG level by PBS of 1.006 g/mL density. Standard human CMs from each volunteer was separately stored at 4°C for less than 24 h before association assay.

2.4.3. Association assay

The uptake of tested compound by artificial and natural CMs emulsion were evaluated as previously described with minor modifications [138,177,191]. Stock solutions of tested compounds (0.1 mM) were prepared in propylene glycol with 1% ethanol (*v/v*). An appropriate volume of stock solution was spiked into 1 mL of previously prepared artificial emulsion or human CMs (1 mg/mL TG) to obtain a final concentration of tested compounds of 1.75 µM [138]. For control sample, same amount of stock solution was added in the PBS (1 mL) without adding CMs. The mixture was then incubated at 37°C with magnetic stirring at 170 rpm.

Following 1 h incubation, 0.9 mL of mixture was added into 0.157 g of KBr to achieve a density of 1.1 g/mL. A density gradient was then built using PBS buffers with the density of 1.036, 1.019 and 1.006 g/mL. The CMs fraction was isolated by gradient density ultracentrifugation as described in Section 2.4.2. Following ultracentrifugation, the upper layer (approximately 1 mL) was collected using a glass pipette and kept in -80°C until analysis. Sample preparation and chromatographic system were described in Section 2.2. The value of CMs association (%) was calculated using the amount of tested compounds in collected fraction (upper layer) divided by the total amount of tested compounds. Each compound was performed in quintuplicate. To evaluate the potential loss of compounds during the procedure of the assay (such as unspecific binding or drug degradation), the calculation of mass recovery percentage was conducted. The value of mass recovery (%) was calculated by using the amount of tested compounds in the mixture following 1 h incubation divided by the total amount of tested compounds. Each compound was performed in triplicate. In this study, the mass recovery (%) > 90% can be considered as acceptable value for calculation of CMs association (%).

2.5. Prodrug conversion assay

The release of LPV from the prodrugs was assessed in rat plasma and fasted state simulated intestinal fluid (FaSSIF, pH = 6.5) supplemented by esterases (mixture of esterases from porcine liver, mainly carboxylesterase, at 20 IU/mL) [177,192,193]. The preparation of FaSSIF was performed as previously reported (**Table 2-3**) [194]. Plasma contains similar composition and levels of enzymes to lymph fluid in many species [195,196]. Therefore, rat plasma was used as an acceptable surrogate to assess the potential stability of tested prodrug in lymphatic system. Following pre-incubation at 37°C for 5 minutes, stock solution of tested compound (1 mM) in acetonitrile was spiked into the media to reach a final concentration of 10 µM. The mixture was incubated at 37°C, 200 rpm on a temperature-controlled orbital shaker (Thermo Scientific MaxQ4000, Waltham, MA, USA). One hundred microliters of the incubation mixture was withdrawn at pre-determined time points, and reaction was terminated by 300 µL of cooled (-20°C) acetonitrile containing 10 µL of internal standard (IS). The samples were analysed for the prodrug and LPV concentrations by means of HPLC-UV as described in Section 2.2. All experiments were performed in triplicate. The slope (*k*) was obtained using the plotted percentage of natural logarithm of prodrug concentration against the pre-determined time points. The half-life ($t_{1/2}$) of tested prodrug was calculated from an equation: $t_{1/2} = -0.693/k$.

Table 2- 3. Preparation of fasted state simulated intestinal fluid (FaSSIF) [194]

	FaSSIF (500 mL)	
Content	**Concentration (mM)**	**in DDW (g)**
NaTc	3	0.807
Lecithin	0.75	0.286
NaOH (pellets)	8.7	0.174
NaH2PO4	28.65	1.977
NaCl	105.9	3.093

Adjusted pH to 6.50

2.6. Long-chain triglyceride solubility test

Tested compound was weighed (> 5 mg) and added into sesame oil (100 µL) with constant mixing using a magnetic stirrer at 37°C for 72 h. Samples were then filtered by centrifugation in Costar Spin-X Centrifuge Tubes (Fisher Scientific, Loughborough, UK) at 2400 *g* for 20 min. The collected filtrates were diluted with ethanol (1:10^4, *v/v*) and analysed by means of HPLC-UV. All experiments were performed in triplicate.

2.7. *In vitro* antiretroviral activity assay

2.7.1. Cell culture and virus preparation

HIV Rev-dependent GFP indicator cells Rev-A3R5-GFP [197] were cultured in RPMI 1640 plus 10% FBS supplemented with 1 μg/ml G418 and 1 μg/ml puromycin. HEK293T cells were maintained in Dulbecco-modified Eagle's medium (DMEM) containing 10% FBS and 1x penicillin-streptomycin. All cells were maintained at 37°C, 95% relative humidity and 5% CO_2. To produce HIV-1 particles, HEK293T cells were transfected with 20 μg of the infectious HIV-1 molecular clone pNL4-3 using Lipofectamine 2000 in 100 mm cell culture dish. Virus supernatant was collected at 48 h post transfection and filtered through a 0.45 μm nitrocellulose membrane. HIV-1 p24 was detected using an in-house p24 ELISA determination kit and the procedure was described in previous publication [198].

2.7.2. Viral infection assay

For each infection, 0.3 million Rev-A3R5-GFP cells were infected with HIV-1 (NL4-3) for 2 h (150 ng p24 per infection). Cells were then washed twice and cultured in fresh media with adding the working standard solutions of LPV and its prodrugs (in DMSO) to yield concentrations of 10^{-3}, 10^{-2}, 10^{-1}, 10^{0}, 10^{1}, 10^{2}, 10^{3}, 10^{4} nM (**Table 2-4**). The percentage of GFP+ cells was quantified by flow cytometry (FACSCalibur; BD Biosciences, San Jose, CA, USA) at 72 h post infection [198].

Table 2- 4. Experimental conditions of cell culture-based antiretroviral activity assay

Tube	Cell [a] (0.3 million)	Virus [b]	After wash, add fresh media [c]	Add tested compound [d]	Final conc.of tested compounds (nM)
1	100 µL	(media 300 µL)	1mL	(DMSO 10 µL)	Negative control
2	100 µL	300 µL	1mL	(DMSO 10 µL)	Positive control
3	100 µL	300 µL	1mL	10 µL	10^4
4	100 µL	300 µL	1mL	10 µL	10^3
5	100 µL	300 µL	1mL	10 µL	10^2
6	100 µL	300 µL	1mL	10 µL	10^1
7	100 µL	300 µL	1mL	10 µL	10^0
8	100 µL	300 µL	1mL	10 µL	10^{-1}
9	100 µL	300 µL	1mL	10 µL	10^{-2}
10	100 µL	300 µL	1mL	10 µL	10^{-3}
	Viral infection time: 2 h		Incubation time: 72h		

[a] Rev-A3R5-GFP cells

[b] HIV-1 (NL4-3 wild-type) (150 ng p24 per infection)

[c] RPMI 1640 plus 10% FBS supplemented with 1 µg/ml G418 and 1 µg/ml puromycin

[d] All tested compounds were dissolved in DMSO

2.7.3. Prodrug stability in cell culture media

The stability of prodrugs was assessed in cell culture media (RPMI 1640 + 10% FBS). Stock solution of tested compound (1 mM) in DMSO was spiked into the media to yield a final concentration of 10 µM. The mixture was incubated at 37°C for 72 h to mimic the time frame of the antiretroviral activity assay. One hundred microliters of the incubation mixture were withdrawn at 48 and 72 h, and proteins were precipitated by 300 µL of cooled (-20°C) acetonitrile. The samples were analysed for the prodrugs and LPV concentrations by means of HPLC-UV as described in Section 2.2. All experiments were performed in triplicate.

2.8. Animal experiments

2.8.1. Animals

Animal welfare and all experimental procedures were reviewed and approved by the University of Nottingham Ethical Review Committee under the Animals [Scientific Procedures] Act 1986. Male Sprague Dawley (SD) rats (300-380g) were obtained from Charles River Laboratories UK and housed at Bio Support Unit, University of Nottingham. They were kept in an environmentally controlled room (12:12h light-dark cycle) with free access to food and water for at least six days before starting experiment.

2.8.2. Right external jugular vein cannulation

2.8.2.1. Preparation of rats for surgery

Jugular vein cannulation surgery was performed under general anaesthesia in order to allow blood sampling in conscious, freely moving rats. On the surgery day, the rat was initially weighed, then anaesthesia was induced by the inhalation of 2.5% isoflurane blending in oxygen [177,199]. After the rat was sedated, the fur in the dorsal neck and the area of right ventral neck toward the upper thorax was gently shaved. The shaved areas were sterilised with alcohol 2% chlorhexidine skin wipes (Clinell®, GAMA Healthcare Ltd., London, UK). In order to prevent corneal dryness during the surgery, eye protection ointment was applied on the eyes. Four millilitres of saline were injected subcutaneously to maintain body fluid balance, followed by injection of 1 mg/kg of meloxicam. The prepared rat was wrapped using the self-adhesive drape (GLAD® Press'n Seal) and transferred to the theatre for surgery.

2.8.2.2. Surgery procedure

The rat was placed on the heating pad, and laid on back with head toward to the surgeon. The mouth and nose of rat were kept in the mask which continuously provided 2.5% isoflurane in oxygen. The anatomical position above the right external jugular vein was identified before skin incision. Blunt dissection was performed to separate the muscle and fat layers until the jugular vein was clearly visible. Jugular vein was isolated from the surrounded connective and fat tissues using cotton swabs, while keeping it moist with normal saline. A small incision was made on the dorsal neck skin for making a subcutaneous tunnel from back toward the front incision using a long metal pin. The silastic-polyethlylene (PE-50) tubing was inserted through the tunnel with silastic end near the isolated part of the jugular vein. A small incision on the vein was made using iris scissors, followed by implantation 2.5 cm of the catheter toward the heart which was secured by a silk suture. A small volume of heparinised saline (100 IU/mL) was slowly injected and withdrawn through the newly inserted catheter to check its function. Once the function of the cannula was validated, the muscle and skin layers were sutured. Three to four centimetres of PE-50 tubing was left away from the dorsal neck and plugged with a sterile metal pin. Animals were observed for the lack of visible pain and distress signs and were allowed to recover for two nights before pharmacokinetic experiments [188,200,201].

2.8.3. Pharmacokinetic study

Prior to the experiment day, rats were fasted overnight with free access to water. For intravenous bolus administration, LPV, prodrugs **1** and **7** were solubilised in a mixture of propylene glycol–sterile water–ethanol (70:20:10, *v*/*v*/*v*) at concentrations of 4 mg/mL, 10 mg/mL and 2.37 mg/mL, respectively, on the day of administration. Formulation (1 mL/kg) was injected intravenously within 30 seconds *via* the jugular vein catheter followed by 0.3 mL heparinised saline (50 IU/mL). For oral administration of LPV in lipid-free group, the formulation was prepared by dissolving LPV in 100% propylene glycol (20 mg/mL). For oral administration of LPV in lipid-based group, LPV solubilised in 100% propylene glycol (20 mg/mL) was administered, followed by fresh sesame oil administration (1 mL/kg) due to the low solubility of LPV in TG. For oral administration of prodrugs/codrugs in lipid-based groups, prodrugs/codrugs were solubilized in fresh sesame oil at concentrations equivalent to 20 mg/mL of LPV. All oral formulations were administered by an oral gavage (1 mL/kg), followed by 1 mL of water. Blood samples (0.25 mL) were withdrawn *via* the jugular vein catheter before dosing and at predetermined time points following administration. Eppendorf tubes contained EDTA (1.5 M) to prevent blood coagulation and NaF (10 mg/mL) [177] as an esterase inhibitor. Plasma samples were placed on ice immediately following the collection for no longer than 5 min and plasma was separated by centrifugation (3000 *g*, at 0°C for 3 min) and stored at -80°C until analysis. At the end of pharmacokinetic study, rats were euthanised by CO_2 inhalation, and MLNs, liver, spleen, brain and testes were harvested and stored at -80°C until analysis.

2.8.4. Biodistribution study

Rats were fasted overnight with free access to water. Lipid-based formulations of tested compounds were prepared as described in Section 2.8.3.2 on the day of administration. Following oral administration of LPV or prodrugs, rats were euthanised by CO_2 inhalation at plasma t_{max} and t_{max-1}. Lymph sample was immediately collected from the mesenteric lymph duct. The MLNs were collected as previously reported [177,191]. Briefly, mesenteric tissues were removed from the abdominal cavity and placed in a clean weigh boat and MLNs were gently isolated from mesenteric adipose tissue. Other tissues, including spleen, brain, liver, and testes were also harvested, and stored at -80°C until analysis. All the collected tissues were homogenised (POLYTRON® PT 10-35 GT, Kinematica AG, Luzern, Switzerland) with NaF in water (10 mg/mL) (1:3, *w/v*) on ice bath prior to sample preparation for drug analysis. The drug and TG levels in the harvested lymph samples were analysed on the day of collection. The procedure for sample preparation was described in Section 2.2.3. TG levels in lymph fluid were measured by serum TG determination kit (Sigma, Gillingham, UK) with following manufacture's instructions.

2.9. Pharmacokinetic analysis

A Non-compartmental analysis (NCA) was applied to calculate pharmacokinetic parameters derived from plasma concentration-time profiles using Phoenix WinNonlin 6.3 software (Pharsight, Mountain View, CA, USA). The oral bioavailability can subsequently be calculated by comparing respective AUCs, as shown by the following equation:

$$F = \frac{AUC_{oral}}{AUC_{IV}} \times \frac{Dose_{IV}}{Dose_{oral}} \text{ (Eq. 1).}$$

2.10. Statistical analysis

The data are shown as mean ± standard deviation (SD). Statistical analysis between two data sets was performed by two-tailed unpaired *t*-test. One-way ANOVA followed by Dunnett's or Tukey's test was used to compare between three or more data sets. A *p*-value lower than 0.05 was considered to represent a significant difference. Statistical analysis was performed using GraphPad Prism version 7.04 (GraphPad Software, Inc., La Jolla, CA, USA).

3. DEVELOPMENT AND VALIDATION OF A SENSITIVE BIOANALYTICAL HPLC-UV METHOD FOR DETERMINATION OF LOPINAVIR IN RAT AND HUMAN PLASMA [202]

The results described in the Chapter have been published in peer-reviewed literature: Qin, C., Feng, W., Chu, Y., Lee, J., Berton, M., Bettonte, S., Teo, Y., Stocks, M., Fischer, P. and Gershkovich, P. (2020). Development and validation of a cost-effective and sensitive bioanalytical HPLC-UV method for determination of lopinavir in rat and human plasma. *Biomedical Chromatography*, 34 (11) e4934.

3.1. Introduction

Lopinavir (LPV) is an HIV protease inhibitor (PI) co-administered with a low dose of ritonavir (RTV) under the brand Kaletra® (LPV/r) as part of antiretroviral treatment (ART) in people affected by HIV. The combination was approved by the U.S. Food and Drug Administration (FDA) two decades ago [203]. Since 2006, the World Health Organization (WHO) guidelines have consistently recommended LPV/r as one of PIs in second-line regimens [69]. In the latest WHO guidelines (2019), LPV/r is still recommended as the preferred PI therapy for second-line ART regimen, alternative first-line ART regimen in children, and in special circumstances in neonates [70]. Most recently, due to the global outbreak of Severe Acute Respiratory Syndrome Coronavirus 2 (SARS-CoV-2) infection leading to COVID-19 disease, LPV/r is being considered as one of potential candidates undergoing several clinical trials (ChiCTR2000029496, ChiCTR2000029539, NCT04307693, NCT04252885). It has been recently reported that early administration of LPV/r could prevent COVID-19 progression to severe stage [204]. Moreover, Gregoire *et al.,* [205] noted a good safety profile in COVID-19 patients undergoing LPV/r treatment in their studies.

By the end of 2018, an estimated 37.9 million people globally were living with HIV (including 1.7 million children). Moreover, 1.7 million in total were newly infected with HIV (including 0.16 million children) in 2018 alone [206]. However, only US$ 19 billion was available for HIV/AIDS response in low- and middle-income countries (end 2018), US$ 1 billion less than 2017 (US$ 19.9 billion) [206]. The relatively low funding, as well as the stagnation in the rate of new HIV infections in recent years is a challenge for efficient and rapid diagnostics and monitoring for people in resource-limited settings. More than 70% patients from low- to middle-income countries undergoing second line regimens are receiving LPV/r [71]. Therefore, a sensitive bioanalytical method for therapeutic drug monitoring (TDM) of LPV are needed, mostly in developing countries. In order to be relevant for TDM, these methods need to cover the range of clinically relevant plasma concentrations of LPV in HIV-infected individuals undergoing LPV/r regimen [207,208]. In addition, the bitter taste reported with various formulations of LPV/r combination [209], is likely to affect adherence, which increases the need for TDM in HIV-infected children. Moreover, application of the new bioanalytical method for the preclinical studies in rats also allows more convenient preclinical research, and, importantly, inclusion of resource-limited developing countries in the research activities.

To date, a large number of bioanalytical methods was developed for the determination of LPV with other antiretroviral drugs in plasma by means of high-performance liquid chromatography (HPLC) with UV detection [210–216] or tandem mass spectrometry (LC-MS/MS) [217–220]. However, previously reported bioanalytical methods for determination of LPV utilizing HPLC-UV methodology are not sensitive enough when low-volume samples are used [221]. On the other hand, LC-MS/MS methodology does provide sufficient sensitivity, but is too expensive for efficient TDM or preclinical research in resource-limited countries. One published bioanalytical method achieved good sensitivity with lower limit of quantification (LLOQ) of 5 ng/mL using HPLC-UV for determination of LPV [210], while another published method utilized LC-MS/MS to obtain LLOQ as low as 1 ng/mL [218]. However, a relatively high volume of plasma (600 µL and 200 µL, respectively) was needed to achieve these high sensitivities in both methods. The relatively high volume of plasma on the scale of 600 µL is problematic for TDM in children, while the scale of 200 µL is still quite high for pharmacokinetic studies in small laboratory animals, such as rats or mice. Additionally, due to the fact that safe handling of HIV positive biological samples in clinics is a priority, drug stability in heat-inactivated conditions (56°C, 30 mins [222]) has been mostly validated in published methods [214,220,223,224]. As a result, the proposed validation of our bioanalytical method also covers drug stability in heat-inactivated conditions, as well as a full validation recommended by FDA guidelines [225].

Therefore, in this work, a simple, sensitive and low sample volume bioanalytical method for determination of LPV in rat plasma was developed and fully validated using HPLC with ultra-violet (UV) detection. This method was successfully implemented in a pharmacokinetic study following intravenous administration in rats. Moreover, the method has been also fully validated for human plasma to provide an option for clinical research and therapeutic drug monitoring (TDM).

3.2. Experimental design

Plasma sample preparation for HPLC analysis is described in Section 2.2.1, and chromatographic system is described in Section 2.2.5. Plasma pharmacokinetic study following intravenous administration of LPV is described in Section 2.8.3. Formulation of LPV was prepared at concentration of 4 mg/mL. The general scheme flowchart of experimental design is shown in **Figure 3-1**.

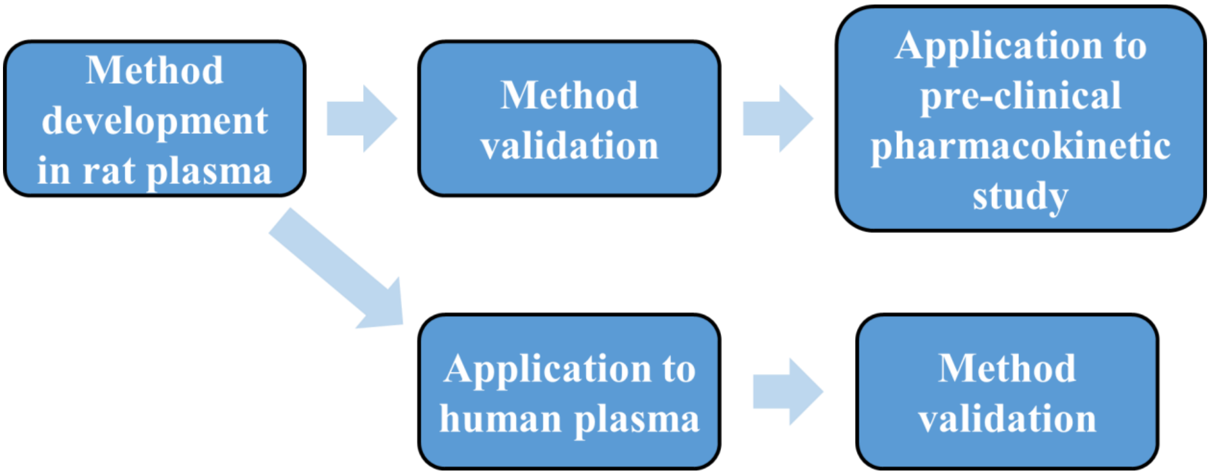

Figure 3- 1. Schematic diagram of workflow for method development and validation in rat plasma, preclinical pharmacokinetic study in rats; application and validation in human plasma.

3.3. Method validation

A full validation of the new method was carried out in accordance with the FDA guidance for Bioanalytical Method Validation [225].

3.3.1. Selectivity

The selectivity of this new HPLC-UV analytical method was assessed by comparing the chromatograms of pooled blank rat plasma samples with the chromatograms of six replicates of plasma samples spiked with LPV at LLOQ standard solution. The selectivity was further assessed in the samples from intravenous (IV) bolus administration of LPV to rats.

3.3.2. Accuracy and Precision

Accuracy was expressed as relative error (RE) and precision as relative standard deviation (RSD). The intra-day accuracy and precision were validated using six-replicate analysis of QC samples (LQC, MQC and HQC) and LLOQ samples on the same day. The inter-day accuracy and precision were also assessed at the same concentrations on 6 separate days. Based on FDA guidelines, the mean value of accuracy should be within ± 15% of the nominal concentration except for the LLOQ which should be within ± 20%. The percentage of precision should not exceed 15% except for the LLOQ in which 20% deviation is accepted [225].

3.3.3. Sensitivity

The LLOQ was defined as the lowest tested concentration of the drug with the RE within ± 20% and RSD ≤ 20%, for both intra-day and inter-day runs [225].

3.3.4. Linearity

Calibration curves (the ratio of LPV peak to IS peak area versus nominal concentration) were fitted by least squares linear regression analysis using a weighted factor (1/X). To validate linearity, correlation coefficient (r^2) should be over 0.99 and accuracy should be within ± 15% (expect for LLOQ in which variability within ± 20% is allowed) [225].

3.3.5. Recovery

Percentage (%) recovery for LPV was determined by comparing the chromatographic peak areas of QC samples following extraction with peak areas obtained from equivalent levels dissolved directly in reconstitution solvent. The recovery of IS was determined in the same way.

3.3.6. Stability

Stability assays were designed to mimic the likely conditions in which samples will be stored, transferred, processed and analysed. QC Samples (LQC, MQC and HQC) were prepared by spiking LPV solution into blank rat plasma. Stability during thermisation (heat-inactivation of HIV) was validated by incubating six replicates of QC samples (LQC, MQC and HQC) at 56°C for 30 min [222]. Freeze-thaw stability was assessed by 3 cycles of freezing the samples at -80°C for 24 h and then thawing at room temperature. Benchtop stability was assessed for 6 h at room temperature. Short term stability was studied for 24 h at -20°C, and long term stability for 4 and 8 weeks at -80°C. Autosampler stability was also assessed by storing six replicates of processed QC samples (LQC, MQC and HQC) at 4°C for 24 hours. Working standard solutions (0.25, 4 and 80 μg/mL) were prepared and stored at room temperature for 6 hours, and then used to prepare six replicates of QC samples (LQC, MQC and HQC) for assessing stock solution stability. Analytes were considered to be stable in plasma when accuracy and precision were within acceptable limits (RE within ± 15% and RSD ≤ 15%, respectively) [225].

3.3.7. Method application and validation in human plasma

The method of sample preparation procedure, chromatography conditions and method validation (excluding long-term stability conditions) of LPV in human plasma were identical to those reported for rat plasma above.

3.4. Results and discussion

3.4.1. Method development

Since LPV is not a highly lipophilic compound (Log P = 1.7, experimental result [226]), n-hexane (non-polar organic solvent) was not efficient in extraction of LPV from plasma (the absolute recovery was zero). Adding 30% ethyl acetate to n-hexane enhanced extraction efficiency dramatically and the mixture of n-hexane–ethyl acetate 7:3 (*v*/*v*) was selected as the optimum extraction solvent. In addition to the extracting solvent composition, the duration of the extraction was also optimized in this assay. It was observed that LPV was extracted very rapidly (within 3 min vortex-mixing) into organic phase during liquid-liquid extraction procedure. Further increase in the duration of the extraction did not improve the recovery. Similar to a previously reported work from our group for bioanalysis of phytocannabinoids, addition of water following plasma protein precipitation before the liquid-liquid extraction improved the extraction efficiency and the chromatography baseline [188]. Cannabidiol was selected as an IS because it had similar extraction procedure and efficiency to LPV in our previous work [188], as well as longer retention time than LPV in chromatography conditions developed in this work.

A simple buffer-free gradient mobile phase, starting from a mixture of acetonitrile–water (50:50, *v*/*v*), gave optimal separation of LPV from background peaks. A higher percentage of acetonitrile was gradually blended in mobile phase to elute IS (**Table 3-1**). Both LPV and IS were monitored at 211 nm, as LPV had the highest UV absorbance and chromatography baseline was clean at LPV retention time at this wavelength.

Table 3- 1. Gradient conditions

Time (min)	***Flow (mL/min)***	***Water (%)***	***Acetonitrile (%)***
0	0.30	50	50
10	0.30	50	50
11	0.30	30	70
19	0.30	30	70
20	0.30	50	50
25	0.30	50	50

3.4.2. Method validation for rat plasma

3.4.2.1. Selectivity

This analytical method showed good selectivity and the peak of LPV was well-separated from endogenous peaks in blank rat plasma (**Figure 3-2 (A)-(C)**), indicating minimum matrix effect and absence of carryover. In addition, this method was applied to evaluate drug concentrations in rat plasma following intravenous administration, and in these samples there was also no interference between the LPV, IS and endogenous peaks (**Figure 3-2 (D)**). Therefore, this method is selective for determination of LPV in rat plasma and suitable for pharmacokinetic experiments in these species.

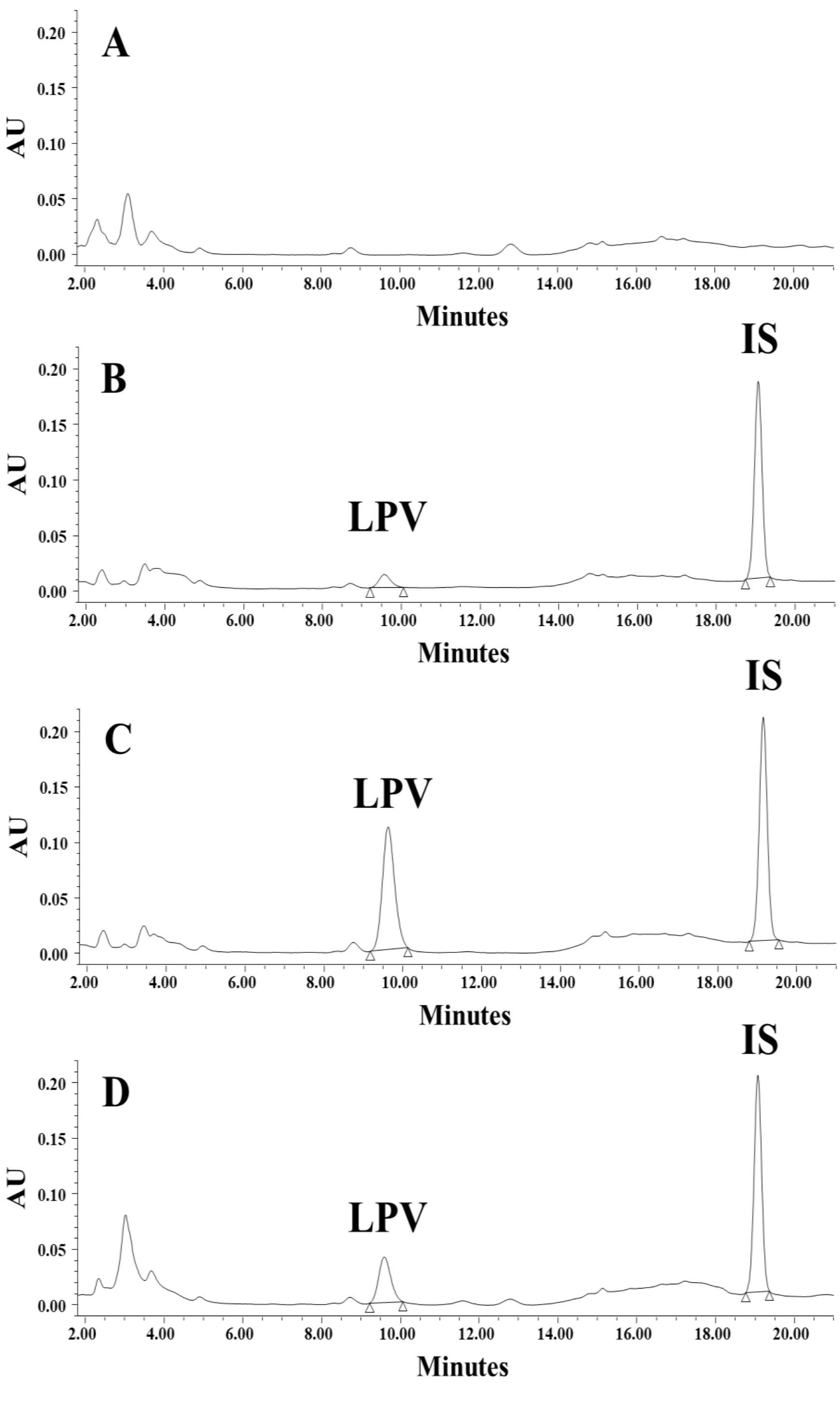

Figure 3- 2. Representative chromatograms of (A) rat plasma blank sample; (B) rat plasma spiked with 1000 ng/mL LPV; and (C) rat plasma spiked with 8000 ng/mL LPV; (D) plasma obtained at 5 minutes following intravenous administration of LPV in rat (4 mg/kg). All chromatograms are observed at λ = 211 nm. LPV, lopinavir; IS, internal standard.

3.4.2.2. Accuracy and precision

Samples were assessed at four different concentrations in 6 replicates to evaluate accuracy (RE) and precision (RSD), respectively. Results for intra- and inter-day validation of LLOQ and QC samples are listed in **Table 3-2**. For accuracy and precision validation, the mean values of all QC samples (LQC, MQC and HQC) were within acceptable range (RE within ± 15% and RSD ≤ 15%). For the LLOQ, RE was within ± 20% and RSD ≤ 20%. These results indicate that this analytical method is suitable for determination of LPV levels in rat plasma in an accurate and precise manner [225].

Table 3- 2. Intra- and inter-day validation results for determination of lopinavir in rat plasma

Nominal concentration levels	***intra-day (n=6)***		***inter-day (n=6)***	
	Accuracy (RE, %)	**Precision (RSD, %)**	**Accuracy (RE, %)**	**Precision (RSD, %)**
LLOQ (10 ng/mL)	5.59	15.80	15.36	2.93
LQC (25 ng/mL)	-7.02	1.64	-2.09	10.90
MQC (400 ng/mL)	-5.67	2.26	-2.91	8.61
HQC (8000 ng/mL)	-1.78	3.69	1.22	5.68

RE, relative error; RSD, relative standard deviation; LLOQ, lower limit of quantification; LQC, low quality control; MQC, medium quality control; HQC, high quality control.

3.4.2.3. Sensitivity and linearity

In this method, 10 ng/mL was determined as LLOQ, since intra- and inter-day accuracy and precision validations for LLOQ samples were within acceptable range (RE within ± 20% and RSD ≤ 20%) (**Table 3-2**). The method was linear for LPV with correlation coefficient (r^2) greater than 0.99 in all calibration curves in the range of 10–10,000 ng/mL, indicating dilution integrity in this range in the conditions of this assay. To note, a low volume of plasma (100 µL) was needed to achieve the LLOQ of 10 ng/mL which makes this assay sufficiently sensitive to perform preclinical pharmacokinetic studies in small laboratory animals or other situations when sample volume is limited. In previously reported studies, some bioanalytical methods achieved better sensitivities (LLOQ less than 10 ng/mL), but required higher volume of plasma and/or more expensive analytic equipment such as LC-MS/MS [210,218].

3.4.2.4. Recovery

Mean absolute recoveries of LPV in LQC, MQC and HQC samples were 88.7 ± 2.1%, 96.5 ± 1.0% and 96.4 ± 2.1%, respectively (mean ± SD, n = 6). The absolute recovery of IS was 70.6 ± 2.5% (mean ± SD, n = 3). The optimised liquid-liquid extraction step contributed to excellent recovery of LPV from rat plasma, thereby achieving good sensitivity of this method.

3.4.2.5. Stability

The results of all stability experiments are shown in **Table 3-3**. All QC samples (LQC, MQC and HQC) were considered to be stable under different realistic storage conditions, with the values of accuracy (RE) and precision (RSD) in the acceptable range (RE within ± 15%, RSD ≤ 15%). Very limited LPV stability data in rat plasma have been reported in previous works and only included freeze-thaw, short-term and autosampler stability experiments [221]. To the best of our knowledge, this is the first report that covers full validation and stability of LPV in rat plasma according to FDA guidelines [225]. Moreover, the stability of LPV in rat plasma was originally validated at heat-inactivated conditions only [222].

Table 3- 3. Stability results of lopinavir in rat plasma under various storage conditions (n=6)

Concentration levels	***Inactivation stability (56°C , 30 min)***		***Benchtop stability (25°C , 6 h)***		***Stock solution stability (25°C , 6 h)***		***Autosampler stability (4°C , 24 h)***		***Short term stability (-20°C , 24 h)***		***Freeze-thaw stability (-80°C , 3 cycles)***		***Long term stability (-80°C , 4 weeks)***		***Long term stability (-80°C , 8 weeks)***	
	RE (%)	**RSD (%)**	**RE (%)**	**RSD (%)**	**RE (%)**	**RSD (%)**	**RE (%)**	**RSD (%)**	**RE (%)**	**RSD (%)**	**RE (%)**	**RSD (%)**	**RE (%)**	**RSD (%)**	**RE (%)**	**RSD (%)**
LQC (25 ng/mL)	3.91	8.02	0.92	10.89	0.23	2.68	6.57	4.19	8.03	4.03	-0.16	3.94	4.61	4.90	12.76	1.68
MQC (400 ng/mL)	-3.89	6.26	1.39	1.65	-5.96	4.20	-11.18	1.34	-8.99	6.07	-0.20	3.94	-2.03	4.00	-9.73	1.35
HQC (8000 ng/mL)	-7.42	6.33	7.42	2.59	-3.22	2.82	-3.23	3.30	-1.29	2.92	-0.94	3.51	5.23	2.88	-0.91	3.38

RE, relative error; RSD, relative standard deviation; LQC, low quality control; MQC, medium quality control; HQC, high quality control.

3.4.3. Pharmacokinetic study in rats

The developed bioanalytical method was applied to a preclinical pharmacokinetic study in rats following single intravenous bolus administration. The individual plasma concentration-time profiles of LPV in three rats are shown in **Figure 3-3**, and mean plasma pharmacokinetic parameters obtained using non-compartmental analysis are shown in **Table 3-4**. Limited number of preclinical pharmacokinetic studies following single intravenous bolus of LPV in rats have been reported [221,227]. The elimination $t_{1/2}$ (0.49 ± 0.01 h) obtained in this study is shorter than the $t_{1/2}$ (0.82 ± 0.03 h) previously reported using HPLC-UV method for the detection of LPV [221]. The lower sensitivity of the previously reported method (LLOQ = 250 ng/mL) limited sampling up to 3 h, which resulted in sampling duration of less than 4 times the elimination $t_{1/2}$. However, to better characterize a pharmacokinetic profile, sampling should preferably be 4–5 times the elimination $t_{1/2}$ [228]. In the current study, a high sensitivity (LLOQ = 10 ng/mL) allows sampling up to 4 h (more than 8 times the elimination $t_{1/2}$), thereby accurately characterizing the pharmacokinetic profile of LPV. Kumar *et al*. reported a significantly longer elimination $t_{1/2}$ (mean value of 2.07 h) compared to other studies [227]. This prolonged elimination $t_{1/2}$ is probably a result of the analytical assay which was using radiolabelled LPV. This trend has been previously observed for other compounds in which radioactivity-based bioanalytical methods were used [229].

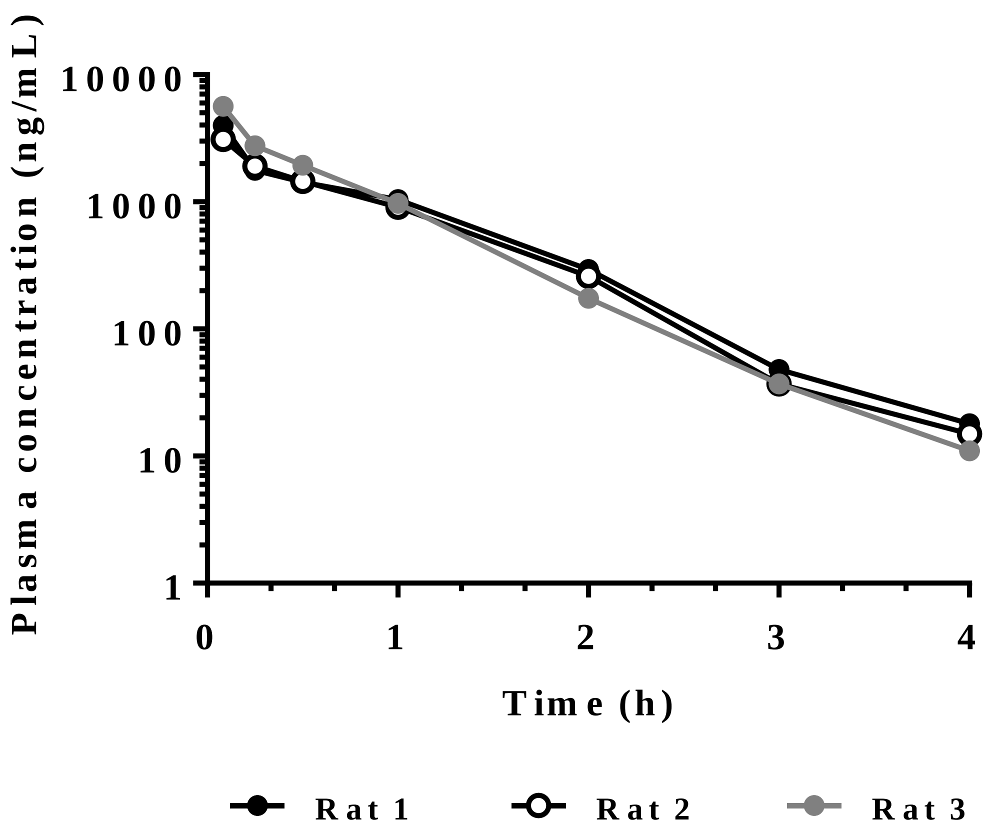

Figure 3- 3. Plasma concentration-time profiles of LPV in rats following intravenous administration at 4 mg/kg (n=3). LPV, lopinavir.

Table 3- 4. Pharmacokinetic parameters of lopinavir following a single i.v. administration of 4 mg/kg to rats (n=3)

Parameters	***Mean***	***SD***
AUC_{inf} (h·ng/mL)	2709	371
$AUC_{0\rightarrow t}$ (h·ng/mL)	2699	372
C_0 (ng/mL)	5992	2033
$t_{1/2}$ (h)	0.49	0.01
V_{ss} (mL/kg)	1053	271
CL (mL/h/kg)	1495	200

AUC_{inf}, area under the curve from time zero to infinity; $AUC_{0\rightarrow t}$, area under the curve from time zero to the last sampling time point; C_0, concentration extrapolated to time zero; $t_{1/2}$, elimination half-life; V_{ss}, volume of distribution at steady state; CL, clearance.

3.4.4. Assessment and validation of the developed bioanalytical method in human plasma for clinical therapeutic drug monitoring (TDM)

Following the development and validation of the bioanalytical method for determination of LPV in rat plasma, the suitability of this method for clinical research and clinical TDM of HIV-infected patients undergoing LPV/r was assessed. A routine TDM plays an important role in ART to assist clinicians in assessing adherence and optimizing the regimens for HIV-infected patients, and therefore to reduce the risks of insufficient therapeutic response, drug resistance or toxicity. This is particularly important in relation to PIs, as the pharmacokinetics of PIs is known to have high inter-individual variability [230–232]. Very high concentrations of LPV can lead to adverse effects such as hyperlipidaemia [233–235] and gastrointestinal disorders [236,237], while concentrations below the therapeutic window would lead to therapeutic failure and drug resistance [237,238]. Moreover, the poor palatability of LPV/r liquid formulations [209] increases the risk of suboptimal antiretroviral efficiency in children due to poor adherence. Therefore, this sensitive bioanalytical method, involving low volume samples of plasma could be useful for monitoring plasma concentrations of LPV in adults and children in both developed and resource-limited countries.

The same calibration curve range (10–10,000 ng/mL) was used in the assessment of the newly developed bioanalytical method for human plasma, since the mean C_{max}, C_{min} and C_{trough} of LPV were reported to be within this range during LPV/r regimen (400/100 mg b.i.d.) in HIV-infected adults [207,208]. The reported mean C_{trough} levels of LPV following LPV/r regimens based on body weight in HIV-infected children were also within this range [239]. Same sample preparation procedure and chromatography conditions used for rat plasma were also applied to human plasma. Good selectivity was observed by comparison of chromatograms between

LPV/RTV spiked samples and blank human plasma samples (**Figure 3-4**). Intra-day and inter-day accuracy (RE) and precision (RSD) were assessed by 6 spiked human plasma samples at four different concentrations (LLOQ and QCs) for LPV (**Table 3-5**). Same sensitivity (LLOQ = 10 ng/mL) and linearity range (r^2 greater than 0.99) as for rat plasma were achieved when the method was applied to human plasma. The extraction recovery of human plasma LQC, MQC and HQC samples were 94.3 ± 4.9%, 99.6 ± 2.2% and 99.5 ± 3.5%, respectively (mean ± SD, n = 6).

Table 3- 5. Intra- and inter-day validation results for determination of lopinavir in human plasma

Nominal concentration levels	***intra-day (n=6)***		***inter-day (n=6)***	
	Accuracy (RE, %)	**Precision (RSD, %)**	**Accuracy (RE, %)**	**Precision (RSD, %)**
LLOQ (10 ng/mL)	5.61	5.60	6.53	10.44
LQC (25 ng/mL)	3.54	4.52	2.11	5.20
MQC (400 ng/mL)	-1.79	4.35	-1.92	2.77
HQC (8000 ng/mL)	-5.57	2.95	2.40	3.56

RE, relative error; RSD, relative standard deviation; LLOQ, lower limit of quantification; LQC, low quality control; MQC, medium quality control; HQC, high quality control.

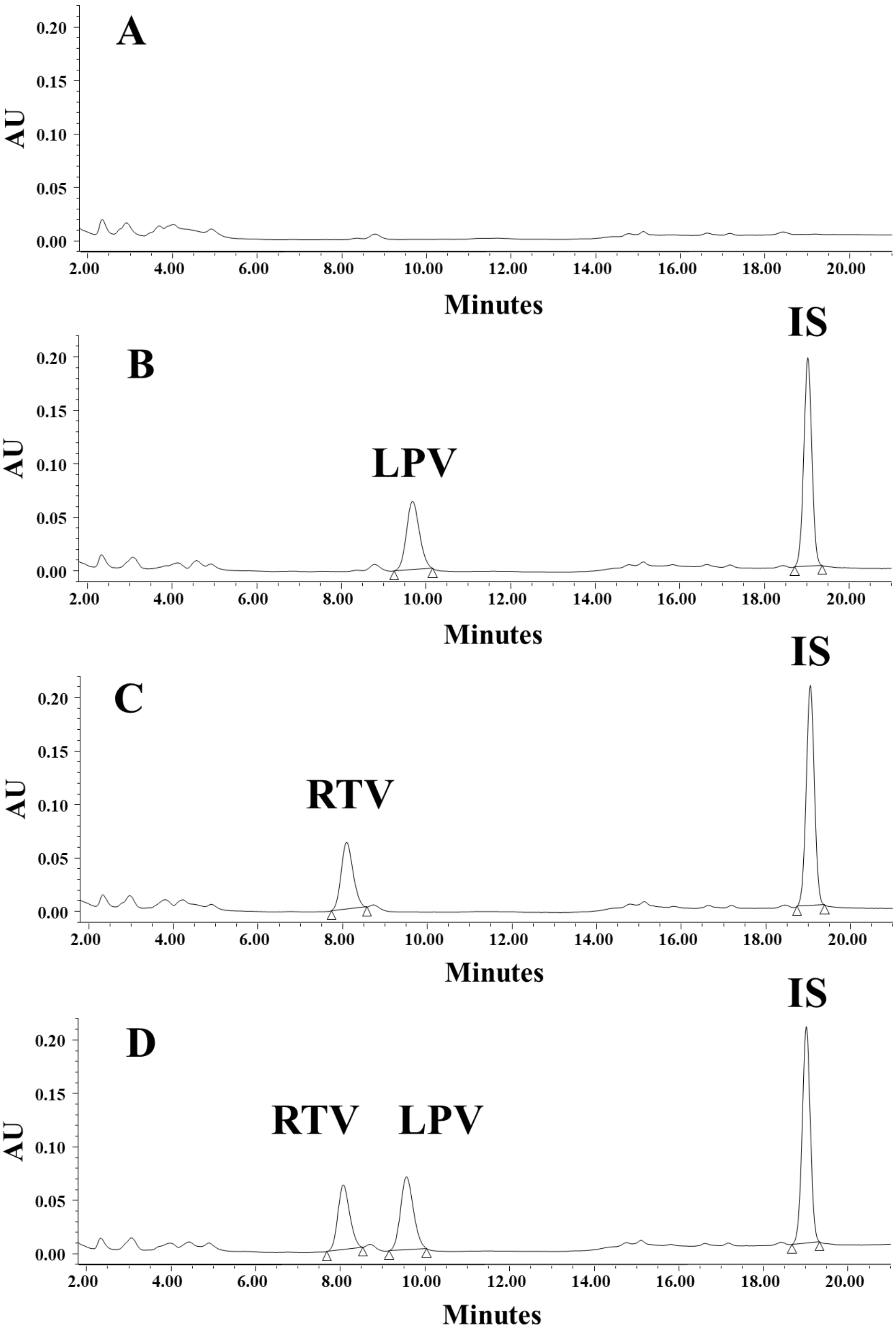

Figure 3- 4. Representative chromatograms of (A) blank human plasma; (B) and (C) human plasma spiked with 5000 ng/mL of LPV and 5000 ng/mL of RTV, respectively; (D) human plasma sample spiked with 5000 ng/mL of LPV and RTV simultaneously. All chromatograms are observed at λ = 211 nm. LPV, lopinavir; RTV, ritonavir; IS, internal standard.

The stability of LPV at 3 concentrations (QCs) in human plasma under different realistic storage conditions is shown in **Table 3-6**. The LPV was stable in human plasma samples under all tested conditions, since the values of RE and RSD are within acceptable range (RE within ± 15%, RSD ≤ 15% [225]). The heat-inactivation stability has demonstrated that the samples are stable during patient plasma HIV inactivation procedure prior to sample preparation. The bench-top stability and stock solution stability show that samples and stock solutions are stable during sample preparation procedure. The processed samples are also stable at 4°C for 24 hours, mimicking the condition in an autosampler. Freeze-thaw stability indicated that samples are stable after undergoing three cycles of freeze and thaw, which should allow TDM even after the samples have been previously used for other tests, such as viral load monitoring. Plasma samples are also stable under short-term storage conditions with the acceptable values of RE and RSD. Therefore, a low plasma volume, good extraction efficiency, high sensitivity and good stability in human plasma at different storage situations make this versatile and robust bioanalytical method suitable for clinical research and clinical TDM of HIV-infected adult and paediatric patients. This new method of determination of LPV in plasma using HPLC-UV detection is less sensitive compared to previously achieved by LC-MS/MS methodology [218,240,241], but requires much lower volume of plasma (100 µL) compared to previously reported HPLC-UV method (600 µL) [210]. Importantly, this method compared to much more expensive LC-MS/MS methodology allows TDM and clinical research activity in resources-limited countries in the developing world.

Table 3- 6. Stability results of lopinavir in human plasma under various storage conditions (n=6)

Concentration levels	***Inactivation stability (56°C , 30 min)***		***Benchtop stability (25°C , 6 h)***		***Stock solution stability (25°C , 6 h)***		***Autosampler stability (4°C , 24 h)***		***Short term stability (-20°C , 24 h)***		***Freeze-thaw stability (-80°C , 3 cycles)***	
	RE (%)	**RSD (%)**	**RE (%)**	**RSD (%)**	**RE (%)**	**RSD (%)**	**RE (%)**	**RSD (%)**	**RE (%)**	**RSD (%)**	**RE (%)**	**RSD (%)**
LQC (25 ng/mL)	-1.69	5.78	-7.72	2.73	-3.71	6.46	7.43	4.87	-10.10	4.39	7.50	4.45
MQC (400 ng/mL)	-2.14	5.28	-3.27	3.12	-5.19	4.21	-7.82	3.76	7.04	3.56	4.28	3.39
HQC (8000 ng/mL)	9.80	3.06	12.27	1.91	2.63	5.59	-2.05	4.64	8.04	4.38	6.29	4.88

RE, relative error; RSD, relative standard deviation; LQC, low quality control; MQC, medium quality control; HQC, high quality control.

3.5. Conclusion

A simple and sensitive HPLV-UV method for the determination of LPV in rat plasma was developed and fully validated. This assay achieved higher sensitivity using lower volume of plasma compared to previously reported HPLC-UV methods. This method will allow preclinical pharmacokinetic and drug delivery studies in rats in the developed and developing countries in a reliable manner. Moreover, the newly developed bioanalytical method was applied and validated for human plasma with similar good selectivity, sensitivity, linearity and stability under different storage conditions. Therefore, this method can be used for clinical research and clinical TDM of HIV-infected and potentially SARS-CoV-2-infected patients undergoing LPV/r treatment in the resource-rich and resource-limited settings.

4. TARGETED DELIVERY OF LOPINAVIR TO HIV RESERVOIRS IN THE MESENTERIC LYMPHATIC SYSTEM BY LIPOPHILIC ESTER PRODRUG APPROACH [242]

The results described in this Chapter have been accepted by the *Journal of Controlled release*: Qin, C., Chu, Y., Feng, W., Fromont, C., He, S., Ali, J., Lee, J., Zgair, A., Berton, M., Bettonte, S., Liu, R., Yang, L., Monmaturapoj, T., Medrano-Padial, C., Ugalde, A., Vetrugno, D., Ee, S.Y., Sheriston, C., Wu, Y., Stocks, M., Fischer, P. and Gershkovich, P. (2020). Targeted delivery of lopinavir to HIV reservoirs in the mesenteric lymphatic system by lipophilic ester prodrug approach. Online ahead of print.

4.1. Introduction

The combined antiretroviral therapy (cART) can efficiently reduce viral load and keep it undetectable in the blood of HIV-infected patients for the duration of treatment [243,244]. However, as soon as the therapy is interrupted, rebound viremia can occur within a few weeks [44,245,246]. This is partially due to the persistence of HIV-1 in anatomical and cellular viral reservoirs [247], which are established during early primary infection stage [248–250] and are extremely stable even during fully suppressive cART [52,251–254]. The gut-associated lymphoid tissue (GALT), including mesenteric lymph and mesenteric lymph nodes (MLNs), harbors a large proportion of body's lymphocytes [104]. During primary HIV infection, severe CD4+ T cells depletion in GALT can impair effective immune response against HIV-1, thereby contributing to poor clinical outcomes [30,34]. Initiation of early cART can partially preserve and reconstitute immune function [255], but does not prevent GALT eventually becoming one of the most important and persistent anatomical reservoirs of HIV [52–55].

Unfortunately, presently known antiretroviral drugs poorly permeate into lymphoid tissues and particularly low levels can be detected in MLNs, resulting in suboptimal concentrations in these important viral reservoirs [52,54,159,253]. In the past, almost all attempts to enhance the delivery of antiretroviral agents to lymph nodes (LNs) involved a general idea of subcutaneous or intramuscular injection of different types of nano-sized drug delivery systems [159–162]. The rationale for this common approach is that due to the nano-scale size of these drug delivery systems, nanoparticles are taken up preferentially by the lymphatics rather than permeate into blood capillaries. However, the main drawback of this common approach is that due to the pattern of anatomical drainage of lymph from subcutaneous space or muscle, the drug could be delivered only to peripheral LNs. Moreover, only those limited individual peripheral LNs collecting the lymph fluid directly from the local region of injection site could be reached using this approach.

In this work, a physiological pathway of absorption of dietary lipids *via* intestinal lymphatic transport was utilized for delivery of antiretroviral drug lopinavir (LPV) to the mesenteric lymphatic system. It has been previously shown in multiple studies that highly lipophilic compounds with appropriate physicochemical characteristics (Log $D_{7.4}$ > 5, long-chain triglyceride (LCT) solubility > 50 mg/mL) have substantial intestinal lymphatic transport when administered orally with lipids [256,257]. Highly lipophilic compounds can associate with chylomicrons (CMs), large lipoproteins which are assembled in the enterocytes in the presence of long-chain triglyceride or long-chain fatty acids. CMs are too large to penetrate into blood capillaries, and therefore are taken up preferentially by lymph lacteals together with the associated highly lipophilic drugs. This mechanism promotes the absorption of drugs into the mesenteric lymphatic system before they reach the systemic circulation (**Figure 4-1**) [104]. A linear correlation between the *in vivo* lymphatic absorption of lipophilic compounds and the degree of drug-CMs association *in vitro* has been previously reported [138]. Therefore, the degree of drug-CMs association could be used as a useful tool to select potential candidates which are likely to have intestinal lymphatic transport and therefore could be delivered to the mesenteric lymph and MLNs in an efficient and selective manner.

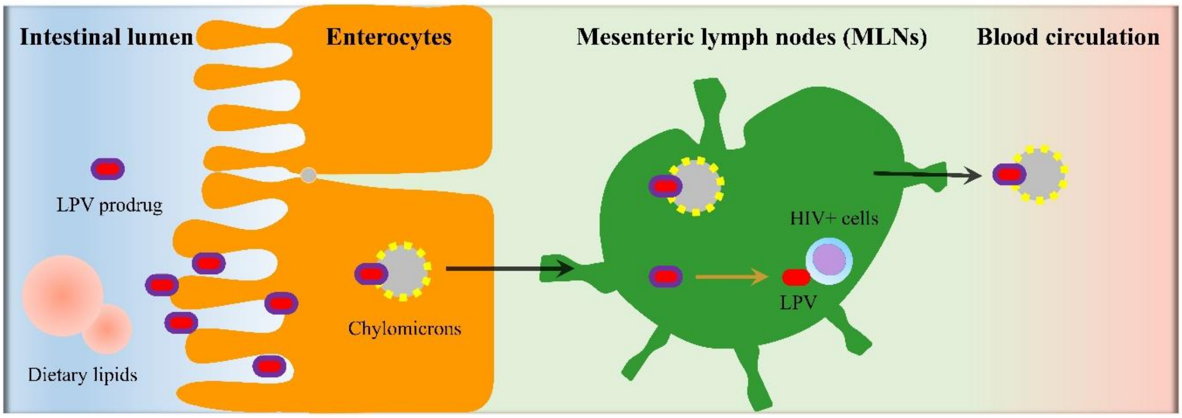

Figure 4- 1. Schematic diagram of delivery of LPV to the mesenteric lymphatic system. Lipophilic prodrugs of LPV have high affinity to chylomicrons (CMs) in the enterocytes, leading to intestinal lymphatic transport and high local concentrations in mesenteric lymph and MLNs. LPV released from the prodrugs by enzymatic cleavage of the ester bond exerts its pharmacological effect within the mesenteric lymph and MLNs.

Previous studies from our and other groups showed efficient delivery of highly lipophilic compounds to the mesenteric lymph and MLNs following oral administration with lipid-based formulations [177,191,256,257]. For example, it was found that the levels of cannabidiol (CBD) and Δ9-tetrahydrocannabinol (THC) in the mesenteric lymph were as high as 250- and 100-fold higher in lymph than in plasma, respectively, when co-administered with long-chain triglyceride formulation [191]. Moreover, it was also found that when the active drug does not have sufficient lipophilicity for the intestinal lymphatic transport, a lipophilic prodrug approach can still achieve efficient delivery of the drug to the mesenteric lymphatic system [177]. Recently, a number of clinically used protease inhibitors (PIs) were screened *in vitro* for their potential for intestinal lymphatic transport in unmodified form. Only tipranavir (TPV) showed some experimental association with CMs. However, *in vivo* results showed that the distribution of chemically unmodified TPV to the mesenteric lymph was moderate and to MLNs was minimal [258].

LPV has been consistently recommended as the preferred PI in the second-line cART regimens [70]. However, similar to most other PIs, LPV does not possess sufficient lipophilicity for delivery to mesenteric lymph and MLNs without chemical modification [258]. Therefore, the aim of this study was to design and synthesize lipophilic ester prodrugs that possess the necessary physicochemical properties for improved association with CMs and lead to efficient delivery of LPV to HIV reservoirs within the mesenteric lymph and MLNs. The efficiency of bioconversion of inactive prodrugs to active agent (LPV) have been evaluated in physiologically relevant media. Subsequently, candidates which possess moderate to high affinity to CMs, good stability in conditions mimicking intestinal tract and rapid release to LPV in conditions mimicking the lymphatic system have been selected for *in vivo* assessment. Finally, the efficiency of the novel prodrug approach in targeting LPV to viral reservoirs in mesenteric lymphatic system has been assessed *in vivo* in rats.

4.2. Experimental design

The procedure of chemical synthesis is described in Section 2.3. *In vitro* and *ex vivo* chylomicrons association, prodrug conversion and antiretroviral activity assays were performed as described in Sections 2.4., 2.5. and 2.7., respectively. Long chain triglycerides (LCTs) solubility measurement is described in Section 2.6. Pharmacokinetic studies are described in Section 2.8.3. Formulations of LPV, prodrugs **1** and **7** were prepared at concentrations equivalent to 4, 9, and 2 mg/mL of LPV, respectively. Biodistribution studies following oral administration are described in Section 2.8.4. Procedures of sample preparation followed the methods described in Section 2.2. The general scheme flowchart of experimental design is shown in **Figure 4-2**.

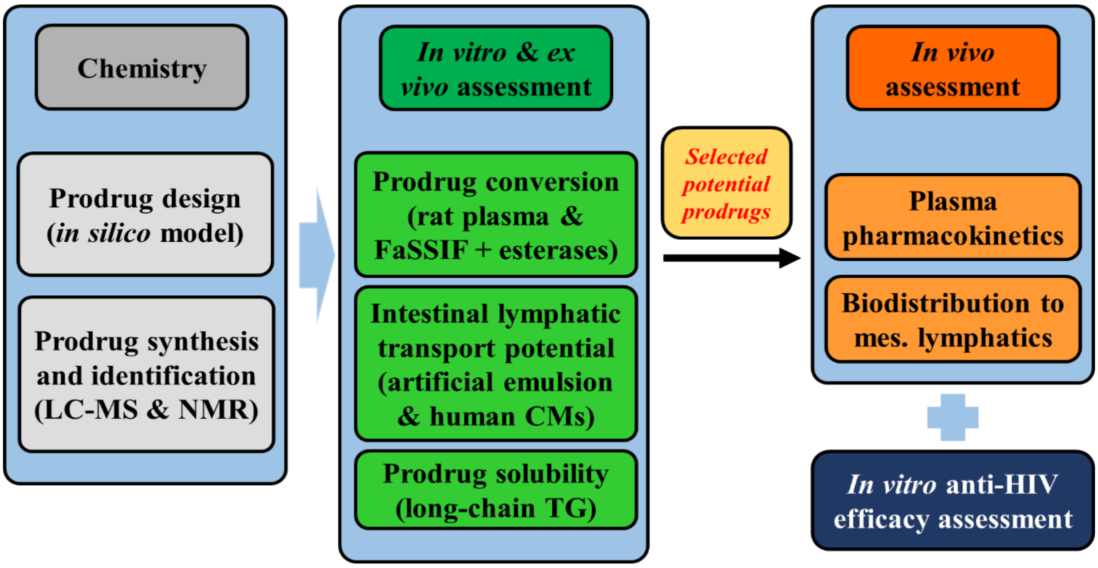

Figure 4- 2. A workflow of experimental design for lipophilic prodrug approach to target mesenteric lymphatic system. FaSSIF, fast state simulated intestinal fluid; CMs, chylomicrons; GALTs, gut-associated lymphoid tissues; TG, triglyceride.

4.3. Results

4.3.1. Design of LPV prodrugs

Prodrugs **1-5** were simple alkyl esters. For prodrug **6**, the enzymatic recognition site (acetamide) was designed to be further away from the main scaffold for better access and diketopiperazine cyclisation to liberate the drug LPV [259]. For prodrug **7**, an electronegative heteroatom (oxygen) was introduced in the β position relative to the acyl group [260]. Due to those specific features, compounds **6** and **7** will be referred in this Chapter as activated ester prodrugs. Chemical structures of all synthesised prodrugs are shown in **Figure 4-3**.

4.3.2. Prodrug synthesis and structural characterisation

All designed ester prodrugs were synthesised and purified. Calculated physicochemical parameters used for *in-silico* prediction of association with CMs, as well as predicted values of affinity to CMs and water solubility are shown in **Table 4-1**. The schematic presentation of the chemical synthetic route and the chemical structures of prodrugs are shown in **Figure 4-3**. The characterisation of individual molecules is available in **Appendix 1**. Prodrugs **1-5** were alkyl esters with a short to medium chain fatty acid. The activated ester prodrugs **6** and **7** were then designed and synthesised following the assessment of prodrugs **1-5**.

Table 4- 1. Physicochemical parameters of LPV and its prodrugs used for *in-silico* prediction of association with CMs, as well as predicted values of affinity to CMs and water solubility.

Compounds	**Log $D_{7.4}$**	**Log P - Log $D_{7.4}$**	**PSA**	**H-acceptors**	**FRB**	**Density (g/cm^3)**	**Molar volume (cm^3)**	**H-donors**	**Predicted association (%) with chylomicrons**	**water solubility (μg/mL)**
LPV	5.88	0.38	120	9	15	1.163	540.4	4	54.6	2.1
1	6.82	1.26	126.07	10	19	1.141	612.4	3	69.6	2.9
2	8.96	0.19	126.07	10	21	1.126	645.4	3	97.4	0.007
3	9.83	0.38	126.07	10	23	1.112	678.4	3	99.2	0.00049
4	10.77	0.5	126.07	10	25	1.1	711.4	3	99.8	0.00017
5	11.54	0.79	126.07	10	27	1.089	744.5	3	99.9	0.000027
6	4.84	0.74	184.27	14	21	1.194	657.3	5	16.7	18
7	7.61	0.84	135.3	11	22	1.139	651.8	3	88.5	0.069

Physicochemical parameter values were obtained using ACD I-Lab. CMs, chylomicrons; PSA, polar surface area; FRB, freely rotatable bonds; LPV, lopinavir

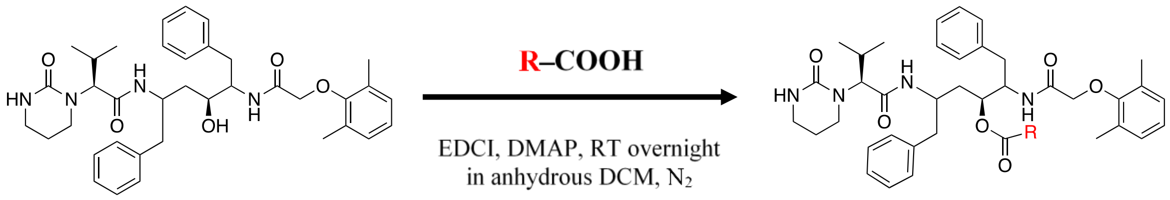

Lopinavir (LPV) **Ester prodrugs**

Alkyl esters

- **1**: **R** = $CH_3(CH_2)_2$
- **2**: **R** = $CH_3(CH_2)_4$
- **3**: **R** = $CH_3(CH_2)_6$
- **4**: **R** = $CH_3(CH_2)_8$
- **5**: **R** = $CH_3(CH_2)_{10}$

Activated esters

- **6**: **R** = Ac-Gly-NH-CH_2
- **7**: **R** = $CH_3(CH_2)_3O(CH_2)$

Figure 4- 3. Chemical structures of LPV and its prodrugs. Prodrugs **1-5** are short to medium chain fatty acid alkyl esters; Prodrugs **6** and **7** are activated esters which should promote more rapid release of LPV in the lymphatic system. EDCI, 1-ethyl-3-(3-dimethylaminopropyl) carbodiimide; DMAP, 4-dimethylaminopyridine; DCM, dichloromethane; RT; room temperature.

4.3.3. Uptake of LPV and its prodrugs by CMs

The association of LPV and prodrugs **1-7** with artificial and natural CMs is shown in **Figure 4-4 (A)**. There was no uptake of unmodified LPV and prodrug **6** by CMs. Prodrugs **1-5** and **7** showed moderate to high affinity to CMs, indicating substantial potential for delivery of these prodrugs to the mesenteric lymphatic system following oral administration with lipid-based formulation. As shown in **Figure 4-3**, the leaving groups of prodrugs **1-4** are short (4 carbons) to medium (10 carbons) chain fatty acids. The longer the fatty acid chain, the higher was the affinity to CMs for prodrugs **1-4**. However, further increase in the lipophilicity and molecular weight by addition of the C12 chain fatty acid (prodrug **5**) resulted in reduction in affinity to

CMs, suggesting that there is a defined lipophilicity and molecular weight range which leads to optimal association with CMs.

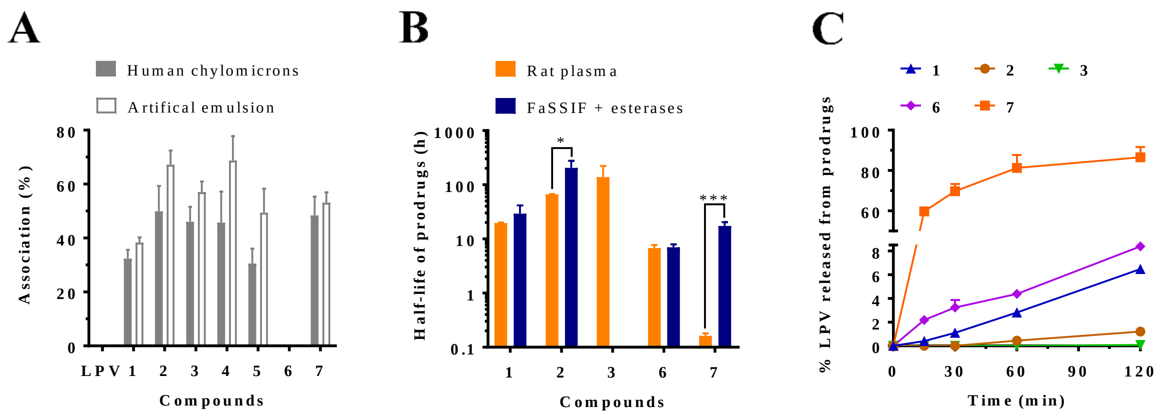

Figure 4- 4. ***In vitro*** **and** ***ex vivo*** **assessment for LPV and its prodrugs.** (**A**) The association (%) of LPV and its prodrugs with human chylomicrons and artificial emulsion (Intralipid®), representing their potential for the delivery to the mesenteric lymphatic system (n = 5). The final concentration of each tested compound in incubation media was 1.75 µM [138]; (**B**) The degradation half-lives of the respective prodrugs in fasted state simulated intestinal fluid (FaSSIF) with added esterases (20 IU/mL) and in rat plasma, representing the stability of prodrugs in the intestinal tract and lymphatic system, respectively (n = 3). Two-tailed unpaired *t*-test was used for statistical analysis, *, $p < 0.05$; ***, $p < 0.001$. (**C**) The relative percentage of released active drug LPV from its corresponding prodrugs in rat plasma (n = 3). Data are expressed as mean ± SD.

4.3.4. *In vitro* and *ex vivo* biotransformation of prodrugs

In this study, the stability of prodrugs and release of the active drug LPV were conducted in rat plasma and fasted state simulated intestinal fluid with added esterase activity (FaSSIF, representing intestinal tract environment). Plasma contains similar composition and levels of enzymes to lymph fluid in many species (including humans and rats) [195,196]. Therefore, rat plasma was chosen as an acceptable surrogate to represent lymph fluid in these studies. Similar approach was implemented in previous work by us [177] and other groups [171,261].

The degradation half-lives of the respective prodrugs in both matrixes are shown in **Figure 4-4 (B)**. The degradation half-lives of prodrug **3** in FaSSIF, as well as prodrugs **4** and **5** in both matrixes could not be calculated reliably due to their extremely high stabilities. Alkyl ester prodrug **1** showed efficient release of LPV in plasma compared to prodrugs **2** and **3** (**Figure 4-4 (C)**). Activated ester prodrugs **6** and **7** were substantially less stable in plasma than alkyl ester prodrugs. In particular, prodrug **7** was relatively stable in FaSSIF (half-life: 17.3 ± 3.0 h) but rapidly converted (half-life: 0.16 ± 0.02 h) to LPV in plasma (**Figure 4-4 (B)** and **(C)**). This is in line with previous literature suggesting that insertion of a heteroatom in the 3rd position (β position) of acyl moiety in the carboxyl esters can enhance plasma and lymph carboxylesterases (CEs) sensitivity [260]. Based on combined CMs association data, plasma and intestinal stability assessments, prodrugs **1** and **7** were selected for subsequent antiretroviral activity and *in vivo* pharmacokinetics and biodistribution studies.

4.3.5. Antiretroviral activities of LPV and selected prodrugs

The 50% inhibition concentration (IC_{50}) of LPV and selected prodrugs against HIV-1 (NL4-3) were derived from released GFP signals where the cell lines responded to infectious HIV-1 stimuli (**Figure 4-6**). The IC_{50} of both prodrugs increased after chemical modification, compared to that of unmodified LPV (**Figure 4-5 (A)**). This, combined with the data of LPV release from prodrugs in cell culture media (**Figure 4-5 (B)** and **(C)**), suggests that efficient release of active drug from prodrugs is necessary for pharmacological effect of LPV to take place in the lymphatic system.

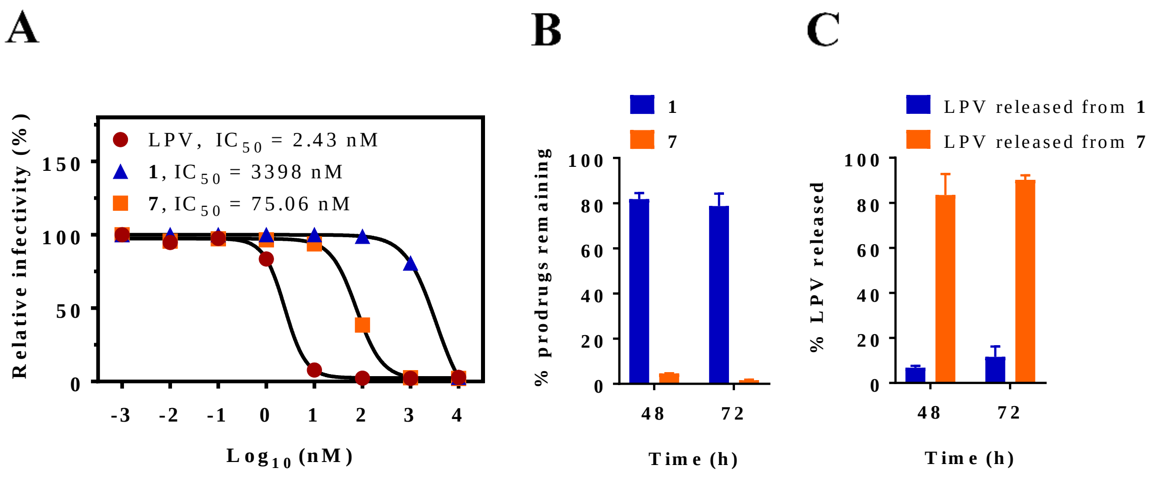

Figure 4- 5. Assessment of the antiretroviral efficacy of LPV and selected prodrugs. (**A**) *In vitro* anti-HIV-1 activity of LPV and its prodrugs following 72 h incubation. Inhibition curves and IC_{50} were generated from plotting relative infectivity (%) against drug concentrations using GraphPad Prism version 7.04; (**B**) The relative percentage of prodrugs remaining; (**C**) the relative percentage of released LPV from its corresponding prodrugs in cell culture media at 48 and 72 h. Data are shown as mean ± SD, n = 3.

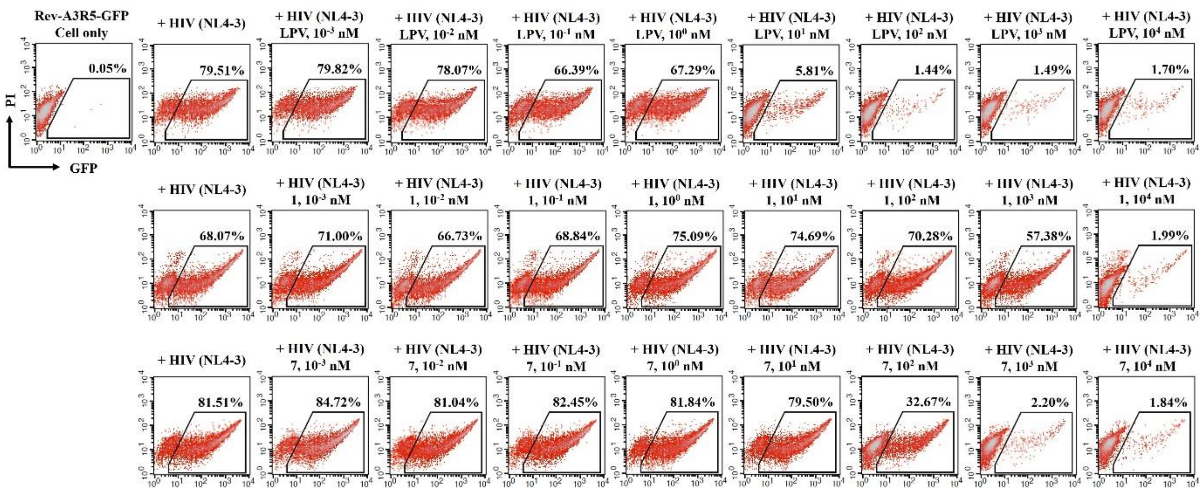

Figure 4- 6. HIV-1 (NL4-3) infectivity assay was performed using Rev-A3R5-GFP cell line after drug (10^{-3}–10^{4} nM) treatment. The percentage of GFP+ cells was measured by flow cytometry at 72 h post infection. PI, Propidium iodide; GFP, Green fluorescent protein.

4.3.6. Long-chain triglyceride solubility of LPV and selected prodrugs

Triglyceride (TG) solubility was tested for LPV and prodrugs selected for *in vivo* studies. The TG solubility for LPV and prodrug **7** were 1.8 ± 0.1 and 24.2 ± 1.4 mg/mL, respectively (mean ± SD, n = 3). Prodrug **1** solubility was above 50 mg/mL (n = 3).

4.3.7. Plasma pharmacokinetics of LPV and selected prodrugs

`

The *in vivo* plasma pharmacokinetic profiles of LPV and its prodrugs were obtained following intravenous and oral (in lipid-free and lipid-based formulation) administrations in rats (**Figure 4-7**). The pharmacokinetic parameters derived from these plasma concentration-time profiles are shown in **Table 4-2** and **Table 4-3**. A significant difference between half-lives of LPV was observed in oral lipid-based group versus intravenous or oral lipid-free group (**Figure 4-7 (A)** and **(B)**; **Table 4-2**), suggesting flip-flop kinetics following oral administration in lipidic formulation, most probably due to delayed gastric emptying [262]. The oral bioavailability values of LPV were not significantly different between oral administrations of LPV in lipid-free and lipid-based groups (**Table 4-1**).

A long elimination half-life of prodrug **1**, as well as relatively low levels of released LPV following single intravenous bolus administration of prodrug **1** have been observed in plasma (**Figure 4-7 (C)** and **Table 4-3**). The very long circulation time of prodrug **1** was also observed in plasma up to 3 days when dosed orally, indicating there could be a re-distribution of this lipophilic prodrug between plasma and deep tissue compartments. Importantly, in parallel with prolonged systemic exposure to prodrug **1**, a continuous release of LPV was observed in plasma (**Figure 4-7 (D)**). Oral administration of short alkyl ester prodrug **1** resulted in relatively high bioavailability of unchanged prodrug (**Table 4-3**). However, the absolute bioavailability of released LPV was lower than following administration of unmodified LPV (**Table 4-2**), most probably due to slow release of LPV from the prodrug.

On the other hand, in case of activated ester prodrug **7**, the elimination half-life of prodrug in systemic circulation was extremely short following single intravenous bolus administration (**Figure 4-7 (E)** and **Table 4-3**). When prodrug **7** was orally administered with lipids, only the released LPV could be detected in systemic blood circulation (**Figure 4-7 (F)**), suggesting that the ester bond of prodrug **7** was rapidly hydrolyzed, and most probably while still in the lymphatic system. This is in agreement with the rapid release of active drug in plasma *ex vivo* (**Figure 4-4 (C)**). The oral bioavailability of released LPV following oral administration of prodrug **7** was nearly 2-fold higher than following administration of unmodified LPV in lipid-free formulation or with lipids (**Table 4-2**).

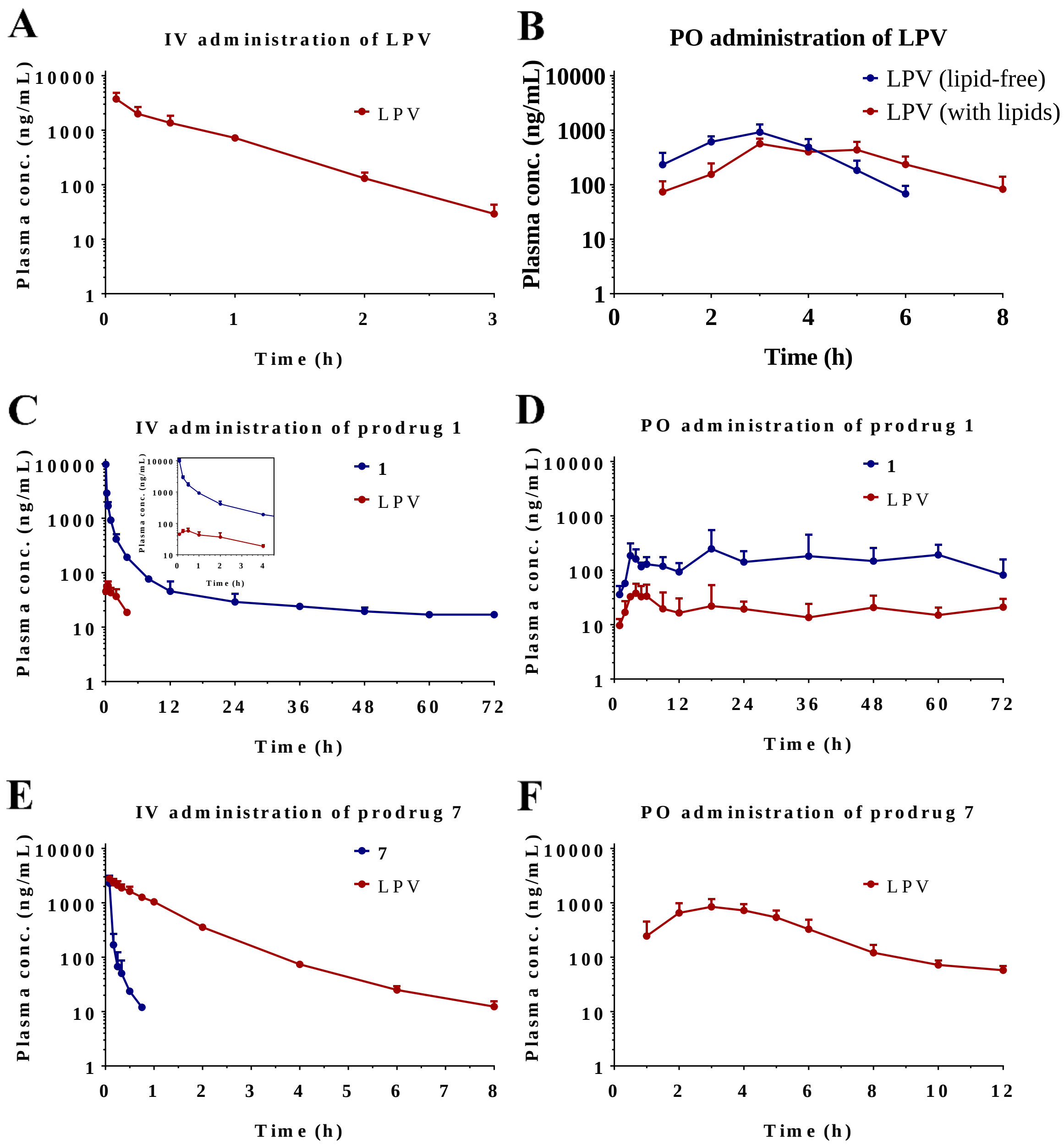

Figure 4- 7. Plasma pharmacokinetic profiles of LPV and selected prodrugs in rats. Plasma concentration-time curves following: (**A**) intravenous bolus administration of LPV (4 mg/kg, n = 4); (**B**) oral administration of LPV in lipid-free formulation and with lipids (20 mg/kg, n = 4); (**C**) intravenous administration of prodrug **1** (10 mg/kg, n = 3); (**D**) oral administration of prodrug **1** in lipid-based formulation (equivalent to 20 mg/kg of LPV, n = 7); (**E**) intravenous administration of prodrug **7** (equivalent to 2 mg/kg of LPV, n = 3); (**F**) oral administration of prodrug **7** in lipid-based formulation (equivalent to 20 mg/kg of LPV, n = 6). Data are expressed as mean ± SD.

Table 4- 2. Plasma pharmacokinetic (PK) parameters of LPV following administration of LPV and its prodrugs to rats. LPV (4 mg/kg), prodrug **1** (10 mg/kg) and prodrug **7** (2.37 mg/kg) following intravenous bolus administration; LPV (20 mg/kg) and its prodrugs (equivalent to 20 mg/kg of LPV) following oral administration in rats (mean ± SD).

	PK parameters of LPV following administration of LPV			**PK parameters of LPV following administration of prodrug 1**		**PK parameters of LPV following administration of prodrug 7**	
Route of administration	***i.v.* (n = 4)**	***p.o.* (lipid-free, n = 4)**	***p.o.* (with lipids, n = 4)[a]**	***i.v.* (n = 3)**	***p.o.* (in lipids, n = 7)**	***i.v.* (n = 3)**	***p.o.* (in lipids, n = 6)[b]**
AUC_{inf} (h·ng/mL)	2176 ± 403	2483 ± 649	2231 ± 396	232 ± 44	-	2913 ± 261	4100 ± 731
$AUC_{0\rightarrow t}$ (h·ng/mL)	2157 ± 407	2419 ± 676	2031 ± 375	144 ± 23	1163 ± 677	2884 ± 253	3868 ± 714
C_0 or C_{max} (ng/mL)	5171 ± 1796	920 ± 360	591 ± 112	63 ± 7	50 ± 26	3421 ± 385	927 ± 181
t_{max} (h)	-	3.0 ± 0.0	3.5 ± 1.0	0.3 ± 0.1	4.3 ± 1.0	-	3.3 ± 1.0
$t_{1/2}$ (h)	0.4 ± 0.1	0.8 ± 0.2	1.5 ± 0.6**	3.1 ± 2.0	96.6 ± 72.4	1.6 ± 0.3	2.8 ± 0.6
V_{ss} (L/kg)	1.18 ± 0.41	-	-	-	-	-	-
CL (L/h/kg)	1.89 ± 0.36	-	-	-	-	-	-
F_{oral} (%)	-	22.8 ± 6.0[c]	20.5 ± 3.6[c]	-	10.8 ± 6.3[d]	-	37.3 ± 6.7[c] **

AUC_{inf}, area under the curve from time zero to infinity; $AUC_{0\rightarrow t}$, area under the curve from time zero to the last sampling time point; C_0, concentration extrapolated to time zero; C_{max}, maximum observed concentration; t_{max}, time to reach peak concentration; $t_{1/2}$, half-life; V_{ss}, volume of distribution at steady state; CL, clearance; F_{oral}, oral bioavailability.

[a] One-way ANOVA followed by Dunnett's test was used for statistical analysis, **, $p < 0.01$ compared to $t_{1/2}$ obtained following *i.v.* administration of LPV.

[b] One-way ANOVA followed by Tukey's test was used for statistical analysis, **, $p < 0.01$ compared to F_{oral} (%) obtained following *p.o.* administration of LPV in lipid-free formulation and with lipids.

[c] Calculated based on the AUC_{inf}.

[d] Calculated based on the $AUC_{0\rightarrow t}$.

Table 4- 3. Plasma pharmacokinetic (PK) parameters of prodrugs **1** and **7** following administration of LPV prodrugs to rats (mean ± SD).

	PK parameters of prodrug 1 following administration of prodrug 1		**PK parameters of prodrug 7 following administration of prodrug 7**	
Route of administration	***i.v.* (n = 3)**	***p.o.* (in lipids, n = 7)**	***i.v.* (n = 3)**	***p.o.* (in lipids, n = 6)**
AUC_{inf} (h·ng/mL)	8210 ± 407	-	1061 ± 290	-
$AUC_{0\rightarrow t}$ (h·ng/mL)	6631 ± 443	10208 ± 4077	1056 ± 292	-
C_0 or C_{max} (ng/mL)	17857 ± 2680	220 ± 110	33701 ± 9384	-
t_{max} (h)	-	3.6 ± 0.8	-	-
$t_{1/2}$ (h)	64.5 ± 1.3	-	0.3 ± 0.1	-
V_{ss} (L/kg)	48.09 ± 5.69	-	0.10 ± 0.04	-
CL (L/h/kg)	1.22 ± 0.06	-	2.34 ± 0.61	-
F_{oral} (%)[a]	-	69.3 ± 27.7	-	-

AUC_{inf}, area under the curve from time zero to infinity; $AUC_{0\rightarrow t}$, area under the curve from time zero to the last sampling time point; C_0, concentration extrapolated to time zero; C_{max}, maximum observed concentration; t_{max}, time to reach peak concentration; $t_{1/2}$, half-life; V_{ss}, volume of distribution at steady state; CL, clearance; F_{oral}, oral bioavailability.

[a] Calculated based on the $AUC_{0\rightarrow t}$.

4.3.8. Biodistribution of LPV and selected prodrugs

For the assessment of drug distribution to the mesenteric lymph and MLNs following oral administration, t_{max} observed in plasma during pharmacokinetic studies and 1 h before t_{max} (t_{max-1}) were considered as the two important sampling time points. As previously reported [177,191], the levels of drugs in mesenteric lymphatic system are usually higher at t_{max-1}, compared to t_{max}. In addition to the mesenteric lymph and MLNs, other tissues representing important HIV reservoirs were harvested and analysed for prodrugs and LPV concentrations at the same time points, as well as following the completion of the pharmacokinetic studies (**Figure 4-8**). The concentrations of LPV were below the limit of detection in both mesenteric lymph and MLNs following administration of unmodified LPV, even in presence of lipids (**Figure 4-8 (A)**). However, high TG levels were observed in mesenteric lymph fluid (**Figure 4-10**). This indicates that despite the fact that lipids were efficiently absorbed, unmodified LPV could not be delivered to the mesenteric lymphatic system even when co-administered with lymphotropic lipids.

On the other hand, oral administration of prodrug **1** in lipid-based formulation resulted in high levels of the prodrug in the mesenteric lymphatic system (**Figure 4-8 (B)** and (**C)**). The concentrations of prodrug **1** were 52- and 55-fold higher in mesenteric lymph and MLNs, respectively, compared to plasma at t_{max-1} (**Figure 4-8 (B)**), whereas relatively low levels of released LPV were observed (**Figure 4-8 (C)**). Although the concentrations of prodrug **1** were substantially higher in mesenteric lymph and MLNs compared to plasma, slow release of active drug in lymphatic system seems to be the limitation of simple alkyl ester prodrug approach.

Following oral administration of activated ester prodrug **7** in lipid-based formulation, high concentrations of the prodrug were observed in mesenteric lymph and MLNs (**Figure 4-8 (D)**), which is in line with its high affinity to CMs (approximately 50%) (**Figure 4-4 (A)**). Importantly, administration of prodrug **7**, featuring an oxygen in the β position relative to the acyl group, led to an impressive improvement of delivery of active LPV to the mesenteric lymphatic system. The levels of LPV in mesenteric lymph and MLNs following oral administration of prodrug **7** were 10.3- and 6.8-fold higher, respectively, compared to administration of prodrug **1** (**Figure 4-9 (A)** and **(B)**). Importantly, the levels of LPV were above the PA-IC_{90} (140 ng/mL) in both lymph fluid and MLNs for both prodrugs. The maximum levels of LPV in mesenteric lymph were 1.6- and 16.9-fold higher than PA-IC_{90} of LPV for HIV-1 (140 ng/mL) following oral administration of simple alkyl ester prodrug and activated ester prodrug, respectively. The concentrations of LPV in MLNs were 1.1- and 7.2-fold higher than PA-IC_{90} following administration of simple alkyl ester prodrug and activated ester prodrug, respectively. Moreover, substantial levels of released LPV were observed in MLNs even at 12 h following oral administration of prodrug **7** (**Figure 4-8 (E)**). Therefore, this approach not only leads to the delivery of the prodrug to the mesenteric lymphatic system, but also to efficient release of the active drug LPV at the site of action within this viral reservoir.

It should be noted that high levels of LPV and prodrugs could be also detected in liver following oral administrations of LPV and prodrugs (**Figure 4-8**). The concentrations of prodrug **1** (but not prodrug **7**) were detectable in spleen (**Figure 4-8 (B)**), but no LPV could be detected in this tissue (**Figure 4-8 (C)**) after oral administration of prodrug **1**. Interestingly, the levels of LPV could be observed in spleen at t_{max} after administration of prodrug **7** (**Figure 4-8 (E)**), probably due to improved systemic exposure to LPV (**Figure 4-6 (F)** and **Table 4-2**). The drug levels in other harvested tissues representing viral reservoirs (such as brain and testes) were below the limit of detection.

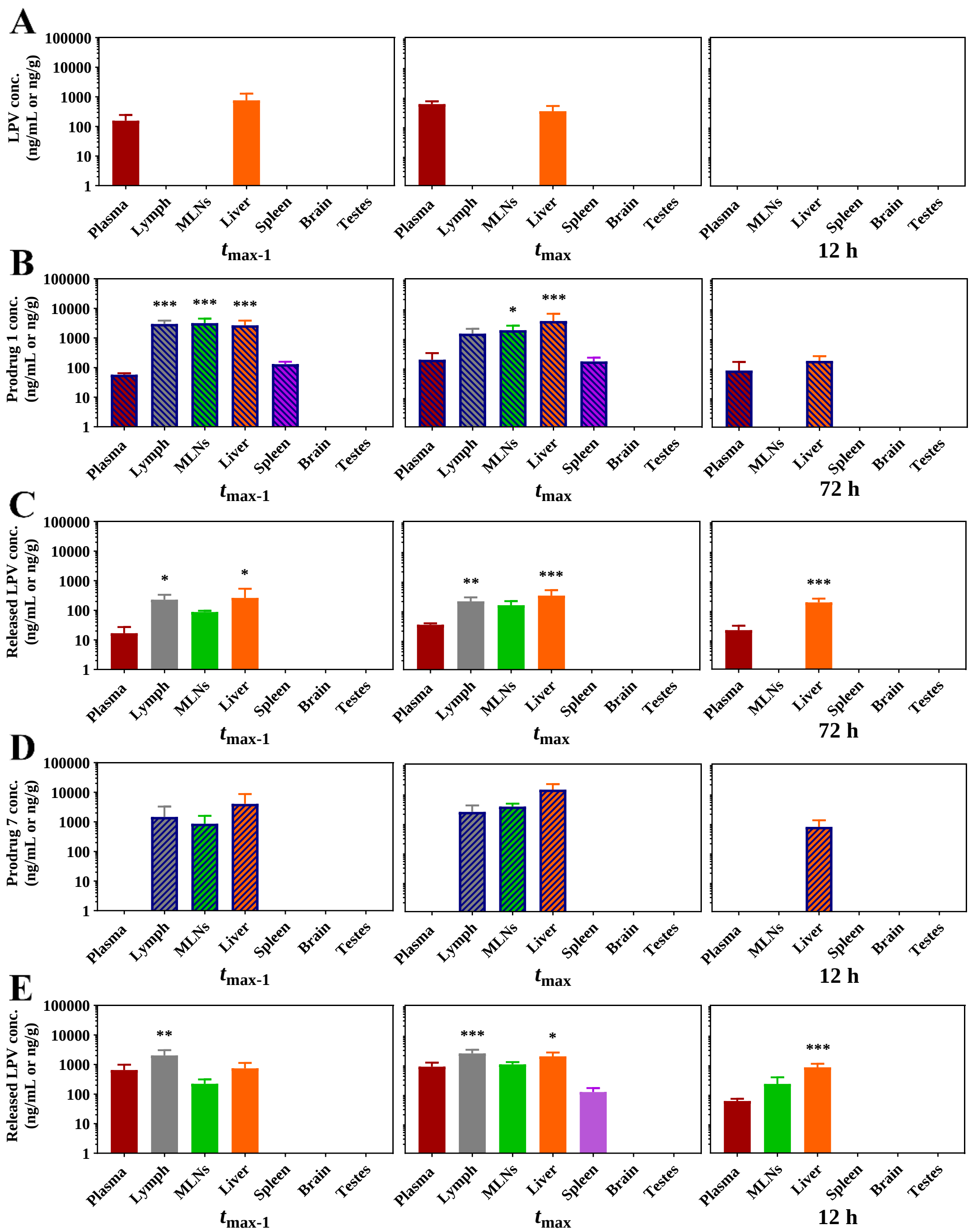

Figure 4- 8. Biodistribution profiles of LPV and selected prodrugs. Rats were administered a 20 mg/kg LPV-equivalent dose of LPV, prodrugs **1** and **7** with lipids by an oral gavage. Biodistribution profiles of (**A**) LPV following administration of unmodified LPV (n = 4); (**B**) prodrug **1** and (**C**) released LPV from prodrug **1** following administration of prodrug **1** (n = 8); (**D**) prodrug **7** and (**E**) released LPV from prodrug **7** following administration of prodrug **7** (n = 4). Data are expressed as mean ± SD. Plasma concentrations were generated in pharmacokinetic studies. MLNs, mesenteric lymph nodes. One-way ANOVA followed by Dunnett's test and two-tailed unpaired *t*-test were used for statistical analysis, *, $p < 0.05$, **, $p < 0.01$, ***, $p < 0.001$.

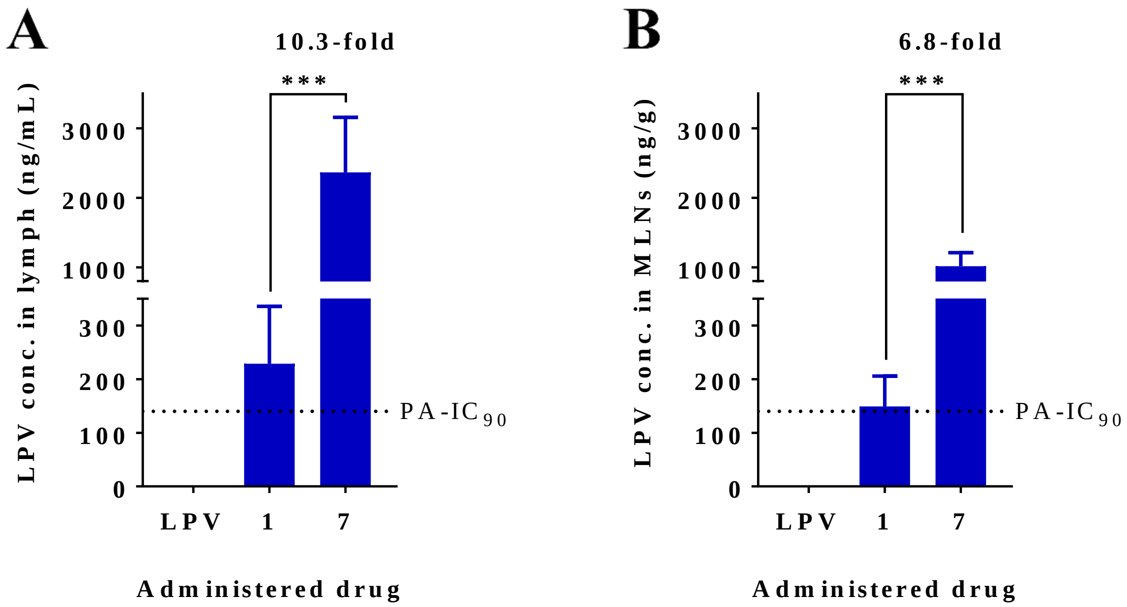

Figure 4- 9. Maximum concentrations of LPV in mesenteric lymphatic system. Concentrations of LPV in (**A**) mesenteric lymph fluid (ng/mL) and (**B**) MLNs (ng/g) were obtained following oral administration of LPV (n = 4), prodrugs **1** (n = 8) and **7** (n = 4) with lipids during biodistribution studies. Limit of detection for lymph fluid and MLNs were 100 ng/mL and 80 ng/g, respectively. The dotted line represents the plasma PA-IC_{90} of LPV (140 ng/mL). Data are expressed as mean ± SD (***, $p < 0.001$ by two-tailed unpaired *t*-test). MLNs, mesenteric lymph nodes. PA-IC_{90}, protein binding-adjusted concentration required for 90% viral inhibition.

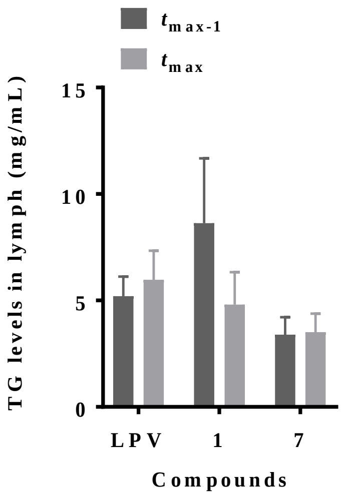

Figure 4- 10. Assessment of the TG levels in biodistribution studies in rats. Triglyceride (TG) levels obtained in mesenteric lymph following oral administration of LPV (n = 4) and prodrugs **1** (n = 7) and **7** (n = 4) with lipids (mean ± SD).

4.4. Discussion

The GALT (including mesenteric lymphatic system) is the largest viral reservoir in HIV-infected individuals [52–55]. Limited penetration of antiretroviral drugs to the mesenteric lymphatic system is a significant barrier for HIV eradication from these important viral reservoirs [52,54,159,253]. In this study, we aimed to deliver antiretroviral drug (LPV) to the mesenteric lymph and MLNs by novel lipophilic ester prodrug approach. The rationale behind this approach is based on physiological process of intestinal lipid absorption and transport.

4.4.1. LPV prodrugs with high potential for delivery to mesenteric lymphatic system

Initially, we assessed the potential of unmodified LPV for intestinal lymphatic transport. The affinity of drugs to CMs is usually highly predictive for intestinal lymphatic transport *in vivo* [137,138]. Although *in-silico* modelling predicted moderate affinity of LPV to CMs (**Table 4-1**), the experimental association of the drug with CMs was negligible, in accordance with the relatively low experimental lipophilicity (log P = 1.7 [226]). Therefore, increasing the lipophilicity of the molecule by adding fatty acid to form ester prodrugs was considered as a reasonable approach to promote high affinity to CMs. We chemically masked the polar and ionisable hydroxyl group within the LPV scaffold to obtain highly lipophilic alkyl ester prodrugs. Results indicate that increasing the lipophilicity dramatically improved the degree of association with CMs by 30% to 50%, compared to the unmodified LPV (**Figure 4-4 (A)**). Previous studies demonstrated that the increased association of highly lipophilic prodrugs with CMs resulted in efficient delivery of drugs to the mesenteric lymph and MLNs, compared to the unmodified moderately lipophilic active drug [177].

4.4.2. *In vitro* screening and selection of prodrug candidates for *in vivo* studies

In order to efficiently deliver drugs to the mesenteric lymphatic system by a prodrug approach, two critical factors have to be considered in the process of prodrug design and assessment. First, the ideal prodrug should have good chemical and enzymatic stability in the gastrointestinal tract prior to absorption. Second, the prodrug should rapidly and efficiently release the active drug as soon as it reaches the lymphatic system. The good stability of prodrugs in FaSSIF (**Figure 4-4 (B)**) suggests that all these prodrugs are likely to remain at least partially intact in the intestinal tract before they reach the enterocytes where association with CMs takes place. Therefore, given the similar stability of all synthesised prodrugs in this study in the intestinal environment, the stability in rat plasma (as an appropriate surrogate to lymph) becomes a critical aspect for screening of potential candidates and their selection for *in vivo* studies. Among the alkyl ester prodrugs, prodrug **1** (shortest alkyl ester) demonstrated the most efficient release of LPV in plasma (**Figure 4-4 (C)**), and therefore was initially selected as a candidate for *in vivo* studies. Following the results of the *in vivo* assessment of prodrug **1** (discussed below), activated ester prodrugs were designed, synthesised and evaluated *in vitro* before potential for selection for *in vivo* studies. The release of LPV from activated ester prodrug **7** was more efficient than from prodrug **1** (86.6% vs 6.5%) at 2 h time point (**Figure 4-4 (C)**), therefore this prodrug was chosen for the subsequent studies. Taken together, high affinity to CMs, good stability in intestinal tract environment and rapid conversion to active drug in lymphatics were considered the major requirements in selection of prodrugs for *in vivo* studies.

4.4.3. *In vitro* antiretroviral activity of the selected prodrugs and released LPV

The *in vitro* antiretroviral efficacy tests confirm the need for the release of LPV from the prodrugs for the efficacy against HIV-1 (**Figure 4-5 (A)**). This is not surprising, as LPV's hydroxyl group is a critical functional group for the inhibition of HIV-1 protease [263]. Prodrug **7** showed significantly higher anti-HIV activity compared to prodrug **1**, indicating the antiretroviral activity of prodrugs in cell culture media was in fact closely linked to the amount of released LPV (**Figure 4-5 (C)**). Previously published report suggests similar tendency for zidovudine prodrugs [264]. To note, the *in vitro* IC_{50} cannot be directly translated to *in vivo* IC_{50}, as LPV is highly plasma protein bound drug (>99% [265]). It has been reported previously that a highly effective viral inhibition is achieved at a plasma concentration higher than protein binding-adjusted IC_{90} (PA-IC_{90}) of LPV for wild-type HIV-1 (140 ng/mL) [266].

4.4.4. Pharmacokinetics of selected prodrugs

The pharmacokinetic profiles following intravenous and oral administrations of prodrug **1** exhibited a prolonged exposure to the prodrug and released LPV in blood (**Figure 4-7 (C)** and **(D)**). The long circulation time of the prodrug is likely due to the tissue distribution of highly lipophilic prodrug **1**, which is similar to other lipophilic, lymphatically transported compounds [267,268]. Compared to relatively low released levels of LPV from prodrug **1** in systemic circulation (**Figure 4-7 (C)** and **(D)**), activated ester prodrug **7** achieved much higher systemic exposure to LPV *in vivo* (**Figure 4-7 (E)** and **(F)**).

The increase in oral bioavailability of LPV achieved in this work is comparable to other studies showing the increase in oral bioavailability of LPV using others approaches [269–271]. In a study carried out by Patel *et al.* [269], a proliposome formulation of LPV led to increase in bioavailability by 2.24-fold compared to pure LPV after oral administration in rats. Furthermore, Patel *et al.* [270] and Negi *et al.* [271] reported 2.97- and 3.56-fold enhancement in oral bioavailability using solid self-nanoemulsifying drug delivery system (S-SNEDDS) and solid lipid nanoparticles (SLNs), respectively, compared to pure LPV following oral administration in rats. In clinical practice, LPV is co-administered with a low dose of ritonavir, a strong inhibitor of cytochrome P450 3A4 (CYP3A4), which results in increased plasma exposure to LPV. However, co-administration of ritonavir with other drugs may lead to serious drug-drug interactions (DDIs) mediated by inhibition of CYP3A4 [272,273]. Therefore, the prodrug approach described in this work can lead, in addition to targeting viral reservoirs in mesenteric lymph and MLNs (discussed below), to higher oral bioavailability of LPV without DDIs issues in HIV-infected patients undergoing ritonavir-boosted lopinavir (LPV/r) regimen.

4.4.5. Delivery of prodrugs and LPV to the mesenteric lymphatic systems

Our results showed that the levels of LPV were below the limit of detection in both mesenteric lymph and MLNs when unmodified LPV was administered orally, even in conditions facilitating lymphatic transport (with lipids) (**Figure 4-8 (A)**). This indicates that oral administration of unmodified LPV does not result in substantial intestinal lymphatic transport and therefore cannot achieve protective concentration in lymphatic system to prevent HIV-1 replication. It is clear that the concentrations of prodrugs **1** and **7** in mesenteric lymph and MLNs were substantially higher than in plasma (**Figure 4-8 (B)** and **(D)**). However, the levels of released LPV were much higher in mesenteric lymphatic system following administration of prodrug **7** compared to prodrug **1** (**Figure 4-9**), probably due to the different LPV release rates (**Figure 4-4 (C)**). A similar pattern of results was obtained in our previous work with anticancer compounds bexarotene and retinoic acid, showing more efficient delivery of active drugs to the mesenteric lymphatic system by activated ester prodrug approach compared to simple alkyl ester prodrug [177]. Although the extent of cumulative lymph transport was not directly measured in this study, we would expect, based on lymph and plasma concentrations, the total amount of prodrug to access the lymph to be similar to that described previously for simple esters [274] and lower than we have described previously for cannabidiol and Δ9-tetrahydrocannabinol [191]. The advantage of the approach taken here, however, is that more effective release of active drug from prodrug in case of activated ester leads to high levels of LPV in mesenteric lymph and MLNs.

Despite the importance of antiretroviral drugs delivery to viral reservoirs such as mesenteric lymph and MLNs, there is a very limited number of studies in which the delivery of LPV to the intestinal lymphatic system has been attempted. A number of publications have assessed the potential of solid-lipid nanoparticles (SLNs) to improve the delivery of LPV to the mesenteric lymphatic system [271,275–277]. It has been reported that the concentrations of LPV observed in MLNs were 3.4- [275] and 2.6-fold [276] higher, respectively, compared to those in plasma 1 h following oral administration of LPV-loaded SLNs to rats. Other studies showed that optimized SLNs approaches achieved 6.6- [277] and 9.1-fold [271] higher levels of LPV in mesenteric lymph fluid, respectively, compared to plasma 2 h following oral administration of LPV-loaded SLNs. Although it seems that SLNs indeed can increase the concentration of LPV in both mesenteric lymph and MLNs, it is unclear if LPV in these tissues is free or is still encapsulated within the SLNs flowing through the intestinal lymphatics to the systemic circulation. In the current study, we achieved 6.2- and 2.8-fold higher levels of released LPV in mesenteric lymph, as well as 4.6- and 1.2-fold in MLNs, compared to those in plasma 3 h following oral administration of lipophilic ester prodrugs **1** and **7**, respectively (**Figure 4-8 (C)** and **(E)**). We have shown previously that drug associated with CMs (approach implemented in this work) has full pharmacological access to lymphocytes [278], probably due to the activity of lipoprotein lipase (LPL) interacting with Apo-C-II proteins on chylomicrons surface [191]. As noted above, an effective viral inhibition is achieved at LPV concentration higher than PA-IC_{90} [266]. The levels of free released LPV from equivalent dose of both prodrugs **1** and **7** in mesenteric lymphatic system substantially exceeds the critical PA-IC_{90} of 140 ng/mL (**Figure 4-9**). Moreover, these efficient levels were extended up to 12 h in MLNs in the case of prodrug **7** (**Figure 4-8 (E)**).

4.5. Conclusion

In this study, we proposed a highly lipophilic prodrug approach, combined with oral lipid-based drug delivery to selectively and efficiently deliver LPV to the difficult-to-penetrate HIV reservoirs in mesenteric lymphatic system. LPV has negligible CMs association, which indeed results in the lack of substantial delivery of unmodified LPV to the mesenteric lymphatic system even when administered with lipids promoting intestinal lymphatic absorption. Simple alkyl ester prodrug approach resulted in substantially higher levels of the prodrug in mesenteric lymphatic system compared to plasma, but poor release of active drug within the lymphatic system. On the other hand, an activated ester prodrug approach showed good stability of the prodrug in the intestinal tract and rapid release of LPV in lymphatic system, thereby leading to high levels of LPV in the MLNs and mesenteric lymph. Moreover, oral administration of activated ester prodrug also increased the oral bioavailability of LPV by nearly 2-fold, and substantially prolonged the circulation time of LPV. This approach, especially if can be translated to other antiretroviral drugs, has potential for reducing the size of HIV reservoirs within the mesenteric lymphatic system.

5. SIMULTANEOUS DELIVERY OF LOPINAVIR AND SALICYLIC ACID TO MESENTERIC LYMPHATIC SYSTEM BY SELF-IMMOLATIVE CODRUG APPROACH

5.1. Introduction

It is well known that acute immune activation is attributed to the loss of gut mucosal integrity and microbial translocation following the occurrence of HIV-1 infection. This leads to a severe depletion of CD4+ T cells (mostly activation-induced cell apoptosis) in gastrointestinal (GI) mucosal tissues during the acute HIV or SIV infection stage [279–282]. With the progression to chronic HIV-1 infection stage, the reduced numbers of CD4+ T cells result in an inverted CD4+/CD8+ ratio which indicates immunologic exhaustion [283–285]. HIV-associated immune activation in viral cellular reservoirs within both systemic circulation and anatomical sites is considered as a main driving force of disease progression to acquired immunodeficiency syndrome (AIDS) [286]. Therefore, reduction of immune activation within viral reservoirs can potentially delay or even prevent disease progression.

The gastrointestinal barrier is severely damaged during the early HIV infection stage, leading to high levels of microbial products, such as lipopolysaccharide (LPS), translocating into systemic blood circulation. In 2006, Jason M. Brenchey *et al.* reported that plasma LPS levels were significantly increased in chronically HIV-infected individuals and SIV-infected rhesus macaques, and effective ART could only partially reduce microbial translocation [31]. This result is in agreement with recent findings that the plasma LPS remained elevated in HIV-infected patients in the chronic HIV infection stage under suppressive ART [287–290].

Therefore, the plasma LPS level is an important biomarker for monitoring microbial translocation and systemic immune activation. [291].

It is well known that LPS can efficiently increase the levels of extracellular high mobility group box 1 (HMGB1) protein [292–294], thereby stimulating toll-like receptor 4 (TLR4), which responds to both LPS [295] and HMGB1 [296]. As a result, triggered TLR4 signalling pathway leads to the activation of intracellular transcription factor, nuclear factor-kappaB (NF-kB) [297], which mediates the activation of HIV transcription and the release of proinflammatory cytokines/chemokines [296] (**Figure 5-1**). In addition, HIV and HIV-specific CD8+ T cell-induced cytopathic effect (necrosis/apoptosis) contributes to passive secretion of HMGB1 [296,298,299], which takes place in both systemic circulation and viral anatomical reservoirs [300]. In 2007, it has been reported that plasma HMGB1 levels in HIV-1-infected patients at chronic stage of the disease were significantly higher than healthy controls, but with the highest levels in immunologic nonresponders [301]. In 2010, this finding was further confirmed by Trøseid *et al*. [302], who demonstrated that the plasma levels of LPS and HMGB1 in ART treatment naïve HIV-1-infected patients were higher compared with 2-year ART treatment immunologic responders, but no significant difference was observed in comparison with immunologic nonresponders. P. Nowak *et al.* [299] and S. Thierry *et al.* [303] reported that HMGB1 singling pathway activated viral transcription and replication in latent HIV-1-infected cells through *in vitro* and *ex vivo* studies. Therefore, the increased levels of released HMGB1 contribute to the activation of HIV-1-infected latent cells, resulting in reproduction of infectious virions in viral reservoirs within both blood and tissues. Furthermore, K. Takeuchi *et al*. [304] found that aspirin and salicylic acid possess cytoprotective function which can inhibit intestinal hypermotility and bacterial translocation to protect intestinal integrity in rats. In 2015, it was demonstrated that salicylic acid/salicylates can specifically bind to HMGB1 and prevent further NF-kB singling pathway, thereby avoiding HMGB1-mediated immune activation [305].

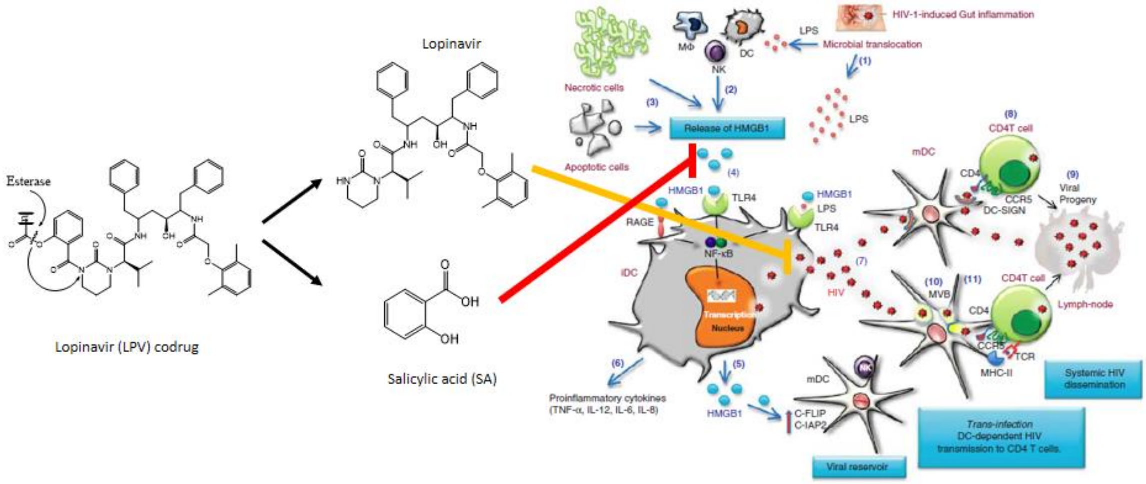

Figure 5 - 1. Schematic diagram of codrug self-immolation and pharmacological effects of released active agents. The self-immolative codrug is described as follows: an enzymatic substrate of esterase is attached to a self-immolative linker (salicylic acid) with adequate length to avoid steric hindrance of lopinavir. As soon as the ester bond is hydrolysed, lopinavir and salicylic acid will be released simultaneously. Therefore, lopinavir can prevent targeted cells from releasing infectious virions (yellow line) and salicylic acid-incorporated HMGB1 will downregulate immune activation (red line), respectively. HMGB1, high mobility group box 1 protein. Adapted from [296].

In this study, lipophilic codrug approach combined with oral lipid-based formulation was designed to efficiently and simultaneously deliver two active agents to HIV reservoirs within the mesenteric lymphatic system. LPV (antiretroviral agent) and salicylic acid (an agent preventing immune activation) were co-administered *via* a novel self-immolative codrug approach, based on previously published literature [306–311]. The two active agents (LPV and salicylic acid) were covalently chemically combined to form a single molecular unit which is then attached to an enzymatic trigger (a fatty acid ester). Subsequently, the linker is hydrolysed in the body by esterase activity in the body thus releasing the two active agents. Here, we designed a series of LPV and salicylic acid codrugs using an *in-silico* modelling tool for prediction of CMs association. The designed codrugs were then chemically synthesised. The potential of synthesised codrugs for mesenteric lymphatic targeting were then assessed using *in vitro* CMs association assay, and the release of active drugs was assessed in biorelevant media. The optimal candidates were subsequently assessed in further *in vivo* studies.

5.2. Experimental design

The procedure of chemical synthesis is described in Section 2.3. *In vitro* chylomicrons association and prodrug conversion assays were performed as described in Sections 2.4. and 2.5., respectively. Long chain triglycerides (LCTs) solubility measurement is described in Section 2.6. Pharmacokinetic studies following oral administration of codrug **4** were performed as described in Section 2.8.3. Procedures for sample preparation are outlined in methods of Section 2.2. The general scheme flowchart of experimental design is shown in **Figure 5-2**.

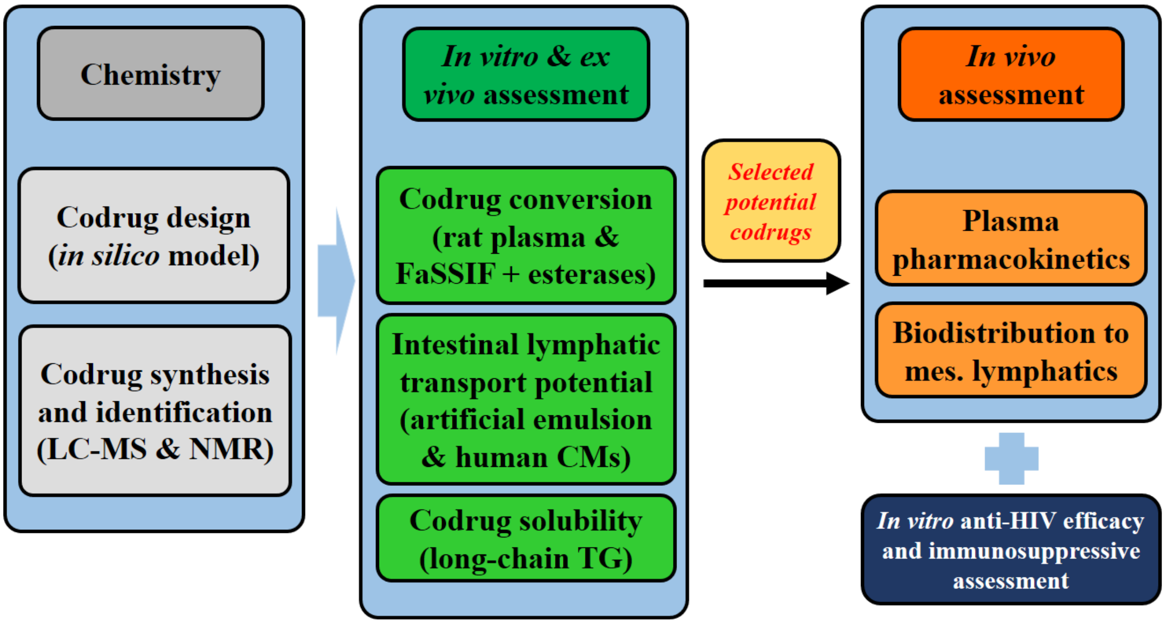

Figure 5 - 2. Schematic diagram of workflow for lipophilic codrug approach to target mesenteric lymphatic systems. FaSSIF, fasted state simulated intestinal fluid; CMs, chylomicrons; TG, triglyceride.

5.3. Results

5.3.1. *In-silico* modelling-assisted design of codrugs of lopinavir and salicylic acid

The predicted physicochemical properties of all designed codrugs were obtained using ACD/Lab (Advanced Chemistry Development Inc., Toronto, Canada). Five codrugs of LPV and salicylic acid were designed using *in-silico* modelling tool [137]. The high predicted values of CMs association (%) with all these codrugs (**Table 5-1**) indicate high potential for the mesenteric lymphatic targeting [138]. Codrugs **1-5** were self-immolative codrug is described as follows: an enzymatic substrate of esterase is attached to a self-immolative linker (salicylic acid) with adequate length to avoid steric hindrance of LPV. As soon as the ester bond is hydrolysed, LPV and salicylic acid will be released simultaneously **Figure 5-1**.

5.3.2. Chemical synthesis

The methodologies of synthesis and characterisation of codrugs are described in Chapter 2 (Sections 2.3.2 and 2.3.3). The yield of codrugs are from low to medium (**Table 5-1**). Compound characterisation is described in **Appendix 2**. The chemical structures are shown in **Figure 5-3.**

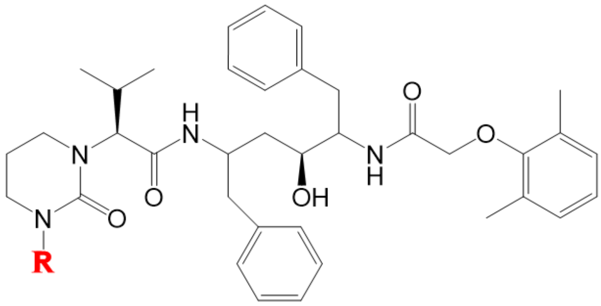

R: Position of substituent

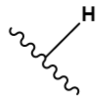

LPV (lopinavir)

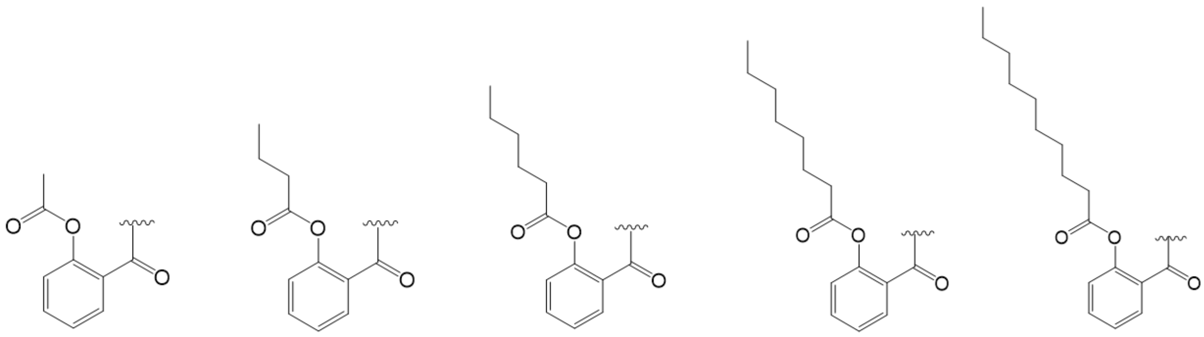

1 **2** **3** **4** **5**

Figure 5 - 3. The chemical structures of lopinavir and its codrugs (1-5). The codrug consists of lopinavir-salicylic acid as a main unit and a short to medium chain fatty acid leaving group. The characterisation of these codrugs are shown in **Appendix 2**.

Table 5- 1. The log P, predicted CM association, yield (%) and purities of codrugs **1-5**

Codrugs	1	2	3	4	5
Log P	6.44	6.82	8.73	10.05	11.13
Predicted association (%)	59.6	79.8	96.9	99.4	99.9
Yield (%)	11%	30%	59%	14%	9%
Purity	>95%	>95%	>95%	>95%	>90%

5.3.3. Uptake of codrugs by chylomicrons

The process of drug-CMs association in intestinal wall enterocytes is the crucial step for intestinal lymphatic transport. Although all codrugs showed moderate to high affinity to CMs in *in-silico* modelling prediction (**Table 5-1**), the experimental association of codrug **1** with artificial CMs-like emulsion (Intralipid®) was negligible (**Figure 5-4 (A)**). Codrugs **2-5** showed moderate to high affinity to artificial CMs-like emulsion, indicating that codrugs **2-5** possess high potential for mesenteric lymphatic targeting following oral administration with lipid-based formulation. As shown in **Figure 5-3**, the chemical structures of codrugs **1-5** consist of LPV, salicylic acid and short (2C) to medium (10C) fatty acid chain alkyl esters. Initial increase of the length of fatty acid chain improved significantly the drug affinity to CMs (**Figure 5-4 (A)**). However, further increase the length of fatty acid moiety (codrug **5**) did not contribute to additional improvement of association with CMs, which is in line with the CMs association results with prodrugs described in chapter 4. Similar phenomenon observed in both codrugs and prodrugs of LPV suggested a defined range of optimal association with CMs to derivatives of LPV. The mass recovery (%) of all test compounds was around 100% (**Figure 5-4 (B)**), indicating that no unspecific drug binding took place during incubation. In addition, the levels of released LPV and intermediate metabolites could not be observed in chromatograms, indicating all codrugs were stable during this assay.

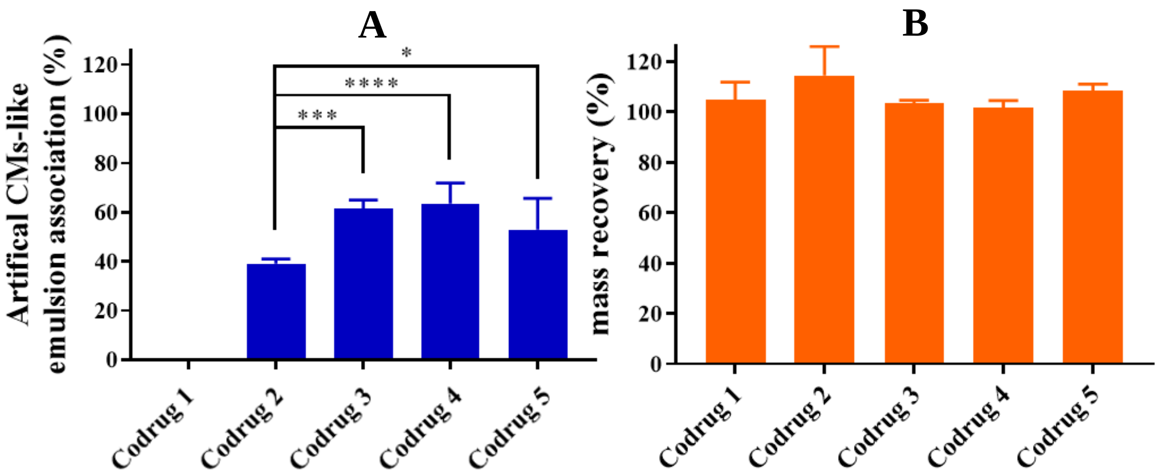

Figure 5 - 4. (A) Association (%) of codrugs with artificial CMs-like emulsion prepared from Intralipid®, indicating the potential of the molecule for intestinal lymphatic transport. One-way ANOVA followed by Tukey's test was used to compare the CMs association (%) values in codrugs **2-5**, *, $p < 0.05$; ***, $p < 0.001$; ****, $p < 0.0001$ (n = 5); **(B)** Mass recovery (%) of all tested codrugs. The concentrations of codrugs in chylomicron emulsion (1 mL) were measured by means of HPLC-UV following 1 h incubation prior to ultracentrifugation. The mass recovery (%) was calculated using the amount of tested compound experimentally measured divided by the amount of compound the medium was spiked with (n = 3). Data are shown as mean ± SD.

5.3.4. *In vitro* bioactivation of codrugs

An ideal codrug should possess good stability in gastrointestinal tract but rapid release of active drugs in lymphatic systems. The *in vitro* stability of the codrugs was assessed in fasted state simulated intestinal fluid (FaSSIF) with added esterase enzyme activity (20 IU/mL), which represents the stability of codrugs in intestinal tract prior to absorption. The *in vitro* conversion of codrugs should also be tested in lymphatic systems, where active drugs work pharmacologically. However, the volume of lymph fluid that can be collected from rats by sampling technique in this work was too low for screening of all tested compounds. In addition, Plasma contains similar composition and levels of enzymes to lymph fluid in many species [195,196]. Therefore, in this study, rat plasma was chosen as surrogate to represent lymph fluid, as the composition and levels of enzymes in plasma are similar to those in lymph fluid in many species (i.e. human and rats) [195,196].

Figure 5-5 and **Figure 5-6** show chromatograms of codrugs stability and bioconversion to LPV in FaSSIF and rat plasma, respectively. It is assumed that all codrugs were firstly hydrolysed to the same metabolites and only then released LPV, rather than releasing aspirin derivatives directly. Subsequently, the HPLC analytical profile of synthesised aspirin derivatives **1-5** (**Figure 5-3**) were determined by means of HPLC-UV using the same analytical method as described for the codrug (**Figure 5-7**). As a result, the peaks of synthesised aspirin derivatives could not be observed in the chromatograms during stability studies (**Figure 5-5** and **5-6**) when compared to the retention times of the reference peaks in **Figure 5-7**.

The degradation half-lives of codrugs **1-3** were extremely short in FaSSIF (less than 15 min), indicating that the codrugs would be unlikely to remain intact in intestinal tract prior to absorption. However, following addition of medium fatty acid chains (8C and 10C), the degradation half-lives of codrugs **4** and **5** in FaSSIF were prolonged to 30.5 ± 9.0 and 66.6 ± 3.0 min (mean ± SD, n = 3), respectively (**Figure 5-8**). For the assessment of codrug stability in rat plasma, codrugs **1-3** were extremely unstable, the peaks of codrugs **1-3** could only be observed at the first time point in chromatograms (**Figure 5-6 (A-C)**). However, codrugs **4** and **5** were more stable in rat plasma (**Figure 5-6 (D)** and **(E)**), compared to codrugs **1-3**. This indicates that increasing the length of fatty acid chain leads to increased steric hindrance of the enzymatic cleavage. The degradation half-life of intermediate metabolite is significantly shorter than alkyl ester prodrug **1** (data in chapter 4) (**Figure 5-9 (A)**). There was no statistically difference in the levels of LPV released from codrugs **1-4** during the tested time frame (up to

2 h) (**Figure 5-9 (B)**), indicating the converting rate to active drugs from intermediate metabolite is consistent.

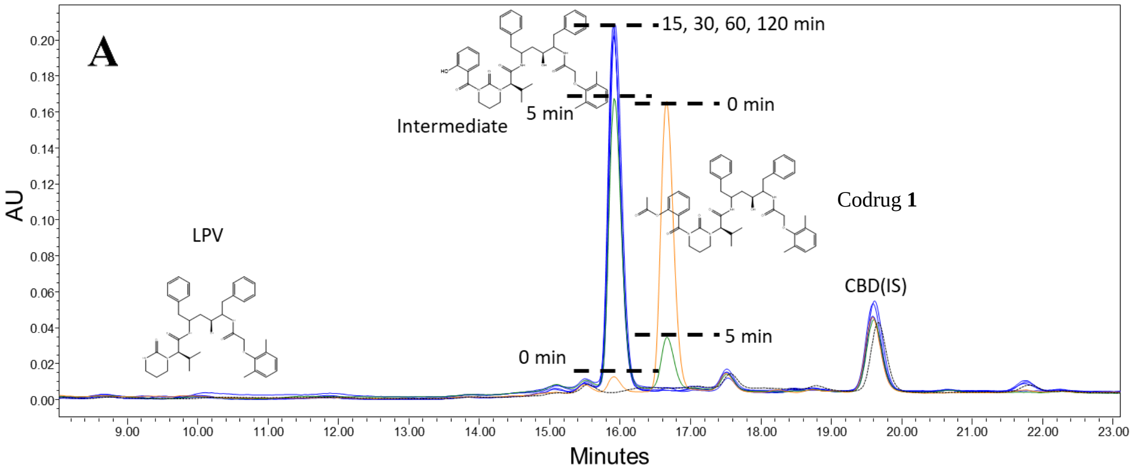
A
15, 30, 60, 120 min
0 min
5 min
Intermediate
Codrug 1
LPV
CBD(IS)
5 min
0 min
AU
Minutes

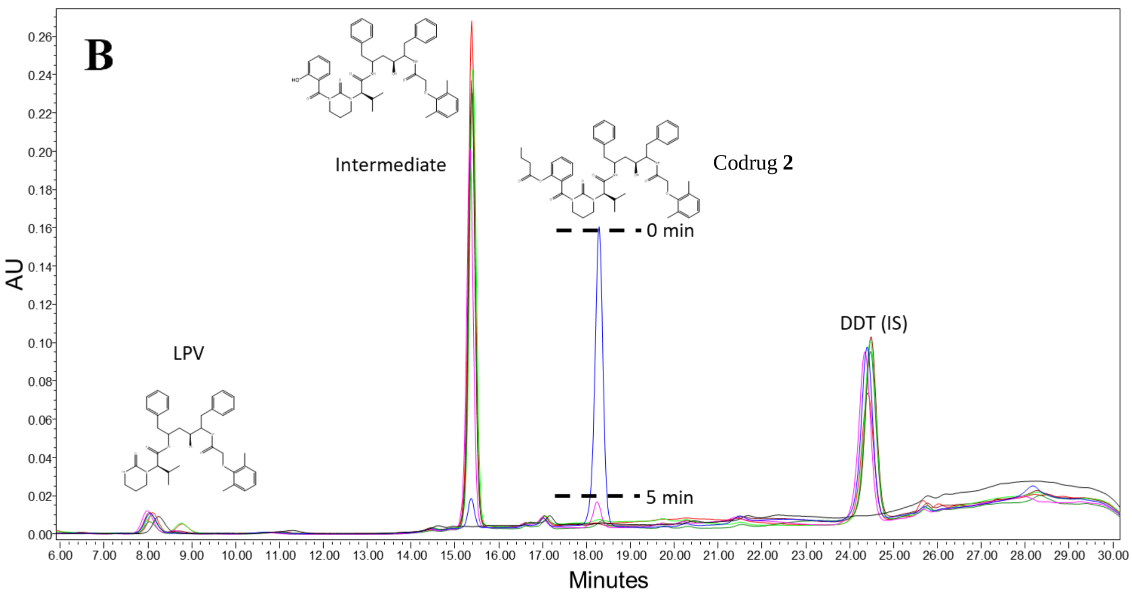
B
Intermediate
Codrug 2
0 min
LPV
DDT (IS)
5 min
AU
Minutes

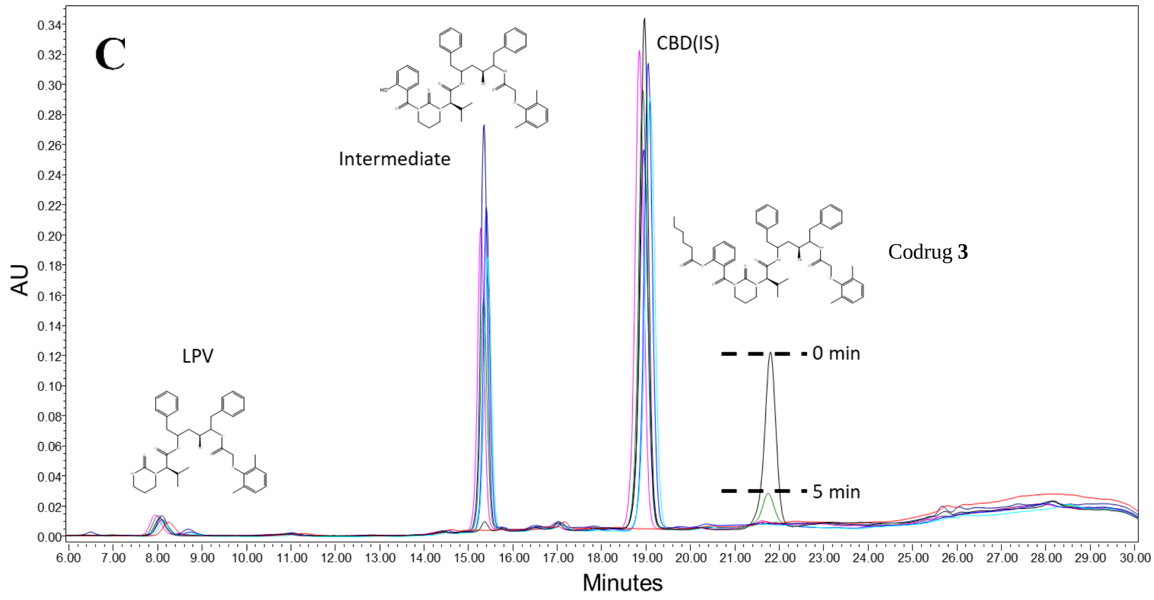
C
CBD(IS)
Intermediate
Codrug 3
LPV
0 min
5 min
AU
Minutes

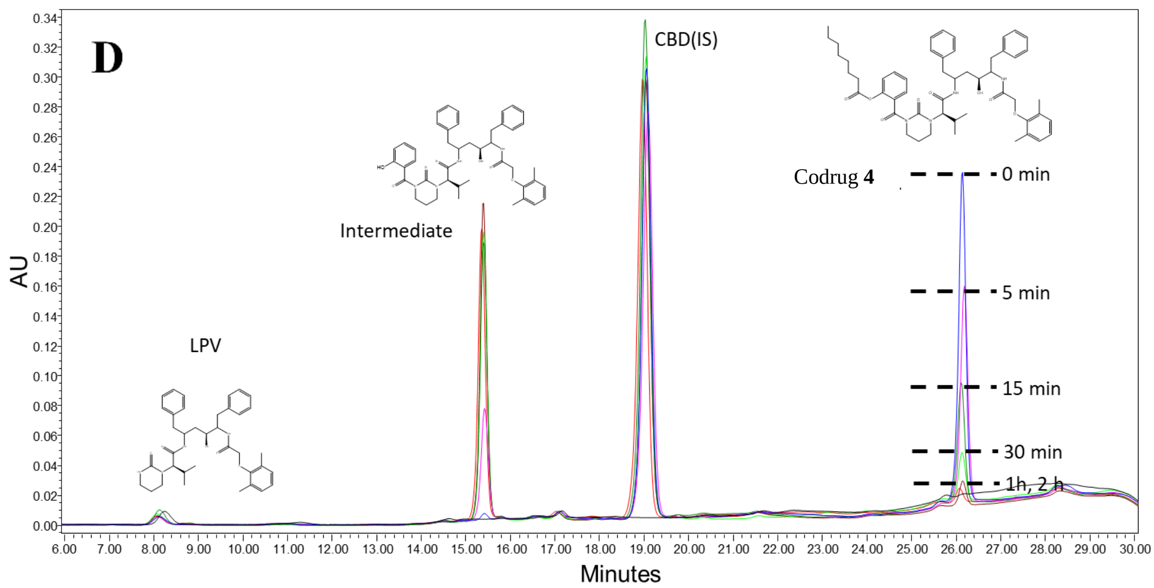
D
CBD(IS)
Intermediate
Codrug 4
LPV
0 min
5 min
15 min
30 min
1h, 2 h
AU
Minutes

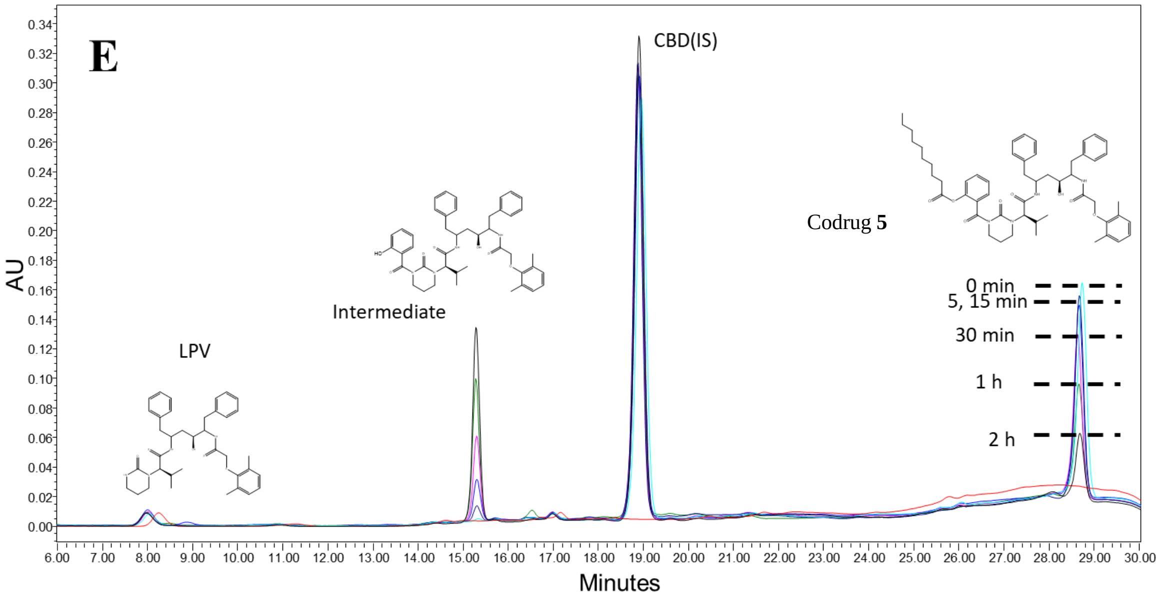

Figure 5 - 5. The stability of codrugs in fasted state simulated intestinal fluid (FaSSIF) supplemented with esterases activity (20 IU/mL). Three compounds, including LPV, intermediate metabolite and corresponding codrug, are represented by three peaks separated in chromatogram. The stability of (**A**) codrug **1**; (**B**) codrug **2**; (**C**) codrug **3**; (**D**) codrug **4** and (**E**) codrug **5** are presented in chromatograms, respectively. LPV: lopinavir; CBD (IS): cannabidiol; DDT: dichlorodiphenyltrichloroethane. Bioanalytical conditions were described in **Table 2-2**.

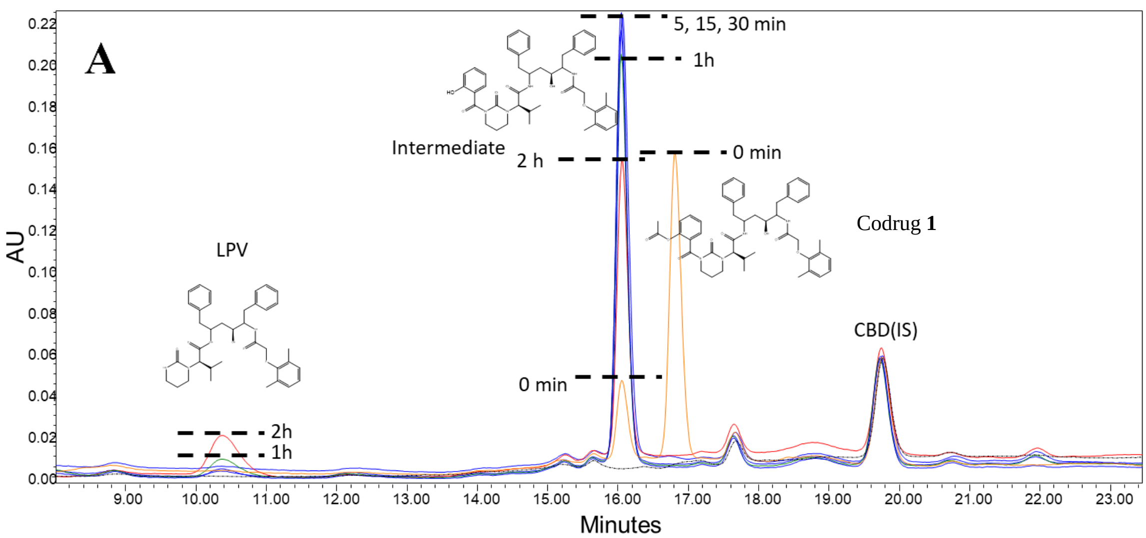
A
5, 15, 30 min
1h
Intermediate
2 h
0 min
Codrug 1
LPV
CBD(IS)
0 min
2h
1h
AU
Minutes

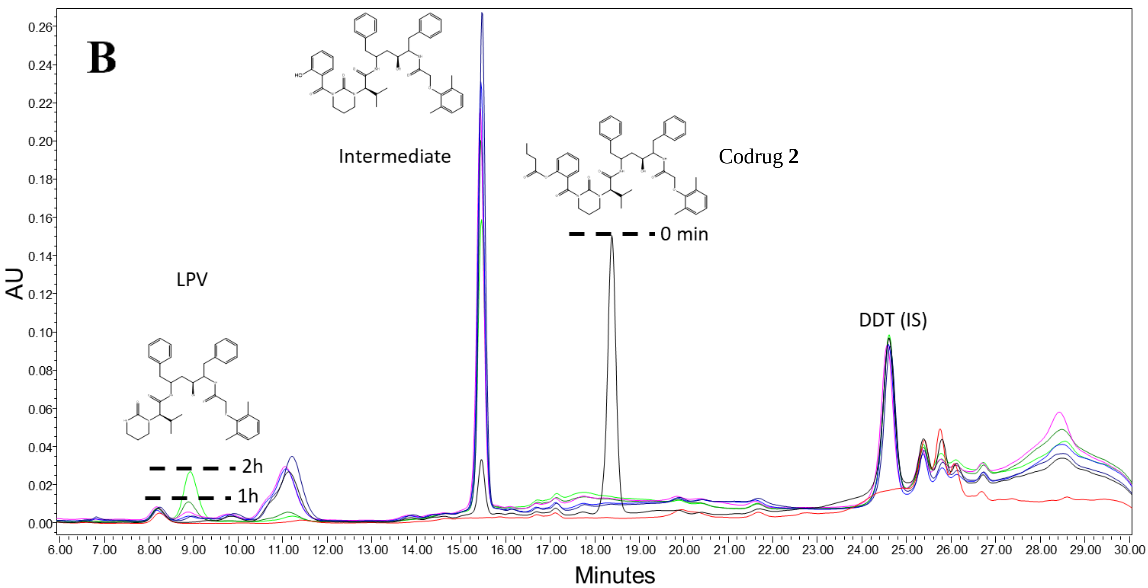
B
Intermediate
Codrug 2
0 min
LPV
DDT (IS)
2h
1h
AU
Minutes

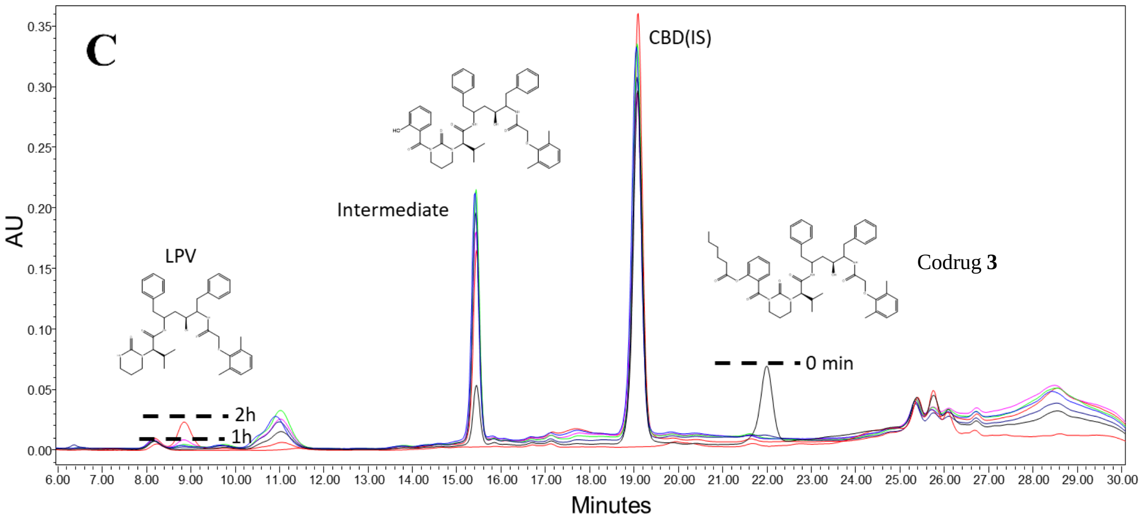
C
CBD(IS)
Intermediate
LPV
Codrug 3
0 min
2h
1h
AU
Minutes

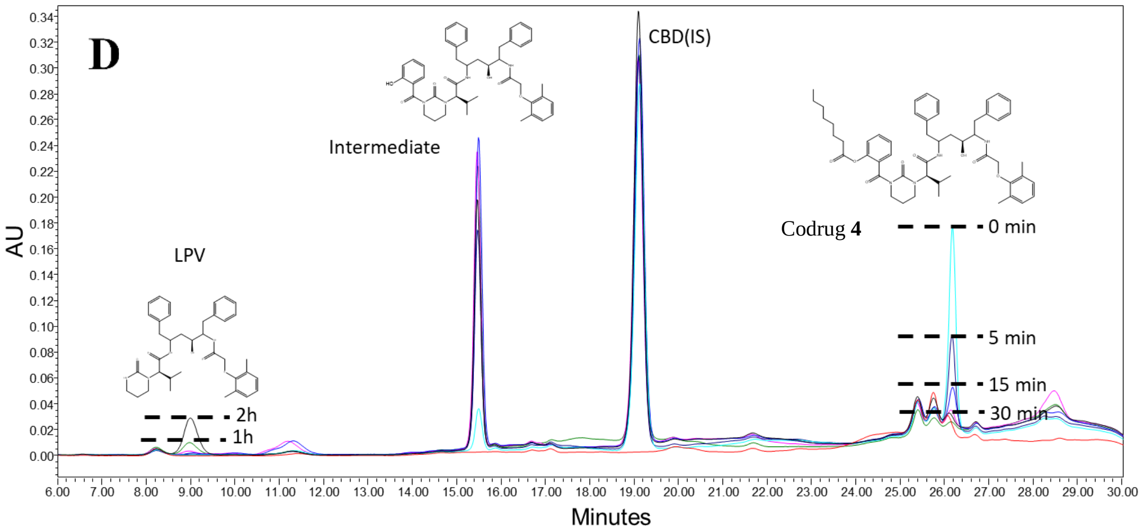
D
CBD(IS)
Intermediate
LPV
Codrug 4
0 min
5 min
15 min
30 min
2h
1h
AU
Minutes

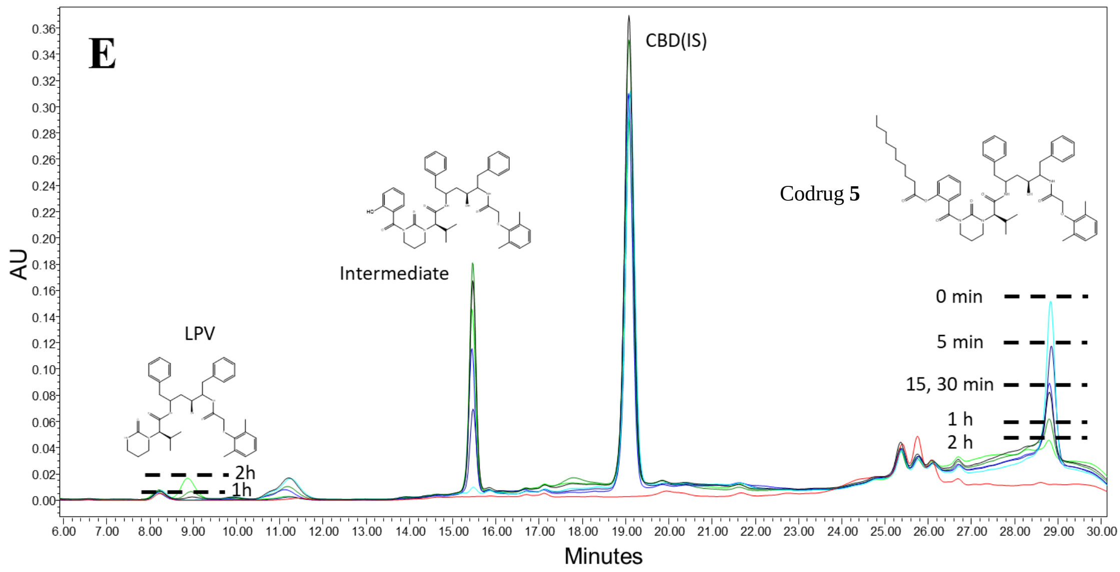

Figure 5 - 6. The stability of codrugs **1-5** in rat plasma. Three compounds, including LPV, intermediate metabolite and corresponding codrug are represented by three peaks separated in chromatogram. The stability of (**A**) codrug **1**; (**B**) codrug **2**; (**C**) codrug **3**; (**D**) codrug **4** and (**E**) codrug **5** are presented in chromatograms, respectively. LPV: lopinavir; CBD (IS): cannabidiol; DDT (IS): dichlorodiphenyltrichloroethane. Bioanalytical conditions were described in **Table 2-2**.

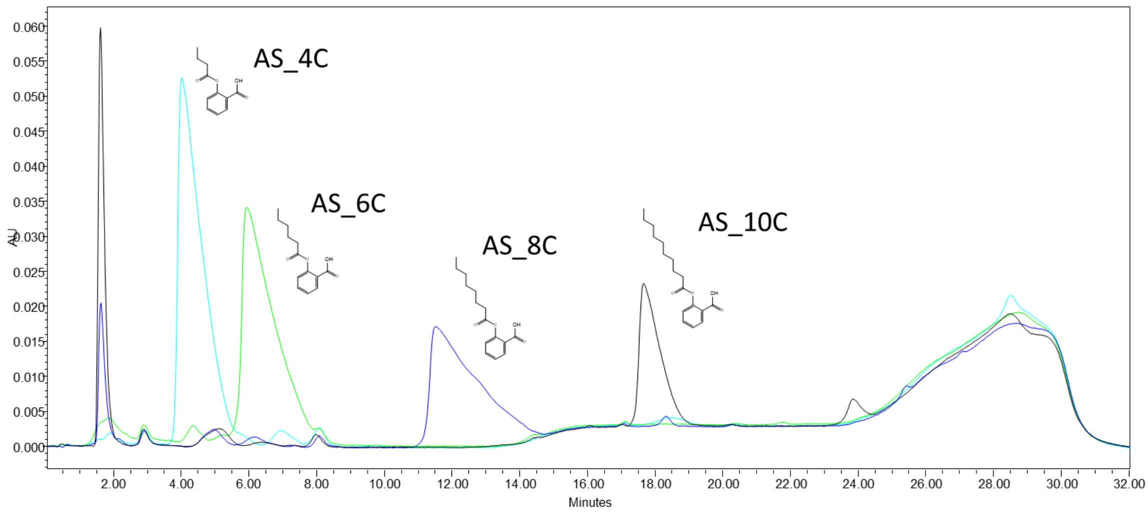

Figure 5 - 7. The chromatograms of synthesised aspirins with short to moderate fatty acid chain. All these compounds were separated using the same analytical methods as codrugs **2**-**5** by means of HPLC-UV.

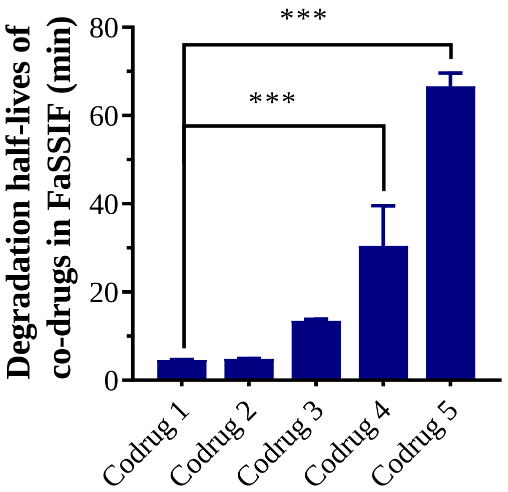

Figure 5 - 8. Degradation half-lives of codrugs **1**-**5** in fasted state simulated intestinal fluid (FaSSIF) supplemented with esterases activity (20 IU/mL) (mean ± SD, n=3). One-way ANOVA followed by Dunnett's test was used for statistical analysis, ***, $p < 0.001$.

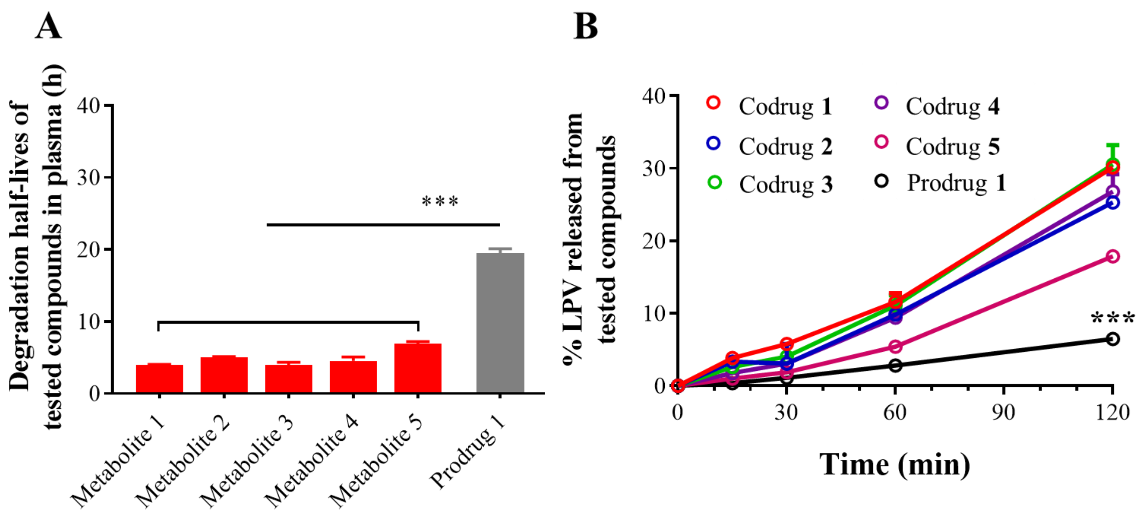

Figure 5 - 9. (**A**) Degradation half-lives of intermediate metabolites **1**-**5** (released from codrugs **1**-**5**) and prodrug **1** (data from in chapter 4) in rat plasma. (**B**) Levels of released active drug LPV from codrugs **1**-**5** and prodrug **1** in rat plasma. One-way ANOVA followed by Dunnett's or Tukey's test was used for statistical analysis, ***, $p < 0.001$.

5.3.5. Preliminary pharmacokinetic studies following oral administration of codrug 4 in lipid-based formulation

The *in vivo* plasma pharmacokinetics of codrug **4** was assessed in a preliminary study following oral administration in lipid-based formulation in rats (n = 2). The long-chain triglyceride solubility of codrug **4** was over 30 mg/mL. However, the levels of codrug **4**, intermediate metabolite and released LPV were undetectable at all sampled time points. On the other hand, the plasma pharmacokinetic profiles of both prodrugs and released LPV could be obtained following oral administration of corresponding ester prodrugs in lipids in rats (Chapter 4). This indicates that ester prodrugs may have lower rate of metabolism in intestinal wall before reaching systemic circulation compared to orally administered codrugs. Further investigation of intestinal microsomal stability of codrugs and prodrugs should be conducted.

5.4. Discussion

5.4.1. Codrugs with high potential for mesenteric lymphatic targeting

The CMs association percentage of all codrugs were predicted using *in-silico* model [137], guiding codrug design. However, the experimental CMs association of codrug **1** was negligible (**Figure 5-4 (A)**), which is same as the results of unmodified LPV (data from chapter 4). Although codrug **1** is more lipophilic than unmodified LPV, the increased lipophilicity did not result in higher affinity to CMs. Therefore, codrugs **2**-**5** were designed to further increase lipophilicity and molecular weight, thereby achieving moderate to high affinity to CMs (**Figure 5-4 (A)**). Taken together, fatty acid chain (4C-12C) did significantly improve the drug association with CMs for both codrugs **2**-**5** in this chapter and prodrugs **1**-**5** in chapter 4. This indicates that fatty acid chains of certain length could be selected as good candidates in early design of codrug/prodrug for delivery of active drugs to mesenteric lymphatic systems.

5.4.2. Bioconversion of codrugs in physiological media

In this study, a good stability of codrugs in gastrointestinal (GI) tract is a key step for ensuring higher fraction of orally administered compounds is in intact form prior to absorption. Codrugs **1**-**3** are extremely unstable in FaSSIF (**Figure 5-8**), whereas only codrugs **4** and **5** appear to be stable in GI tract. Another important step is efficient release of active agents in mesenteric lymphatic systems. The *in vitro* stability of the codrugs assessed in rat plasma was used for mimicking the release efficiency when codrugs reach mesenteric lymph and MLNs. The alkyl ester prodrugs **1**-**5** were too stable to rapidly release LPV in rat plasma (data shown in chapter 4), indicating that simple fatty acid chain esters increase the steric hindrance of the enzymatic cleavage. In order to avoid steric hindrance, a self-immolative linker (salicylic acid) was introduced, which also worked as an active agent for reducing excessive immune activation in lymphatic and systemic systems. Indeed, the release of LPV from all codrugs was much more efficient compared to prodrug **1** (the most promising one amongst alkyl esters in chapter 4) (**Figure 5-9 (B)**). Self-immolative prodrug approaches have been known as an advanced strategy for drug delivery to achieve efficient release of active drug [312]. Some self-immolative prodrugs were designed to release active drugs using a single bond leaving group [312–314]. Other prodrugs consist of enzymatic substrates, self-immolative linkers and active drugs, which, following enzymatic cleavage, cause the subsequent ‘self-immolation’ of the linker and thereby release of active drug [315,316]. In general, self-immolative prodrug approach is well studied in chemotherapy for reducing cytotoxicity of the active moiety by controllable release, real-time tracking of drug’s release and localization [317]. In this study, the primary aim is rapid release of LPV by introducing self-immolative linker. In addition, this linker contributed as an active agent to reduce immune activation. Due to the limitations of bioanalytical methods, the peak of released salicylic acid could not be observed in chromatograms. However, as the molar concentrations of released LPV can be determined by means of HPLC-UV, it could be assumed that the same molar levels of released salicylic acid can be achieved from codrugs.

The increased degree of steric hindrance is a main reason for delay of enzymatic cleavage of protecting groups (ester bond) [177,318]. Interestingly, this delay of enzymatic recognition did not affect the following spontaneous hydrolysis of self-immolative linker (salicylic acid), therefore the release rate of active drug LPV has no significant difference between codrugs **1-4** in rat plasma (**Figure 5-8 (B)**). Moreover, the chromatograms clearly showed the phenomenon of enzymatic cleavage and self-immolative degradation mechanism throughout the experimental time frame (**Figure 5-6**). As a result, all codrugs converted to the same intermediate following the cleavage of protecting groups by esterases, which is similar to the reported self-immolative approaches involving the use of ‘hemiacetal’ [311] or ‘hydrocymethyl disulfide’ [310] as unstable intermediates in prodrug design.

5.4.3. Selection of candidates for *in vivo* studies

In this study, the criteria for selection of codrugs for subsequent *in vivo* studies was based on *in vitro* CMs association and stability assays. In essence, high affinity of codrugs to CMs, good stability in FaSSIF and rapid release of active drugs in rat plasma are the key criteria for selection potential candidates. Based on the results of *in vitro* assessments, codrugs **4** and **5** were firstly selected as good candidates due to their high percentage of association with artificial CMs-like (intralipid®), as well as good stability (half-lives > 30 min) in FaSSIF. However, codrug **5** possesses prolonged release of active drug (LPV) in plasma, compared to the rest of the codrugs (**Figure 5-8 (B)**). Therefore, codrug **4** was ultimately chosen for subsequent *in vivo* studies.

5.4.4. Pharmacokinetic study following oral administration of codrug 4 in lipids

Unfortunately, the levels of codrug **4**, intermediate metabolite and released LPV were below the limit of detection in plasma in all pre-determined time points following oral administration of codrug **4**. There is no indication that degradation of codrug **4** and extensive release of LPV take place in GI tract prior to intestinal absorption. Our results in Chapter 4 and other studies [221,319] showed that plasma pharmacokinetic profiles of LPV could be obtained following oral administration of unmodified LPV in rats. This indicates that there is little chance of extensive release of LPV in intestinal lumen prior to absorption following oral administration of codrug **4** in lipids. Therefore, we hypothesise that the main reason for these results is likely to be that the molecules (codrug **4** or its intermediate) are absorbed into enterocytes but rapidly metabolised in intestinal wall, liver or both. It is reported that salicylic acid can be extensive metabolised by CYP450-mediated oxidation and glucuronidation in intestinal wall [320], which might increase the degradation of the molecule. However, it is well known that RTV, which works as potent inhibitors of CYP3A4 [67], is co-administered with LPV to increase the systemic exposure to LPV in clinical practice [66,68]. Therefore, co-administration of a small dose of RTV may potentially increase the absorption of codrugs.

Further investigation should be conducted to test the proposed hypothesis using intestinal microsomal stability assays and transport studies. In this chapter, the bioanalytical method developed for simultaneous detection of the released salicylic acid and other compounds has substantial limitations. The logP of salicylic acid is significantly lower than codrugs and LPV, and salicylic acid is completely ionized under the analytical conditions developed for codrugs and LPV (pH is nearly 7). Therefore, different analytical conditions should be developed for determination of salicylic acid by means of HPLC-UV or a simultaneous analytical method for all molecules in question using LC-MS/MS methodology.

5.5. Conclusion

In this chapter, we designed and synthesised a series of self-immolative codrugs with moderate to high potential for intestinal lymphatic transport and controllable release of active agents. The 'self-immolation' of codrugs was triggered by an esterase-mediated hydrolysis mechanism, which resulted in a cleavage of ester bond, following a release of active drugs lopianvir and salicylic acid. Following the *in vitro* assessment, codrug **4** was selected for the subsequent *in vivo* studies. Unfortunately, codrug or released LPV could not be detected in plasma at all sampled time points. Although the reason for negative *in vivo* results is unclear, it is likely that first-pass intestinal or hepatic metabolic loss is the main reason. Further investigation will be needed to assess the feasibility of self-immolative codrug approach.

6. GENERAL DISCUSSION AND FUTURE WORK

6.1. General discussion

In this PhD project, we have focused on optimisation of the treatment of HIV/AIDS by lipophilic ester prodrug approach. It aims to selectively and efficiently deliver antiretroviral drug lopinavir (LPV) to the mesenteric lymph nodes (MLNs), an important difficult-to-penetrate viral reservoir. It demonstrates a novel avenue of therapeutic strategy for eradication of HIV reservoirs.

6.1.1. Simple and sensitive bioanalytical method for determination of LPV by means of HPLC-UV method

A simple and sensitive bioanalytical method for determination of LPV was developed and fully validated in rat plasma (Chapter 3). This method was also applied to the detection of synthesised LPV prodrugs/codrugs in plasma and tissues with slight modifications throughout this PhD project. High sensitivity of HPLC-UV method for determination of LPV (LLOQ = 10 ng/mL) allowed accurate demonstration of *in vivo* pharmacokinetic and biodistribution profiles in this project. A full validation, including benchtop, stock solution, autosampler, freeze-thaw, short-term and long-term stabilities, ensured the accuracy and precision of this bioanalytical method undergoing sample preparation and storage conditions. In addition, this method was assessed and validated in human plasma with the intention that it may provide clinical therapeutic drug monitoring (TDM) in HIV-infected patients in resource-limited settings.

There are dozens of bioanalytical methods reported in literature for determination of LPV for clinical TDM in HIV-infected patients [210–217,240,321–333], but only a small amount of methods is reported for preclinical studies in animals [221,334,335]. One published bioanalytical method achieved good sensitivity with LLOQ of 5 ng/mL by means of HPLC-UV for determination of LPV [210], while another method utilized LC-MS/MS to obtain LLOQ as low as 1 ng/mL [331]. Both bioanalytical methods demonstrated better sensitivity for analysis of LPV in plasma compared to the sensitivity of our method reported in Chapter 3 (LLOQ = 10 ng/mL). However, substantially higher volume of plasma (600 and 200 µL, respectively) was applied in these previously published assays compared to ours (100 µL), indicating that our bioanalytical method is more suitable for preclinical studies in small animals.

Moreover, Chapter 3 reports full validation and stability of LPV in rat plasma according to FDA guidelines [225]. The nearest comparison for method validation and stability to our work is the one carried out by Vats *et al.* [221]. However, in that method only the stabilities of LPV in rat plasma under the conditions of freeze-thaw (3 cycles between -20 °C and room temperature), short/long-term frozen (-20 °C) and autosampler (4 °C for 24 h) were validated. In addition, the stability of LPV in rat plasma was originally validated at heat-inactivated condition only.

6.1.2. LPV and simple alkyl ester prodrugs

All ester prodrugs of LPV were designed through masking the hydroxyl group (esterification) coupled with *in-silico* modification of structures [137]. Following design and synthesis of prodrugs, they were subsequently assessed for drug-CMs association and active drug release in physiological media. The alkyl esters of LPV with simple fatty acid chains (a widely studied prodrug approach [318]) were initially developed and assessed. In this study, these prodrugs were designed to mask the hydroxyl group of LPV by esterification, thereby optimising multiple physicochemical properties for the improvement of association with CMs. As a result, all alkyl esters showed significantly increased affinity to CMs compared to unmodified LPV (zero association), indicating the improvement of their potential for delivery to mesenteric lymphatic systems. However, the alkyl esters of LPV were relatively stable in rat plasma (representing lymphatic system), thereby delaying the conversion to active drug LPV in both blood and lymphatic systems. It was also observed that the length of fatty acid chain correlated with the release rate of active drug LPV. Among the alkyl esters, prodrug **1** (shortest alkyl ester) possessed the fastest conversion to active LPV in rat plasma (degradation half-life: 19.5 h) and a moderate CMs association of 32%; therefore prodrug **1** was selected for the following *in vivo* studies.

Following pharmacokinetic and biodistribution studies of LPV and alkyl ester prodrug **1**, several major findings are described as follows: Oral administration of unmodified LPV with lipids did not alter the overall oral bioavailability of LPV, but prolonged the half-life of LPV, compared to administration of LPV in lipid-free formulation. In addition, co-administration of lipids led to flip-flop kinetic phenomenon, indicating delayed gastric emptying. Limited numbers of published works reported the oral bioavailability of LPV in animals and humans [66,276,319,334]. Ravi *et al*. reported that the oral bioavailabilities of LPV in different works were 4.6% [319], 5.0% [276] and 12.4% [334], respectively, following oral administration of 20 mg/kg of LPV in sodium citrate solution (3.8%, *w*/*v*) to rats. The oral bioavailability of LPV, reported in our work, are 22.8% and 20.5% (**Table 4-2**, Chapter 4), respectively, following oral administration of 20 mg/kg of LPV in lipid-free formulation and in lipid-based formulation to rats. The closest oral bioavailability to our result is around 25% following oral administration of 10mg/kg of LPV to rats [66]. In addition, it was reported in that work that oral bioavailability was 0% following oral administration of 10 and 5 mg/kg of LPV in monkeys and dogs, respectively, while less than 1% in humans after administration of 400 mg of LPV alone. Therefore, LPV normally is co-administered with a low dose of ritonavir in HIV-infected patients in clinical practice. It was confirmed that the levels of LPV were below the limit of detection in mesenteric lymph and MLNs following administration of unmodified LPV with lipids. Several studies reported the concentrations of LPV in lymph and lymphatic tissues when free LPV was administered in animals [160,275,276,336]. Freeling *et al*. [160] found that the levels of LPV in inguinal lymph nodes were undetectable following subcutaneous administration of free LPV in primates. This is similar to our findings in which the levels of LPV in mesenteric lymph and MLNs were below limit of detection at t_{max} and t_{max-1} h following oral administration in rats (**Figure 4-8**, Chapter 4). This indicates that poor delivery of LPV to lymphatic tissues can be expected when free LPV is administered through either oral or parenteral routes. Different concentrations of LPV in MLNs following oral administration of unmodified LPV in rats were observed by Ravi *et al*. [275,276] and Alex *et al*. [336]. In their findings, approximately 3000 ng/g and 2000 ng/g of LPV were observed in MLNs at 1 h after administration of a 20 mg/kg dose [275,276], and 500 ng/mL of LPV was found in mesenteric lymph fluid at 1 h after administration of a10 mg/kg dose [336]. Moreover, the concentrations of LPV in MLNs at 1 h following oral administration were significantly higher than the levels in plasma at plasma t_{max} [275,276], indicating that LPV was probably delivered to the systemic circulation through intestinal lymphatic transport. However, the calculated absolute oral bioavailability was about 4-fold lower compared to our results. To note, when given orally, LPV is extensively metabolised *via* the hepatic first-pass effect [227], while lipophilic drugs utilising intestinal lymphatic transport can efficiently avoid this effect [104]. Therefore, the relatively high exposure of LPV to MLNs followed by extremely low systemic exposure in works by Ravi *et al*. [275,276] and Alex *et al*. [336] is a bit contradictive. In our work high levels of prodrug were achieved in mesenteric lymph and MLNs (52- and 55-fold higher than plasma) following oral administration of prodrug **1**, but inefficient release of active drug LPV is the drawback of simple alkyl esters (**Figure 4-8** (**B**) and (**C**), Chapter 4). Similar alkyl ester prodrug approach was utilized in our previous work [177] and others' [176,337,338] in which the goals were lymphatic targeting for drugs to work within the lymphatic system and as a secondary goal – the potential effect of lymphatic transport on systemic bioavailability. Lee *et al*. [177] reported that substantial levels of simple ester prodrug of bexarotene were achieved in intestinal lymphatics with 41- and 6.0-fold levels higher in mesenteric lymph and MLNs, respectively, compared to plasma. However, the levels of the released active bexarotene within mesenteric lymph and MLNs were comparable to plasma. To note, in a work by other group, when alkyl ester prodrug approach was applied to mycophenolic acid (MPA) in rats, the levels of 8C-chain alkyl ester prodrug (MPA-C8E) could not be detected in lymph, and only 0.07% of dose of released MPA was found in lymph fluid [337]. In another study, testosterone was assessed for lymphatic transport (%) of dose following oral administration of testosterone undecanoate (11C-chain alkyl ester prodrug) in thoracic duct cannulated dogs [176]. The cumulative recoveries of free testosterone were around 3% of dose after administration of testosterone undecanoate, which significantly improved the systemic exposure compared to administration of unmodified testosterone. Similarly, Sugihara *et al.* [338] reported poor lymphatic absorption of alkyl esters to the lymph (< 3% of dose) for 24 h when administered alkyl ester derivatives of TA-594 and trimetoquinol in rats. Taken together, the data from our work and others suggest that simple alkyl ester prodrug approach may not be the most promising for delivery of active drugs to the lymphatics or improvement of systemic bioavailability through lymphatic transport. The prolonged duration of prodrug **1** and released LPV in systemic blood circulation was observed up to 72 h following oral administration (**Figure 4-7** (**D**), Chapter 4). Similar phenomenon was observed previously following administration of other highly lipophilic compounds, such as dichlorodiphenyltrichloroethane (DDT) [267], lumefantrine [339] and amiodarone [340].

6.1.3. Activated ester prodrugs

Following investigation of alkyl ester prodrugs, it became clear that the efficient release of LPV in rat plasma is a critical step for successful delivery of LPV to mesenteric lymphatic systems. In addition, following the failed codrug approach, the rationale of next designs should maintain similar characteristics of alkyl esters with reasoned modification. Subsequently, two activated esters of LPV were designed and chemically synthesised using the same route of esterification as alkyl esters. Between activated esters, prodrug **7** possessed all the key elements for delivery of LPV to mesenteric lymphatic systems, e.g. high CMs association of 48%, good stability in FaSSIF (half-life: 17.3 h) and rapid release of LPV in plasma (half-life: 0.16 h). As a result, this proposed prodrug approach significantly delivered 10.2- and 6.8-fold higher levels of LPV to the mesenteric lymph and MLNs, respectively, compared to alkyl ester prodrug **1**. In addition, this approach improved oral bioavailability of LPV by nearly 2-fold, as well as prolonged the circulation time compared to unmodified LPV. Taken together, all these achievement take advantage of intestinal lymphatic transport for delivery of drugs to mesenteric lymphatic system, and bypass hepatic first pass metabolism.

A similar lipophilic activated ester prodrug approach was previously reported by our group, and was successfully applied to two anti-cancer agents (bexarotene and retinoic acid) for improvement of active drug delivery to the mesenteric lymphatic system [177]. It was reported that the maximum levels of released bexarotene in MLNs were 2.7-fold higher following oral administration of activated ester of bexarotene, compared to administration of alkyl ester. In other studies, tenofovir (TFV), a nucleotide reverse transcriptase inhibitor, was successfully delivered to the lymphatic system in dogs [341] and HIV-infected patients [178] when prodrug approach was applied to TFV. As a result, following oral administration of activated prodrug tenofovir alafenamide (TAF) in dogs, the levels of TFV in inguinal, axillary, iliac and mesenteric lymph nodes were 15.0-, 14.8-, 10.6- and 5.7-fold higher, respectively, compared to the commercially available prodrug tenofovir disproxil fumarate (TDF) [341]. A recent study has shown that the levels of tenofovir diphosphate (TFV-DP) (pharmacologic-active moiety of TFV) in inguinal lymph nodes were 6.4-fold higher following oral administration of TAF in HIV-infected patients, compared to commercially available prodrug TDF [178]. In our current work, we achieved as high as 6.8-fold higher levels of active drug LPV in MLNs following oral administration of activated ester prodrug **7** in rats, compared to administration of simple alkyl ester prodrug **1** (**Figure 4-9 (B)**, Chapter 4). Even more importantly, the levels of LPV in MLNs were 7.2-fold higher than the protein binding-adjusted IC_{90} (PA-IC_{90}) (140 ng/mL) 3 h following administration of the activated ester prodrug. These high levels of active drug (LPV) ensure reduction in production of infectious virions by infected CD4+ cells in HIV reservoirs within MLNs.

6.1.4. Self-immolative codrugs

The codrug comprises of active drug (LPV), self-immolative linker (salicylic acid) and an enzymatic substrate as a trigger, which is away from the main scaffold in order to reduce steric hindrance of the enzymatic cleavage. All codrugs of LPV and salicylic acid were designed coupled with *in-silico* modification of structures [137]. Following design and synthesis of codrugs, they were subsequently assessed for drug-CMs association and active drugs release in physiological media. All codrugs are less stable and provide faster release of LPV in both tested physiological media (plasma and FaSSIF), compared to alkyl ester prodrugs. In addition, codrugs **2-5** achieved moderate to high association with artificial CMs-like emulsion (Intralipid®). As a result, codrug **4** has good stability in FaSSIF (degradation half-life: 30.5 min), fast release of LPV in rat plasma, and high association with CMs, therefore making it a good candidate for *in vivo* studies. However, the levels of codrug and released LPV were below the limit of detection in blood following oral administration of codrug **4** in lipids. One hypothesis is that codrug **4** was extensively metabolised in the intestinal wall before reaching systemic circulation when it was orally administered in rats. Further investigation of intestinal microsomal stability of codrugs should be conducted to test this hypothesis.

Self-immolative prodrug approaches have been developed to overcome the limitation of inefficient release of active compound in many previous publications [306–311]. It is reported that the half-life of a novel paclitaxel prodrug associated with a self-immolative spacer was 10.5-fold shorter compared to prodrugs containing conventional spacers [342]. To note, for the nearest comparison, in a work by other group self-immolative prodrug approach was applied to acivicin. The half-life was over 3-fold shorter than for carbamate prodrug in rat plasma [343]. This is comparable with our result, showing that the half-life of self-immolative codrug **4** is nearly 5-fold shorter compared to prodrug **1** (shortest simple alkyl ester) (**Figure 5-9** (**A**)).

6.2. Future work

6.2.1. Delivery of other classes of antiretroviral drugs to mesenteric lymphatic system by lipophilic prodrug approach

LPV is recommended as the preferred protease inhibitor (PI) therapy in second-line ART regimen in the latest WHO guidelines (2019) [70]. In addition, combined ART normally consists of three or more different active drugs from two or more classes to achieve efficient treatment, whilst reducing the risk of drug resistance. Therefore, single antiretroviral drug (LPV) has its limitations for further investigation in preclinical and clinical studies. In future work, other classes of antiretroviral drugs, especially those recommended in first-line regimens [70], will be developed for mesenteric lymphatic targeting by lipophilic ester prodrug approach. For the study of delivery of other class of antiretroviral drugs to the mesenteric lymphatic system (as discussed in Section 6.1.3), tenofovir (TFV) was successfully delivered to the lymphatic system (including MLNs) in dogs by prodrug approach [341]. To conclude, efficient delivery of WHO-recommended antiretrovirals to the mesenteric lymphatic system (mainly MLNs) by lipophilic activated prodrugs is a promising approach for reduction of HIV reservoirs.

6.2.2. Delivery of antiretroviral drugs to other lymph nodes or lymphatic tissues

The GALT (mainly MLNs) contains the largest numbers of HIV cellular reservoirs in the body, and is one of the most difficult-to-penetrate reservoirs for antiretroviral drugs targeting [34,109–111]. In this work, selected antiretroviral drug (LPV) was efficiently delivered to the

MLNs and mesenteric lymph by lipophilic activated ester prodrug approach. This approach, especially if can be translated to other antiretroviral drugs, has potential for reducing the size of HIV reservoirs within the mesenteric lymphatic system. However, other lymph nodes and lymphatic tissues are also important anatomical and cellular HIV reservoirs into which antiretroviral drugs poorly penetrate. Therefore, delivery of antiretroviral drugs to the broader lymphatic system in the body can significantly shrink the size of HIV reservoirs compared to mainly targeting single compartment. A number of studies have been carried out by other groups showing that efficient levels of antiretroviral drugs can be delivered to the peripheral lymphoid tissues by nanoparticle approaches [163–165]. To note, lymph nodes were biopsied in anatomical regions after IM injection in these papers above, which means all lymph nodes targeted in these works were from peripheral regions around the site of injection. For example, Hilaire *et al*. [163] prolonged the half-life of rilpivirne (RPV) in blood and improved tissue distribution following single intramuscular (IM) injection of lipophilic RPV prodrug nanoformulation in mice and macaques. In particular, the levels of RPV in lymph nodes were over 20-fold higher at day 56 after injection of 100 mg/kg RPV-eq. of prodrug nanoformulation in mice, compared to unmodified RPV. Moreover, the levels of RPV in lymph nodes were around 16-fold higher 204 days after injection of 45 mg/kg RPV-eq. of prodrug nanoformulation in macaques, compared to unmodified RPV. In another example, Sillman *et al*. [164] found that the levels of dolutegravir (DTG) in lymph nodes were nearly 30-fold higher 28 days after single IM injection of 45 mg/kg DTG-eq. of prodrug nanoformulation in mice, compared to unmodified DTG. In their recent work, the levels of cabotegravir (CAB) in lymph nodes were around 23-fold higher at day 364 after injection of 45 mg/kg CAB-eq. of prodrug nanoformulation in mice, compared to unmodified CAB [165]. Delivery of antiretroviral drugs to HIV reservoirs within global lymphatic system using combined oral lipophilic prodrug (presented in this work) with injectable or transdermal nanoformulation approaches could be a future direction for enhancement of lymphatic targeting efficiency of antiretroviral drugs.

6.2.3. Selection of successful prodrug candidates for assessment of therapeutic efficacy in humanized mice/rats and SIV-infected macaques

Following the assessment of pharmacokinetics and drug distribution to mesenteric lymphatic system in rats, the therapeutic efficacy of potential prodrug candidates can be evaluated using SIV-infected macaques [344,345] or HIV-infected humanized mice/rats models [346–349]. It is very important to evaluate therapeutic efficacy and functional cure using these models prior to clinical trials in patients. The key advantages of SIV-infected macaque models include the ability to extensively study therapeutic efficacy in viral reservoirs (including selective necropsy), and to obtain the parameters that are virtually impossible to assess in humans (such as drug levels in MLNs, brain, spleen etc.). However, the limitations of SIV-infected macaque models include the limited availability, high-cost and difference of infection and pathogenesis between SIV and HIV-1 [344,350]. Recently, HIV-infected humanized mice/rats models have been developed to investigate HIV-1 infection and immunopathogenesis, as well as to investigate HIV vaccine and therapeutics [347,349]. These animal models constructed with human immune system can assist in evaluating of the efficacy of prodrug approach against viral reservoirs more accurately, and are much cheaper compared to non-human primate models. However, rodents are limited in the length of life-span and body size for long-term study, as well as less similar physiological to humans compared to non-human primates. Taken together, the prodrug approach can be tested in various animal models that would fully demonstrate the therapeutic effectiveness against HIV reservoirs (mainly MLNs in this project), thereby achieving the final goal–functional cure.

APPENDICES

Appendix 1. Characterisation of ester prodrugs of lopinavir

1 (lopinavir butyl ester), (3S)-2-(2-(2, 6-dimethylphenoxy) acetamido)-5-((R)-3-methyl-2-(2-oxotetrahydropyrimidin-1(2H)-yl) butanamido)-1, 6-diphenylhexan-3-yl butyrate was synthesised using LPV and butyric acid as the reactants. The purity of the final compound was more than 98% by HPLC-UV, white solid (85% yield), melting point 54.0-56.0°C. H^1 NMR (400 MHz, DMSO-d_6): δ 7.60-7.70 (m, 2H), 7.10-7.27 (m, 10H), 6.99-7.04 (m, 2H), 6.90-6.96 (m, 1H), 6.30 (s, 1H), 5.06-5.14 (m, 1H), 4.61-4.72 (m, 1H), 4.34 (d, J = 10.96 Hz, 1H), 4.13-4.24 (m, 1H), 4.10 (s, 2H), 2.96-3.07 (m, 2H), 2.54-2.93 (m, 6H), 2.29-2.44 (m, 2H), 2.16 (s, 6H), 2.00-2.09 (m, 1H), 1.46-1.76 (m, 6H), 0.92 (t, J = 7.31 Hz, 3H), 0.83 (d, J = 6.4 Hz, 3H), 0.75 (d, J = 6.7 Hz, 3H). ^{13}C NMR (100 MHz, DMSO-d_6): δ 172.31, 169.45, 167.68, 155.45, 154.69, 138.91, 138.41, 130.27, 129.12, 129.04, 128.79, 127.99, 127.9, 126.07, 125.61, 124.21, 72.74, 70.18, 61.46, 50.83, 46.64, 37.32, 37.18, 35.55, 25.40, 21.62, 19.59, 18.66, 18.00, 15.9, 13.5. HR-MS (ESI$^+$): *m/z* [M+ H]$^+$ calculated for $C_{41}H_{55}N_4O_6$, 699.4116, found 699.4102.

2 (lopinavir hexyl ester), (3S)-2-(2-(2,6-dimethylphenoxy)acetamido)-5-((S)-3-methyl-2-(2-oxotetrahydropyrimidin-1(2H)-yl)butanamido)-1,6-diphenylhexan-3-yl hexanoate was synthesised using LPV and hexanoic acid as the reactants. The purity of the final compound was more than 98% by HPLC-UV, white solid (80% yield), melting point 52.0-54.0°C. H^1 NMR (400 MHz, DMSO-d_6): δ 7.58-7.70 (m, 2H), 7.10-7.26 (m, 10H), 6.99-7.04 (m, 2H), 6.91-6.96 (m, 1H), 6.29 (s, 1H), 5.06-5.12 (m, 1H), 4.60-4.69 (m, 1H), 4.33 (d, J = 10.97 Hz, 1H), 4.12-4.22 (m, 1H), 4.09 (s, 2H), 2.96-3.05 (m, 2H), 2.54-2.92 (m, 6H), 2.30-2.43 (m, 2H), 2.15 (s, 6H), 1.89-1.99 (m, 1H), 1.55-1.76 (m, 4H), 1.19-1.32 (m, 6H), 0.80-0.86 (m, 6H), 0.74 (d, J = 6.65 Hz, 3H). ^{13}C NMR (100 MHz, DMSO-d_6): δ 172.44, 169.44, 167.44, 155.43, 154.65, 138.91, 138.39, 130.26, 129.11, 129.03, 128.79, 128.00, 127.9, 126.08, 125.62, 124.22, 72.73, 70.16, 61.44, 50.83, 46.64, 37.31, 37.20, 33.63, 30.72, 25.41, 24.19, 21.81, 21.62, 19.59, 18.67, 15.89, 13.77. HR-MS (ESI^+): *m/z* $[M+H]^+$ calculated for $C_{43}H_{59}N_4O_6$, 727.4429, found 727.4415.

3 (lopinaivr octyl ester), (3S)-2-(2-(2,6-dimethylphenoxy)acetamido)-5-((S)-3-methyl-2-(2-oxotetrahydropyrimidin-1(2H)-yl)butanamido)-1,6-diphenylhexan-3-yl decanoate was synthesised using LPV and octanoic acid as the reactants. The purity of the final compound was more than 95% by HPLC-UV, colourless oil (65% yield). H^1 NMR (400 MHz, DMSO-d_6): δ 7.59-7.66 (m, 2H), 7.10-7.27 (m, 10H), 6.99-7.04 (m, 2H), 6.90-6.96 (m, 1H), 6.28 (s, 1H), 5.06-5.12 (m, 1H), 4.60-4.69 (m, 1H), 4.34 (d, *J* = 11.39 Hz, 1H), 4.12-4.19 (m, 1H), 4.09 (s, 2H), 2.96-3.06 (m, 2H), 2.54-2.92 (m, 6H), 2.34-2.41 (m, 2H), 2.15 (s, 6H), 1.99-2.05 (m, 1H), 1.55-1.74 (m, 4H), 1.19-1.30 (m, 10H), 0.80-0.85 (m, 6H), 0.74 (d, *J* = 6.9 Hz, 3H). ^{13}C NMR (100 MHz, DMSO-d_6): δ 172.44, 169.42, 167.66, 155.43, 154.64, 138.90, 138.38, 130.26, 129.10, 129.03, 128.79, 128.00, 127.9, 126.1, 125.62, 124.23, 72.72, 70.15, 61.44, 50.83, 46.63, 37.33, 37.22, 33.70, 31.11, 28.88, 25.41, 24.62, 23.55, 21.62, 19.59, 18.66, 15.89, 13.77. HR-MS (ESI^+): *m/z* $[M+H]^+$ calculated for $C_{45}H_{63}N_4O_6$, 755.4742, found 755.4737.

4 (lopinavir decanyl ester), (3S)-2-(2-(2,6-dimethylphenoxy)acetamido)-5-((S)-3-methyl-2-(2-oxotetrahydropyrimidin-1(2H)-yl)butanamido)-1,6-diphenylhexan-3-yl dodecanoate was synthesised using LPV and decanoic acid as the reactants. The purity of the final compound was more than 95% by HPLC-UV, colourless oil (89% yield). H^1 NMR (400 MHz, DMSO-d_6): δ 7.58-7.67 (m, 2H), 7.10-7.26 (m, 10H), 6.99-7.04 (m, 2H), 6.90-6.96 (m, 1H), 6.29 (s, 1H), 5.05-5.12 (m, 1H), 4.61-4.70 (m, 1H), 4.34 (d, *J* = 11.07 Hz, 1H), 4.13-4.23 (m, 1H), 4.09 (s, 2H), 2.96-3.07 (m, 2H), 2.53-2.93 (m, 6H), 2.32-2.41 (m, 2H), 2.15 (s, 6H), 1.98-2.09 (m, 1H), 1.53-1.74 (m, 4H), 1.18-1.28 (m,14H), 0.81-0.86 (m, 6H), 0.74 (d, J = 6.65 Hz, 3H). ^{13}C NMR (100 MHz, DMSO-d_6): δ 172.42, 169.43, 167.65, 155.44, 154.64, 138.90, 138.37, 130.24, 129.10, 129.02, 128.78, 127.98, 127.89, 126.09, 125.61, 124.22, 72.74, 70.15, 61.43, 50.82, 46.63, 37.34, 37.26, 33.70, 31.26, 28.92, 28.88, 28.52, 25.40, 24.52, 22.08, 21.62, 19.59, 18.65, 15.90, 13.92. HR-MS (ESI$^+$): m/z [M+ H]$^+$ calculated for $C_{47}H_{67}N_4O_6$, 783.5055, found 783.5035.

5 (lopinavir dodecanyl ester), (3S)-2-(2-(2,6-dimethylphenoxy)acetamido)-5-((S)-3-methyl-2-(2-oxotetrahydropyrimidin-1(2H)-yl)butanamido)-1,6-diphenylhexan-3-yl dodecanoate was synthesised using LPV and dodecanoic acid as the reactants. The purity of the final compound was more than 95% by HPLC-UV, colourless oil (85% yield). H^1 NMR (400 MHz, DMSO-d_6): δ 7.58-7.66 (m, 2H), 7.11-7.28 (m, 10H), 6.99-7.04 (m, 2H), 6.90-6.96 (m, 1H), 6.29 (s, 1H), 5.05-5.12 (m, 1H), 4.60-4.71 (m, 1H), 4.33 (d, J = 11.06 Hz, 1H), 4.12-4.22 (m, 1H), 4.09 (s, 2H), 2.97-3.05 (m, 2H), 2.54-2.92 (m, 6H), 2.34-2.41 (m, 2H), 2.15 (s, 6H), 1.99-2.07 (m, 1H), 1.55-1.74 (m, 4H), 1.18-1.26 (m, 18H), 0.80-0.86 (m, 6H), 0.74 (d, J = 6.6 Hz, 3H). ^{13}C NMR (100 MHz, DMSO-d_6): δ 172.42, 169.42, 167.65, 155.43, 154.64, 138.90, 138.37, 130.24, 129.11, 129.02, 128.78, 127.98, 127.89, 126.08, 125.42, 124.21, 72.75, 70.15, 61.93, 50.82, 46.64, 37.35, 37.27, 33.71, 31.29, 28.99, 28.88, 28.71, 28.52, 25.41, 24.52, 22.09, 21.62, 19.59, 18.65, 15.90, 13.93. HR-MS (ESI$^+$): m/z [M+ H]$^+$ calculated for $C_{49}H_{71}N_4O_6$, 811.5368, found 811.5374.

6 (lopinavir N-Acetylglycylglycinyl ester), (3S)-2-(2-(2,6-dimethylphenoxy)acetamido)-5-((R)-3-methyl-2-(2-oxotetrahydropyrimidin-1(2H)-yl)butanamido)-1,6-diphenylhexan-3-yl acetylglycylglycinate was synthesised using LPV and 2-(2-acetamidoacetamido) acetic acid as the reactants. The purity of the final compound was more than 95% by HPLC-UV, colourless oil (46% yield). H^1 NMR (400 MHz, DMSO-d_6): δ 8.32 (t, *J* = 5.9 Hz, 1H), 8.20 (t, *J* = 5.9 Hz, 1H), 7.70 (d, *J* = 9.7 Hz, 1H), 7.63 (d, *J* = 9.1 Hz, 1H), 7.10-7.25 (m, 10H), 7.00-7.02 (m, 2H), 6.90-6.94 (m, 1H), 6.28 (s, 1H), 5.05-5.09 (m, 1H), 4.70-4.77 (m, 1H), 4.33 (d, *J* = 11 Hz, 1H), 4.14-4.28 (m, 1H), 3.85-4.06 (m, 2H), 3.70-3.72 (m, 2H), 2.98-3.03 (m, 2H), 2.56-2.90 (m, 6H), 2.15 (s, 6H), 2.02-2.06 (m, 1H), 1.54-1.73 (m, 4H), 1.24-1.39 (m, 2H), 1.83 (s, 3H), 0.82 (d, *J* = 6.4 Hz, 3H), 0.74 (d, *J* = 6.7 Hz, 3H). ^{13}C NMR (100 MHz, DMSO-d_6): δ 169.82, 169.69, 169.60, 169.30, 167.89, 155.42, 154.92, 138.87, 138.49, 130.32, 129.16, 129.01, 128.75, 127.99, 127.90, 126.05, 125.61, 124.13, 73.91, 70.28, 61.44, 50.51, 46.65, 41.98, 40.81, 37.28, 37.20, 29.03, 25.39, 22.44, 21.61, 19.63, 18.66, 15.96. HR-MS (ESI^+): *m/z* $[M+H]^+$ calculated for $C_{43}H_{57}N_6O_8$, 785.4232, found 785.4223.

7 (lopinavir butoxyacetyl ester), (2S,3S,5R)-2-(2-(2,6-dimethylphenoxy)acetamido)-5-((S)-3-methyl-2-(2-oxotetrahydropyrimidin-1(2H)-yl)butanamido)-1,6-diphenylhexan-3-yl 2-butoxyacetate was synthesised using LPV and 2-butoxyacetic acid as the reactants. The purity of the final compound was more than 98% by HPLC-UV, white solid (87% yield), melting point 72.0-75.0°C. H^1 NMR (400 MHz, DMSO-d_6): δ 7.68 (d, *J* = 9.1 Hz, 2H), 7.63 (d, *J* = 9.8 Hz, 1H), 7.11-7.28 (m, 10H), 7.00-7.02 (m, 2H), 6.91-6.95 (m, 1H), 6.30 (s, 1H), 5.13-5.17 (m, 1H), 4.66-4.73 (m, 1H), 4.35 (d, *J* = 11 Hz, 1H), 4.12-4.25 (m, 1H), 4.03 (quintet, *J* = 7.0 Hz, 2H), 3.46-3.51 (m, 2H), 2.99-3.04 (m, 2H), 2.57-2.92 (m, 6H), 2.14 (s, 6H), 1.99-2.07 (m, 1H), 1.55-1.77 (m, 4H), 1.15-1.53 (m, 6H), 0.82-0.86 (m, 6H), 0.75 (d, *J* = 6.7 Hz, 3H). ^{13}C NMR (100 MHz, DMSO-d_6): δ 169.90, 169.53, 167.74, 155.44, 154.62, 138.86, 138.34, 130.29, 129.12, 129.02, 128.78, 128.01, 127.91, 126.11, 125.65, 124.24, 73.41, 70.44, 70.13, 61.46, 50.74, 46.68, 37.28, 37.22, 33.63, 31.22, 25.42, 21.63, 20.75, 19.59, 18.73, 18.67, 15.89, 13.66. HR-MS (ESI^+): *m/z* $[M+H]^+$ calculated for $C_{43}H_{58}N_4O_7$, 743.4378, found 743.4384.

Appendix 2. Characterisation of codrugs of lopinavir and salicylic acid

Codrug 1, 2-(3-((2R)-1-(((4S)-5-(2-(2,6-dimethylphenoxy)acetamido)-4-hydroxy-1,6-diphenylhexan-2-yl)amino)-3-methyl-1-oxobutan-2-yl)-2-oxohexahydropyrimidine-1-carbonyl)phenyl acetate. The synthetic scheme was described in **Section 2.3.2**., acetate chloride was used for codrug 2 was acetyl chloride (7.2 mmol). The desired product was a white solid, with the purity of over 95% by HPLC-UV detection. The yield is 11%. H^1 NMR (400 MHz, DMSO-d6, δ = 2.50 ppm): δ 7.80 (d, *J* = 8.47 Hz, 1H), 7.44 (d, *J* = 9.92 Hz, 1H), 7.08-7.27 (m, 10H), 7.00-7.02 (m, 2H), 6.93-6.95 (m, 1H), 4.98 (d, *J* = 5.69 Hz, 1H), 4.02-4.36 (m, 5H), 3.51-3.84 (m, 3H), 2.58-3.10 (m, 6H), 2.14 (s, 6H), 1.98-2.07 (m, 1H), 1.38-1.72 (m, 4H), 1.21-1.36 (m, 3H), 0.78 (d, *J* = 7.42 Hz, 3H), 0.73 (d, *J* = 7.07 Hz, 3H). ^{13}C NMR (100 MHz, DMSO-d6, δ = 39.52 ppm): δ 168.64, 168.50, 168.20, 167.29, 154.50, 152.42, 146.10, 138.97, 138.88, 132.22, 130.24, 129.67, 129.28, 129.12, 128.80, 127.99, 127.65, 127.53, 125.90, 125.61, 125.24, 124.23, 122.33, 70.20, 68.26, 62.21, 52.40, 46.87, 42.73, 37.89, 28.88, 26.07, 23.56, 21.51, 20.64, 19.30, 18.62, 15.86. HR-MS (ESI^+): *m/z* $[M+ H]^+$ calculated for $C_{46}H_{54}N_4O_8$, 791.4014, found 791.4015.

Codrug 2, 2-(3-((2R)-1-(((4S)-5-(2-(2,6-dimethylphenoxy)acetamido)-4-hydroxy-1,6-diphenylhexan-2-yl)amino)-3-methyl-1-oxobutan-2-yl)-2-oxohexahydropyrimidine-1-carbonyl)phenyl butyrate. The synthetic scheme was described in **Section 2.3.2**., specific chloride was used for codrug 2 was butyric chloride (7.2 mmol). The desired product was a white solid, with the purity of over 95% by HPLC-UV detection. The yield is 30%. H^1 NMR (400 MHz, DMSO-d6, δ = 2.50 ppm): δ 7.80 (d, *J* = 8.95 Hz, 1H), 7.44 (d, *J* = 9.69 Hz, 1H), 7.08-7.27 (m, 10H), 7.00-7.02 (m, 2H), 6.93-6.95 (m, 1H), 4.98 (d, *J* = 5.81 Hz, 1H), 4.02-4.36 (m, 5H), 3.51-3.84 (m, 3H), 2.58-3.10 (m, 6H), 2.14 (s, 6H), 1.98-2.07 (m, 1H), 1.38-1.72 (m, 4H), 1.21-1.36 (m, 9H), 0.78 (d, *J* = 6.59 Hz, 3H), 0.73 (d, *J* = 6.48 Hz, 3H). ^{13}C NMR (100 MHz, DMSO-d6, δ = 39.52 ppm): δ 170.98, 168.63, 168.18, 167.30, 154.50, 152.35, 146.08, 138.97, 138.89, 132.33, 130.24, 129.53, 129.29, 129.12, 128.80, 127.99, 127.64, 127.32, 125.91, 125.59, 125.15, 124.24, 122.41, 70.21, 68.26, 62.19, 52.40, 46.88, 42.82, 37.89, 35.21, 28.88, 26.09, 23.56, 22.09, 21.47, 19.27, 18.60, 17.84, 15.86, 13.95, 13.34. HR-MS (ESI$^+$): *m/z* $[M+H]^+$ calculated for $C_{48}H_{58}N_4O_8$, 819.4327, found 819.4369.

Codrug 3, 2-(3-((2R)-1-(((4S)-5-(2-(2,6-dimethylphenoxy)acetamido)-4-hydroxy-1,6-diphenylhexan-2-yl)amino)-3-methyl-1-oxobutan-2-yl)-2-oxohexahydropyrimidine-1-carbonyl)phenyl hexanoate. The synthetic scheme was described in **Section 2.3.2.**, specific chloride was used for codrug 3 was hexanoyl chloride (7.2 mmol). The desired product was a white solid, with the purity of over 95% by HPLC-UV detection. The yield is 59%. H^1 NMR (400 MHz, DMSO-d6, δ = 2.50 ppm): δ 7.80 (d, *J* = 9.00 Hz, 1H), 7.44 (d, *J* = 9.65 Hz, 1H), 7.08-7.27 (m, 10H), 7.00-7.02 (m, 2H), 6.93-6.95 (m, 1H), 4.98 (d, *J* = 5.75 Hz, 1H), 4.02-4.36 (m, 5H), 3.51-3.84 (m, 3H), 2.58-3.10 (m, 6H), 2.14 (s, 6H), 1.98-2.07 (m, 1H), 1.38-1.72 (m, 4H), 1.21-1.36 (m, 13H), 0.78 (d, *J* = 6.61 Hz, 3H), 0.73 (d, *J* = 6.47 Hz, 3H).^{13}C NMR (100 MHz, DMSO-d6, δ = 39.52 ppm): δ 171.11, 168.62, 168.19, 167.30, 154.50, 152.35, 146.10, 138.97, 138.89, 132.31, 130.24, 129.53, 129.30, 129.12, 128.80, 127.99, 127.63, 127.33, 125.91, 125.57, 125.14, 124.43, 122.39, 70.21, 68.26, 67.02, 62.19, 52.39, 46.89, 42.80, 37.90, 33.34, 30.56, 28.89, 26.09, 25.13, 23.89, 23.56, 21.75, 21.49, 19.26, 18.61, 15.86, 13.78. HR-MS (ESI$^+$): *m/z* $[M+H]^+$ calculated for $C_{50}H_{62}N_4O_8$, 847.4640, found 847.4643.

Codrug 4, 2-(3-((2R)-1-(((4S)-5-(2-(2,6-dimethylphenoxy)acetamido)-4-hydroxy-1,6-diphenylhexan-2-yl)amino)-3-methyl-1-oxobutan-2-yl)-2-oxohexahydropyrimidine-1-carbonyl)phenyl octanoate. The synthetic scheme was described in **Section 2.3.2.**, specific chloride was used for codrug 4 was octanoyl chloride (7.2 mmol). The desired product was a white solid, with the purity of over 95% by HPLC-UV detection. The yield is 14%. H^1 NMR (400 MHz, DMSO-d6, δ = 2.50 ppm): δ 7.80 (d, *J* = 8.98 Hz, 1H), 7.44 (d, *J* = 9.67 Hz, 1H), 7.08-7.27 (m, 10H), 7.00-7.02 (m, 2H), 6.93-6.95 (m, 1H), 4.98 (d, *J* = 5.74 Hz, 1H), 4.02-4.36 (m, 5H), 3.51-3.84 (m, 3H), 2.58-3.10 (m, 6H), 2.14 (s, 6H), 1.98-2.07 (m, 1H), 1.38-1.72 (m, 4H), 1.21-1.36 (m, 17H), 0.77 (d, *J* = 6.60 Hz, 3H), 0.72 (d, *J* = 6.49 Hz, 3H). ^{13}C NMR (100 MHz, DMSO-d6, δ = 39.52 ppm): δ 171.12, 168.63, 168.19, 167.30, 154.50, 152.35, 146.10, 138.97, 138.89, 132.32, 130.24, 129.54, 129.30, 129.12, 128.81, 127.99, 127.63, 127.33, 125.91, 125.57, 125.15, 124.24, 122.39, 70.21, 68.26, 62.19, 60.72, 52.40, 46.89, 42.81, 37.90, 33.38, 32.55, 31.29, 31.07, 29.04, 29.01, 28.70, 28.31, 26.10, 25.50, 24.29, 22.09, 22.02, 21.49, 19.26, 18.62, 15.87, 13.91. HR-MS (ESI^+): *m/z* $[M+H]^+$ calculated for $C_{52}H_{66}N_4O_8$, 875.4953, found 875.4926.

Codrug 5, 2-(3-((2R)-1-(((4S)-5-(2-(2,6-dimethylphenoxy)acetamido)-4-hydroxy-1,6-diphenylhexan-2-yl)amino)-3-methyl-1-oxobutan-2-yl)-2-oxohexahydropyrimidine-1-carbonyl)phenyl decanoate. The synthetic scheme was described in **Section 2.3.2.**, specific chloride was used for codrug 5 was decanoyl chloride (7.2 mmol). The desired product was a white solid, with the purity of over 90% by HPLC-UV detection. The yield is 9%. H^1 NMR (400 MHz, DMSO-d6, δ = 2.50 ppm): δ 7.80 (d, *J* = 9.00 Hz, 1H), 7.44 (d, *J* = 9.51 Hz, 1H), 7.08-7.27 (m, 10H), 7.00-7.02 (m, 2H), 6.93-6.95 (m, 1H), 4.98 (d, *J* = 5.76 Hz, 1H), 4.02-4.36 (m, 5H), 3.51-3.84 (m, 3H), 2.58-3.10 (m, 6H), 2.14 (s, 6H), 1.98-2.07 (m, 1H), 1.38-1.72 (m, 4H), 1.21-1.36 (m, 21H), 0.77 (d, *J* = 6.59 Hz, 3H), 0.72 (d, *J* = 6.46 Hz, 3H). ^{13}C NMR (100 MHz, DMSO-d6, δ = 39.52 ppm): δ 171.67, 171.11, 168.62, 168.18, 167.29, 165.64, 154.50, 152.34, 138.97, 138.89, 133.74, 132.32, 130.24, 129.52, 129.30, 129.12, 128.80, 127.98, 127.62, 127.32, 125.90, 125.56, 124.23, 122.38, 70.21, 68.25, 62.18, 52.39, 46.89, 42.80, 37.89, 33.48, 33.37, 31.28, 31.25, 28.85, 28.80, 28.67, 28.62, 28.42, 28.34, 26.09, 24.28, 24.05, 22.09, 21.48, 19.25, 18.62, 15.86, 13.95. HR-MS (ESI$^+$): *m/z* $[M+ H]^+$ calculated for $C_{54}H_{70}N_4O_8$, 903.5266, found 903.5235.

REFERENCE

[1] Centers for Disease Control and Prevention, Kaposi's sarcoma and Pneumocystis pneumonia among homosexual men—New York City and California., MMWR Morb. Mortal Wkly. Rep. 30. (1981) 305–308.

[2] Centers for Disease Control and Prevention, Pneumocystis pneumonia—Los Angeles., MMWR Morb. Mortal Wkly. Rep. 30,. (1981) 250–252.

[3] Centers for Disease Control and Prevention, Persistent, generalized lymphadenopathy among homosexual males., MMWR Morb. Mortal Wkly. Rep. 31,. (1982) 249–251.

[4] Centers for Disease Control and Prevention, Update on acquired immune deficiency syndrome (AIDS)—United States., MMWR Morb. Mortal Wkly. Rep. 31,. (1982) 507–508, 513–514.

[5] Centers for Disease Control and Prevention, Prevention of acquired immune deficiency syndrome (AIDS): report of interagency recommendations., MMWR Morb. Mortal Wkly. Rep. 32,. (1983) 101–103.

[6] F. Barre-Sinoussi, J. Chermann, F. Rey, M. Nugeyre, S. Chamaret, J. Gruest, C. Dauguet, C. Axler-Blin, F. Vezinet-Brun, C. Rouzioux, W. Rozenbaum, L. Montagnier, Isolation of a T-Lymphotropic Retrovirus from a Patient at Risk for Acquired Immune Deficiency Syndrome (AIDS), Science. 220 (1983) 868–871.

[7] R.C. Gallo, S. Salahuddin, M. Popovic, G. Shearer, M. Kaplan, B. Haynes, T. Palker, R. Redfield, J. Oleske, B. Safai, Frequent detection and isolation of cytopathic retroviruses (HTLV-III) from patients with AIDS and at risk for AIDS, Science. 224 (1984) 500–503.

[8] J. Levy, A. Hoffman, S. Kramer, J. Landis, J. Shimabukuro, L. Oshiro, Isolation of lymphocytopathic retroviruses from San Francisco patients with AIDS, Science. 225 (1984) 840–842.

[9] S.G. Deeks, J. Overbaugh, A. Phillips, S. Buchbinder, HIV infection, Nature Reviews Disease Primers. 1 (2015). https://doi.org/10.1038/nrdp.2015.35.

[10] D.E. Mosier, How HIV changes its tropism: evolution and adaptation?, Current Opinion in HIV and AIDS. (2008) 1. https://doi.org/10.1097/COH.0b013e3283223d61.How.

[11] P.R. Gorry, G. Bristol, J.A. Zack, K. Ritola, R. Swanstrom, C.J. Birch, J.E. Bell, N. Bannert, K. Crawford, H.U.I. Wang, D. Schols, E.D.E. Clercq, K. Kunstman, S.M. Wolinsky, D. Gabuzda, Macrophage Tropism of Human Immunodeficiency Virus Type 1 Isolates from Brain and Lymphoid Tissues Predicts Neurotropism Independent of Coreceptor Specificity, Journal of Virology. 75 (2001) 10073–10089. https://doi.org/10.1128/JVI.75.21.10073.

[12] G. Alkhatib, C. Combadiere, C.. Broder, Y. Feng, P.. Kennedy, P.. Murphy, E.. Berger, CC CKR5: A RANTES, MIP-1 , MIP-1 Receptor as a Fusion Cofactor for Macrophage-Tropic HIV-1, Science. 272 (1996) 1955–1958.

[13] H. Deng, R. Liut, W. Ellmeier, S. Choet, D. Unutmaz, M. Burkhart, P. Di Marziot, S. Marmon, R.E. Sutton, C.M. Hill, C.B. Davis, S.C. Peiper, T.J. Schall, D.R. Littman, N.R. Landaut, Identification of a major co-receptor for primary isolates of HIV-1, Nature. 381 (1996) 661–666.

[14] T. Dragic, V. Litwint, G.P. Allawayt, S.R. Martin, Y. Huang, K.A. Nagashimat, C. Cayanan, P.J. Maddont, R.A. Koup, J.P. Moore, W.A. Paxton, T. Aaron, HIV-1 entry into CD4 + cells is mediated by the chemokine receptor CC-CKR-5, Nature. 381 (1996) 667–673.

[15] Y. Feng, C.C. Broder, P.E. Kennedy, E.A. Berger, HIV-1 Entry Cofactor : Functional cDNA Cloning of a Seven-Transmembrane , G Protein-Coupled Receptor, Science. 272 (1996) 872–877.
[16] E.A. Berger, P.M. Murphy, J.M. Farber, CHEMOKINE RECEPTORS AS HIV-1 CORECEPTORS : Roles in Viral Entry , Tropism , and Disease, Annual Review of Immunology. 17 (1999) 657–700.
[17] W. Hu, S.H. Hughes, HIV-1 Reverse Transcription, Cold Spring Harbor Perspectives in Medicine. 2 (2012) a006882–a006882.
[18] R. Craigie, F.D. Bushman, HIV DNA Integration, Cold Spring Harbor Perspectives in Medicine. 2 (2012) a006890–a006890.
[19] W.I. Sundquist, H. Kra, HIV-1 Assembly, Budding, and Maturation, Cold Spring Harbor Perspectives in Medicine. 2 (2012) a006924–a006924.
[20] K.D. Pedro, A.J. Henderson, L.M. Agosto, Mechanisms of HIV-1 cell-to-cell transmission and the establishment of the latent reservoir, Virus Research. 265 (2019) 115–121. https://doi.org/10.1016/j.virusres.2019.03.014.
[21] S. Benichou, Mechanisms for Cell-to-Cell Transmission of HIV-1, Frontiers in Immunology. 9 (2018) 1–14. https://doi.org/10.3389/fimmu.2018.00260.
[22] L.M. Agosto, M.B. Herring, W. Mothes, A.J. Henderson, L.M. Agosto, M.B. Herring, W. Mothes, A.J. Henderson, HIV-1-Infected CD4 + T Cells Facilitate Latent Infection of Resting CD4 + T Cells through Cell-Cell Article HIV-1-Infected CD4 + T Cells Facilitate Latent Infection of Resting CD4 + T Cells through Cell-Cell Contact, CellReports. 24 (2018) 2088–2100. https://doi.org/10.1016/j.celrep.2018.07.079.
[23] J.M. Carr, H. Hocking, P. Li, C.J. Burrell, Rapid and Efficient Cell-to-Cell Transmission of Human Immunodeficiency Virus Infection from Monocyte-Derived Macrophages to Peripheral Blood Lymphocytes, Virology. 329 (1999) 319–329.
[24] P. Chen, W. Hu, M.A. Spinelli, B.K. Chen, Predominant Mode of Human Immunodeficiency Virus Transfer between T Cells Is Mediated by Sustained Env-Dependent Neutralization-Resistant Virological Synapses □ †, Journal of Virology. 81 (2007) 12582–12595. https://doi.org/10.1128/JVI.00381-07.
[25] G. Doitsh, W.C. Greene, S. Francisco, S. Francisco, S. Francisco, S. Francisco, Dissecting How CD4 T Cells Are Lost During HIV Infection, Cell Host Microbe. 19 (2017) 280–291. https://doi.org/10.1016/j.chom.2016.02.012.Dissecting.
[26] M. Vassallo, P. Mercié, J. Cottalorda, M. Ticchioni, P. Dellamonica, The role of lipopolysaccharide as a marker of immune activation in HIV-1 infected patients : a systematic literature review, Virology Journal. 9 (2012) 1–8.
[27] G. Alter, N. Teigen, R. Ahern, H. Streeck, A. Meier, E.S. Rosenberg, M. Altfeld, Evolution of Innate and Adaptive Effector Cell Functions during Acute HIV-1 Infection, The Journal of Infectious Diseases. 195 (2007) 1452–1460. https://doi.org/10.1086/513878.
[28] P. Borrow, Innate immune responses in primary HIV-1 infection Persephone, Current Opinion in HIV and AIDS. 3 (2009) 36–44. https://doi.org/10.1097/COH.0b013e3282f2bce7.Innate.
[29] H. Streeck, J.S. Jolin, Y. Qi, B. Yassine-diab, R.C. Johnson, D.S. Kwon, M.M. Addo, C. Brumme, J. Routy, S. Little, H.K. Jessen, A.D. Kelleher, F.M. Hecht, R. Sekaly, E.S. Rosenberg, B.D. Walker, M. Carrington, M. Altfeld, Human Immunodeficiency Virus Type 1-Specific CD8 + T-Cell Responses during Primary Infection Are Major Determinants of the Viral Set Point and Loss of CD4 + T Cells □ †, Journal of Virology. 83 (2009) 7641–7648. https://doi.org/10.1128/JVI.00182-09.
[30] J.M. Brenchley, T.W. Schacker, L.E. Ruff, D.A. Price, J.H. Taylor, G.J. Beilman, P.L. Nguyen, A. Khoruts, M. Larson, A.T. Haase, D.C. Douek, CD4 + T Cell Depletion

during all Stages of HIV Disease Occurs Predominantly in the Gastrointestinal Tract, The Journal of Experimental Medicine. 200 (2004) 749–759. https://doi.org/10.1084/jem.20040874.
[31] J.M. Brenchley, D.A. Price, T.W. Schacker, T.E. Asher, G. Silvestri, S. Rao, Z. Kazzaz, E. Bornstein, O. Lambotte, D. Altmann, B.R. Blazar, B. Rodriguez, L. Teixeira-Johnson, A. Landay, J.N. Martin, F.M. Hecht, L.J. Picker, M.M. Lederman, S.G. Deeks, D.C. Douek, Microbial translocation is a cause of systemic immune activation in chronic HIV infection, Nature Medicine. 12 (2006) 1365–1371. https://doi.org/10.1038/nm1511.
[32] R.S. Veazey, M. Demaria, L. V Chalifoux, D.E. Shvetz, D.R. Pauley, H.L. Knight, M. Rosenzweig, R.P. Johnson, R.C. Desrosiers, A.A. Lackner, Gastrointestinal Tract as a Major Site of CD4 + T Cell Depletion and Viral Replication in SIV Infection, Science. 280 (1998) 427–431.
[33] J.J. Mattapallil, D.C. Douek, B. Hill, Y. Nishimura, M. Martin, M. Roederer, Massive infection and loss of memory CD4 T cells in multiple tissues during acute SIV infection, Nature. 434 (2005) 1093–1097.
[34] M. Guadalupe, E. Reay, S. Sankaran, T. Prindiville, J. Flamm, A. Mcneil, S. Dandekar, Severe CD4 + T-Cell Depletion in Gut Lymphoid Tissue during Primary Human Immunodeficiency Virus Type 1 Infection and Substantial Delay in Restoration following Highly Active Antiretroviral Therapy, Journal of Virology. 77 (2003) 11708–11717. https://doi.org/10.1128/JVI.77.21.11708.
[35] P.R. Johnson, V.M. Hirsch, SIV Infection of Macaques as a Model for AIDS Pathogenesis, International Reviews of Immunology. 8 (1992) 55–63. https://doi.org/10.3109/08830189209056641.
[36] T.-W. Chun, D. Engel, M.. Berrey, T. Shea, L. Corey, A.. Fauci, Early establishment of a pool of latently infected , resting CD4 + T cells during primary HIV-1 infection, Proceedings of the National Academy of Sciences. 95 (1998) 8869–8873. https://doi.org/10.1073/pnas.1318249111.
[37] T. Chun, J.S. Justement, S. Moir, C.W. Hallahan, J. Maenza, J.I. Mullins, A.C. Collier, L. Corey, A.S. Fauci, Decay of the HIV Reservoir in Patients Receiving Antiretroviral Therapy for Extended Periods : Implications for Eradication of Virus, The Journal of Infectious Diseases. 195 (2007) 1762–1764. https://doi.org/10.1086/518250.
[38] A. Couëdel-Courteille, C. Butor, V. Juillard, J.-G. Guillet, A. Venet, Dissemination of SIV after Rectal Infection Preferentially Involves Paracolic Germinal Centers, Virology. 260 (1999) 277–294.
[39] B.A.I. Spira, P.A. Marx, B.K. Patterson, J. Mahoney, A. Koup, S.M. Wolinsky, D.D. Ho, Cellular targets of infection and route of viral dissemination after an intravaginal inoculation of simian immunodeficiency virus into rhesus macaques., The Journal of Experimental Medicine. 183 (1996) 215–225.
[40] Q. Li, L. Duan, J.D. Estes, Z. Ma, Peak SIV replication in resting memory CD4 + T cells depletes gut lamina propria CD4 + T cells, Nature. 434 (2005) 1148–1152. https://doi.org/10.1038/nature03546.Published.
[41] J.B. Whitney, A.L. Hill, S. Sanisetty, P. Penaloza-macmaster, J. Liu, M. Shetty, L. Parenteau, C. Cabral, J. Shields, S. Blackmore, J.Y. Smith, A.L. Brinkman, L.E. Peter, S.I. Mathew, K.M. Smith, E.N. Borducchi, D.I.S. Rosenbloom, M.G. Lewis, J. Hattersley, B. Li, J. Hesselgesser, R. Geleziunas, M.L. Robb, J.H. Kim, N.L. Michael, D.H. Barouch, Rapid seeding of the viral reservoir prior to SIV viraemia in rhesus monkeys, Nature. 512 (2014) 74–77. https://doi.org/10.1038/nature13594.
[42] G. Dornadula, H. Zhang, B. VanUitert, J. Stern, L. Livornese, M.J. Ingerman, J. Wiek, R.J. Kedanis, J. Natkin, J. DeSimone, R.J. Pomerantz, Residual HIV-1 RNA in Blood

Plasma of Patients Taking Suppressive Highly Active Antiretroviral Therapy, JAMA. 282 (1999) 1627–1632.
[43] D.J. Colby, L. Trautmann, S. Pinyakorn, L. Leyre, A. Pagliuzza, E. Kroon, M. Rolland, H. Takata, S. Buranapraditkun, J. Intasan, N. Chomchey, R. Muir, E.K. Haddad, S. Tovanabutra, S. Ubolyam, D.L. Bolton, B.A. Fullmer, R.J. Gorelick, L. Fox, T.A. Crowell, R. Trichavaroj, R.O. Connell, N. Chomont, J.H. Kim, N.L. Michael, M.L. Robb, N. Phanuphak, J. Ananworanich, Rapid HIV RNA rebound after antiretroviral treatment interruption in persons durably suppressed in Fiebig I acute HIV infection, Nature Medicine. 24 (2018) 923–926. https://doi.org/10.1038/s41591-018-0026-6.
[44] R.T. Davey, N. Bhat, C. Yoder, T. Chun, J.A. Metcalf, R. Dewar, V. Natarajan, R.A. Lempicki, J.W. Adelsberger, K.D. Miller, J.A. Kovacs, M.A. Polis, R.E. Walker, J. Falloon, H. Masur, D. Gee, M. Baseler, D.S. Dimitrov, A.S. Fauci, H.C. Lane, HIV-1 and T cell dynamics after interruption of highly active antiretroviral therapy (HAART) in patients with a history of sustained viral suppression, Proceedings of the National Academy of Sciences. 96 (1999) 1–6. https://doi.org/10.1073/pnas.96.26.15109.
[45] R. Calin, C. Hamimi, S. Lambert-niclot, G. Carcelain, J. Bellet, L. Assoumou, R. Tubiana, V. Calvez, Y. Dudoit, D. Costagliola, B. Autran, C. Katlama, S. Group, Treatment interruption in chronically HIV-infected patients with an ultralow HIV reservoir, AIDS. 30 (2016) 761–769. https://doi.org/10.1097/QAD.0000000000000987.
[46] M.K. Rothenberger, B.F. Keele, S.W. Wietgrefe, C. V Fletcher, G.J. Beilman, J.G. Chipman, A. Khoruts, J.D. Estes, J. Anderson, S.P. Callisto, T.E. Schmidt, A. Thorkelson, C. Reilly, K. Perkey, T.G. Reimann, N.S. Utay, Large number of rebounding / founder HIV variants emerge from multifocal infection in lymphatic tissues after treatment interruption, Proceedings of the National Academy of Sciences. 112 (2015) E1126–E1134. https://doi.org/10.1073/pnas.1414926112.
[47] D.A. Kulpa, N. Chomont, HIV persistence in the setting of antiretroviral therapy : when , where and how does HIV hide ?, Journal of Virus Eradication. (2015) 59–66.
[48] J.D. Siliciano, J. Kajdas, D. Finzi, T.C. Quinn, K. Chadwick, J.B. Margolick, C. Kovacs, J. Stephen, R.F. Siliciano, L. Hiv-, Long-term follow-up studies confirm the stability of the latent reservoir for HIV-1 in resting, Nature Medicine. 9 (2003) 727–728. https://doi.org/10.1038/nm880.
[49] D. Finzi, J. Blankson, J.D. Siliciano, J.B. Margolick, K. Chadwick, T. Pierson, K. Smith, J. Lisziewicz, F. Lori, C. Flexner, T.C. Quinn, R.E. Chaisson, E. Rosenberg, B. Walker, S. Gange, J. Gallant, R.F. Siliciano, Latent infection of CD4 + T cells provides a mechanism for lifelong persistence of HIV-1 , even in patients on effective combination therapy, Nature Medicine. 5 (1999) 512–517.
[50] A.M. Crooks, R. Bateson, A.B. Cope, N.P. Dahl, M.K. Griggs, J.D. Kuruc, C.L. Gay, J.J. Eron, D.M. Margolis, R.J. Bosch, N.M. Archin, Precise Quantitation of the Latent HIV-1 Reservoir : Implications for Eradication Strategies, Journal of Infectious Diseases. 212 (2015) 1361–1365. https://doi.org/10.1093/infdis/jiv218.
[51] L. Shen, R.F. Siliciano, Viral reservoirs, residual viremia, and the potential of highly active antiretroviral therapy to eradicate HIV infection, Journal of Allergy and Clinical Immunology. 122 (2008) 22–28. https://doi.org/10.1016/j.jaci.2008.05.033.Viral.
[52] C. V Fletcher, K. Staskus, S.W. Wietgrefe, M. Rothenberger, C. Reilly, J.G. Chipman, G.J. Beilman, A. Khoruts, A. Thorkelson, T.E. Schmidt, J. Anderson, K. Perkey, M. Stevenson, A.S. Perelson, D.C. Douek, A.T. Haase, T.W. Schacker, Persistent HIV-1 replication is associated with lower antiretroviral drug concentrations in lymphatic

tissues, Proceedings of the National Academy of Sciences. 111 (2014) 2307–2312. https://doi.org/10.1073/pnas.1318249111.
[53] S. Siddiqui, S. Perez, Y. Gao, L. Doyle-Meyers, B.T. Foley, Q. Li, B. Ling, Persistent Viral Reservoirs in Lymphoid Tissues in Suppressive Antiretroviral Therapy, Viruses. 11 (2019) 105. https://doi.org/10.3390/v11020105.
[54] J.D. Estes, C. Kityo, F. Ssali, L. Swainson, K.N. Makamdop, G.Q. Del Prete, S.G. Deeks, P.A. Luciw, J.G. Chipman, G.J. Beilman, T. Hoskuldsson, A. Khoruts, J. Anderson, C. Deleage, J. Jasurda, T.E. Schmidt, M. Hafertepe, S.P. Callisto, H. Pearson, T. Reimann, J. Schuster, J. Schoephoerster, P. Southern, K. Perkey, L. Shang, S.W. Wietgrefe, C. V. Fletcher, J.D. Lifson, D.C. Douek, J.M. McCune, A.T. Haase, T.W. Schacker, Defining total-body AIDS-virus burden with implications for curative strategies, Nature Medicine. 23 (2017) 1271–1276. https://doi.org/10.1038/nm.4411.
[55] M. Horiike, S. Iwami, M. Kodama, A. Sato, Y. Watanabe, M. Yasui, Y. Ishida, T. Kobayashi, T. Miura, T. Igarashi, Lymph nodes harbor viral reservoirs that cause rebound of plasma viremia in SIV-infected macaques upon cessation of combined antiretroviral therapy, Virology. 423 (2012) 107–118. https://doi.org/10.1016/j.virol.2011.11.024.
[56] J.M. Brenchley, D.A. Price, T.W. Schacker, T.E. Asher, G. Silvestri, S. Rao, Z. Kazzaz, E. Bornstein, O. Lambotte, D. Altmann, B.R. Blazar, B. Rodriguez, L. Teixeira-johnson, A. Landay, J.N. Martin, F.M. Hecht, L.J. Picker, M.M. Lederman, S.G. Deeks, D.C. Douek, Microbial translocation is a cause of systemic immune activation in chronic HIV infection, Nature Medicine. 12 (2006) 1365–1371. https://doi.org/10.1038/nm1511.
[57] R. Yarchoan, K.J. Weinhold, H.K.I.M. Lyerly, E. Gelmann, R.M. Blum, G.M. Shearer, J.M. Collins, C.E. Myers, P.D. Markham, D.T. Durack, D.W. Barry, M.A. Fischl, D.P. Bolognesi, S. Broder, Administration of 3´-azido-3´-deoxythymidine, an inhibitor of HTLV-III/LAV replication, to patients with AIDS or AIDS-related complex, The Lancet. 327 (1983) 575–580.
[58] A.S. Perelson, P. Essunger, Y. Cao, M. Vesanen, A. Hurley, K. Saksela, M. Markowitz, D.D. Ho, Decay characteristics of HIV-1-infected compartments during combination therapy, Nature. 387 (1997) 188–191.
[59] L. Zhang, B. Ramratnam, K. Tenner-Racz, Y. He, M. Vesanen, S. Lewin, A. Talal, P. Racz, A.S. Perelson, B.T. Korber, M. Markowitz, Y. Guo, M. Duran, A. Hurley, J. Tsay, Y.-C. Huang, C.-C. Wang, D.D. Ho, QUANTIFYING RESIDUAL HIV-1 REPLICATION IN PATIENTS RECEIVING COMBINATION ANTIRETROVIRAL THERAPY, New England Journal of Medicine. 340 (1999) 1605–1613.
[60] FDA-Approved HIV Medicines, Https://Aidsinfo.Nih.Gov/Understanding-Hiv-Aids/Fact-Sheets/21/58/Fda-Approved-Hiv-Medicines. (2020).
[61] E.J. Arts, D.J. Hazuda, HIV-1 Antiretroviral Drug Therapy, Cold Spring Harbor Perspectives in Medicine. 2 (2012) a007161–a007161.
[62] S. Gulnik, J.W. Erickson, D. Xie, HIV Protease : Enzyme Function and Drug Resistance *, Vitamins & Hormones. 58 (2000) 213–256. https://doi.org/10.1016/S0083-6729(00)58026-1.
[63] E. De Clercq, The history of antiretrovirals : key discoveries over the past 25 years, Reviews in Medical Virology. 19 (2009) 287–299. https://doi.org/10.1002/rmv.624.
[64] S.A. Rabi, R.D. Moore, R.F. Siliciano, S.A. Rabi, G.M. Laird, C.M. Durand, S. Laskey, L. Shan, J.R. Bailey, S. Chioma, R.D. Moore, R.F. Siliciano, Multi-step inhibition explains HIV-1 protease inhibitor pharmacodynamics and resistance Find the latest version : Multi-step inhibition explains HIV-1 protease inhibitor pharmacodynamics and resistance, Journal of Clinical Investigation. 123 (2013) 3848–

3860. https://doi.org/10.1172/JCI67399.3848.
[65] E.M. Mangum, K.K. Graham, Lopinavir-Ritonavir: A New Protease Inhibitor, Pharmacotherapy. 21 (2001) 1352–1363. https://doi.org/10.1592/phco.21.17.1352.34419.
[66] H.L. Sham, D.J. Kempf, A. Molla, K.C. Marsh, G.N. Kumar, C.M. Chen, W. Kati, K. Stewart, R. Lal, A. Hsu, D. Betebenner, M. Korneyeva, S. Vasavanonda, E. McDonald, A. Saldivar, N. Wideburg, X. Chen, P. Niu, C. Park, V. Jayanti, B. Grabowski, G.R. Granneman, E. Sun, A.J. Japour, J.M. Leonard, J.J. Plattner, D.W. Norbeck, ABT-378, a highly potent inhibitor of the human immunodeficiency virus protease, Antimicrobial Agents and Chemotherapy. 42 (1998) 3218–3224. https://doi.org/10.1128/AAC.42.12.3218.
[67] R.A.B. Van Waterschoot, R. Heine, E. Wagenaar, C.M.M. Van Der Kruijssen, R.W. Rooswinkel, A.D.R. Huitema, J.H. Beijnen, A.H. Schinkel, Effects of cytochrome P450 3A (CYP3A) and the drug transporters P-glycoprotein (MDR1 / ABCB1) and MRP2 (ABCC2) on the pharmacokinetics of lopinavir, British Journal of Pharmacology. 160 (2010) 1224–1233. https://doi.org/10.1111/j.1476-5381.2010.00759.x.
[68] N.A. Qazi, J.F. Morlese, A.L. Pozniak, Lopinavir/ritonavir (ABT-378/r), Expert Opinion on Pharmacotherapy. 3 (2002) 315–327. https://doi.org/10.1517/14656566.3.3.315.
[69] World Health Organization, Antiretroviral therapy for HIV infection in adults and adolescents: Recommendations for a public health approach., 2006.
[70] World Health Organization, UPDATE OF FIRST- AND SECOND-LINE ANTIRETROVIRAL REGIMENS, 2019.
[71] World Health Organization, Updated recommendations on first-line and second-line antiretroviral regimens and post-exposure prophylaxis and recommendations on early infant diagnosis of HIV: interim guidelines, 2018.
[72] N.M. Archin, A.L. Liberty, A.D. Kashuba, S.K. Choudhary, J.D. Kuruc, A.M. Crooks, D.C. Parker, E.M. Anderson, M.F. Kearney, M.C. Strain, D.D. Richman, M.G. Hudgens, R.J. Bosch, J.M. Coffin, J.J. Eron, D.J. Hazuda, D.M. Margolis, Administration of vorinostat disrupts HIV-1 latency in patients on antiretroviral therapy, Nature. 489 (2012) 460. https://doi.org/10.1038/nature11286.
[73] S.G. Deeks, Shock and kill, Nature. 487 (2012) 439–440. https://doi.org/10.1038/487439a.
[74] G. Jiang, S. Dandekar, Targeting NF-κB signaling with protein kinase C agonists as an emerging strategy for combating HIV latency, AIDS Research and Human Retroviruses. 31 (2015) 4–12.
[75] S. Lim, C.E. Osuna, P.T. Hraber, J. Hesselgesser, J.M. Gerold, T.L. Barnes, S. Sanisetty, M.S. Seaman, M.G. Lewis, R. Geleziunas, M.D. Miller, T. Cihlar, W.A. Lee, A.L. Hill, J.B. Whitney, TLR7 agonists induce transient viremia and reduce the viral reservoir in SIV-infected rhesus macaques on antiretroviral therapy, Science Translational Medicine. 10 (2018) eaao4521.
[76] T. Cells, G.R. Campbell, R.S. Bruckman, Y. Chu, R.N. Trout, S.A. Spector, G.R. Campbell, R.S. Bruckman, Y. Chu, R.N. Trout, S.A. Spector, SMAC Mimetics Induce Autophagy-Dependent Article SMAC Mimetics Induce Autophagy-Dependent Apoptosis of HIV-1-Infected Resting Memory CD4 + T Cells, Cell Host and Microbe. 24 (2018) 689–702.e7. https://doi.org/10.1016/j.chom.2018.09.007.
[77] G. Darcis, A. Kula, S. Bouchat, K. Fujinaga, F. Corazza, A. Ait-ammar, A. Melard, K. Kabeya, F. Pianowski, L. Gama, C. Schwartz, J. Vila, An In-Depth Comparison of An In-Depth Comparison of Latency-Reversing Agent Combinations in Various In Vitro

and Ex Vivo HIV-1 Latency Models Identified Bryostatin-1+JQ1 and Ingenol-B+JQ1 to Potently Reactivate Viral Gene Expression, PLOS Pathogens. 11 (2015) e1005063. https://doi.org/10.1371/journal.ppat.1005063.

[78] J.H. Elliott, F. Wightman, A. Solomon, K. Ghneim, J. Ahlers, M.J. Cameron, M.Z. Smith, T. Spelman, J. Mcmahon, P. Velayudham, G. Brown, J. Roney, J. Watson, M.H. Prince, J.F. Hoy, N. Chomont, F.A. Procopio, J. Zeidan, S. Palmer, L. Odevall, S.R. Lewin, Activation of HIV Transcription with Short-Course Vorinostat in HIV-Infected Patients on Suppressive Antiretroviral Therapy, PLoS Pathogens. 10 (2014) e1004473. https://doi.org/10.1371/journal.ppat.1004473.

[79] L. Vibholm, M.H. Schleimann, J.F. Højen, T. Benfield, R. Offersen, K. Rasmussen, R. Olesen, Short-Course Toll-Like Receptor 9 Agonist Treatment Impacts Innate Immunity and Plasma Viremia in Individuals With Human Immunodeficiency Virus Infection, Clinical Infectious Diseases. 64 (2017) 1686–1695. https://doi.org/10.1093/cid/cix201.

[80] E.N. Borducchi, J. Liu, P. Joseph, T. Broge, P. Abbink, N.B. Mercado, A. Chandrashekar, D. Jetton, L. Peter, K. Mcmahan, E.T. Moseley, E. Bekerman, J. Hesselgesser, W. Li, M.G. Lewis, G. Alter, R. Geleziunas, Antibody and TLR7 agonist delay viral rebound in SHIV-infected monkeys, Nature. 564 (2018) E8–E8. https://doi.org/10.1038/s41586-018-0600-6.

[81] Y. Ho, L. Shan, N.N. Hosmane, J. Wang, S.B. Laskey, D.I.S. Rosenbloom, J. Lai, J.N. Blankson, J.D. Siliciano, R.F. Siliciano, Replication-Competent Noninduced Proviruses in the Latent Reservoir Increase Barrier to HIV-1 Cure, Cell. 155 (2013) 540–551. https://doi.org/10.1016/j.cell.2013.09.020.

[82] L. Shan, K. Deng, N.S. Shroff, C.M. Durand, S.A. Rabi, H. Yang, H. Zhang, J.B. Margolick, J.N. Blankson, R.F. Siliciano, Stimulation of HIV-1-Specific Cytolytic T Lymphocytes Facilitates Elimination of Latent Viral Reservoir after Virus Reactivation, Immunity. 36 (2012) 491–501. https://doi.org/10.1016/j.immuni.2012.01.014.

[83] K. Deng, M. Pertea, A. Rongvaux, L. Wang, C.M. Durand, G. Ghiaur, J. Lai, H.L. Mchugh, H. Hao, H. Zhang, J.B. Margolick, C. Gurer, A.J. Murphy, D.M. Valenzuela, G.D. Yancopoulos, S.G. Deeks, T. Strowig, P. Kumar, J.D. Siliciano, S.L. Salzberg, Broad CTL response is required to clear latent HIV-1 due to dominance of escape mutations, Nature. 517 (2014) 381–385. https://doi.org/10.1038/nature14053.

[84] J. Rosenthal, W. Tyor, Aging , comorbidities , and the importance of finding biomarkers for HIV-associated neurocognitive disorders, Journal of NeuroVirology. 25 (2019) 673–685.

[85] S. Eilebrecht, V. Le Douce, R. Riclet, B. Targat, V. Driessche, C. Schwartz, H. Hallay, C. Van Lint, O. Rohr, A.G. Benecke, I.H. E, HMGA1 recruits CTIP2-repressed P-TEFb to the HIV-1 and cellular target promoters, Nucleic Acids Research. 42 (2014) 4962–4971. https://doi.org/10.1093/nar/gku168.

[86] C. Méndez, S. Ledger, K. Petoumenos, C. Ahlenstiel, A.D. Kelleher, RNA - induced epigenetic silencing inhibits HIV - 1 reactivation from latency, Retrovirology. 15 (2018) 1–18. https://doi.org/10.1186/s12977-018-0451-0.

[87] V. Interactions, H. Takata, C. Kessing, A. Sy, N. Lima, J. Sciumbata, L. Mori, R.B. Jones, N. Chomont, N.L. Michael, S. Valente, L. Trautmann, Modeling HIV-1 Latency Using Primary CD4+ T Cells from Virally Suppressed HIV-1-Infected Individuals on Antiretroviral Therapy, Journal of Virology. 93 (2019) 1–11.

[88] M.J. Jean, T. Hayashi, H. Huang, J. Brennan, S. Simpson, A. Purmal, K. Gurova, M.C. Keefer, J.J. Kobie, N.G. Santoso, J. Zhu, Curaxin CBL0100 Blocks HIV-1 Replication and Reactivation through Inhibition of Viral Transcriptional Elongation, Frontiers in

Microbiology. 8 (2017) 1–13. https://doi.org/10.3389/fmicb.2017.02007.
[89] C.F. Kessing, C.C. Nixon, C. Li, P.M. Tsai, H. Takata, G. Mousseau, P.T. Ho, J.B. Honeycutt, M. Fallahi, J.V. Garcia, S.T. Valente, In Vivo Suppression of HIV Rebound by Didehydro-Cortistatin A, a “Block-and-Lock” Strategy for HIV-1 Treatment, Cell Reports. 21 (2017) 600–611. https://doi.org/10.1016/j.celrep.2017.09.080.In.
[90] P. Joshi, E. Maidji, C.A. Stoddart, Inhibition of Heat Shock Protein 90 Prevents HIV Rebound, 291 (2016) 10332–10346. https://doi.org/10.1074/jbc.M116.717538.
[91] M.M. Elsheikh, Y. Tang, D. Li, G. Jiang, Deep latency : A new insight into a functional HIV cure, EBioMedicine. 45 (2019) 624–629. https://doi.org/10.1016/j.ebiom.2019.06.020.
[92] M. Di Mascio, J.D. Lifson, S. Srinivasula, I. Kim, P. Degrange, B.F. Keele, A.J. Belli, K.A. Reimann, Y. Wang, M. Proschan, H.C. Lane, A.S. Fauci, Evaluation of an antibody to a 4 b 7 in the control of SIVmac239- nef-stop infection, Science. 365 (2019) 1025–1029.
[93] C.C. Denucci, A.J. Pagán, J.S. Mitchell, J.S. Mitchell, Y. Shimizu, Control of α 4 β 7 Integrin Expression and CD4 T Cell Homing by the β 1 Integrin Subunit, The Journal of Immunology. 184 (2010) 2458–2467. https://doi.org/10.4049/jimmunol.0902407.
[94] A. Sivro, A. Schuetz, D. Sheward, V. Joag, S. Yegorov, L.J. Liebenberg, N. Yende, A. Stalker, R.S. Mwatelah, N. Garrett, N. Samsunder, A. Balgobin, F. Nawaz, J. Arthos, A.S. Fauci, A.O. Anzala, J. Kimani, Integrin α4β7 expression on peripheral blood CD4+ T cells predicts HIV acquisition and disease progression outcomes, Science Translational Medicine. 10 (2019) eaam6354. https://doi.org/10.1126/scitranslmed.aam6354.Integrin.
[95] S. He, Y. Fu, J. Guo, M. Spear, J. Yang, B. Trinité, C. Qin, S. Fu, Y. Jiang, Z. Zhang, J. Xu, H. Ding, D.N. Levy, W. Chen, E.P. Iii, Cofilin hyperactivation in HIV infection and targeting the cofilin pathway using an anti-α4β7 integrin antibody, Science Advances. 5 (2019) eaat7911.
[96] Q. Liu, Y. Lai, P. Zhang, M.K. Louder, A. Pegu, R. Rawi, M. Asokan, X. Chen, C. Shen, G. Chuang, E.S. Yang, H. Miao, Y. Wang, A.S. Fauci, P.D. Kwong, J.R. Mascola, P. Lusso, Improvement of antibody functionality by structure-guided paratope engraftment, Nature Communications. 10 (2019) 1–13. https://doi.org/10.1038/s41467-019-08658-4.
[97] S.N. Byrareddy, J. Arthos, C. Cicala, F. Villinger, K.T. Ortiz, D. Little, N. Sidell, M.A. Kane, J. Yu, J.W. Jones, P.J. Santangelo, C. Zurla, L.R. Mckinnon, K.B. Arnold, C.E. Woody, L. Walter, C. Roos, A. Noll, D. Van Ryk, K. Jelicic, R. Cimbro, S. Gumber, T.G. Parslow, A.S. Fauci, A.A. Ansari, Sustained virologic control in SIV+ macaques after antiretroviral and α4β7 antibody therapy, Science. 354 (2016) 197–202.
[98] S.N. Byrareddy, B. Kallam, J. Arthos, C. Cicala, J. Hiatt, E.N. Kersh, J.M. Mcnicholl, D. Hanson, A. Keith, M. Brameier, L. Walter, K. Rogers, A.E. Mayne, T. Villinger, D. Little, T.G. Parslow, P.J. Santangelo, Targeting α4β7 integrin reduces mucosal transmission of simian immunodeficiency virus and protects gut-associated lymphoid tissue from infection, Nature Medicine. 20 (2014) 1397–1400. https://doi.org/10.1038/nm.3715.Targeting.
[99] M.C. Sneller, K.E. Clarridge, C. Seamon, V. Shi, M.D. Zorawski, J.S. Justement, J. Blazkova, E.D. Huiting, M.A. Proschan, J.R. Mora, M. Shetzline, S. Moir, H.C. Lane, T. Chun, A.S. Fauci, An open-label phase 1 clinical trial of the anti-α4β7 monoclonal antibody vedolizumab in HIV-infected individuals, Science Translational Medicine. 11 (2019) eaax3447.
[100] M. Mcguinty, J. Angel, A. Kumar, R. Sy, S. Murthy, D. Kilby, E. Lavoie, S.B.

Schinkel, N. Tremblay, D.W. Cameron, H. Ctnpt, S. Team, Seeking Suppression in HAVARTI : Viremia & T Cells After Vedolizumab & ATI in HIV / ART, CROI, Seattle, Washington. (2019). https://doi.org/10.1038/nm.3715.Byrareddy.
[101] M.A. Swartz, The physiology of the lymphatic system, Advanced Drug Delivery Reviews. 50 (2001) 3–20.
[102] G.M. Ryan, L.M. Kaminskas, C.J.H. Porter, Nano-chemotherapeutics : Maximising lymphatic drug exposure to improve the treatment of lymph-metastatic cancers, Journal of Controlled Release. 193 (2014) 241–256. https://doi.org/10.1016/j.jconrel.2014.04.051.
[103] M.L. Forchielli, W.A. Walker, The role of gut-associated lymphoid tissues and mucosal defence, British Journal of Nutrition. 1 (2005) 41–48. https://doi.org/10.1079/BJN20041356.
[104] A. Zgair, J.C.M. Wong, P. Gershkovich, Targeting Immunomodulatory Agents to the Gut-Associated Lymphoid Tissue, in: Neuro-Immuno-Gastroenterology, Springer International Publishing Switzerland, 2016: pp. 237–261. https://doi.org/10.1007/978-3-319-28609-9.
[105] R.D. Berg, A.W. Garlingtont, Translocation of Certain Indigenous Bacteria from the Gastrointestinal Tract to the Mesenteric Lymph Nodes and Other Organs in a Gnotobiotic Mouse Model, Infection and Immunity. 23 (1979) 403–411. https://doi.org/10.1128/iai.23.2.403-411.1979.
[106] M.J. Weiss, Cytokines in liver , biliary , and pancreatic disease, Fifth Edition, Elsevier Inc., 2009. https://doi.org/10.1016/B978-1-4377-1454-8.00010-2.
[107] A.J. Macpherson, K. Smith, Mesenteric lymph nodes at the center of immune anatomy, 203 (2006) 497–500. https://doi.org/10.1084/jem.20060227.
[108] B.S. Sheridan, L. Lefrançois, Intraepithelial Lymphocytes: To Serve and Protect, Current Gastroenterology Reports. 12 (2010) 513–521. https://doi.org/10.1007/s11894-010-0148-6.Intraepithelial.
[109] S. Yukl, S. Gianella, E. Sinclair, L. Epling, Q. Li, A.L.M. Choi, V. Girling, T. Ho, P. Li, K. Fujimoto, C.B. Hare, M. Pandori, A.T. Haase, H.F. Günthard, M. Fischer, A. Shergill, K. Mcquaid, D. V Havlir, K. Joseph, Differences in HIV Burden and Immune Activation within the Gut of HIV+ Patients on Suppressive Antiretroviral Therapy, Journal of Infectious Diseases. 202 (2011) 1553–1561. https://doi.org/10.1086/656722.Differences.
[110] S.A. Yukl, A.K. Shergill, T. Ho, M. Killian, V. Girling, L. Epling, P. Li, L.K. Wong, P. Crouch, S.G. Deeks, D. V Havlir, K. Mcquaid, E. Sinclair, J.K. Wong, The Distribution of HIV DNA and RNA in Cell Subsets Differs in Gut and Blood of HIV-Positive Patients on ART : Implications for Viral Persistence, Journal of Infectious Diseases. 208 (2013) 1212–1220. https://doi.org/10.1093/infdis/jit308.
[111] T. Chun, D.C. Nickle, J.S. Justement, J.H. Meyers, C.W. Hallahan, S. Kottilil, S. Moir, J.M. Mican, I. James, D.J. Ward, K.J. A, P.J. Mannon, A.S. Fauci, T. Chun, D.C. Nickle, J.S. Justement, J.H. Meyers, G. Roby, C.W. Hallahan, S. Kottilil, S. Moir, J.M. Mican, J.I. Mullins, D.J. Ward, J.A. Kovacs, P.J. Mannon, A.S. Fauci, Persistence of HIV in Gut-Associated Lymphoid Tissue despite Long-Term Antiretroviral Therapy, Journal of Infectious Diseases. 197 (2008) 714–720. https://doi.org/10.1086/527324.
[112] P. Lerner, M. Guadalupe, R. Donovan, J. Hung, J. Flamm, T. Prindiville, S. Sankaran-walters, M. Syvanen, J.K. Wong, M.D. George, S. Dandekar, The Gut Mucosal Viral Reservoir in HIV-Infected Patients Is Not the Major Source of Rebound Plasma Viremia following Interruption of Highly Active Antiretroviral Therapy, Journal of Virology. 85 (2011) 4772–4782. https://doi.org/10.1128/JVI.02409-10.
[113] B. Vrancken, S. Dellicour, P. Lemey, S. Palmer, D. Scheerder, B. Vrancken, S.

Dellicour, T. Schlub, E. Lee, W. Shao, HIV Rebound Is Predominantly Fueled by Genetically Identical Viral Expansions from Diverse Reservoirs, Cell Host & Microbe. 26 (2019) 347–358. https://doi.org/10.1016/j.chom.2019.08.003.

[114] A. Chaillon, B. Vrancken, D.M. Smith, A. Chaillon, S. Gianella, S. Dellicour, S.A. Rawlings, T.E. Schlub, M.F. De Oliveira, C. Ignacio, M. Porrachia, B. Vrancken, D.M. Smith, HIV persists throughout deep tissues with repopulation from multiple anatomical sources, The Journal of Clinical Investigation. 130 (2020) 1699–1712. https://doi.org/10.1172/JCI134815.

[115] H. Rabezanahary, F. Moukambi, D. Palesch, J. Clain, G. Racine, G. Andreani, G. Benmadid-Laktout, O. Zghidi-Abouzid, C. Soundaramourty, C. Tremblay, G. Silvestri, J. Estaquier, Despite early antiretroviral therapy effector memory and follicular helper CD4 T cells are major reservoirs in visceral lymphoid tissues of SIV-infected macaques, Mucosal Immunology. 13 (2020) 149–160. https://doi.org/10.1038/s41385-019-0221-x.

[116] S.M. Pond, T.N. Tozer, Basic Concepts and Clinical Consequences First-Pass Elimination, Clinical Pharmacokinetics. 25 (1984) 1–25. https://doi.org/10.2165/00003088-198409010-00001.

[117] C.J.H. Porter, W.N. Charman, Uptake of drugs into the intestinal lymphatics, Advanced Drug Delivery Reviews. 25 (1997) 71–89. https://doi.org/10.1016/s0169-409x(96)00492-9.

[118] J.A. Yáñez, S.W.J. Wang, I.W. Knemeyer, M.A. Wirth, K.B. Alton, Intestinal lymphatic transport for drug delivery ☆, Advanced Drug Delivery Reviews. 63 (2015) 923–942. https://doi.org/10.1016/j.addr.2011.05.019.

[119] C.J.H. Porter, N.L. Trevaskis, W.N. Charman, Lipids and lipid-based formulations : optimizing the oral delivery of lipophilic drugs, Nature Reviews Drug Discovery. 6 (2007) 231–248. https://doi.org/10.1038/nrd2197.

[120] N.L. Trevaskis, L.M. Kaminskas, C.J.H. Porter, From sewer to saviour — targeting the lymphatic system to promote drug exposure and activity, Nature Reviews Drug Discovery. 14 (2015) 781–803. https://doi.org/10.1038/nrd4608.

[121] M. Loukas, S.S. Bellary, M. Kuklinski, J. Ferrauiola, A. Yadav, M.M. Shoja, K. Shaffer, R.S. Tubbs, The Lymphatic System : A Historical Perspective, Clinical Anatomy. 24 (2011) 807–816. https://doi.org/10.1002/ca.21194.

[122] S.W. Mcdonald, D. Russell, William Hunter and Lymphatics, Annals of Anatomy - Anatomischer Anzeiger. 218 (2018) 40–48. https://doi.org/10.1016/j.aanat.2018.03.002.

[123] Y. Shiau, Mechanisms of intestinal fat absorption, American Journal of Physiology-Gastrointestinal and Liver Physiology. 240 (1981) G1–G9. https://doi.org/10.1152/ajpgi.1981.240.1.g1.

[124] A.B.W. Thomson, M. Keelan, M.L. Garg, M.T. Clandinin, Intestinal aspects of lipid absorption : in review, Canadian Journal of Physiology and Pharmacology. 67 (1989) 179–191. https://doi.org/10.1139/y89-031.

[125] M.C. Carey, D.M. Small, C.M. Bliss, LIPID DIGESTION AND ABSORPTION, Annual Review of Physiology. 45 (1983) 651–677. https://doi.org/10.1146/annurev.ph.45.030183.003251.

[126] A. Giammanco, A.B. Cefalù, D. Noto, M.R. Averna, The pathophysiology of intestinal lipoprotein production, Frontiers in Physiology. 6 (2015). https://doi.org/10.3389/fphys.2015.00061.

[127] C.M.M. Ii, F. Gorelick, Development and Physiological Regulation of Intestinal Lipid Absorption . II . Dietary lipid absorption , complex lipid synthesis , and the intracellular packaging and secretion of chylomicrons, American Journal of

Physiology-Gastrointestinal and Liver Physiology. 293 (2007) 645–650. https://doi.org/10.1152/ajpgi.00299.2007.
[128] N.A. Abumrad, N.O. Davidson, Role of the gut in lipid homeostasis, Physiological Reviews. 92 (2012) 1061–1085. https://doi.org/10.1152/physrev.00019.2011.
[129] M.M. Hussain, A proposed model for the assembly of chylomicrons, Atherosclerosis. 148 (2000) 1–15. https://doi.org/10.1016/s0021-9150(99)00397-4.
[130] E. Levy, S. Stan, E. Delvin, D. Me, C. Shoulders, C. Garofalo, I. Slight, E. Seidman, Localization of Microsomal Triglyceride Transfer Protein, THE JOURNAL OF BIOLOGICAL CHEMISTRY. 277 (2002) 16470–16477. https://doi.org/10.1074/jbc.M102385200.
[131] I.J. Cartwright, D. Plonné, J.A. Higgins, Intracellular events in the assembly of chylomicrons in rabbit enterocytes, Journal of Lipid Research. 41 (2000) 1728–1739.
[132] K.R. Feingold, C. Grunfeld, Introduction to Lipids and Lipoproteins, in: Endotext [Internet], 2018.
[133] I.J. Goldberg, R.H. Eckel, N.A. Abumrad, Regulation of fatty acid uptake into tissues : lipoprotein lipase- and CD36-mediated pathways, Journal of Lipid Research. 50 (2008) 86–90. https://doi.org/10.1194/jlr.R800085-JLR200.
[134] A.D. Cooper, Hepatic uptake of chylomicron remnants, Journal of Lipid Research. 38 (1997) 2173–2192.
[135] C.J.H. Porter, W.N. Charman, Intestinal lymphatic drug transport: An update, Advanced Drug Delivery Reviews. 50 (2001) 61–80. https://doi.org/10.1016/S0169-409X(01)00151-X.
[136] S. Sengupta, R.F. Siliciano, Targeting the Latent Reservoir for HIV-1, Immunity. 48 (2018) 872–895. https://doi.org/10.1016/j.immuni.2018.04.030.
[137] P. Gershkovich, J. Fanous, B. Qadri, A. Yacovan, S. Amselem, A. Hoffman, The role of molecular physicochemical properties and apolipoproteins in association of drugs with triglyceride-rich lipoproteins: in-silico prediction of uptake by chylomicrons, Journal of Pharmacy and Pharmacology. 61 (2009) 31–39. https://doi.org/10.1211/jpp/61.01.0005.
[138] P. Gershkovich, A. Hoffman, Uptake of lipophilic drugs by plasma derived isolated chylomicrons: Linear correlation with intestinal lymphatic bioavailability, European Journal of Pharmaceutical Sciences. 26 (2005) 394–404. https://doi.org/10.1016/j.ejps.2005.07.011.
[139] A. Zagir, J.B. Lee, J.C.M. Wong, A. Jehan, P.M. Fischer, D.A. Barrett, C.S. Constantinescu, P. Gershkovich, Targeting Cannabidiol to the Intestinal Lymphatic System for Enhanced Immunomodulatory Effects in the Treatment of Autoimmune Diseases, Proceedings of Annual Meeting of American Association of Pharmaceutical Scientists. Denver, US (2016).
[140] L. Koleva, E. Bovt, F. Ataullakhanov, E. Sinauridze, Erythrocytes as Carriers : From Drug Delivery to Biosensors, Pharmaceutics. 12 (2020) 1–44. https://doi.org/10.3390/pharmaceutics12030276.
[141] J. Herskovitz, H.E. Gendelman, HIV and the Macrophage : From Cell Reservoirs to Drug Delivery to Viral Eradication, Journal of Neuroimmune Pharmacology. 14 (2019) 52–67. https://doi.org/10.1007/s11481-018-9785-6.
[142] D.A. Lewis, H.O. Alpar, Therapeutic possibilities of drugs encapsulated in erythrocytes, International Journal of Pharmaceutics. 22 (1984) 137–146. https://doi.org/10.1016/0378-5173(84)90017-6.
[143] K. KINOSITA, T.Y. TSONG, Survival of sucrose-loaded erythrocytes in the circulation, Nature. 272 (1978) 258–260. https://doi.org/10.1038/272258a0.
[144] M. Knutson, M. Wessling-resnick, Iron Metabolism in the Reticuloendothelial, Critical

Reviews in Biochemistry and Molecular Biology. 38 (2003) 61–88. https://doi.org/10.1080/713609210.
[145] M. Magnani, L. Rossi, G. Brandit, G.F. Schiavano, M. Montroni, G. Piedimonte, Targeting antiretroviral nucleoside analogues in phosphorylated form to macrophages : In vitro and in vivo studies, Proceedings of the National Academy of Sciences. 89 (1992) 6477–6481. https://doi.org/10.1073/pnas.89.14.6477.
[146] A. Fraternale, A. Casabianca, C. Orlandi, A. Cerasi, L. Chiarantini, Macrophage protection by addition of glutathione (GSH) - loaded erythrocytes to AZT and DDI in a murine AIDS model, Antiviral Research. 56 (2002) 263–272. https://doi.org/10.1016/s0166-3542(02)00128-6.
[147] L. Rossi, G. Brandi, G.F. Schiavano, E. Balestra, E. Millo, S. Scarfi, G. Damonte, A. Gasparini, M. Magnani, C. Perno, U. Benatti, A.D.E. Flora, Macrophage Protection Against Human Immunodeficiency Virus or Herpes Simplex Virus by Red Blood Cell-Mediated Delivery of a Heterodinucleotide of Azidothymidine and Acyclovir, AIDS Research and Human Retroviruses. 14 (1998) 435–444. https://doi.org/10.1089/aid.1998.14.435.
[148] S. Grimaldi, A. Lisi, D. Pozzi, N. Santoro, Attempts to use liposomes and RISC ghosts as vectors in drug and antisense therapy of virus infection, Research in Virology. 148 (1997) 177–180. https://doi.org/10.1016/s0923-2516(97)89906-2.
[149] M. Hamidi, A. Zarrin, M. Foroozesh, S. Mohammadi-samani, Applications of carrier erythrocytes in delivery of biopharmaceuticals, Journal of Controlled Release. 118 (2007) 145–160. https://doi.org/10.1016/j.jconrel.2006.06.032.
[150] S. Vemuri, C.T. Rhodes, Preparation and characterisation of liposomes as therapeutic delivery systems: a review, Pharmaceutica Acta Helvetiae. 70 (1995) 95–111. https://doi.org/10.1016/0031-6865(95)00010-7.
[151] A. Samad, Y. Sultana, M. Aqil, Liposomal Drug Delivery Systems : An Update Review, Current Drug Delivery. 4 (2007) 297–305. https://doi.org/10.2174/156720107782151269.
[152] J. Bestman-Smith, P. Gourde, A. Désormeaux, M.J. Tremblay, M.G. Bergeron, Sterically stabilized liposomes bearing anti-HLA-DR antibodies for targeting the primary cellular reservoirs of HIV-1, Biochimica et Biophysica Acta (BBA) - Biomembranes. 1468 (2000) 161–174. https://doi.org/10.1016/s0005-2736(00)00254-6.
[153] C.D. Kaur, M. Nahar, N.K. Jain, Lymphatic targeting of zidovudine using surface-engineered liposomes, Journal of Drug Targeting. 16 (2008) 798–805. https://doi.org/10.1080/10611860802475688.
[154] J.-F. Gagné, A. Désormeaux, S. Perron, M.J. Tremblay, M.G. Bergeron, Targeted delivery of indinavir to HIV-1 primary reservoirs with immunoliposomes, Biochimica et Biophysica Acta (BBA) - Biomembranes. 1558 (2002) 198–210. https://doi.org/10.1016/s0005-2736(01)00432-1.
[155] J. Kim, Liposomal drug delivery system, Journal of Pharmaceutical Investigation. 46 (2016) 387–392. https://doi.org/10.1007/s40005-016-0260-1.
[156] S.A. Wissing, O. Kayser, R.H. Müller, Solid lipid nanoparticles for parenteral drug delivery, Advanced Drug Delivery Reviews. 56 (2004) 1257–1272. https://doi.org/10.1016/j.addr.2003.12.002.
[157] A. zur Mühlen, C. Schwarz, W. Mehnert, Solid lipid nanoparticles (SLN) for controlled drug delivery – Drug release and release mechanism, European Journal of Pharmaceutics and Biopharmaceutics. 45 (1998) 149–155. https://doi.org/10.1016/s0939-6411(97)00150-1.
[158] R.H. Müller, M. Radtke, S.A. Wissing, Solid lipid nanoparticles (SLN) and

nanostructured lipid carriers (NLC) in cosmetic and dermatological preparations, Advanced Drug Delivery Reviews. 54 (2002) 131–155. https://doi.org/10.1016/s0169-409x(02)00118-7.
[159] J.P. Freeling, R.J.Y. Ho, Anti-HIV drug particles may overcome lymphatic drug insufficiency and associated HIV persistence, Proceedings of the National Academy of Sciences. 111 (2014) 2512–2513. https://doi.org/10.1073/pnas.1406554111.
[160] J.P. Freeling, J. Koehn, C. Shu, J. Sun, R.J.Y. Ho, Long-acting three-drug combination anti-HIV nanoparticles enhance drug exposure in primate plasma and cells within lymph nodes and blood, AIDS. 29 (2015) 1727. https://doi.org/10.1097/QAD.0000000000000421.
[161] J.P. Freeling, J. Koehn, C. Shu, J. Sun, R.J.Y. Ho, Anti-HIV Drug-Combination Nanoparticles Enhance as Well as Triple-Drug Combination Levels in Cells Within Lymph Nodes and Blood in Primates, AIDS Research and Human Retroviruses. 31 (2015) 107–114. https://doi.org/10.1089/aid.2014.0210.
[162] L.A. Mcconnachie, L.M. Kinman, J. Koehn, J.C. Kraft, S. Lane, W. Lee, A.C. Collier, R.J.Y. Ho, Long-Acting Profile of 4 Drugs in 1 Anti-HIV Nanosuspension in Nonhuman Primates for 5 Weeks After a Single Subcutaneous Injection, Journal of Pharmaceutical Sciences. 107 (2018) 1787–1790. https://doi.org/10.1016/j.xphs.2018.03.005.Long-Acting.
[163] J.R. Hilaire, A.N. Bade, B. Sillman, N. Gautam, J. Herskovitz, B. Laxmi, D. Shetty, M.S. Wojtkiewicz, A. Szlachetka, B.G. Lamberty, S. Sravanam, H.S. Fox, Y. Alnouti, P.K. Dash, J.M. Mcmillan, B.J. Edagwa, H.E. Gendelman, Creation of a long-acting rilpivirine prodrug nanoformulation, Journal of Controlled Release. 311–312 (2019) 201–211. https://doi.org/10.1016/j.jconrel.2019.09.001.
[164] B. Sillman, A.N. Bade, P.K. Dash, B. Bhargavan, T. Kocher, S. Mathews, H. Su, G.D. Kanmogne, L.Y. Poluektova, S. Gorantla, J. Mcmillan, N. Gautam, Y. Alnouti, B. Edagwa, H.E. Gendelman, Creation of a long-acting nanoformulated dolutegravir, Nature Communications. 9 (2018). https://doi.org/10.1038/s41467-018-02885-x.
[165] T.A. Kulkarni, A.N. Bade, B. Sillman, B. Laxmi, D. Shetty, M.S. Wojtkiewicz, N. Gautam, J.R. Hilaire, S. Sravanam, A. Szlachetka, B.G. Lamberty, B.M. Morsey, H.S. Fox, Y. Alnouti, J.M. Mcmillan, R.L. Mosley, J. Meza, P.L. Domanico, T. Yue, G. Moore, B.J. Edagwa, H.E. Gendelman, A year-long extended release nanoformulated cabotegravir prodrug, Nature Materials. (2020). https://doi.org/10.1038/s41563-020-0674-z.
[166] M. Schäfer-korting, W. Mehnert, H. Korting, Lipid nanoparticles for improved topical application of drugs for skin diseases ☆, Advanced Drug Delivery Reviews. 59 (2007) 427–443. https://doi.org/10.1016/j.addr.2007.04.006.
[167] S. Cai, Q. Yang, T.R. Bagby, M.L. Forrest, Lymphatic drug delivery using engineered liposomes and solid lipid nanoparticles ☆, Advanced Drug Delivery Reviews. 63 (2011) 901–908. https://doi.org/10.1016/j.addr.2011.05.017.
[168] P.M. Dandagi, P.D. Patel, A.P. Gadad, A.K. Aravapalli, RES and brain targeting stavudine-loaded solid lipid nanoparticles for AIDS therapy, Asian Journal of Pharmaceutics. 6 (2012) 116. https://doi.org/10.4103/0973-8398.102934.
[169] R. Shegokar, K.K. Singh, Stavudine entrapped lipid nanoparticles for targeting lymphatic HIV reservoirs, Pharmazie. 66 (2011) 264–271. https://doi.org/10.1691/ph.2011.0149.
[170] V. Makwana, R. Jain, K. Patel, M. Nivsarkar, A. Joshi, Solid lipid nanoparticles (SLN) of Efavirenz as lymph targeting drug delivery system : Elucidation of mechanism of uptake using chylomicron flow blocking approach, International Journal of Pharmaceutics. 495 (2015) 439–446. https://doi.org/10.1016/j.ijpharm.2015.09.014.

[171] S. Han, L. Hu, T. Quach, J.S. Simpson, N.L. Trevaskis, C.J.H. Porter, Profiling the Role of Deacylation-Reacylation in the Lymphatic Transport of a Triglyceride-Mimetic Prodrug, Pharmaceutical Research. 32 (2015) 1830–1844. https://doi.org/10.1007/s11095-014-1579-9.
[172] C. Tian, J. Guo, G. Wang, B. Sun, K. Na, X. Zhang, Z. Xu, M. Cheng, Z. He, J. Sun, Efficient Intestinal Digestion and On Site Tumor-Bioactivation are the Two Important Determinants for Chylomicron-Mediated Lymph-Targeting Triglyceride-Mimetic Docetaxel Oral Prodrugs, Advanced Science. 6 (2019) 1901810. https://doi.org/10.1002/advs.201901810.
[173] A. Dahan, R. Duvdevani, I. Shapiro, A. Elmann, E. Finkelstein, A. Hoffman, The oral absorption of phospholipid prodrugs : In vivo and in vitro mechanistic investigation of trafficking of a lecithin-valproic acid conjugate following oral administration, Journal of Controlled Release. 126 (2008) 1–9. https://doi.org/10.1016/j.jconrel.2007.10.025.
[174] S. Han, L. Hu, T. Quach, J.S. Simpson, G.A. Edwards, N.L. Trevaskis, C.J.H. Porter, Lymphatic Transport and Lymphocyte Targeting of a Triglyceride Mimetic Prodrug Is Enhanced in a Large Animal Model: Studies in Greyhound Dogs, Molecular Pharmaceutics. 13 (2016) 3351–3361. https://doi.org/10.1021/acs.molpharmaceut.6b00195.
[175] S. Han, L. Hu, T. Quach, J.S. Simpson, N.L. Trevaskis, C.J.H. Porter, Constitutive Triglyceride Turnover into the Mesenteric Lymph Is Unable to Support Ef fi cient Lymphatic Transport of a Biomimetic Triglyceride Prodrug, Journal of Pharmaceutical Sciences. 105 (2016) 786–796. https://doi.org/10.1002/jps.24670.
[176] D.M. Shackleford, W.A.F. Faassen, N. Houwing, H. Lass, G.A. Edwards, C.J.H. Porter, W.N. Charman, Contribution of Lymphatically Transported Testosterone Undecanoate to the Systemic Exposure of Testosterone after Oral Administration of Two Andriol Formulations in Conscious Lymph Duct-Cannulated Dogs, Journal of Pharmacology and Experimental Therapeutics. 306 (2003) 925–933. https://doi.org/10.1124/jpet.103.052522.after.
[177] J.B. Lee, A. Zgair, J. Malec, T.H. Kim, M.G. Kim, J. Ali, C. Qin, W. Feng, M. Chiang, X. Gao, G. Voronin, A.E. Garces, C.L. Lau, T.H. Chan, A. Hume, T.M. McIntosh, F. Soukarieh, M. Al-Hayali, E. Cipolla, H.M. Collins, D.M. Heery, B.S. Shin, S.D. Yoo, L. Kagan, M.J. Stocks, T.D. Bradshaw, P.M. Fischer, P. Gershkovich, Lipophilic activated ester prodrug approach for drug delivery to the intestinal lymphatic system, Journal of Controlled Release. 286 (2018) 10–19. https://doi.org/10.1016/j.jconrel.2018.07.022.
[178] C. V Fletcher, A.T. Podany, A. Thorkelson, L.C. Winchester, T. Mykris, J. Anderson, S. Jorstad, J. V Baker, T.W. Schacker, The Lymphoid Tissue Pharmacokinetics of Tenofovir Disoproxil Fumarate and Tenofovir Alafenamide in HIV-Infected Persons, Clinical Pharmacology & Therapeutics. (2020). https://doi.org/10.1002/cpt.1883.
[179] N. Das, M. Dhanawat, B. Dash, R.C. Nagarwal, S.K. Shrivastava, Codrug : An efficient approach for drug optimization, European Journal of Pharmaceutical Sciences. 41 (2010) 571–588. https://doi.org/10.1016/j.ejps.2010.09.014.
[180] W.M. Lau, A.W. White, S.J. Gallagher, M. Donaldson, G. Mcnaughton, C.M. Heard, Scope and Limitations of The Co-Drug Approach to Topical Drug Delivery, Current Pharmaceutical Design. 14 (2008) 794–802.
[181] S. De Castro, M.-J. Camarasa, Polypharmacology in HIV inhibition: can a drug with simultaneous action against two relevant targets be an alternative to combination, European Journal of Medicinal Chemistry. 150 (2018) 206–227. https://doi.org/10.1016/j.ejmech.2018.03.007.
[182] K. Ijichi, M. Fujiwara, K. Mori, M. Morozumi, H. Machida, S. Shigeta, K. Konno, T.

Yokota, M. Baba, Antiviral activities of nucleotide heterodimers against human immunodeficiency virus type 1 in vitro, Antiviral Research. 31 (1996) 115–120. https://doi.org/10.1016/0166-3542(96)00945-x.

[183] P. Taylor, M. Taourirte, L.A. Mohamed, A. Rochdi, J.J. Vasseur, S. Fernández, Nucleosides , Nucleotides and Nucleic Acids Chemoenzymatic Syntheses of Homo - and Heterodimers of AZT and d4T , and Evaluation of Their Anti - HIV Activity, Nucleosides, Nucleotides and Nucleic Acids. 23 (2004) 701–714. https://doi.org/10.1081/NCN-120037749.

[184] H. Matsumoto, T. Hamawaki, H. Ota, T. Kimura, T. Goto, K. Sano, Y. Kiso, `Double-Drugs' - A New Class of Prodrug Form of an HIV Protease Inhibitor Conjugated with a Reverse Transcriptase Inhibitor by a Spontaneously Cleavable Linker, Bioorganic & Medicinal Chemistry Letters. 10 (2000) 1227–1231. https://doi.org/10.1016/s0960-894x(00)00202-x.

[185] T. Kimura, H. Matsumoto, T. Matsuda, T. Hamawaki, K. Akaji, Y. Kiso, A new class of anti-HIV agents: Synthesis and activity of conjugates of HIV protease inhibitors with a reverse transcriptase inhibitors, Bioorganic & Medicinal Chemistry Letters. 9 (1999) 803–806. https://doi.org/10.1016/s0960-894x(99)00089-x.

[186] X. Sun, Q. Wu, N. Wang, Y. Cai, X. Lin, Novel mutual pro-drugs of 2′,3′-dideoxyinosine with 3-octadecyloxy-propane-1,2-diol by straightforward enzymatic regioselective synthesis in acetone, Biotechnology Letters. 27 (2005) 113–117. https://doi.org/10.1007/s10529-004-7335-1.

[187] P. Vlieghe, T. Clerc, C. Pannecouque, M. Witvrouw, E. De Clercq, Synthesis of New Covalently Bound K -Carrageenan - AZT Conjugates with Improved Anti-HIV Activities, J. Med. Chem. 45 (2002) 1275–1283. https://doi.org/10.1021/jm010969d.

[188] A. Zgair, J.C.M. Wong, A. Sabri, P.M. Fischer, D.A. Barrett, C.S. Constantinescu, P. Gershkovich, Development of a simple and sensitive HPLC-UV method for the simultaneous determination of cannabidiol and δ^9-tetrahydrocannabinol in rat plasma, Journal of Pharmaceutical and Biomedical Analysis. 114 (2015) 145–151. https://doi.org/10.1016/j.jpba.2015.05.019.

[189] B. Neises, W. Steglich, Simple Method for the Esterification of Carboxylic Acids, Angewandte Chemie International Edition in English. 17 (1978) 522–524. https://doi.org/10.1002/anie.197805221.

[190] H.E. Gottlieb, V. Kotlyar, A. Nudelman, NMR Chemical Shifts of Common Laboratory Solvents as Trace Impurities, The Journal of Organic Chemistry. 62 (1997) 7512–7515. https://doi.org/10.1021/jo971176v.

[191] A. Zgair, J.B. Lee, J.C.M. Wong, D.A. Taha, J. Aram, D. Di Virgilio, J.W. McArthur, Y.K. Cheng, I.M. Hennig, D.A. Barrett, P.M. Fischer, C.S. Constantinescu, P. Gershkovich, Oral administration of cannabis with lipids leads to high levels of cannabinoids in the intestinal lymphatic system and prominent immunomodulation, Scientific Reports. 7 (2017) 1–12. https://doi.org/10.1038/s41598-017-15026-z.

[192] J. Stappaerts, S. Geboers, J. Snoeys, J. Brouwers, J. Tack, P. Annaert, P. Augustijns, Rapid conversion of the ester prodrug abiraterone acetate results in intestinal supersaturation and enhanced absorption of abiraterone : In vitro , rat in situ and human in vivo studies, EUROPEAN JOURNAL OF PHARMACEUTICS AND BIOPHARMACEUTICS. 90 (2015) 1–7. https://doi.org/10.1016/j.ejpb.2015.01.001.

[193] G. Xue-jiao, F. Xue-jiao, Q. Bin, G. Zhi-qiang, A lipophilic prodrug of Danshensu : preparation , characterisation , and in vitro and in vivo evaluation, Chinese Journal of Natural Medicines. 15 (2017) 355–362. https://doi.org/10.1016/S1875-5364(17)30056-0.

[194] M. Marques, Dissolution Media Simulating Fasted and Fed States, Dissolution

Technologies. 11 (2004) 16. https://doi.org/10.14227/DT110204P16.
[195] M.Y.Z. Fanous, A.J. Phillips, J. a Windsor, Mesenteric lymph: the bridge to future management of critical illness, Journal of the Pancreas. 8 (2007) 374–399.
[196] J. Lindena, W. Küpper, I. Trautschold, Catalytic Enzyme Activity Concentration in Thoracic Duct , Liver , and Intestinal Lymph of the Dog , the Rabbit , the Rat and the Mouse, Clinical Chemistry and Laboratory Medicine. 24 (1986) 19–33. https://doi.org/10.1515/cclm.1986.24.1.19.
[197] Y. Wu, M.H. Beddall, J.W. Marsh, Rev-Dependent Indicator T Cell Line, Current HIV Research. 5 (2007) 394–402. https://doi.org/10.2174/157016207781024018.
[198] Y. Fu, S. He, A.A. Waheed, D. Dabbagh, Z. Zhou, B. Trinité, Z. Wang, J. Yu, D. Wang, F. Li, D.N. Levy, H. Shang, E.O. Freed, Y. Wu, PSGL-1 restricts HIV-1 infectivity by blocking virus particle attachment to target cells, Proceedings of the National Academy of Sciences. 117 (2020) 9537–9545. https://doi.org/10.1073/pnas.1916054117.
[199] A. Zgair, J.C.M. Wong, J.B. Lee, J. Mistry, O. Sivak, K.M. Wasan, M.H. Ivo, D.A. Barrett, C.S. Constantinescu, P.M. Fischer, P. Gershkovich, Dietary fats and pharmaceutical lipid excipients increase systemic exposure to orally administered cannabis and cannabis-based medicines, American Journal of Translational Research. 8 (2016) 3448–3459.
[200] J.B. Lee, A. Zgair, T.H. Kim, M.G. Kim, S.D. Yoo, P.M. Fischer, Simple and sensitive HPLC-UV method for determination of bexarotene in rat plasma, Journal of Chromatography B. 1040 (2017) 73–80. https://doi.org/10.1111/j.1095-8649.2005.00727.x.
[201] K. V. Thrivikraman, R.L. Huot, P.M. Plotsky, Jugular vein catheterization for repeated blood sampling in the unrestrained conscious rat, Brain Research Protocols. 10 (2002) 84–94. https://doi.org/10.1016/S1385-299X(02)00185-X.
[202] C. Qin, W. Feng, Y. Chu, J.B. Lee, M. Berton, S. Bettonte, Y.Y. Teo, M.J. Stocks, P.M. Fischer, P. Gershkovich, Development and validation of a cost-effective and sensitive bioanalytical HPLC-UV method for determination of lopinavir in rat and human plasma, Biomedical Chromatography. 34 (2020) e4934. https://doi.org/10.1002/bmc.4934.
[203] V. Oldfield, G.L. Plosker, Lopinavir/ritonavir: A review of its use in the management of HIV infection, Drugs. 66 (2006) 1275–1299. https://doi.org/10.2165/00003495-200666090-00012.
[204] E. Klement-Frutos, S. Burrel, G. Peytavin, S. Marot, M.P. Lê, N. Godefroy, V. Calvez, A.-G. Marcelin, E. Caumes, V. Pourcher, D. Boutolleau, Early administration of ritonavir-boosted lopinavir could prevent severe COVID-19, Journal of Infection. (2020). https://doi.org/10.1016/j.jinf.2020.05.039.
[205] M. Gregoire, P. Le Turnier, B.J. Gaborit, G. Veyrac, Lopinavir pharmacokinetics in COVID-19 patients, Journal of Antimicrobial Chemotherapy. (2020) 5–6. https://doi.org/10.1093/jac/dkaa195.
[206] UNAIDS, GLOBAL HIV AND AIDS STATISTICS FACT SHEET– WORLD AIDS DAY 2019, 2019.
[207] E. Ribera, R.M. Lopez, M. Diaz, L. Pou, L. Ruiz, M. Crespo, C. Azuaje, I. Ruiz, Steady-State Pharmacokinetics of a Double-Boosting Regimen of Saquinavir Soft Gel plus Lopinavir plus Minidose Ritonavir in Human Immunodeficiency Virus-Infected Adults, Antimicrobial Agents and Chemotherapy. 48 (2004) 4256–4262. https://doi.org/10.1128/AAC.48.11.4256.
[208] J.J. Eron, J. Feinberg, H.A. Kessler, H.W. Horowitz, M.D. Witt, F.F. Carpio, D.A. Wheeler, P. Ruane, D. Mildvan, B.G. Yangco, R. Bertz, B. Bernstein, M.S. King, E.

Sun, Once-Daily versus Twice-Daily Lopinavir / Ritonavir in Antiretroviral-Naive HIV-Positive Patients : A 48-Week Randomized Clinical Trial, The Journal of Infectious Diseases. 189 (2004) 265–272. https://doi.org/10.1086/380799.
[209] B.R. Phelps, N. Rakhmanina, Antiretroviral Drugs in Pediatric HIV-Infected Patients Pharmacokinetic and Practical Challenges, Pediatric Drugs. 13 (2011) 175–192. https://doi.org/10.2165/11587300-000000000-00000.
[210] S. Notari, A. Bocedi, G. Ippolito, P. Narciso, L.P. Pucillo, G. Tossini, R.P. Donnorso, F. Gasparrini, P. Ascenzi, Simultaneous determination of 16 anti-HIV drugs in human plasma by high-performance liquid chromatography, Journal of Chromatography B: Analytical Technologies in the Biomedical and Life Sciences. 831 (2006) 258–266. https://doi.org/10.1016/j.jchromb.2005.12.016.
[211] D.R. Weller, R.C. Brundage, H.H. Balfour, H.E. Vezina, An isocratic liquid chromatography method for determining HIV non-nucleoside reverse transcriptase inhibitor and protease inhibitor concentrations in human plasma, Journal of Chromatography B. 848 (2007) 369–373. https://doi.org/10.1016/j.jchromb.2006.10.022.
[212] N.L. Rezk, R.R. Tidwell, A.D.M. Kashuba, High-performance liquid chromatography assay for the quantification of HIV protease inhibitors and non-nucleoside reverse transcriptase inhibitors in human plasma, Journal of Chromatography B. 805 (2004) 241–247. https://doi.org/10.1016/j.jchromb.2004.03.002.
[213] J. Faux, N. Venisse, J.C. Olivier, S. Bouquet, Rapid high-performance liquid chromatography determination of lopinavir, a novel HIV-1 protease inhibitor, in human plasma, Chromatographia. 54 (2001) 469–473. https://doi.org/10.1007/BF02491201.
[214] J. Poirier, P. Robidou, P. Jaillon, Simple and Simultaneous Determination of the Nelfinavir Metabolite and the Nonnucleoside Reverse Transcriptase Inhibitors Efavirenz and Nevirapine in Human Plasma by Reversed-Phase Liquid Chromatography, Therapeutic Drug Monitoring. 27 (2005) 186–192. https://doi.org/10.1097/01.ftd.0000152680.36517.5d.
[215] J. Ray, E. Pang, D. Carey, Simultaneous determination of indinavir, ritonavir and lopinavir (ABT 378) in human plasma by high-performance liquid chromatography, Journal of Chromatography B. 775 (2002) 225–230. https://doi.org/10.1016/S1570-0232(02)00295-7.
[216] U.S. Justesen, C. Pedersen, N.A. Klitgaard, Simultaneous quantitative determination of the HIV protease inhibitors indinavir, amprenavir, ritonavir, lopinavir, saquinavir, nelfinavir and the nelfinavir active metabolite M8 in plasma by liquid chromatography, Journal of Chromatography B. 783 (2003) 491–500. https://doi.org/10.1016/S1570-0232(02)00728-6.
[217] J. Martin, G. Deslandes, E. Dailly, C. Renaud, V. Reliquet, F. Raffi, P. Jolliet, A liquid chromatography-tandem mass spectrometry assay for quantification of nevirapine, indinavir, atazanavir, amprenavir, saquinavir, ritonavir, lopinavir, efavirenz, tipranavir, darunavir and maraviroc in the plasma of patients infected with HIV, Journal of Chromatography B. 877 (2009) 3072–3082. https://doi.org/10.1016/j.jchromb.2009.07.031.
[218] R.C.E. Estrela, F.S. Ribeiro, B. V. Seixas, G. Suarez-Kurtz, Determination of lopinavir and ritonavir in blood plasma, seminal plasma, saliva and plasma ultra-filtrate by liquid chromatography/tandem mass spectrometry detection, Rapid Communications in Mass Spectrometry. 22 (2008) 657–664. https://doi.org/10.1002/rcm.3411.
[219] G.A. Temghare, S.S. Shetye, S.S. Joshi, Rapid and sensitive method for quantitative determination of lopinavir and ritonavir in human plasma by liquid chromatography-

tandem mass specrtometry, E-Journal of Chemistry. 6 (2009) 223–230. https://doi.org/10.1155/2009/709478.
[220] L. Else, V. Watson, J. Tjia, A. Hughes, M. Siccardi, S. Khoo, D. Back, Validation of a rapid and sensitive high-performance liquid chromatography-tandem mass spectrometry (HPLC-MS/MS) assay for the simultaneous determination of existing and new antiretroviral compounds, Journal of Chromatography B. 878 (2010) 1455–1465. https://doi.org/10.1016/j.jchromb.2010.03.036.
[221] R. Vats, A.N. Murthy, P.R. Ravi, Simple, rapid and validated LC determination of lopinavir in rat plasma and its application in pharmacokinetic studies, Scientia Pharmaceutica. 79 (2011) 849–863. https://doi.org/10.3797/scipharm.1107-24.
[222] E. Tjøtta, O. Hungnes, B. Grinde, Survival of HIV-1 Activity After Disinfection , Temperature and pH Changes , or Drying, Journal of Medical Virology. 35 (1991) 223–227. https://doi.org/10.1002/jmv.1890350402.
[223] W. Egge-Jacobsen, M. Unger, C.U. Niemann, M. Baluom, S. Hirai, L.Z. Benet, U. Christians, Automated, fast, and sensitive quantification of drugs in human plasma by LC/LC-MS: Quantification of 6 protease inhibitors and 3 nonnucleoside transcriptase inhibitors, Therapeutic Drug Monitoring. 26 (2004) 546–562. https://doi.org/10.1097/00007691-200410000-00014.
[224] A.D. Avolio, M. Simiele, M. Siccardi, L. Baietto, M. Sciandra, V. Oddone, F.R. Stefani, S. Agati, J. Cusato, S. Bonora, G. Di Perri, A HPLC – MS method for the simultaneous quantification of fourteen antiretroviral agents in peripheral blood mononuclear cell of HIV infected patients optimized using medium corpuscular volume evaluation, Journal of Pharmaceutical and Biomedical Analysis. 54 (2011) 779–788. https://doi.org/10.1016/j.jpba.2010.10.011.
[225] Food and Drug Administration, Bioanalytical Method Validation Guidance for Industry, U.S. Department of Health and Human Services. (2018) 1–41.
[226] J. Ford, S.H. Khoo, D.J. Back, The intracellular pharmacology of antiretroviral protease inhibitors, Journal of Antimicrobial Chemotherapy. 54 (2004) 982–990. https://doi.org/10.1093/jac/dkh487.
[227] G.N. Kumar, V.K. Jayanti, M.K. Johnson, J. Uchic, S. Thomas, R.D. Lee, B.A. Grabowski, H.L. Sham, D.J. Kempf, J.F. Denissen, K.C. Marsh, E. Sun, S.A. Roberts, Metabolism and Disposition of the HIV-1 Protease Inhibitor Lopinavir (ABT-378) Given in Combination with Ritonavir in Rats, Dogs, and Humans, Pharmaceutical Research. 21 (2004) 1622–1630. https://doi.org/10.1023/b:pham.0000041457.64638.8d.
[228] K. Dunnington, N. Benrimoh, C. Brandquist, N. Cardillo-marricco, M. Di Spirito, J. Grenier, Application of Pharmacokinetics in Early Drug Development Development-Chapter 4, 2018. https://doi.org/10.5772/intechopen.74189.
[229] E.M. Isin, C.S. Elmore, G.N. Nilsson, R.A. Thompson, L. Weidolf, Use of Radiolabeled Compounds in Drug Metabolism and Pharmacokinetic Studies, Chemical Research in Toxicology. 25 (2012) 532–542.
[230] M.G. Barry, C. Merry, J. Lloyd, K. Halifax, P. Carey, F. Mulcahy, D.J. Back, Variability in trough plasma saquinavir concentrations in HIV patients—a case for therapeutic drug monitoring, British Journal of Clinical Pharmacology. 45 (1998) 501–502. https://doi.org/10.1046/j.1365-2125.1998.00714.x.
[231] M.B. Regazzi, P. Villani, R. Maserati, L. Cocchi, R. Giacchino, D. Burroni, M. Rettani, Pharmacokinetic variability and strategy for therapeutic drug monitoring of saquinavir (SQV) in HIV-1 infected individuals, British Journal of Clinical Pharmacology. 47 (1999) 379–382. https://doi.org/10.1046/j.1365-2125.1999.00919.x.
[232] M.R. Van Der Leur, D.M. Burger, C.J.L. Porte, P.P. Koopmans, A Retrospective TDM

Database Analysis of Interpatient Variability in the Pharmacokinetics of Lopinavir in HIV-infected Adults, Therapeutic Drug Monitoring. 28 (2006) 650–653. https://doi.org/10.1097/01.ftd.0000245681.12092.d6.
[233] M.L. Montes, F. Pulido, C. Barros, E. Condes, R. Rubio, F. Dronda, A. Antela, E. Navas, P. Miralles, J. Berenguer, S. Pe, J.R. Arribas, J.M. Pen, Lipid disorders in antiretroviral-naive patients treated with lopinavir/ritonavir-based HAART: frequency, characterisation and risk factors, Journal of Antimicrobial Chemotherapy. 55 (2005) 800–804. https://doi.org/10.1093/jac/dki063.
[234] S. Limsreng, O. Marcy, S. Ly, V. Ouk, H. Chanroeurn, Dyslipidemias and Elevated Cardiovascular Risk on Lopinavir-Based Antiretroviral Therapy in Cambodia, PLOS ONE. 11 (2016) e0160306. https://doi.org/10.1371/journal.pone.0160306.
[235] Gutiérrez，Félix, Padilla，Sergio, Navarro，Andrés, Masiá，Mar, Hernández，Ildefonso, Ramos，José, Esteban，Angel, Martin-Hidalgo，Alberto, Lopinavir Plasma Concentrations and Changes in Lipid Levels During Salvage Therapy with Lopinavir/Ritonavir-Containing Regimens, Journal of Acquired Immune Deficiency Syndromes. 33 (2003) 594–600. https://doi.org/10.1097/00126334-200308150-00007.
[236] M. Boffito, E. Acosta, D. Burger, C. V Fletcher, C. Flexner, R. Garaffo, Current status and future prospects of therapeutic drug monitoring and applied clinical pharmacology in antiretroviral therapy, Antiviral Therapy. 10 (2005) 375–392.
[237] D. Breilh, I. Pellegrin, K. Berthoin, F. Xuereb, Virological, intracellular and plasma pharmacological parameters predicting response to lopinavir/ritonavir (KALEPHAR Study), AIDS. 18 (2004) 1305–1310. https://doi.org/10.1097/01.aids.0000125993.32646.b1.
[238] B. Masquelier, D. Breilh, D. Neau, S. Lawson-ayayi, J. Ragnaud, M. Dupon, P. Morlat, F. Dabis, H. Fleury, P. Ame, Human Immunodeficiency Virus Type 1 Genotypic and Pharmacokinetic Determinants of the Virological Response to Lopinavir-Ritonavir-Containing Therapy in Protease Inhibitor-Experienced Patients, Antimicrobial Agents and Chemotherapy. 46 (2002) 2926–2932. https://doi.org/10.1128/AAC.46.9.2926.
[239] T. Puthanakit, K. Chokephaibulkit, P. Suntarattiwong, M. Gorowara, N. Vanprapar, P. Leawsrisuk, T. Suwanlerk, P. Boonrak, K. Ruxrungtham, Therapeutic drug monitoring of lopinavir in HIV infected children receiving adult tablets, The Pediatric Infectious Disease Journal. 29 (2010) 79–82. https://doi.org/10.1097/inf.0b013e3181b21040.
[240] S. Agarwal, S.H.S. Boddu, R. Jain, S. Samanta, D. Pal, A.K. Mitra, Peptide prodrugs: Improved oral absorption of lopinavir, a HIV protease inhibitor, International Journal of Pharmaceutics. 359 (2008) 7–14. https://doi.org/10.1016/j.ijpharm.2008.03.031.
[241] M. Wang, M.S. Halquist, Y. Zhang, P.M. Gerk, Simultaneous determination of lopinavir and three ester prodrugs by LC – MS / MS in lysates of BeWo cells, Journal of Chromatography B. 975 (2015) 84–90. https://doi.org/10.1016/j.jchromb.2014.10.032.
[242] C. Qin, Y. Chu, W. Feng, C. Fromont, S. He, J. Ali, J. Bong, A. Zgair, M. Berton, S. Bettonte, R. Liu, L. Yang, A. Alonso, R. Ugalde, D. Vetrugno, S.Y. Ee, C. Sheriston, Y. Wu, M.J. Stocks, P.M. Fischer, P. Gershkovich, Targeted delivery of lopinavir to HIV reservoirs in the mesenteric lymphatic system by lipophilic ester prodrug approach, Journal of Controlled Release. (2020). https://doi.org/10.1016/j.jconrel.2020.10.036.
[243] S.M. Hammer, K.E. Squires, M.D. Hughes, J.M. Grimes, L.M. Demeter, J.S. Currier, J.J. Eron, J.E. Feinberg, H.H. Balfour, L.R. Deyton, J.A. Chodakewitz, M.A. Fischl, J.P. Phair, L. Pedneault, B.-Y. Nguyen, J.C. Cook, A Controlled Trial of Two

Nucleoside Analogues plus Indinavir in Persons with Human Immunodeficiency Virus Infection and CD4 Cell Counts of 200 per Cubic Millimeter or Less, New England Journal of Medicine. 337 (1997) 725–733. https://doi.org/10.1056/nejm199709113371101.
[244] R.M. Gulick, J.W. Mellors, D. Havlir, J.J. Eron, C. Gonzalez, D. McMahon, D.D. Richman, F.T. Valentine, L. Jonas, A. Meibohm, E.A. Emini, J.A. Chodakewitz, P. Deutsch, D. Holder, W.A. Schleif, J.H. Condra, Treatment with Indinavir, Zidovudine, and Lamivudine in Adults with Human Immunodeficiency Virus Infection and Prior Antiretroviral Therapy, New England Journal of Medicine. 337 (1997) 734–739. https://doi.org/10.1056/nejm199709113371102.
[245] SMART, CD4+ Count–Guided Interruption of Antiretroviral Treatment, New England Journal of Medicine. 355 (2006) 2283–2296. https://doi.org/10.1056/nejmoa062360.
[246] P.G. Cardiello, E. Hassink, J. Ananworanich, P. Srasuebkul, T. Samor, A. Mahanontharit, K. Ruxrungtham, B. Hirschel, J. Lange, P. Phanuphak, D.A. Cooper, A Prospective, Randomized Trial of Structured Treatment Interruption for Patients with Chronic HIV Type 1 Infection, Clinical Infectious Diseases. 40 (2005) 594–600. https://doi.org/10.1086/427695.
[247] E. Eisele, R.F. Siliciano, Redefining the Viral Reservoirs that Prevent HIV-1 Eradication, Immunity. 37 (2012) 377–388. https://doi.org/10.1016/j.immuni.2012.08.010.Redefining.
[248] J. Ananworanich, A. Schuetz, C. Vandergeeten, I. Sereti, M. De, R. Rerknimitr, R. Dewar, M. Marovich, F. Van Griensven, R. Sekaly, S. Pinyakorn, N. Phanuphak, R. Trichavaroj, W. Rutvisuttinunt, N. Chomchey, R. Paris, S. Peel, V. Valcour, F. Maldarelli, N. Chomont, N. Michael, P. Phanuphak, J.H. Kim, Impact of Multi-Targeted Antiretroviral Treatment on Gut T Cell Depletion and HIV Reservoir Seeding during Acute HIV Infection, PLoS ONE. 7 (2012) e33948. https://doi.org/10.1371/journal.pone.0033948.
[249] J. Ananworanich, C.P. Sacdalan, S. Pinyakorn, N. Chomont, M. De Souza, T. Luekasemsuk, A. Schuetz, S.J. Krebs, R. Dewar, L. Jagodzinski, S. Ubolyam, R. Trichavaroj, S. Tovanabutra, S. Spudich, V. Valcour, I. Sereti, N. Michael, M. Robb, P. Phanuphak, J.H. Kim, N. Phanuphak, Virological and immunological characteristics of HIV-infected individuals at the earliest stage of infection, Journal of Virus Eradication. 2 (2016) 43–48.
[250] T. Schacker, S. Little, E. Connick, K. Gebhard, Z. Zhang, J. Krieger, J. Pryor, D. Havlir, J.K. Wong, R.T. Schooley, D. Richman, Productive Infection of T Cells in Lymphoid Tissues during Primary and Early Human Immunodeficiency Virus Infection, The Journal of Infectious Diseases. 183 (2001) 555–562. https://doi.org/10.1086/318524.
[251] T.-W. Chun, L. Stuyver, S.B. Mizell, L.A. Ehler, J.A.M. Mican, M. Baseler, A.L. Lloyd, M.A. Nowak, A.S. Fauci, Presence of an inducible HIV-1 latent reservoir during highly active antiretroviral therapy, Proceedings of the National Academy of Sciences. 94 (1997) 13193–13197. https://doi.org/10.1073/pnas.94.24.13193.
[252] D. Finzi, M. Hermankova, T. Pierson, L.M. Carruth, C. Buck, R.E. Chaisson, T.C. Quinn, K. Chadwick, J. Margolick, R. Brookmeyer, J. Gallant, M. Markowitz, D.D. Ho, D.D. Richman, R.F. Siliciano, Identification of a Reservoir for HIV-1 in Patients on Highly Active Antiretroviral Therapy, Science. 278 (1997) 1295–1300. https://doi.org/10.1126/science.278.5341.1295.
[253] R. Lorenzo-redondo, H.R. Fryer, T. Bedford, E. Kim, J. Archer, S.L.K. Pond, Y. Chung, S. Penugonda, J.G. Chipman, V. Fletcher, Courtney, T.W. Schacker, M.H. Malim, A. Rambaut, A.T. Haase, A.R. McLean, S.M. Wolinsky, Persistent HIV-1

replication maintains the tissue reservoir during therapy, Nature. 530 (2016) 51–56. https://doi.org/10.1038/nature16933.
[254] J.D. Siliciano, J. Kajdas, D. Finzi, T.C. Quinn, K. Chadwick, J.B. Margolick, C. Kovacs, S.J. Gange, R.F. Siliciano, Long-term follow-up studies confirm the stability of the latent reservoir for HIV-1 in resting, Nature Medicine. 9 (2003) 727–728. https://doi.org/10.1038/nm880.
[255] R. Rajasuriar, E. Wright, S.R. Lewin, Impact of antiretroviral therapy (ART) timing on chronic immune activation/inflammation and end-organ damage, Current Opinion in HIV and AIDS. 10 (2015) 35–42. https://doi.org/10.1097/coh.0000000000000118.
[256] W.N.A. Charman, V.J. Stella, Estimating the maximal potential for intestinal lymphatic transport of lipophilic drug molecules, International Journal of Pharmaceutics. 34 (1986) 175–178. https://doi.org/10.1016/0378-5173(86)90027-x.
[257] N.L. Trevaskis, W.N. Charman, C.J.H. Porter, Lipid-based delivery systems and intestinal lymphatic drug transport: A mechanistic update, Advanced Drug Delivery Reviews. 60 (2008) 702–716. https://doi.org/10.1016/j.addr.2007.09.007.
[258] Y. Chu, C. Qin, W. Feng, J. Ali, C. Sheriston, B. Ling, M. Stocks, P. Fischer, P. Gershkovich, Targeting tipranavir to mesenteric lymph nodes (MLNs) for improved treatment of HIV/AIDS, in: 23rd International AIDS Conference, 2020.
[259] J.M. Férriz, J. Vin, Prodrug Design of Phenolic Drugs, Current Pharmaceutical Design. 16 (2010) 2033–2052. https://doi.org/10.2174/138161210791293042.
[260] T.L. Huang, T. Shiotsuki, T. Uematsu, B. Borhan, Q.X. Li, B.D. Hammock, Structure activity relationships for substrates and inhibitors of mammalian liver microsomal carboxylesterases, Pharmaceutical Research. 13 (1996) 1495–1500. https://doi.org/10.1023/A:1016071311190.
[261] V. Bala, S. Rao, P. Li, S. Wang, C.A. Prestidge, Lipophilic Prodrugs of SN38 : Synthesis and in Vitro Characterisation toward Oral Chemotherapy, Molecular Pharmaceutics. 13 (2016) 287–294. https://doi.org/10.1021/acs.molpharmaceut.5b00785.
[262] P. Gershkovich, E.K. Wasan, M. Lin, O. Sivak, C.G. Leon, J.G. Clement, K.M. Wasan, Pharmacokinetics and biodistribution of amphotericin B in rats following oral administration in a novel lipid-based formulation, Journal of Antimicrobial Chemotherapy. 65 (2009) 101–108. https://doi.org/10.1093/jac/dkp140.
[263] G.S.K.K. Reddy, A. Ali, M.N.L. Nalam, S.G. Anjum, H. Cao, R.S. Nathans, C.A. Schiffer, T.M. Rana, Design and Synthesis of HIV-1 Protease Inhibitors Incorporating Oxazolidinones as P2/P2′ Ligands in Pseudosymmetric Dipeptide Isosteres, Journal of Medicinal Chemistry. 50 (2007) 4316–4328. https://doi.org/10.1021/jm070284z.Design.
[264] J.-F. Liotard, M. Mehiri, A. Di Giorgio, N. Boggetto, M. Reboud-Ravaux, A.-M. Aubertin, R. Condom, N. Patino, AZT and AZT-monophosphate Prodrugs Incorporating HIV-protease Substrate Fragment: Synthesis and Evaluation as Specific Drug Delivery Systems, Antiviral Chemistry and Chemotherapy. 17 (2006) 193–213. https://doi.org/10.1177/095632020601700404.
[265] A. Gulati, F.D. Boudinot, P.M. Gerk, Binding of Lopinavir to Human 1-Acid Glycoprotein and Serum Albumin, Drug Metabolism and Disposition. 37 (2009) 1572–1575. https://doi.org/10.1124/dmd.109.026708.
[266] R.L. Murphy, S. Brun, C. Hicks, J.J. Eron, R. Gulick, M. King, A.C. White, C. Benson, M. Thompson, H.A. Kessler, S. Hammer, R. Bertz, A. Hsu, A. Japour, E. Sun, ABT-378/ritonavir plus stavudine and lamivudine for the treatment of antiretroviral-naive adults with HIV-1 infection : 48-week results, AIDS. 15 (2001) F1–F9. https://doi.org/10.1097/00002030-200101050-00002.

[267] P. Gershkovich, A. Hoffman, Effect of a high-fat meal on absorption and disposition of lipophilic compounds : The importance of degree of association with triglyceride-rich lipoproteins, European Journal of Pharmaceutical Sciences. 32 (2007) 24–32. https://doi.org/10.1016/j.ejps.2007.05.109.
[268] L. Hu, S. Han, C.J.H. Porter, N.L. Trevaskis, The Impact of Lymphatic Transport on the Systemic Disposition of Lipophilic Drugs, Journal of Pharmaceutical Sciences. 102 (2013) 2395–2408. https://doi.org/10.1002/jps.23597.
[269] G.M. Patel, P.K. Shelat, A.N. Lalwani, QbD based development of proliposome of lopinavir for improved oral bioavailability, European Journal of Pharmaceutical Sciences. 108 (2016) 50–61. https://doi.org/10.1016/j.ejps.2016.08.057.
[270] G. Patel, P. Shelat, A. Lalwani, Statistical modeling , optimization and characterisation of solid self-nanoemulsifying drug delivery system of lopinavir using design of experiment, Drug Delivery. 23 (2016) 3027–3042. https://doi.org/10.3109/10717544.2016.1141260.
[271] J.S. Negi, P. Chattopadhyay, A.K. Sharma, V. Ram, Development and evaluation of glyceryl behenate based solid lipid nanoparticles (SLNs) using hot self-nanoemulsification (SNE) technique, Archives of Pharmacal Research. 37 (2014) 361–370. https://doi.org/10.1007/s12272-013-0154-y.
[272] Y. Gong, S. Haque, P. Chowdhury, T.J. Cory, S. Kodidela, M.M. Yallapu, J.M. Norwood, S. Kumar, Pharmacokinetics and pharmacodynamics of cytochrome P450 inhibitors for HIV treatment, Expert Opinion on Drug Metabolism & Toxicology. 15 (2019) 417–427. https://doi.org/10.1080/17425255.2019.1604685.
[273] A. Stolbach, K. Paziana, H. Heverling, P. Pham, A Review of the Toxicity of HIV Medications II : Interactions with Drugs and Complementary and Alternative Medicine Products, Journal of Medical Toxicology. 11 (2015) 326–341. https://doi.org/10.1007/s13181-015-0465-0.
[274] A. Coert, J. Geelen, J. De Visser, van der V. J, The pharmacology and metabolism of testosterone undecanoate (TU), a new orally active androgen, Acta Endocrinologica. 4 (1975) 789–800. https://doi.org/10.1530/acta.0.0790789.
[275] P.R. Ravi, R. Vats, V. Dalal, A.N. Murthy, A hybrid design to optimize preparation of lopinavir loaded solid lipid nanoparticles and comparative pharmacokinetic evaluation with marketed lopinavir/ritonavir coformulation, Journal of Pharmacy and Pharmacology. 66 (2014) 912–926. https://doi.org/10.1111/jphp.12217.
[276] P.R. Ravi, R. Vats, Comparative pharmacokinetic evaluation of lopinavir and lopinavir-loaded solid lipid nanoparticles in hepatic impaired rat model, Journal of Pharmacy and Pharmacology. 69 (2017) 823–833. https://doi.org/10.1111/jphp.12716.
[277] S.J. Negi, P. Chattopadhyay, K.S. Ashok, V. Ram, Development of solid lipid nanoparticles (SLNs) of lopinavir using hot self nano-emulsification (SNE) technique, European Journal of Pharmaceutical Sciences. 48 (2013) 231–239. https://doi.org/10.1016/j.ejps.2012.10.022.
[278] A. Zgair, J.B. Lee, J.C.M. Wong, D.A. Taha, J. Aram, D. Di Virgilio, J.W. Mcarthur, Y. Cheng, I.M. Hennig, D.A. Barrett, P.M. Fischer, C.S. Constantinescu, P. Gershkovich, Oral administration of cannabis with lipids leads to high levels of cannabinoids in the intestinal lymphatic system and prominent immunomodulation, Scientific Reports. 7 (2017) 1–12. https://doi.org/10.1038/s41598-017-15026-z.
[279] M. Guadalupe, E. Reay, S. Sankaran, T. Prindiville, J. Flamm, A. Mcneil, S. Dandekar, Severe CD4+ T-Cell Depletion in Gut Lymphoid Tissue during Primary Human Immunodeficiency Virus Type 1 Infection and Substantial Delay in Restoration following Highly Active Antiretroviral Therapy, Journal of Virology. 77 (2003) 11708–11717. https://doi.org/10.1128/JVI.77.21.11708.

[280] J.M. Brenchley, M. Paiardini, K.S. Knox, A.I. Asher, B. Cervasi, T.E. Asher, P. Scheinberg, D.A. Price, C.A. Hage, L.M. Kholi, A. Khoruts, I. Frank, J. Else, T. Schacker, G. Silvestri, D.C. Douek, Differential Th17 CD4 T-cell depletion in pathogenic and nonpathogenic lentiviral infections, Blood. 112 (2016) 2826–2836. https://doi.org/10.1182/blood-2008-05-159301.
[281] R.S. Veazey, M. Demaria, L. V Chalifoux, D.E. Shvetz, D.R. Pauley, H.L. Knight, M. Rosenzweig, R.P. Johnson, R.C. Desrosiers, A.A. Lackner, Gastrointestinal Tract as a Major Site of CD4+ T Cell Depletion and Viral Replication in SIV Infection, Science. 280 (1998) 427–431.
[282] S. Kewenig, T. Schneider, K. Hohloch, K.L. Dreyer, R. Ullrich, N. Stolte, C.S. Hennig, F.J. Kaup, A. Stallmach, M. Zeitz, Rapid mucosal CD4+ T-cell depletion and enteropathy in simian immunodeficiency virus–infected rhesus macaques, Gastroenterology. 116 (1999) 1115–1123.
[283] Z. Liu, W.G. Cumberland, L.E. Hultin, A.H. Kaplan, R. Detels, J. V. Giorgi, CD8+ T-Lymphocyte Activation in HIV-1 Disease Reflects an Aspect of Pathogenesis Distinct From Viral Burden and Immunodeficiency, Journal of Acquired Immune Deficiency Syndromes and Human Retrovirology. 18 (1998) 332–340.
[284] F. Caby, A. Guihot, S. Lambert-niclot, M. Guiguet, D. Boutolleau, R. Agher, M. Valantin, Determinants of a Low CD4 / CD8 Ratio in HIV-1 – Infected Individuals Despite Long-term Viral Suppression, AIDS. 31 (2017) 1685–1695. https://doi.org/10.1093/cid/ciw076.
[285] J. Tang, CD4 : CD8 lymphocyte ratio as a quantitative measure of immunologic health in HIV-1 infection : findings from an African cohort with prospective data, Frontiers in Microbiology. 6 (2015) 1–9. https://doi.org/10.3389/fmicb.2015.00670.
[286] M. Paiardini, M. Müller-Trutwin, HIV-associated chronic immune activation, Immunological Reviews. 254 (2013) 78–101. https://doi.org/10.1111/imr.12079.HIV-associated.
[287] E. Cassol, S. Malfeld, P. Mahasha, S. van der Merwe, S. Cassol, C. Seebregts, M. Alfano, G. Poli, T. Rossouw, Persistent Microbial Translocation and Immune Activation in HIV-1–Infected South Africans Receiving Combination Antiretroviral Therapy, The Journal of Infectious Diseases. 202 (2010) 723–733. https://doi.org/10.1086/655229.
[288] W. Jiang, M.M. Lederman, P. Hunt, S.F. Sieg, K. Haley, A. Landay, J. Martin, E. Sinclair, A.I. Asher, G. Steven, D.C. Douek, J.M. Brenchley, Plasma Levels of Bacterial DNA Correlate with Immune Activation and the Magnitude of Immune Restoration in Persons with Antiretroviral-Treated HIV Infection, The Journal of Infectious Diseases. 199 (2009) 1177–1185. https://doi.org/10.1086/597476.Plasma.
[289] Z. Zhou, A. Maya, V. Ramakrishnan, A. Eckard, Elevated systemic microbial translocation in pregnant HIV-infected women compared to HIV-uninfected women , and its inverse correlations with plasma progesterone levels, Journal of Reproductive Immunology. 127 (2018) 16–18. https://doi.org/10.1016/j.jri.2018.04.001.
[290] W. Xu, Z. Luo, A. V Alekseyenko, L. Martin, Z. Wan, B. Ling, Z. Qin, S.L. Heath, K. Maas, X. Cong, W. Jiang, Distinct systemic microbiome and microbial translocation are associated with plasma level of anti-CD4 autoantibody in HIV infection, Scientific Reports. 8 (2018) 1–12. https://doi.org/10.1038/s41598-018-31116-y.
[291] M.A. Monnig, C.W. Kahler, P.A. Cioe, P.M. Monti, K.H. Mayer, D.W. Pantalone, R.A. Cohen, B. Ramratnam, Markers of Microbial Translocation and Immune Activation Predict Cognitive Processing Speed in Heavy-Drinking Men Living with HIV, Microorganisms. 5 (2017) 64. https://doi.org/10.3390/microorganisms5040064.
[292] K. Tsoyi, T.Y. Lee, Y.S. Lee, H.J. Kim, H.G. Seo, J.H. Lee, K.C. Chang, Heme-

Oxygenase-1 Induction and Carbon Monoxide- Releasing Molecule Inhibit Lipopolysaccharide (LPS) -Induced High-Mobility Group Box 1 Release in Vitro and Improve Survival of Mice in LPS- and Cecal Ligation and Puncture- Induced Sepsis Model in Vivo, Molecular Pharmacology. 76 (2009) 173–182. https://doi.org/10.1124/mol.109.055137.can.
[293] R. Takamiya, C. Hung, S.R. Hall, K. Fukunaga, T. Nagaishi, T. Maeno, C. Owen, A.A. Macias, L.E. Fredenburgh, A. Ishizaka, R.S. Blumberg, R.M. Baron, M.A. Perrella, High-Mobility Group Box 1 Contributes to Lethality of Endotoxemia in Heme Oxygenase-1 – Deficient Mice, American Journal of Respiratory Cell and Molecular Biology. 41 (2009) 129–135. https://doi.org/10.1165/rcmb.2008-0331OC.
[294] M. El Gazzar, HMGB1 modulates infl ammatory responses in LPS-activated macrophages, Inflammation Research. 56 (2007) 162–167. https://doi.org/10.1007/s00011-006-6112-0.
[295] J.C. Chow, D.W. Young, D.T. Golenbock, W.J. Christ, F. Gusovsky, Toll-like Receptor-4 Mediates Lipopolysaccharide-induced Signal Transduction, Journal of Biological Chemistry. 274 (1999) 10689–10692. https://doi.org/10.1074/jbc.274.16.10689.
[296] M.L. Gougeon, M.T. Melki, H. Sadi, HMGB1, an alarmin promoting HIV dissemination and latency in dendritic cells, Cell Death and Differentiation. 19 (2012) 96–106. https://doi.org/10.1038/cdd.2011.134.
[297] T. Kawai, S. Akira, Signaling to NF-κB by Toll-like receptors, Trends in Molecular Medicine. 13 (2007) 460–469. https://doi.org/10.1016/j.molmed.2007.09.002.
[298] M. Trøseid, A. Lind, P. Nowak, B. Barqasho, B. Heger, I. Lygren, K.K. Pedersen, T. Kanda, H. Funaoka, J.K. Dama, Circulating levels of HMGB1 are correlated strongly with MD2 in HIV-infection : Possible implication for TLR4-signalling and chronic immune activation, Innate Immunity. 19 (2012) 290–297. https://doi.org/10.1177/1753425912461042.
[299] S. Thierry, J. Gozlan, A. Jaulmes, R. Boniface, N. Nasreddine, F. Strauss, V. Maréchal, High-mobility group box 1 protein induces HIV-1 expression from persistently infected cells, AIDS. 21 (2007) 283–292. https://doi.org/10.1097/QAD.0b013e3280115b50.
[300] B. Barqasho, P. Nowak, S. Abdurahman, L. Walther-Jallow, A. Sönnerborg, Implications of the release of high-mobility group box 1 protein from dying cells during human immunodeficiency virus type 1 infection in vitro, Journal of General Virology. 91 (2010) 1800–1809. https://doi.org/10.1099/vir.0.016915-0.
[301] P. Nowak, B. Barqasho, A. Sönnerborg, Elevated plasma levels of high mobility group box protein 1 in patients with HIV-1 infection, AIDS. 21 (2007) 869–871.
[302] M. Trøseid, P. Nowak, J. Nyström, A. Lindkvist, S. Abdurahman, A. Sönnerborg, Elevated plasma levels of lipopolysaccharide and high mobility group box-1 protein are associated with high viral load in HIV-1 infection : reduction by 2-year antiretroviral therapy, AIDS. 24 (2010) 1733–1737. https://doi.org/10.1097/QAD.0b013e32833b254d.
[303] P. Nowak, B. Barqasho, C.J. Treutiger, H.E. Harris, K.J. Tracey, J. Andersson, A. Sönnerborg, HMGB1 activates replication of latent HIV-1 in a monocytic cell-line, but inhibits HIV-1 replication in primary macrophages, Cytokine. 34 (2006) 17–23. https://doi.org/10.1016/j.cyto.2006.03.010.
[304] K. Takeuchi, S. Hase, H. Mizoguchi, Y. Komoike, A. Tanaka, Protection by aspirin of indomethacin-induced small intestinal damage in rats: Mediation by salicylic acid, Journal of Physiology Paris. 95 (2001) 51–57. https://doi.org/10.1016/S0928-4257(01)00009-2.

[305] H.W. Choi, M. Tian, F. Song, E. Venereau, A. Preti, S.-W. Park, K. Hamilton, G.V.T. Swapna, M. Manohar, M. Moreau, A. Agresti, A. Gorzanelli, F. De Marchis, H. Wang, M. Antonyak, R.J. Micikas, D.R. Gentile, R. a Cerione, F.C. Schroeder, G.T. Montelione, M.E. Bianchi, D.F. Klessig, Aspirin's Active Metabolite Salicylic Acid Targets High Mobility Group Box 1 to Modulate Inflammatory Responses., Molecular Medicine. 21 (2015) 526–535. https://doi.org/10.2119/molmed.2015.00148.
[306] J. Matson, K. Dillon, C. Powell, Self-Immolative Prodrugs: Effective Tools for the Controlled Release of Sulfur Signaling Species, Synlett. 30 (2019) 525–531. https://doi.org/10.1055/s-0037-1611693.Self-Immolative.
[307] J.L.M. Jourden, K.B. Daniel, S.M. Cohen, Investigation of self-immolative linkers in the design of hydrogen peroxide activated metalloprotein inhibitors, Chemical Communications. 47 (2011) 7968–7970. https://doi.org/10.1039/b000000x/Major.
[308] S.U. Hettiarachchi, B. Prasai, R.L. Mccarley, Detection and Cellular Imaging of Human Cancer Enzyme Using a Turn-On, Wavelength-Shiftable, Self-Immolative Profluorophore, Journal of the American Chemical Society. 136 (2014) 7575–7578. https://doi.org/10.1021/ja5030707.
[309] J.A. Sáez, B. Escuder, J.F. Miravet, Supramolecular hydrogels for enzymatically triggered self-immolative drug delivery, Tetrahedron. 66 (2010) 2614–2618. https://doi.org/10.1016/j.tet.2010.02.033.
[310] Y. Zheng, B. Yu, Z. Li, Z. Yuan, C.L. Organ, R.K. Trivedi, S. Wang, D.J. Lefer, B. Wang, An Esterase-Sensitive Prodrug Approach for Controllable Delivery of Persulfide Species, Angewandte Chemie. 129 (2017) 11911–11915. https://doi.org/10.1002/anie.201704117.
[311] L. Hu, Drug Delivery: Principles and Applications, 2016.
[312] M.E. Roth, O. Green, S. Gnaim, D. Shabat, Dendritic , Oligomeric , and Polymeric Self-Immolative Molecular Amplification, Chemical Reviews. 116 (2016) 1309–1352. https://doi.org/10.1021/acs.chemrev.5b00372.
[313] A. Sagi, R. Weinstain, N. Karton, D. Shabat, Self-Immolative Polymers, Journal of the American Chemical Society. 130 (2008) 5434–5435. https://doi.org/10.1021/ja801065d.
[314] M. Shamis, H.N. Lode, D. Shabat, Bioactivation of Self-Immolative Dendritic Prodrugs by Catalytic Antibody 38C2, Journal of the American Chemical Society. 126 (2004) 1726–1731. https://doi.org/10.1021/ja039052p.
[315] A.D. Corso, M. Caruso, L. Belvisi, D. Arosio, U. Piarulli, C. Albanese, F. Gasparri, A. Marsiglio, F. Sola, S. Troiani, B. Valsasina, L. Pignataro, D. Donati, C. Gennari, Synthesis and Biological Evaluation of RGD Peptidomimetic – Paclitaxel Conjugates Bearing Lysosomally Cleavable Linkers, Chemistry - A European Journal. 21 (2015) 6921–6929. https://doi.org/10.1002/chem.201500158.
[316] E.K.Y. Chen, R.A. Mcbride, E.R. Gillies, Self-Immolative Polymers Containing Rapidly Cyclizing Spacers: Toward Rapid Depolymerization Rates, Macromolecules. 45 (2012) 7364–7374. https://doi.org/10.1021/ma301667c.
[317] B. Li, P. Liu, D. Yan, F. Zeng, S. Wu, A self-immolative and DT-diaphorase-activatable prodrug for drug-release tracking and therapy, Journal of Materials Chemistry B. 5 (2017) 2635–2643. https://doi.org/10.1039/C7TB00266A.
[318] K. Beaumont, R. Webster, I. Gardner, K. Dack, Design of Ester Prodrugs to Enhance Oral Absorption of Poorly Permeable Compounds : Challenges to the Discovery Scientist, Current Drug Metabolism. 4 (2003) 461–485. https://doi.org/10.2174/1389200033489253.
[319] P.R. Ravi, R. Vats, R. Thakur, S. Srivani, N. Aditya, Effect of Grapefruit Juice and Ritonavir on Pharmacokinetics of Lopinavir in Wistar Rats, Phytotherapy Research.

1495 (2012) 1490–1495. https://doi.org/10.1002/ptr.4593.
[320] J.B. Dressman, A. Nair, B. Abrahamsson, D.M. Barends, D.W. Groot, S. Kopp, P. Langguth, J.E. Polli, V.P. Shah, M. Zimmer, Biowaiver Monograph for Immediate-Release Solid Oral Dosage Forms : Acetylsalicylic Acid, Journal of Pharmaceutical Sciences. 101 (2012) 2653–2667. https://doi.org/10.1002/jps.
[321] E. Dailly, F. Raffi, P. Jolliet, Determination of atazanavir and other antiretroviral drugs (indinavir, amprenavir, nelfinavir and its active metabolite M8, saquinavir, ritonavir, lopinavir, nevirapine and efavirenz) plasma levels by high performance liquid chromatography with UV, Journal of Chromatography B. 813 (2004) 353–358. https://doi.org/10.1016/j.jchromb.2004.10.005.
[322] Y.U. Sami, T.O. Ki, M.N. Akai, M.S. Agisaka, T.K. Aneda, A Simple HPLC Method for Simultaneous Determination of Lopinavir, Ritonavir and Efavirenz, CHEMICAL & PHARMACEUTICAL BULLETIN. 51 (2003) 5–8. https://doi.org/10.1248/cpb.51.715.
[323] S.M. Robertson, R.T. Davey, J. Voell, E. Formentini, R.M. Alfaro, Effect of Ginkgo biloba extract on lopinavir, midazolam and fexofenadine pharmacokinetics in healthy subjects, Current Medical Research and Opinion. 24 (2008) 591–599. https://doi.org/10.1185/030079908X260871.
[324] K.V. Kumar, M. Sudhakar, Y.P. Reddy, P. Malleshwari, S.K. Hafeez, RP-HPLC Method Development and Validation for Simultaneous Estimation of Lopinavir and Ritonavir in Dosage form and in Plasma, Journal of Pharmaceutical Research. 3 (2014) 1–8. https://doi.org/10.23880/oajpr-16000140.
[325] N.L. Rezk, R.D. Crutchley, R.F. Yeh, A.D.M. Kashuba, Full Validation of an Analytical Method for the HIV-Protease Inhibitor Atazanavir in Combination With 8 Other Antiretroviral Agents and its Applicability to Therapeutic Drug Monitoring, Therapeutic Drug Monitoring. 28 (2006) 517–525. https://doi.org/10.1097/00007691-200608000-00006.
[326] A. V Sulebhavikar, U.D. Pawar, K. V Mangoankar, HPTLC Method for Simultaneous Determination of Lopinavir and Ritonavir in Capsule Dosage Form, E-Journal of Chemistry. 5 (2008) 706–712. https://doi.org/10.1155/2008/539849.
[327] R. Verbesselt, E. Van Wijngaerden, J. de Hoon, Simultaneous determination of 8 HIV protease inhibitors in human plasma by isocratic high-performance liquid chromatography with combined use of UV and fluorescence detection: Amprenavir, indinavir, atazanavir, ritonavir, lopinavir, saquinavir, nelfinavir, Journal of Chromatography B. 845 (2007) 51–60. https://doi.org/10.1016/j.jchromb.2006.07.068.
[328] C. Marzolini, A. Béguin, A. Telenti, A. Schreyer, T. Buclin, J. Biollaz, L.A. Decosterd, Determination of lopinavir and nevirapine by high-performance liquid chromatography after solid-phase extraction: Application for the assessment of their transplacental passage at delivery, Journal of Chromatography B. 774 (2002) 127–140. https://doi.org/10.1016/S1570-0232(02)00169-1.
[329] L. Else, V. Watson, J. Tjia, A. Hughes, M. Siccardi, S. Khoo, D. Back, Validation of a rapid and sensitive high-performance liquid chromatography-tandem mass spectrometry (HPLC-MS/MS) assay for the simultaneous determination of existing and new antiretroviral compounds, Journal of Chromatography B. 878 (2010) 1455–1465. https://doi.org/10.1016/j.jchromb.2010.03.036.
[330] G.A. Temghare, S.S. Shetye, S.S. Joshi, S.M. Yetal, V. V. Vaidya, Rapid and sensitive method for quantitative determination of azathioprine and 6-mercaptopurine in human plasma by liquid chromatography- tandem mass specrtometry, Ournal of Chemistry. 1 (2009) 223–230.
[331] T. Piper, U. Mareck, H. Geyer, U. Flenker, M. Thevis, P. Platen, W. Schanzer,

Determination of 13C/12C ratios of endogenous urinary steroids: methd validation, reference population and application to doping control purposes, Rapid Communications in Mass Spectrometry : RCM. 22 (2008) 2161–2175. https://doi.org/10.1002/rcm.
[332] S. Jaiswal, A. Sharma, M. Shukla, J. Lal, Simultaneous LC – MS-MS Determination of Lopinavir and Rifabutin in Human Plasma, Journal of Chromatographic Science. 55 (2017) 617–624. https://doi.org/10.1093/chromsci/bmx016.
[333] H. Plasma, W. Egge-jacobsen, M. Unger, C.U. Niemann, M. Baluom, S. Hirai, L.Z. Benet, U. Christians, Automated, Fast, and Sensitive Quantification of Drugs in Human Plasma by LC/LC-MS, Therapeutic Drug Monitoring. 26 (2004) 546–562. https://doi.org/10.1097/00007691-200410000-00014.
[334] P.R. Ravi, R. Vats, V. Dalal, N. Gadekar, N. Aditya, Design, optimization and evaluation of poly-ε-caprolactone (PCL) based polymeric nanoparticles for oral delivery of lopinavir, Drug Development and Industrial Pharmacy. 41 (2015) 131–140. https://doi.org/10.3109/03639045.2013.850710.
[335] J. Sun, L. Yin, J. Chen, H. Lu, Effect of the Tang herb on the pharmacokinetics of lopinavir in rats, Journal of Chinese Pharmaceutical Sciences. 23 (2014) 28–32.
[336] M.R. Aji Alex, A.J. Chacko, S. Jose, E.B. Souto, Lopinavir loaded solid lipid nanoparticles (SLN) for intestinal lymphatic targeting, European Journal of Pharmaceutical Sciences. 42 (2011) 11–18. https://doi.org/10.1016/j.ejps.2010.10.002.
[337] S. Han, T. Quach, L. Hu, A. Wahab, W.N. Charman, V.J. Stella, N.L. Trevaskis, J.S. Simpson, C.J.H. Porter, Targeted delivery of a model immunomodulator to the lymphatic system: Comparison of alkyl ester versus triglyceride mimetic lipid prodrug strategies, Journal of Controlled Release. 177 (2014) 1–10. https://doi.org/10.1016/j.jconrel.2013.12.031.
[338] J. SUGIHARA, S. FURUUCHI, K. NAKANO, S. HARIGAYA, Studies on Intestinal Lymphatic Absorption of Drugs. I. Lymphatic Absorption of Alkyl Ester Derivatives and α-Monoglyceride Derivatives of Drugs, Journal of Pharmacobio-Dynamics. 11 (1988) 369–376. https://doi.org/10.1248/bpb1978.11.369.
[339] Wahajuddin, S.P. Singh, K.S.R. Raju, A. Nafis, S.K. Puri, G.K. Jain, Intravenous pharmacokinetics , oral bioavailability , dose proportionality and in situ permeability of anti-malarial lumefantrine in rats, Malaria Journal. 10 (2011) 1–9. https://doi.org/10.1186/1475-2875-10-293.
[340] A. Shayeganpour, A.S. Jun, D.R. Brocks, Pharmacokinetics of Amiodarone in Hyperlipidemic and Simulated High Fat-Meal Rat Models, Biopharmaceutics & Drug Disposition. 26 (2005) 249–257. https://doi.org/10.1002/bdd.457.
[341] W.A. Lee, G. He, E. Eisenberg, T. Cihlar, S. Swaminathan, A. Mulato, K.C. Cundy, Selective Intracellular Activation of a Novel Prodrug of the Human Immunodeficiency Virus Reverse Transcriptase Inhibitor Tenofovir Leads to Preferential Distribution and Accumulation in Lymphatic Tissue, Antimicrobial Agents and Chemotherapy. 49 (2005) 1898–1906. https://doi.org/10.1128/aac.49.5.1898-1906.2005.
[342] F.M.H. De Groot, W.J. Loos, R. Koekkoek, L.W.A. Van Berkom, G.F. Busscher, A.E. Seelen, C. Albrecht, P. De Bruijn, H.W. Scheeren, Elongated Multiple Electronic Cascade and Cyclization Spacer Systems in Activatible Anticancer Prodrugs for Enhanced Drug Release, J. Org. Chem. 66 (2001) 8815–8830. https://doi.org/10.1021/jo0158884.
[343] R.B. Greenwald, A. Pendri, C.D. Conover, H. Zhao, Y.H. Choe, A. Martinez, Drug Delivery Systems Employing 1 , 4- or 1 , 6-Elimination : Poly (ethylene glycol) Prodrugs of Amine-Containing Compounds, J. Med. Chem. 42 (1999) 3657–3667. https://doi.org/10.1021/jm990166e.

[344] J.A. Levy, The value of primate models for studying human immunodeficiency virus pathogenesis, Journal of Medical Primatology. 25 (1996) 163–174. https://doi.org/10.1111/j.1600-0684.1996.tb00013.x.
[345] D.T. Evans, G. Silvestri, Non-Human Primate Models in AIDS Research, Current Opinion in HIV and AIDS. 8 (2013) 255–261. https://doi.org/10.1097/coh.0b013e328361cee8.
[346] J.V. Garcia, "Humanized mice for HIV and AIDS research," Current Opinion in Virology. 19 (2016) 56–64. https://doi.org/10.1016/j.coviro.2016.06.010.
[347] L. Zhang, G.I. Kovalev, L. Su, HIV-1 infection and pathogenesis in a novel humanized mouse model, Blood. 109 (2006) 2978–2981. https://doi.org/10.1182/blood-2006-07-033159.
[348] O.T. Keppler, F.J. Welte, T.A. Ngo, P.S. Chin, K.S. Patton, C. Tsou, N.W. Abbey, M.E. Sharkey, R.M. Grant, Y. You, J.D. Scarborough, W. Ellmeier, D.R. Littman, M. Stevenson, I.F. Charo, B.G. Herndier, R.F. Speck, M.A. Goldsmith, Progress Toward a Human CD4/CCR5 Transgenic Rat Model for De Novo Infection by Human Immunodeficiency Virus Type 1, Journal of Experimental Medicine. 195 (2002) 719–736. https://doi.org/10.1084/jem.20011549.
[349] Y. Agarwal, C. Beatty, S. Biradar, I. Castronova, S. Ho, K. Melody, M.T. Bility, Moving beyond the mousetrap: current and emerging humanized mouse and rat models for investigating prevention and cure strategies against HIV infection and associated pathologies, Retrovirology. 17 (2020) 1–11. https://doi.org/10.1186/s12977-020-00515-3.
[350] K.C. Williams, T.H. Burdo, HIV and SIV infection: the role of cellular restriction and immune responses in viral replication and pathogenesis, APMIS. 117 (2009) 400–412. https://doi.org/10.1111/j.1600-0463.2009.02450.x.